

Vincent G. Duffy *Editor*

Advances in Applied Digital Human Modeling and Simulation

Proceedings of the AHFE 2016
International Conference on Digital
Human Modeling and Simulation,
July 27–31, 2016, Walt Disney World[®],
Florida, USA

Advances in Intelligent Systems and Computing

Volume 481

Series editor

Janusz Kacprzyk, Polish Academy of Sciences, Warsaw, Poland
e-mail: kacprzyk@ibspan.waw.pl

About this Series

The series “Advances in Intelligent Systems and Computing” contains publications on theory, applications, and design methods of Intelligent Systems and Intelligent Computing. Virtually all disciplines such as engineering, natural sciences, computer and information science, ICT, economics, business, e-commerce, environment, healthcare, life science are covered. The list of topics spans all the areas of modern intelligent systems and computing.

The publications within “Advances in Intelligent Systems and Computing” are primarily textbooks and proceedings of important conferences, symposia and congresses. They cover significant recent developments in the field, both of a foundational and applicable character. An important characteristic feature of the series is the short publication time and world-wide distribution. This permits a rapid and broad dissemination of research results.

Advisory Board

Chairman

Nikhil R. Pal, Indian Statistical Institute, Kolkata, India
e-mail: nikhil@isical.ac.in

Members

Rafael Bello, Universidad Central “Marta Abreu” de Las Villas, Santa Clara, Cuba
e-mail: rbellop@uclv.edu.cu

Emilio S. Corchado, University of Salamanca, Salamanca, Spain
e-mail: escorchado@usal.es

Hani Hagras, University of Essex, Colchester, UK
e-mail: hani@essex.ac.uk

László T. Kóczy, Széchenyi István University, Győr, Hungary
e-mail: koczy@sze.hu

Vladik Kreinovich, University of Texas at El Paso, El Paso, USA
e-mail: vladik@utep.edu

Chin-Teng Lin, National Chiao Tung University, Hsinchu, Taiwan
e-mail: ctlin@mail.nctu.edu.tw

Jie Lu, University of Technology, Sydney, Australia
e-mail: Jie.Lu@uts.edu.au

Patricia Melin, Tijuana Institute of Technology, Tijuana, Mexico
e-mail: epmelin@hafsamx.org

Nadia Nedjah, State University of Rio de Janeiro, Rio de Janeiro, Brazil
e-mail: nadia@eng.uerj.br

Ngoc Thanh Nguyen, Wroclaw University of Technology, Wroclaw, Poland
e-mail: Ngoc-Thanh.Nguyen@pwr.edu.pl

Jun Wang, The Chinese University of Hong Kong, Shatin, Hong Kong
e-mail: jwang@mae.cuhk.edu.hk

More information about this series at <http://www.springer.com/series/11156>

Vincent G. Duffy
Editor

Advances in Applied Digital Human Modeling and Simulation

Proceedings of the AHFE 2016 International
Conference on Digital Human Modeling
and Simulation, July 27–31, 2016,
Walt Disney World[®], Florida, USA

Editor
Vincent G. Duffy
Purdue University
West Lafayette, IN
USA

ISSN 2194-5357 ISSN 2194-5365 (electronic)
Advances in Intelligent Systems and Computing
ISBN 978-3-319-41626-7 ISBN 978-3-319-41627-4 (eBook)
DOI 10.1007/978-3-319-41627-4

Library of Congress Control Number: 2016944333

© Springer International Publishing Switzerland 2017

This work is subject to copyright. All rights are reserved by the Publisher, whether the whole or part of the material is concerned, specifically the rights of translation, reprinting, reuse of illustrations, recitation, broadcasting, reproduction on microfilms or in any other physical way, and transmission or information storage and retrieval, electronic adaptation, computer software, or by similar or dissimilar methodology now known or hereafter developed.

The use of general descriptive names, registered names, trademarks, service marks, etc. in this publication does not imply, even in the absence of a specific statement, that such names are exempt from the relevant protective laws and regulations and therefore free for general use.

The publisher, the authors and the editors are safe to assume that the advice and information in this book are believed to be true and accurate at the date of publication. Neither the publisher nor the authors or the editors give a warranty, express or implied, with respect to the material contained herein or for any errors or omissions that may have been made.

Printed on acid-free paper

This Springer imprint is published by Springer Nature
The registered company is Springer International Publishing AG Switzerland

Advances in Human Factors and Ergonomics 2016

AHFE 2016 Series Editors

Tareq Z. Ahram, Florida, USA
Waldemar Karwowski, Florida, USA

7th International Conference on Applied Human Factors and Ergonomics

Proceedings of the AHFE 2016 International Conference on Digital Human Modeling and Simulation, July 27–31, 2016, Walt Disney World[®], Florida, USA

<i>Advances in Cross-Cultural Decision Making</i>	<i>Sae Schatz and Mark Hoffman</i>
<i>Advances in Applied Digital Human Modeling and Simulation</i>	<i>Vincent G. Duffy</i>
<i>Advances in Human Factors and Ergonomics in Healthcare</i>	<i>Vincent G. Duffy and Nancy Lightner</i>
<i>Advances in Affective and Pleasurable Design</i>	<i>WonJoon Chung and Cliff(Sungsoo) Shin</i>
<i>Advances in Human Aspects of Transportation</i>	<i>Neville A. Stanton, Steven Landry, Giuseppe Di Bucchianico and Andrea Vallicelli</i>
<i>Advances in Ergonomics In Design</i>	<i>Francisco Rebelo and Marcelo Soares</i>
<i>Advances in Ergonomics Modeling, Usability & Special Populations</i>	<i>Marcelo Soares, Christianne Falcão and Tareq Z. Ahram</i>
<i>Advances in Social & Occupational Ergonomics</i>	<i>Richard Goossens</i>
<i>Advances in Neuroergonomics and Cognitive Engineering</i>	<i>Kelly S. Hale and Kay M. Stanney</i>
<i>Advances in Physical Ergonomics and Human Factors</i>	<i>Ravindra Goonetilleke and Waldemar Karwowski</i>
<i>Advances in The Ergonomics in Manufacturing: Managing the Enterprise of the Future</i>	<i>Christopher Schlick and Stefan Trzcielinski</i>
<i>Advances in Safety Management and Human Factors</i>	<i>Pedro Arezes</i>
<i>Advances in Human Factors, Software, and Systems Engineering</i>	<i>Ben Amaba</i>

(continued)

(continued)

<i>Advances in Human Factors and Sustainable Infrastructure</i>	<i>Jerzy Charytonowicz</i>
<i>Advances in The Human Side of Service Engineering</i>	<i>Tareq Z. Ahram and Waldemar Karwowski</i>
<i>Advances in Human Factors in Energy: Oil, Gas, Nuclear and Electric Power Industries</i>	<i>Sacit Cetiner, Paul Fechtelkötter and Michael Legatt</i>
<i>Advances in Human Factors in Sports and Outdoor Recreation</i>	<i>Paul Salmon and Anne-Claire Macquet</i>
<i>Advances in Human Factors and System Interactions</i>	<i>Isabel L. Nunes</i>
<i>Advances in Human Factors, Business Management, Training and Education</i>	<i>Jussi Kantola, Tibor Barath, Salman Nazir and Terence Andre</i>
<i>Advances in Human Factors in Robots and Unmanned Systems</i>	<i>Pamela Savage-Knepshield and Jessie Chen</i>
<i>Advances in Design for Inclusion</i>	<i>Giuseppe Di Bucchianico and Pete Kercher</i>
<i>Advances in Human Factors in Cybersecurity</i>	<i>Denise Nicholson, Janae Lockett-Reynolds and Katherine Muse</i>

Preface

This book, *Advances in Applied Digital Human Modeling*, is concerned with human modeling, biomechanics, and simulation. The benefit of this area of research is to aid in the design of systems. Human modeling and simulation can reduce the need for physical prototyping and incorporate ergonomics and human factors earlier in design processes. These models provide a representation of some human aspects that can be inserted into simulations or virtual environments and facilitate prediction of safety, satisfaction, usability, performance, and sustainability. These may consider the physiological, cognitive, behavioral, emotional, and environmental aspects. The math and science provides a foundation for visualizations that can facilitate decision-making by technical experts, management, or those responsible for public policy.

Explicitly, the book contains the following subject areas:

- I. Situational Awareness, Design and Computational Modeling
- II. Virtual Reality and Simulation
- III. Applied Modeling and Simulation

Each chapter of the book was either reviewed by the members of scientific advisory and editorial board or germinated by them. Our sincere thanks and appreciation go to the board members listed below for their contribution to the highest scientific standards maintained in developing this book:

- T. Ahram, USA
- T. Alexander, Germany
- S. Bogner, USA
- J. Charland, Canada
- Z. Cheng, USA
- T. Convard, France
- B. Corner, USA
- M. Corticeiro Neves, Portugal
- N. Dechy, France
- J. Dell'Anna, Germany

M. Fray, UK
L. Fritzsche, Germany
R. Goonetilleke, Hong Kong
R. Goossens, the Netherlands
B. Gore, USA
R. Green, USA
L. Hanson, Sweden
D. Högberg, Sweden
M. Kimura, Japan
Z. Li, China
A. Luximon, Hong Kong
T. Marler, USA
R. Marshall, UK
M. Mazzola, Italy
M. Merad, France
C. Möbus, Germany
M. Mochimaru, Japan
A. Pereira, Portugal
S. Pickl, Germany
G. Psarros, Norway
K. Radermacher, Germany
H. Rasmussen, Denmark
R. Sudhakar, USA
J. Yang, USA
Z. Yang, UK

West Lafayette, USA
July 2016

Vincent G. Duffy

Contents

Part I Situational Awareness, Design and Computational Modeling	
Field Study on the Application of a Simulation-Based Software Tool for the Strain-Based Staffing in Industrial Manufacturing	3
Peter Gust, Ulf Müller, Nico Feller and Michael Schiffmann	
A Quantitative Comparison of Operator Field of View for Vehicle Design	13
M.D. King, Jeffrey Jinkerson, Teena Garrison, Derek Irby and Daniel W. Carruth	
An Integrated Computational Simulation System for Injury Assessment	23
Sultan Sultan, Karim Abdel-Malek, Jasbir Arora, Rajan Bhatt and Tim Marler	
Identifying the Factors Affecting Automotive Driving Posture and Their Perceived Importance for Seat and Steering Wheel Adjustment	35
Xuguang Wang and Jeanne Bulle	
Optimization-Based Prediction of the Motion of a Soldier Performing the ‘Going Prone’ and ‘Get Up from Prone’ Military Tasks	45
Mahdiar Hariri	
Part II Virtual Reality and Simulation	
FCA Ergonomics Proactive Approach in Developing New Cars: Virtual Simulations and Physical Validation	57
Spada Stefania, Germanà Danila, Sessa Fabrizio and Lidia Ghibaudo	

Virtual Human Motion Design and Ergonomics Analysis in Maintenance Simulation 65
 Fuyang Yu, Qing Xue and Minxia Liu

Virtual Reality for Safety, Entertainment or Education: The Mars Mission Test 75
 Irene Lia Schlacht, Antonio Del Mastro and Salman Nazir

The Argument for Simulation-Based Training in Dietetic Clinical Education: A Review of the Research 85
 Farhood Basiri

The Working Posture Controller—Automated Assessment and Optimisation of the Working Posture During the Process 93
 The Duy Nguyen, Carla Pilz and Jörg Krüger

Older Driver’s Physiological Response Under Risky Driving Conditions—Overtaking, Unprotected Left Turn 107
 Se Jin Park, Murali Subramaniam, Seoung Eun Kim, Seunghye Hong, Joo Hyeong Lee and Chan Min Jo

Part III Applied Modeling and Simulation

Modeling Decision Flow Dynamics for the Reliable Assessment of Human Performance, Crew Size and Total Ownership Cost 117
 Tareq Z. Ahram, Waldemar Karwowski, Serge Sala-Diakanda and Hong Jiang

Modeling the Perception Reaction Time and Deceleration Level for Different Surface Conditions Using Machine Learning Techniques 131
 Mohammed Elhenawy, Ihab El-Shawarby and Hesham Rakha

3D Scanning of Clothing Using a RGB-D Sensor with Application in a Virtual Dressing Room. 143
 Michael B. Holte

Application of Strength Requirements to Complex Loading Scenarios 155
 Scott England and Sudhakar Rajulu

Movement Variability and Digital Human Models: Development of a Demonstrator Taking the Effects of Muscular Fatigue into Account 169
 Jonathan Savin, Martine Gilles, Clarisse Gaudez, Vincent Padois and Philippe Bidaud

Climate Variability, Opposition Group Formation and Conflict Onset. 181
 Zining Yang and Piotr M. Zagorowski

Towards a Comprehensive Simulator for Public Speaking Anxiety Treatment 195
 Esin Söyler, Chathika Gunaratne and Mustafa İlhan Akbaş

The Research on VR-Based of Technology Generating Equipment and Interaction Equipment 207
 Yan Liu and Fan Wang

Assessing Hazard Identification in Surface Stone Mines in a Virtual Environment 217
 Jennica L. Bellanca, Timothy J. Orr, William Helfrich, Brendan Macdonald, Jason Navoyski and Brianna Eiter

Interactive Landslide Simulator: A Tool for Landslide Risk Assessment and Communication 231
 Pratik Chaturvedi, Akshit Arora and Varun Dutt

The Human-Systems Integration (HSI) Concept, Applied in an Observation of a Car Crash Simulation 245
 Nelson Matias, Natália Carvalho, Paulo Sena, Claudia Araújo and Rosinei Ribeiro

Digital Human Modeling Pipeline with a 3D Anthropometry Database 257
 Peng Li, Jeremy Carson, Joseph Parham and Steven Paquette

Integrating Heterogeneous Modeling Frameworks Using the DREAMIT Workspace 267
 Walter Warwick, Matthew Walsh, Stu Rodgers and Christian Lebiere

Lessons Learned in Development of a Behavior Modeling Tool for Health Intervention Design: BehaviorSim 279
 Tylar Murray, Eric Hekler, Donna Spruijt-Metz, Daniel E. Rivera and Andrew Rajj

Experimentation System for Path Planning Applied to 3D Printing 291
 Mateusz Wojcik, Iwona Pozniak-Koszalka, Leszek Koszalka and Andrzej Kasprzak

User Experience Design Based on Eye-Tracking Technology: A Case Study on Smartphone APPs. 303
 Qing-Xing Qu, Le Zhang, Wen-Yu Chao and Vincent Duffy

When Feedback Loops Collide: A Complex Adaptive Systems Approach to Modeling Human and Nature Dynamics. 317
 Zining Yang, Patrick deWerk Neal and Mark Abdollahian

Part I
Situational Awareness, Design and
Computational Modeling

Field Study on the Application of a Simulation-Based Software Tool for the Strain-Based Staffing in Industrial Manufacturing

Peter Gust, Ulf Müller, Nico Feller and Michael Schiffmann

Abstract In the context of demographic changes in industrial nations and the common global megatrend Internet of Things or Industry 4.0, enterprises have to tackle technological, social and economic challenges. To maintain their market position, enterprises have to change their manufacturing processes, amongst others. After a short introduction, the following article presents the objective and proceeding of a field study on the simulation-based software tool WorkDesigner for the strain-based staffing in a medium-sized enterprise of industrial manufacturing. Afterwards, the data acquisition and modelling as well as the analysis of the simulation results is explained. Concluding, the presented results and future developments are discussed.

Keywords WorkDesigner · Strain-based staffing · Age- and stress-based simulation tool · Digital transformation · Internet of things · Industry 4.0

1 Introduction

Digital Transformation, Internet of Things or Industry 4.0 are all representative terms for a new reality: the global crosslinking between humans, products and services as well as resources. This crosslinking has the potential for a great wave of

P. Gust

Engineering Design, University of Wuppertal, Gaußstr. 20, 42119 Wuppertal, Germany
e-mail: peter.gust@uni-wuppertal.de

U. Müller · N. Feller (✉) · M. Schiffmann

Laboratory for Manufacturing Systems, Cologne UAS, Betzdorfer Str. 2,
50679 Cologne, Germany
e-mail: nico.feller@th-koeln.de

U. Müller

e-mail: ulf.mueller@th-koeln.de

M. Schiffmann

e-mail: michael.schiffmann@th-koeln.de

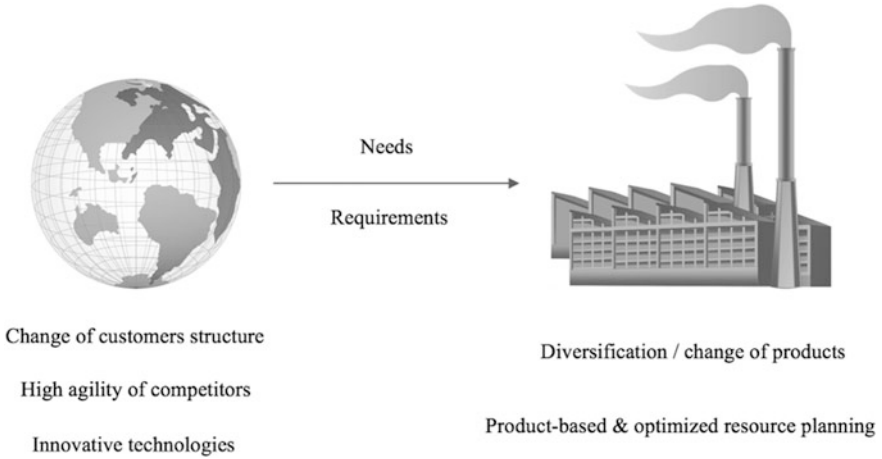


Fig. 1 Simplified overview on challenges connected to the digital transformation

innovation but is also accompanied by significant social and technological challenges (cf. [1]). Figure 1 shows a simplified overview on challenges connected to the Digital Transformation especially for small and medium-sized enterprises of industrial manufacturing.

Change of customer-structure: customers from all over the world, with different socio-cultural backgrounds require new and individualized products and services. For example, today's adolescents—the so-called digital natives—and young adults do not want to buy a car at a local dealer, they want to buy mobility via the internet (carsharing) (cf. [2]).

High agility of competitors: in accordance with the customers' purchase behavior—to buy most products via the internet—completely new markets like Asia Pacific, Sub-Saharan Africa or Middle East and North Africa open up with frequently changing competitors. As crowd funded start-ups or high tech foundations of universities, those competitors have a dramatically different speed and behavior at the market.¹

Innovative technologies: going along with the common fourth industrial revolution the half-life period of knowledge and the development cycles of innovative technologies become shorter and shorter. Agile enterprises like Google Inc. bring innovative ideas in less than six months to the market.²

The described customers' needs and changes force enterprises to diversify into new markets and to redesign their production. Future production systems no longer only have to satisfy the classic factors of success: quality, cost and time. They have to be versatile, real-time capable and network-compatible, too. The adaptation of both

¹For additional information see [3].

²See [3].

work content and responsibility is part of the integration of innovative technologies into industrial manufacturing, and leads to new work stress collectives.

In 2015 Müller et al. [4] introduced WorkDesigner, an affordable and lean simulation software application for the strain-based staffing and design of work processes, to tackle the described challenge. WorkDesigner is based on the approach established by Feller and Müller [5] using an age- and stress-based simulation model for the development and assessment of work systems for employees in industrial manufacturing. In this model employees and work places are the main parameters. Based on the specific age, sex and an absolute term for the individual's ability, the employee's physical ability level and the corresponding work ability level is determined for every discrete simulation step. Every work place is defined by five parameters (stress factors rated from excellent to deficient): lighting, climate, noise, work posture and work intensity. Considering age-related changes in the employees' abilities, all stress factors are individually weighted for every interaction between an employee and a work place. Based on the formulas provided by Feller and Müller [5] the overall stress is calculated for every work process, which leads to the determination of the employee's utilization of his or her work ability at the end (cf. [4, 6]). Overall, the aim of WorkDesigner is to answer the question: how is the staff affected by the digitalization of production?

Now, after several short-term test trails WorkDesigner is applied for the first time under real conditions in a small and medium-sized enterprise of industrial manufacturing.

2 Objective and Proceeding of the Field Study

The field study on the application on WorkDesigner is accompanied by one big question: how can the simulated predictive events be sufficiently validated? The answer is by simulating the already completed work processes for a representatively heterogeneous number of workers for defined periods (past). So the simulated daily utilization of every employee's individual work ability is correlated with employee shift specific enterprise respectively production data to validate WorkDesigner.

2.1 Indicators for Overstraining

As described by Schlick et al. [7, pp. 194 ff.] the employee's fatigue and recovery have to be balanced to avoid strong short-term or even long-lasting serious limitations of the physical ability, as well as the employee's physical and psychological health. Days absent, disease, quickly-occurring fatigue and considerably limited concentration clearly indicate an imbalance. In accordance with Schlick et al. [7, pp. 194 ff.] the following values are selected as indicators for the employee's overstraining in the field study:

- days absent/sick days,
- production failure/accident at work,
- product quality, and
- production volume.

The mentioned indicators for overstraining can easily be extracted from the ERP data: Production Data Acquisition (PDA), Quality Management (QM), Overall Equipment Efficiency (OEE), staff work time logging, etc.³

2.2 *Leading Questions*

The main target of the field study is to validate WorkDesigner as a useful and trustworthy software tool for the strain-based staffing in industrial manufacturing. In this regard the following leading questions are formulated:

- Is there a statistically significant number of workers that shows a temporal correlation of their simulated utilization of work ability and the ERP-extracted indicators for overstraining?
- How does the individual employee's relative distribution of the simulated strain and the indicators for overstraining look like?
- How accurate is the simulated occurrence probability?

2.3 *Usability in the Industrial Manufacturing*

The simulation tool WorkDesigner is realized as a software app for mobile devices with regards to the special needs of small and medium-sized enterprises for lean, intuitive and cost-saving system solutions. The preliminary drafted transformation processes play an enormous challenge especially for small and medium-sized enterprises. As job order production enterprises, small and medium-sized enterprises are confronted with frequently changing products (batch size one up to small-series production), strong competitive pressure and highly limited resources. With regards to costs and usability most common IT system solutions in the area of digital factory are not tailored to suit the needs of small and medium-sized enterprises (cf. [6]).

In this context the field study is set at Maschinenbau Lienenbrügger GmbH (LIDU) a traditional German medium-sized enterprise of industrial manufacturing

³During the field study we use EDM.Cloud by x-dms Datenmanagement Systeme, a cloud-based integral Engineering Data Management System that provides the functionality of Product Data Management (PDM), Enterprise Resource Planning (ERP), Production Planning and Control (PPC) and Manufacturing Execution System (MES).

with a production area of 3400 m², 140,000 machine hours (turning, milling, drilling, welding and steel building) and about 120 employees. LIDU is already using the ERP system EDM.Cloud since several years.

Besides the already mention leading questions, the field study is also accompanied by an additional question regarding the usability and the user experience of WorkDesigner.

3 Data Acquisition and Modeling

3.1 Consideration of the Employees' Leisure During Mid and Long Term Simulation Experiments

As it was already described by Feller and Müller [5] the middle and long term simulation of work systems is attended by a very difficult aspect, the sufficient mapping of the employees' holistic time use during the complete simulation experiment. This means night-time, leisure, weekends and vacations have to be determined and simulated, too.

Based on the time use survey by Statistisches Bundesamt [8] an employee's average weekday is designed (see Fig. 2). Considering the relative attendance of the representative test group three areas of activities are taken for a sufficient, discrete mapping of a weekday:

- personal care activities (about 44 % of the day, simulated as recovery),
- work (about 33 up to 42 % of the day, simulated in detail),
- effective leisure time (about 23 % of the day, simulated as fatigue*).

According to the time spend with work, the durations of personal care activities and of effective leisure time are both proportionately adapted during a simulation experiment.

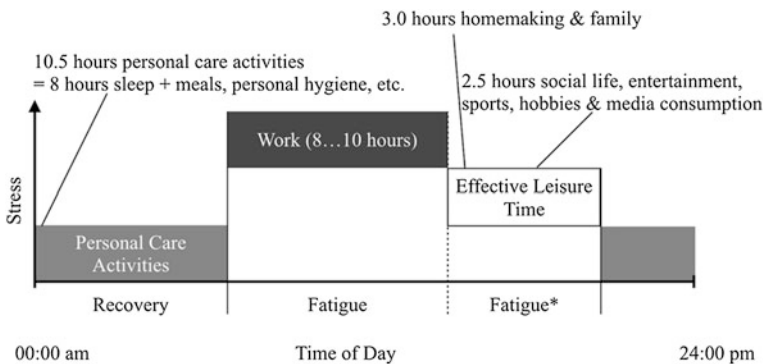


Fig. 2 Time use weekdays

Based on the calculation by Feller and Müller [5] for the individual employee's strain (cf. Formula 1) an additional equation for the strain respectively fatigue during effective leisure time is deduced (cf. Formula 2).

$$s = \begin{cases} s_i + e^{t_w \left(\frac{OS}{WAL}\right)}, & \text{Fatigue} \\ s_i e^{-t_b k}, & \text{Recovery} \end{cases}. \quad (1)$$

The basic assumption is that humans are disposed to spend about 60 % of their physical performance for work and about one third for leisure activities (cf. [9, p. 46; 7, p. 268]).

$$\Rightarrow s = s_i + e^{t_{elt} \left(\frac{0.33 PAL}{0.6 PAL}\right)}, \text{ Fatigue}^*. \quad (2)$$

This leads to a general adaptive and in this case sufficient approximation of an employee's strain during effective leisure time (Formula 3). The employee's recovery during personal care activities is still calculated by Formula 1.

$$\Rightarrow s = s_i + e^{t_{elt}(0.55)}, \text{ Fatigue}^*. \quad (3)$$

s	strain in %
s _i	strain at instant of time i
t _w	duration of work process in h
OS	overall stress in %
WAL	work ability level in %
t _b	duration of break in h
k	absolute term for individual ability
t _{elt}	duration of effective leisure time in h
PAL	physical ability level in %.

For the mapping of weekends and vacations the following assumptions are taken:

- the time use is split into about 45 % personal care activities and 55 % effective leisure time,⁴
- during effective leisure time there is a healthy balance between fatigue and recovery (neutral utilization),
- a potential overload from the earlier week respectively work period is successively reduced day by day.

This leads to formula 4 for the determination of the employee's strain during weekends and vacations:

⁴Referring to this additional time use surveys were consulted such as [10]. It has to be mentioned that there are huge variations with recreational activities depending on the country, the socio-cultural background and the age group.

$$s = \begin{cases} s_i + 0, & \text{Effective Leisure Time (Fatigue)} \\ s_i e^{-t_{pca} k}, & \text{Personal Care Activities (Recovery)} \end{cases} \quad (4)$$

t_{pca} duration of personal care activities in h.

The simulator of WorkDesigner is extended with the introduced formulas.

3.2 Setup of the Field Study on WorkDesigner

Methodology In the range of this field study the completed work processes of two heterogeneous groups of workers are simulated for the past twelve month. One group is recruited from the metal-cutting section's staff, the other group is collected from the welding and steel building section's workforce. Both sections have separate production halls and different environmental conditions.

Compared to the welding and steel building section's work processes, the work processes of the metal-cutting section are classified as less physically stressing with regards to the stress factors work posture and work intensity. But work processes in the metal-cutting section are usually timed by the machinery's program cycle times so the employees are less self-determined and more mentally stressed.

The described methodology makes it possible to prove the general usability of WorkDesigner in the area of industrial manufacturing as well as it gives the ability to assess the deviation of the simulation results caused by unconsidered psychological stress factors.

Subjects Each group of workers consists of ten test persons. The subjects of both groups are collocated from male and female employees under 20 years, from 21 up to 30 years and older than 30 years. The collection is based on three assumptions about the human performance:

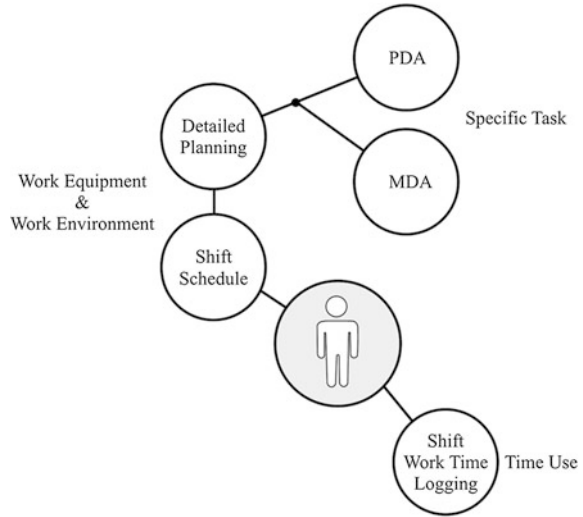
- the individual employee's physical ability (PAL) and the dependent work ability (WAL) grows up to an age of about 20 years,
- at an age of 21 years first physical changes begin like the decrease of the oxygen uptake ability or the regression of the visual ability,
- the continuous decrease of PAL and the dependent WAL starts at an age of about 30 years.

The described changes of human performance are explained in detail by Feller and Müller [5]. As preliminarily mentioned, WorkDesigner takes the age associated changes of PAL and WAL under consideration.

The staff and the work council are informed about the aim and procedure of the field study. The participation is optional. The recorded individual employee's data (age, sex and individual ability/fitness) are made anonymous.

Work Systems Figure 3 shows the crosslinking of EDM.Cloud data to enable the reconstruction of every subject's work systems (specific task/duration, work equipment and work environment) of the past twelve month.

Fig. 3 Schema of work system data acquisition



The shift work time logging provides the individual employee's holistic time use, i.e.: time at work, breaks, overtime, weekends, vacations, days absent/sick days. The shift schedule enables the unambiguous assignment of the subjects, their work equipment and work environment. The detailed planning makes it possible to link the work equipment, work environment and the specific task via the particular job order. Finally, job order related events like setting, reworking, service, etc. collected by PDA and MDA facilitate the detailed mapping of all work systems involved in this field study.

4 Analysis of the Simulation Results

Figure 4 shows examples for the analysis of the simulation results.

The upper left corner indicates the analytical tool OEE (Overall Equipment Efficiency) of MDE-DNC.Net which provides a graphical overview of the performance, capacity and quality of job orders produced with a selected machine and for a picked period of time. The upper right corner shows the MDA and PDA message tool of MDE-DNC.Net. It gives a graphical survey of all machine- and production-specific events for selected machines during a chosen period of time (compare Fig. 3).⁵

⁵MDE-DNC.Net is a stand alone system for machine data acquisition (MDA), production data acquisition (PDA) and machine monitoring (DNC) by MDE-DNC.Net/Smart Factory B.V. It is the link between enterprise-specific data and manufacturing-specific data.

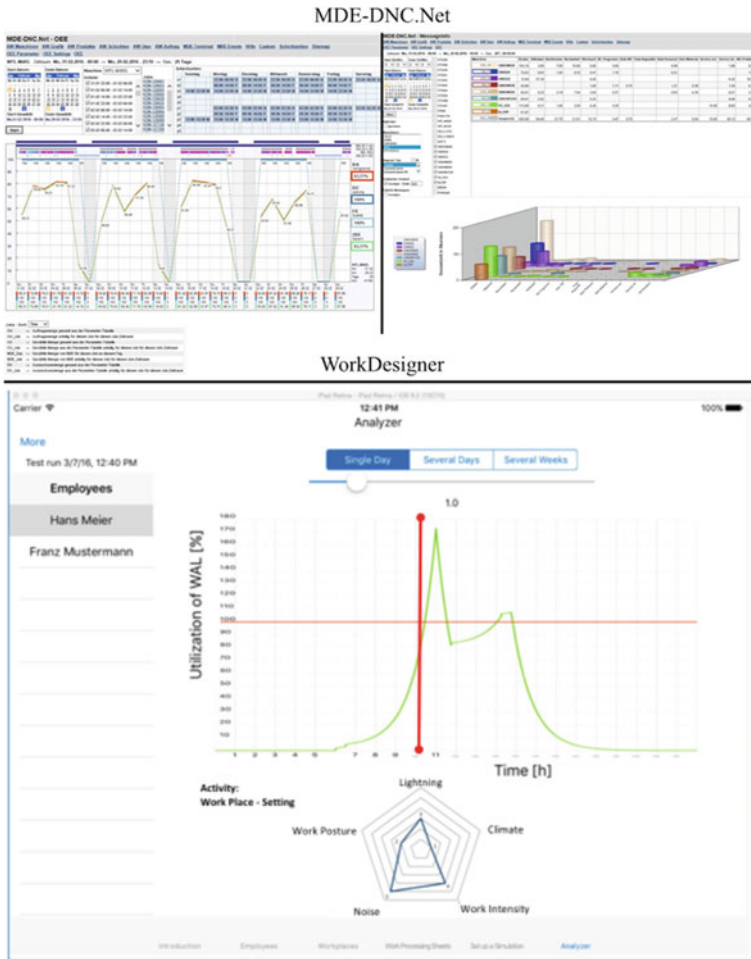


Fig. 4 Analysis tools: MDE.DNC.Net and WorkDesigner (cf. [11])

The lower part of Fig. 4 indicates WorkDesigner’s analysis tool. It provides two stacked charts for every simulated employee. The upper one displays the utilization of the individual employee’s WAL on the y-axis and the simulated period of time on the x-axis. The time resolution can be varied between a single day, several days or several weeks. The lower one gives a detailed view on the weighted stress factors at any selected instant of time (red ruler).

So the simulation results and the existing ERP data can easily be compared as described in Sect. 2.1.

5 Discussion

After the general functionality of WorkDesigner has already been proven in several short-term test trails in 2015, the simulation-based software tool for the strain-based staffing in industrial manufacturing is currently used for the first time in the real production of a medium-sized enterprise (LIDU). As described in this article three essential challenges accompany the field study on the application of WorkDesigner. First, the validation of the simulated predictive events, which is shown in chapter two. The solution is the simulation of already completed work processes for a heterogeneous group of workers and the comparison of the simulation results with the ERP data history. Second, the mapping of the employees' leisure time during the simulation experiment(s). For this purpose, new formulas for the calculation of the employees' fatigue and recovery during leisure, weekends and vacations are introduced in chapter three. Third, the data acquisition and detailed modeling of work systems. Chapter three delineates how the crosslinking of ERP data for the holistic depiction of every activities of the employees can be achieved.

Analytical tools for the investigation of the simulation results are presented in Chap. 4.

The field study is still in progress. So the results will be published soon.

References

1. Steinbrunn, M., Bubner, N.: IT-Strategien in Zeiten der Digitalen Transformation. Detecon Update, Digital Business News. Detecon Consulting GmbH, GER (2015)
2. Becker, D., Pawelke, M.: Blechbieger oder Grid Master? Die Automobilindustrie an der Weggabelung in ein hochdigitalisiertes Zeitalter. KPMG AUTOMOTIVE, Trendanalyse 2015. KPMG AG, GER (2015)
3. Kusch, T., Deprez, F., Nebendahl, J.: Transformation and Peoplemanagement. Detecon Management Report. Detecon International GmbH, Köln (2015)
4. Müller, U., Gust, P., Feller, N., Schiffmann, M.: WorkDesigner: consulting application software for the strain-based staffing and design of work processes. *Procedia Manufact.* **3**, 379–386 (2015)
5. Feller, N., Müller, U.: Development and assessment of work systems for elder employees in industrial manufacturing. In: Trzcielinski, S., Karwowski, W. (eds.) *Advances in the Ergonomics in Manufacturing, Managing the Enterprise of the Future*, pp. 140–151. AHFE Conference ©, USA (2014)
6. Müller, U., Gust, P., Feller, N., Schiffmann, M.: Simulationstool zur alters- und belastungsorientierten Entwicklung und Bewertung von Arbeitssystemen in der industriellen Fertigung. In: Rabe, M., Clausen, U. (eds.) *Simulation in Production and Logistics 2015*, pp. 469–480. Fraunhofer IRB Verlag, Stuttgart (2015)
7. Schlick, C., Bruder, R., Luczak, H.: *Arbeitswissenschaft*. Springer, Berlin (2010)
8. Bundesamt, Statistisches: *Zeitverwendungserhebung, Aktivitäten in Stunden und Minuten für ausgewählte Personengruppen 2012/2013*. Statistisches Bundesamt, Wiesbaden (2015)
9. Bullinger, H.-J.: *Ergonomie, Produkt- und Arbeitsplatzgestaltung*. Teubner, Stuttgart (1994)
10. American Time Use Survey 2014, Bureau of Labor Statistics, U.S. Department of Labor. <http://www.bls.gov/news.release/pdf/atus.pdf> (4 Mar 2016)
11. MDE-DNC.Net. <http://www.mde-dnc.net> (7 Mar 2016)

A Quantitative Comparison of Operator Field of View for Vehicle Design

M.D. King, Jeffrey Jinkerson, Teena Garrison, Derek Irby
and Daniel W. Carruth

Abstract This paper outlines the preliminary application of a quantitative method for assessing field of view using spherical projections of categorical visual information overlaid by occlusion maps based on vehicle geometry. The project goal was to quantitatively assess not only *where* a vehicle operator can see but *what* visual information is available in the operator's field of view. By creating a driving environment dataset coded for visual information, we can indicate the probability of a type of visual information appearing in the operator's field of view in a given vehicle. Next, we overlay probability maps with vehicle and operator eye height-specific occlusion maps, giving us a quantitative representation of visible information. This method was applied to three vehicles: a midsized sedan, a light-duty pickup truck, and a full-sized pickup truck using eye heights corresponding to those of 5th percentile females, 50th percentile females, 50th percentile males, and 95th percentile males.

Keywords Field of view · Driving · Vehicle design

1 Introduction

A key aspect of task performance when operating a vehicle is the ability of the occupant to sense task-relevant visual information in the driving environment. Current methods for quantitatively evaluating field of view in manned ground vehicles allow researchers to assess where operators are likely to look and where

M.D. King (✉) · J. Jinkerson · T. Garrison · D. Irby · D.W. Carruth
Center for Advanced Vehicular Systems, Mississippi State University,
Starkville, MS, USA
e-mail: mdk106@msstate.edu

T. Garrison
e-mail: teenag@cavs.msstate.edu

D.W. Carruth
e-mail: dwc2@cavs.msstate.edu

they are able to see [1, 2]. Recent techniques for evaluation of field of view for manned ground vehicles include the spherical projection of Ray and Teizer [3] and the masking technique of Bostelman et al. [4]. Ray and Teizer’s technique presented an automated method for calculating blind spots in construction vehicles. To do this, the cabin or the exterior of the construction equipment was scanned. From these scans, they created a point cloud representation of the equipment, resulting in a map for measuring blind spots. Bostelman et al. developed a masking technique in which they manually masked digital panoramas in a photo editor, giving a representation of what can be seen from the given eye height position. In addition to using scans of vehicles, CAD models can be used for evaluation of field of view [1, 2].

It is intuitive to assume that the less visual information occluded by vehicle geometry, the better able to safely and effectively operate a vehicle one will be. However, this does not account for where in the field of view task-relevant visual information will appear. Using their volumetric technique, Cook et al. demonstrated that a line of cyclists could easily be obscured in a certain location near a commercial vehicle [5]. This type of additional test of whether critical visual information is occluded by vehicle geometry is necessary as a vehicle design with quantitatively greater field of view as determined by analysis of a spherical or cylindrical projection may not be safer or more effective if what is visible is irrelevant to the operator’s task.

In this paper, we present an initial application of a proposed method for evaluating the occlusion of task-relevant visual information. The authors are unaware of other methods for quantitatively determining the likelihood that general task-relevant visual information will be visible or occluded by vehicle geometry. We have addressed this by creating probability maps of specific categories of visual information for comparison with maps of the occlusion of the visual field by vehicle geometry.

2 Methods

2.1 *Task-Specific Visual Information*

As previously mentioned, one of the primary goals of this project was the development of a quantitative method for assessing the probability that certain task-specific visual information would appear in the driving environment and where in the operator’s field of view that information would likely be present. To address this need, we created a driving environment database using 360°, panoramic, static images. Locations were sampled using GIS software that randomly selected latitude and longitude points within the boundaries of the top 25 most populous cities in the continental United States as defined by US census shapefiles [6]. Images for selected locations were acquired from an online mapping service.

Once acquired, these images were individually coded using digital editing software for the appearance of eight visual information categories relevant to

various ground vehicle operator tasks. The current analysis addresses only three of the eight layers: roadway surfaces, navigation signs, and road side vehicles. The roadway surfaces layer includes drivable roadway surfaces (paved or otherwise). It does not include driveways, parking lots, or other drivable surfaces. The navigation sign layer include all indicators of appropriate traffic behavior visible to the driver. These include, but are not limited to speed limit signs, stop signs, traffic cones, and traffic lights. Road side vehicles include all vehicles stopped on or near roadways and certain areas that they may appear: parked cars, parking lots, driveways, and other vehicle entrances to non-roadway areas.

2.2 Occlusion Maps

As mentioned briefly in Sect. 1, Bostelman et al. developed a physical method for creating panoramic occlusion maps [4]. Using “a standard Red, Green, Blue (RGB) camera and a motorized camera mount,” they obtained images from the driver’s perspective in construction equipment, stitched the images into panoramas, and then manually masked the appropriate regions of the stitched panoramas. Our own researchers mounted a smartphone on a tripod situated at approximate eye points for various vehicles and collected panoramic images using a commercially available application. The portions of the vehicles obscuring the outside environment in the flattened versions of these panoramas were then manually masked. In this way, we were able to create occlusion maps of physical vehicles to compare to our digital models.

Möller and Trumbore [7] developed an algorithm for determining the intersection of rays and triangles. Lagae and Dutré [8] built upon this foundation to develop an efficient test for the intersection of rays and convex quadrilaterals which determines whether intersections exist at all before trying to determine their precise locations. In order to create digital occlusion maps, we employed a modified version of the raytracing method on vehicle models with triangular meshes and a modified version of the methods on vehicle models with quadrilateral meshes [7, 8]. By sending rays from approximate eye locations, we were thus able to render fields of view as spherical projections. When flattened, the images on these spheres became our digital occlusion maps. Figure 1 depicts a digitally rendered occlusion map for an artist’s recreation of a manned ground vehicle.

At this point, our analysis is roughly equivalent to [2]. We can calculate the percentage of the field of view that is visible or occluded by the vehicle geometry. However, as pointed out previously, this analysis treats the entire potential visual field equally and does not address where task-relevant visual information is more or less likely to appear.

Vehicles We selected three vehicles representative of commercially available vehicle classes: a full size pickup, a light-duty pickup, and a midsize sedan. We acquired 3D artist representations of vehicles with geometry based on scan data.

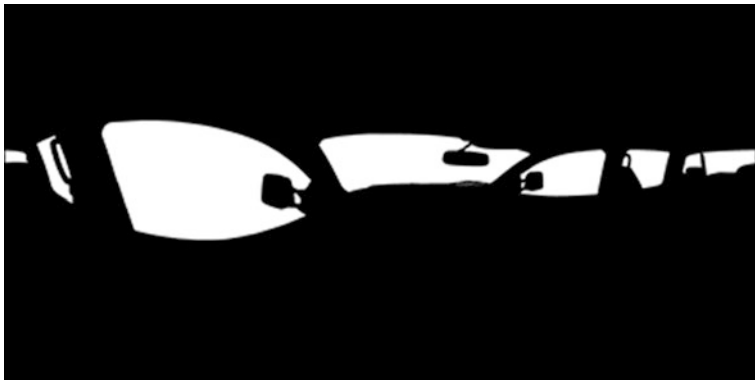


Fig. 1 Example of digitally rendered panoramic occlusion

Our primary calculations of field of view are based on the 3D digital models of these vehicles (see Fig. 2). As described previously, we assessed the validity of the selected digital models, by ensuring that the artistic renderings were accurate in scale and design by comparing them to published vehicle dimensions and comparing with physical vehicles using the masking technique of [4].

Occupants Using SAE anthropometric standards, we calculated approximate eye points for 5th percentile female, 50th percentile female, 50th percentile male and 95th percentile male. These eye heights were chosen to give a range of possible eye heights from small to large. Vehicle reference points (Ball of Foot Reference Point [BOFRP], Seating Reference Point [SgRP], Accelerator Heel Point [AHP], and derived variables [L1, L6, H8, H30, and W20]) were estimated using a simulated H-point device placed relative to the driver's seat of the 3D model. β was set to the default estimated value of 12.0.



Fig. 2 Rendering of the three 3D models selected for the current study

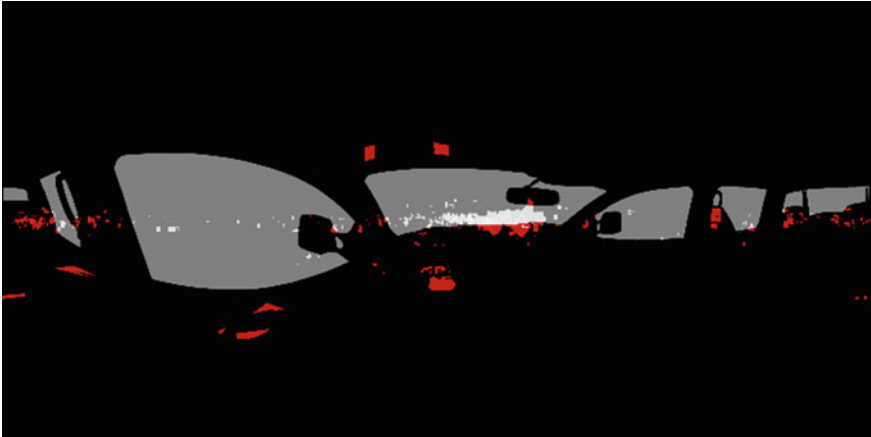


Fig. 3 Visualization of an overlay of occlusion map for the full sized pickup truck on the navigation sign. *Red* indicates occluded information. *White* indicates visible information

2.3 Figures

In the next step of our analysis, we overlay the coded visual information maps from our driving environment dataset with the generated vehicle occlusion maps. Figure 3 provides a visual representation of this overlay. Visual inspection of the overlay provides an impression of the quantity of visual information occluded and by what vehicle geometry.

A quantitative assessment of the quality of the field of view for specific task-relevant information can be calculated by determining the percentage of available visual information that is not occluded by the vehicle geometry. We calculated the percentage of visual information available for the three vehicles (full-size pickup, light-duty pick-up, and four-door sedan) at each eye point (5 % female, 50 % female, 50 % male, 95 % male) for each map of task-relevant visual information (roadway surfaces, navigation signs, and roadside vehicles).

3 Results

The analysis of visibility of roadway surfaces reveals that a very small percentage (0.5–4.5 %) of the total potentially visible roadway surface is not occluded by the vehicle geometry (see Fig. 4). This is not surprising considering that our current analysis evaluates the field of view as a sphere surrounding the operator. While the total potential visible information may be larger than necessary for the current case, the analysis reveals relative differences in visibility not related to the fact that most of the roadway surface is beneath the vehicle. The visibility of roadway surface to

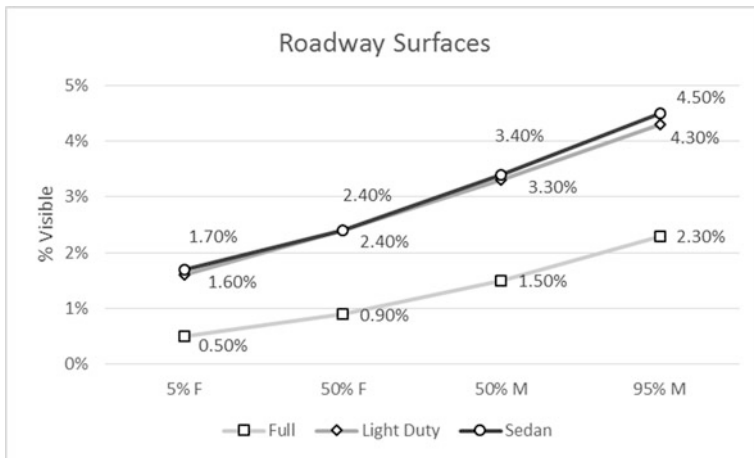


Fig. 4 Comparison of visibility of roadway surfaces by vehicle and eye height

operators of the full size pickup truck (0.5–2.3 %) is approximately 1/3 to 1/2 of the visibility for the pickup truck (1.6–4.3 %) and the sedan (1.7–4.5 %) depending on the height of the operator. Roadway surface visibility increases almost linearly with height. There appears to be no difference in visibility between the light-duty pickup and the sedan.

The visibility of navigation signs for an operator of the full size pickup truck ranges from 23 to 32 % (see Fig. 5). Navigation sign visibility increases almost linearly with height for the full size pickup truck operator. However, while visibility of navigation signs for an operator of both the light-duty pickup truck and sedan are

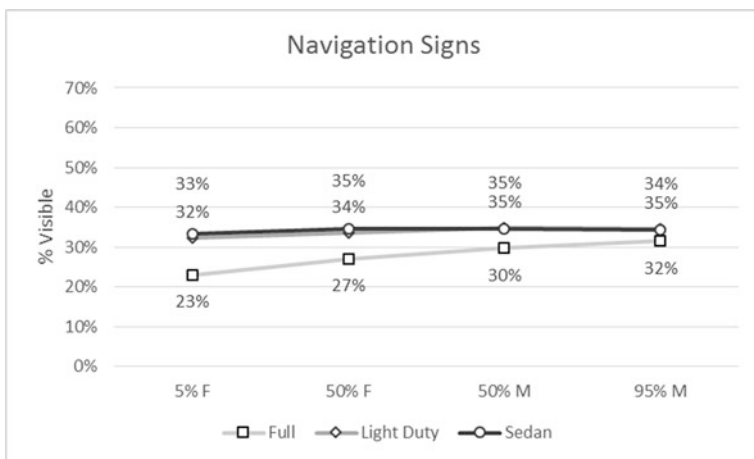


Fig. 5 Comparison of visibility of roadside vehicles by vehicle and eye height

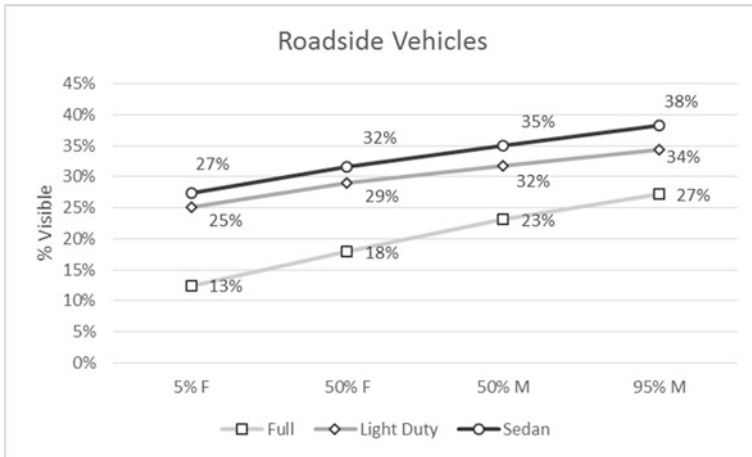


Fig. 6 Comparison of visibility of roadside vehicles by vehicle and eye height

higher than visibility from the full size pickup, visibility does not increase with height.

The visibility of roadside vehicles has a similar profile to the visibility of roadway surfaces (see Fig. 6). Visibility increases linearly with occupant height for all three vehicles. The full-size pickup truck again has the lowest visibility (13–27 %) of the vehicles. However, unlike the visibility of navigation signs and roadway surfaces, the light-duty pickup truck demonstrates consistently lower visibility of roadside vehicles compared to the sedan.

4 Conclusions

This initial analysis indicates relatively poorer performance of a full size pickup truck than a light-duty pickup truck and a sedan. Visibility from the full size pickup truck consistently increases as the height of the operator increases. Flat, superior visibility, as seen for the light-duty pickup truck and sedan for navigation signs, may indicate superior vehicle design to accommodate occupants of varying heights.

The current analysis assessed visibility for three types of visual information. The value of multiple visual information maps is dependent on differences existing in the distribution of task-relevant visual information across the field of view. As demonstrated here, while the relative visibility from the three vehicles was similar across all three maps, there are sufficient differences between the three selected information maps to reveal potentially meaningful differences in the vehicle designs.

The results of the application of this preliminary method demonstrated an extended quantitative analysis of what task-relevant visual information is occluded

by vehicle geometry. The analysis demonstrates differences in field of view across three vehicle models representative of commercially available equipment. The quantitative and task-specific nature of the analysis will allow the analysis tool, following additional development, to provide insights into the impact of vehicle design decisions on the vehicle operator's ability to perceive critical visual information.

4.1 *Limitations*

Because this is a preliminary application of a new method, there are several limitations worth noting and addressing in future research. One significant issue in our analysis is the need to determine an appropriate field of view for analysis. While the analysis of visibility of roadway surfaces allows a comparison of relative performance across the three vehicles, it is difficult to interpret actual visibility of visual information due to the inclusion of visual information that can reasonably be expected to be occluded in all vehicles (i.e., the road beneath the vehicle). This also applies to the inclusion of portions of the sky above the vehicle that, while potentially visible through a sunroof, are unlikely to be the source of visual information critical to the operator's task. However, there are potentially cases where these areas of the field of view are critically relevant. For example, forklift or crane operation may benefit from visibility of overhead portions of the field of view. Similarly, the current analysis does not account for the normal, forward-facing orientation of the human head and weighs visual information available from the side and rear windows as having the same relevance as information available from the front. We expect our next steps in developing this tool will include determining appropriate areas of analysis and providing a method for defining those areas.

An additional concern is the impact of the source of our driving environment database. The cameras used to capture the panoramic source images are not located at eye height and we do not have 3D data associated with the images. In practice, the result is that the visual information maps do not perfectly reflect the location of visual information for a vehicle operator. Future work will be necessary to determine the impact of the difference in camera height and operator height and to determine potential methods for adjusting the results.

Also related to the driving environment database is the time investment necessary to construct the data sets. Many hours were spent manually coding panoramic images of randomly selected locations for the categories of visual information of interest. Generating databases of additional locations or different categories of visual information will require significant investments of time. We are currently undertaking generation of an extended number of datasets and assessing potential for generating representative datasets through simulation.

Acknowledgments Effort sponsored by the Engineering Research and Development Center under Cooperative Agreement number W912HZ-15-2-0004. The views and conclusions contained herein are those of the authors and should not be interpreted as necessarily representing the official policies or endorsements, either expressed or implied, of the Engineering Research and Development Center or the U.S. Government. The authors would also like to acknowledge the invaluable efforts of Patience Judy and Maverick Smith for their many hours of assistance manually coding the images in the driving environment database.

References

1. RAMSIS Cognitive, http://www.human-solutions.com/mobility/front_content.php?idcat=325
2. Marshall, R., Summerskill, S., Cook, S.: Development of a volumetric projection technique for the digital evaluation of field of view. *Ergonomics* **56**(9), 1437–1450 (2013)
3. Ray, S., Teizer, J.: Computing 3D blind spots of construction equipment: implementation and evaluation of an automated measurement and visualization method utilizing range point cloud data. *Autom. Constr.* **36**, 95–107 (2013)
4. Bostelman, R., Teizer, J., Ray, S., Agronin, M., Albanese, D.: Methods for improving visibility measurement standards of powered industrial vehicles. *Saf. Sci.* **62**, 257–270 (2014)
5. Cook, S., Summerskill, S., Marshall, R., Richardson, J., Lawton, C., Grant, R., . . . , Clemo, K.: The development of improvements to drivers' direct and indirect vision from vehicles—Phase 2. Technical Report, Loughborough University (2011)
6. TIGER/Line Shapefile, 2013, 2010 nation, U.S., 2010 Census Urban Area National, http://www2.census.gov/geo/tiger/TIGER2013/UAC10/tl_2013_us_uac10.zip
7. Moller, R., Trumbore, B.: Fast, minimum storage ray-triangle intersection. *J. Graphics Tools* **2**(1), 21–28 (1997)
8. Lagae, A., Dutre, P.: An efficient ray-quadrilateral intersection test. *J. Graph. GPU Game Tools* **10**(4), 23–32 (2005)

An Integrated Computational Simulation System for Injury Assessment

Sultan Sultan, Karim Abdel-Malek, Jasbir Arora, Rajan Bhatt and Tim Marler

Abstract Injury prediction and prevention are subject areas that will significantly benefit from the use of digital human models (DHMs). The subject of this research is to investigate human simulation to predict injuries. This work over the past few years seeks to integrate high-fidelity computational methods for stress/strain analysis, namely finite element analysis (FEA) with biomechanics predictions through DHMS to yield measures (indices) for the propensity for injury. Indeed, a multi-scale FEA model using continuum-mechanics-based theories was developed in order to obtain highly accurate simulations of the segmental stress fields during a specific task. Previous work by this group is a simulation environment called Santos™ that enables the prediction of human motion including all aspects of its biomechanics. The Santos environment provides a joint- on physics-based, predictive capability including a muscle model. While FEA models are certainly useful as independent tools, their benefits can be fully realized when they are integrated with a complete system-level human model. This integration essentially connects the local model to a virtual environment, whereby the DHM model yields the muscle forces and motion profiles (i.e., the kinematics of the motion across time for each degree-of-freedom for the body). These motion profiles and muscle forces are calculated for each task and are used as input for the multi-scale FEA model. The results of the FEA model executed across a statistically viable set of data is fed into a neural network for learning and evaluating a pre-determined injury index measure that was developed by this group. This paper presents the initial promising results for this integrated multi-scale approach to quantify and predict injury in a particular joint that is undergoing a specific motion. The joint injury index system is developed based on the yield stress of the joint components. The injury index includes both the bone and soft tissue structures of the joint where bone was modeled as elastic material and the soft tissue was modeled as hyper-elastic material with the

S. Sultan (✉) · K. Abdel-Malek · J. Arora · R. Bhatt
Virtual Soldier Research (VSR) Program, Center for Computer Aided Design (CCAD),
The University of Iowa, Iowa City, IA, USA
e-mail: asultan@engineering.uiowa.edu

T. Marler
RAND Corporation, Santa Monica, CA, USA

Noe-Hookean method. This integrated system allows one to study the effects of various motions and task-parameters on knee joints so as to modify tasks, save analysis time, and reduce the likelihood of injury.

Keywords Digital human modeling · Multi-scale modeling · FEA modeling · Injury prevention · Neural network

1 Introduction

Joint injuries such as sprains occur with an estimated frequency of one injury per 10,000 people per day, amounting to about 27,000 injuries each day in the United States [1, 2]. The sprained ankle and knee remain the most common injuries.

The impact of injuries is the loss of manpower, increased healthcare costs, and disabilities and fatalities. Injuries have caused 47–57 % of all deaths, 22–63 % of all disabilities, and 22–31 % of all hospitalizations in all services (Army, Navy, Marine Corps, Air Force) [3]. Lower extremity overuse injuries resulted in over 3 million days of limited duty in 2004 for the DoD [3]. Musculoskeletal injuries include problems in muscles, tendons, ligaments, and bone tissue. The injuries may result from high stress (overuse) and potentially advance into chronic conditions [4]. Eighty-two percent of the total injuries reported in the military in 2006 were related to musculoskeletal conditions; 22 % of those were due to knee injuries, and 13 % were due to ankle injuries [5]. Danny and Hollingsworth [6] reported that the most commonly injured body region was the knee, followed by the lower back and ankle. The overall injury problem in the U.S. Army results in about half the deaths, three-fourths of the disability cases, and one-fifth of the hospitalizations [7]. About 80 % of musculoskeletal injuries include bone stress reactions and stress fractures located in the lower extremities [7].

Sultan and Marler [8] introduced a simple multi-scale model for predicting knee joint injury based on static analysis involving joint torque and external ground reaction forces predicted by the DHM Santos. Sultan and Marler [2] also presented a multi-scale model for predicting knee and ankle joint injury based on analysis involving motion data and external ground reaction forces predicted by the DHM Santos in conjunction with muscle force computation by OpenSim software.

The present work provides a multi-scale model to introduce a scale to measure joint injury by considering both the soft tissues and bones in the joint. The measuring system has the ability to quantitatively assess the joint injury. The importance of the proposed system is that it offers a new approach for predicting a quantitative scale of the risk of injury, which can indicate the proper action for prevention.

2 Method

2.1 Santos DHM Dynamic Prediction

Santos is built on a biomechanically accurate musculoskeletal model with 109 predicted degrees of freedom (DOFs) [9]. There is one joint angle for each DOF, and the relationship between the joint angles and the position of points on the series of links (or on the actual avatar) is defined using the Denavit-Hartenberg (DH) notation [10]. Predicting posture while considering external loads is discussed in detail by Liu et al. [11] and Marler et al. [12, 13]. In this study, Santos predicts the motion of land-markers in the form of x-y-z positions and three components of ground reaction force for walking and stair-ascending tasks in four different loading cases: with no backpack, with a 10 kg backpack, with a 17 kg backpack, and with a 33 kg backpack, as shown in Fig. 1. The predicted data for the two tasks (walking and stair ascending) are then exported to OpenSim.

2.2 OpenSim Muscle Force Computation

Predicted data (motion and GRF data) from Santos are fed to OpenSim to compute muscle forces along the tendon direction. In OpenSim, many computational processes are conducted, including model scaling, inverse kinematics, the reduction residual algorithm (RRA), computation of muscle control (CMC), and the analysis process to compute muscle force along the tendon direction. A program is then used to compute the direction of muscle forces with respect to the skeleton.



Fig. 1 Santos with **a** no backpack, **b** 10 kg backpack, **c** 17 kg backpack, **d** 33 kg backpack

2.3 Knee Muscle Analysis

The main active muscles that articulate the knee joint are the rectus femoris (rec-fem), vastus intermediate (vas-int), sartorius (sar), gracilis (grac), biceps femoris short head (bifemsh), biceps femoris long head (bifemlh), and tensor of faciae latae (tfl). The details of muscle forces are illustrated in Fig. 8a in Appendix 1. The muscles that articulate the ankle joint are the soleus (sols), gastrocnemius (med-gas), tibialis anterior (tib-ant), and tibialis posterior (tib-post). A program is used to compute the direction of muscle forces with respect to the skeleton as well as the compression and shear forces acting on the ankle and knee joints. The ground reaction force (GRF) is used in addition to muscle forces to compute compression and shear force. The direction of the compression is normal to the cross-section of the tibia bone, whereas the direction of the shear force is in the plane of the cross-section of the tibia bone. The compression (\mathbf{K}_{comp}) and shear (\mathbf{K}_{shear}) forces acting on the knee joint are computed as shown in Eqs. 1 and 2. Details of all equations are illustrated in Appendix 1 and Fig. 8a [2].

$$\mathbf{K}_{comp} = \mathbf{A}_{comp} + \mathbf{M}_{comp} \quad (1)$$

$$\mathbf{K}_{shear} = \mathbf{A}_{shear} + \mathbf{M}_{shear} \quad (2)$$

where

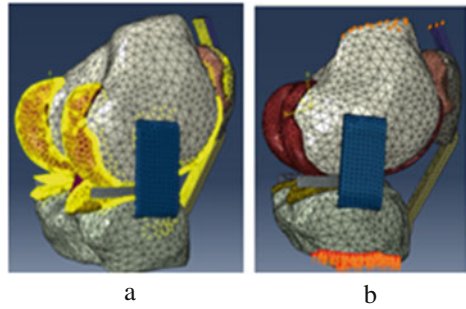
$\mathbf{A}_{comp}, \mathbf{A}_{shear}$ are the compression and shear components of the ankle, respectively
 $\mathbf{K}_{comp}, \mathbf{K}_{shear}$ are the compression and shear components of the knee, respectively
 $\mathbf{M}_{comp}, \mathbf{M}_{shear}$ are the compression and shear components of the muscles in the knee joints, respectively

2.4 Knee FEA Model

A 3D model in IGES format for the knee joint was provided by the Department of Orthopaedics at the University of Iowa. The IGES format model was then exported to Abaqus 6.13 for meshing and analysis. All ligaments and menisci were represented with very basic models in Abaqus 6.13, and knee components were then assembled to form a complete knee joint model. All joint components were meshed using the tetrahedron element (C3D4). Bone was modeled as elastic material, and soft tissue was modeled as hyper-elastic material with the Noe-Hookean method [2].

Contact problems were developed for three pairs of components. In the knee joint model, the first pair included the contact between the femur cartilage and the patella cartilage, the second between the femur cartilage and the tibia cartilage, and the third between the femur cartilage and the menisci, as shown in Fig. 2a. The

Fig. 2 Knee model, **a** contact surfaces, **b** loading



loadings for the knee joint were distributed pressure on the cross-section area and shear force per unit area as shown in Fig. 2b. The coefficient of friction for contact problems was 0.01.

3 Injury Prediction and Assessment

The automated process for predicted injury index proceeds as follows. A user works within the Santos software environment. As the user conducts analyses using dynamic prediction, he or she selects an option for high-fidelity analysis. The motion land-markers' xyz positions and GRF data are then exported to OpenSim to compute muscle forces.

A program to compute both compression and shear force acting on the joint is used. The joint compression and shear force are exported to the FEA model and automatically imposed as boundary conditions. The FEA model is then run. Currently, a set of 20 finite pre-set joint angles (starting with 0° and ending with 95° in increments of 5°) are used for the knee FEA analysis. The current joint component stresses resulting from the FEA model for a few selected frames of the task cycle are fed to a neural network program (NNT) to produce a regressed stress data that covers the whole task cycle and are consequently compared with the component yield stresses to compute the injury index. The prediction process is illustrated in Fig. 3.

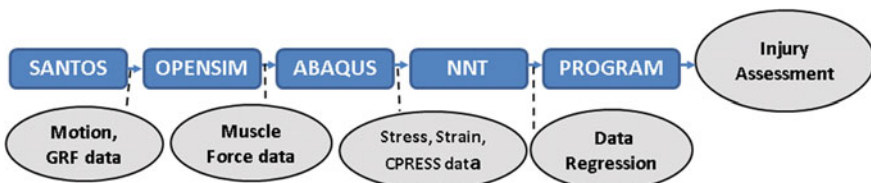


Fig. 3 Integrated injury prediction model

The parameter dictating the likelihood of knee injury of this study is the stresses of all the joint components computed as a result of compressive and shear loading during normal walking and stair-ascending tasks.

4 Results and Discussion

After computing the current stress values of the components of the joint for a few selected frames distributed over the task cycle, the data is fed to an NNT program. The NNT program creates a regression process to produce the stress values for all frames over the whole task cycle. Another computational program is used to compare the current stress values with those of the yield values. In this sense, a quantitative values range from (<1) to (≥ 1) is used. The yield criteria used here is the component maximum Von Mises stresses [14]. The present study used same injury prediction algorithm used by Sultan and Marler [2] and shown in Fig. 8b in Appendix 1. If the current maximum stress value for that component of the joint is less than the yield value during the task (<1), the status of the joint is likely to be healthy. If the current maximum stress value is equal to or higher than the yield stress (≥ 1), the status of the joint is likely to be risky. Certainly, as the load on the joint increases, the risk of injury increases.

The maximum injury index values of 0.455, 0.463, 0.497, and 0.521 were found in the tibia bone of the right knee joint at 71.6 % of the walking cycle for four loading cases, respectively, as presented in Table 2 in Appendix 2. For the same joint under the same conditions and cases in the walking task, the minimum injury index value of less than 0.0001 was found in the patella cartilage.

For the stair-ascending task under the same loading cases for the right knee, values of the maximum injury index of 0.455, 0.476, 0.490, and 0.515 at 66.4 % of the task cycle were also found in the tibia bone, as presented in Table 2 in Appendix 2. The smallest index values were less than 0.0001 in the patella cartilage. In all loading cases, the bone tissue of the tibia has the highest stress for both walking and stair ascending, whereas the soft tissue of the patella cartilage has the lowest stress value. A comparison of the injury index values of all components for the right knee joint in the walking and stair-ascending tasks for 17 kg backpack loading is shown in Figs. 4 and 5, respectively. It was evident in Fig. 6 that the maximum injury index value of the tibia bone of the right knee during walking increased by 1.75 % for 10 kg backpack loading, by 9.23 % for 17 kg backpack loading, and by 14.51 % for 33 kg backpack loading compared to that of no backpack loading. The maximum injury index value for soft tissue in the right knee during the walking task occurred in the lateral meniscus as shown in Fig. 4. In the stair-ascending task, it occurred in the medial meniscus as shown in Fig. 5. Details of the maximum injury index for the lateral meniscus of the right knee in the walking task under different loading cases are provided in Table 3 in Appendix 2. Table 3 in Appendix 2 shows that no increase occurred in the maximum injury index value for the tibia bone and the lateral meniscus due to different loadings at

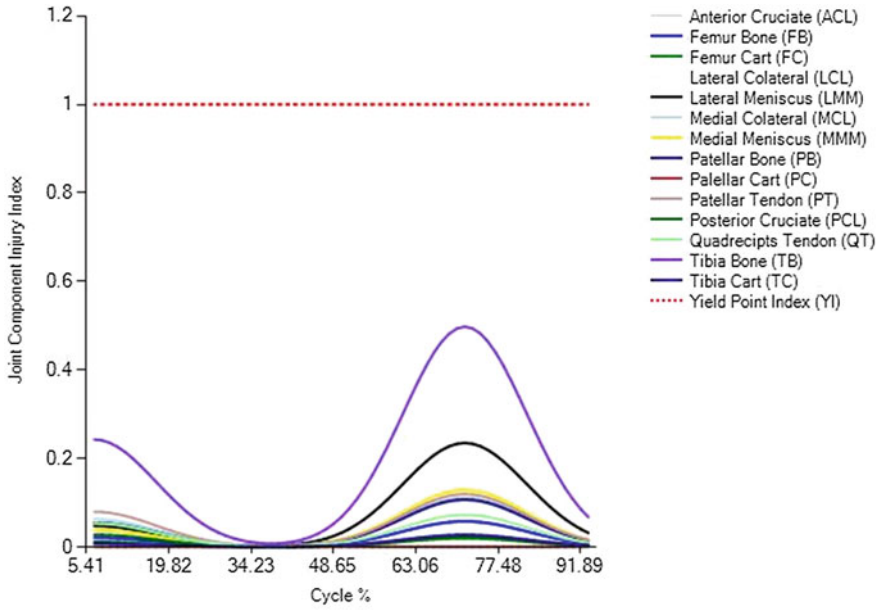


Fig. 4 Right knee components injury index in walking with 17 kg backpack

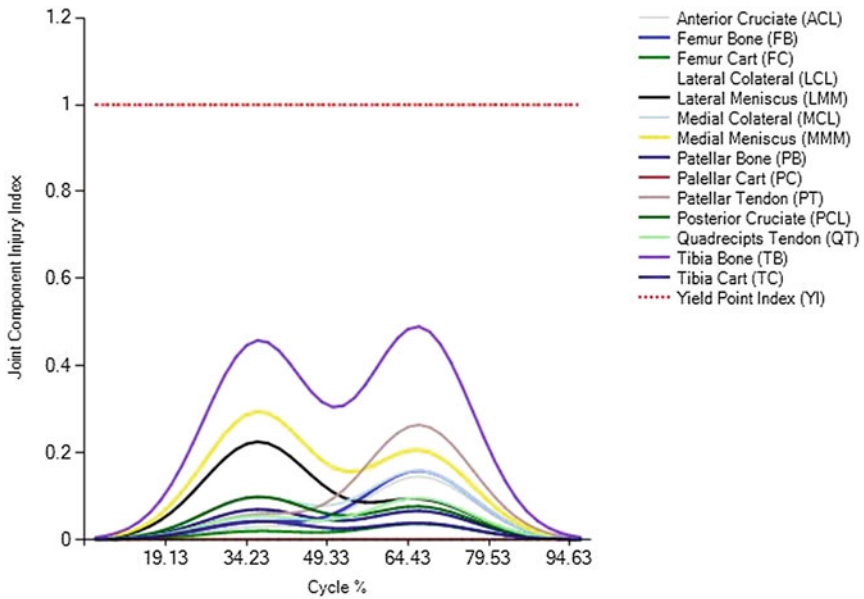


Fig. 5 Right knee components injury index in stair ascending with 17 kg backpack

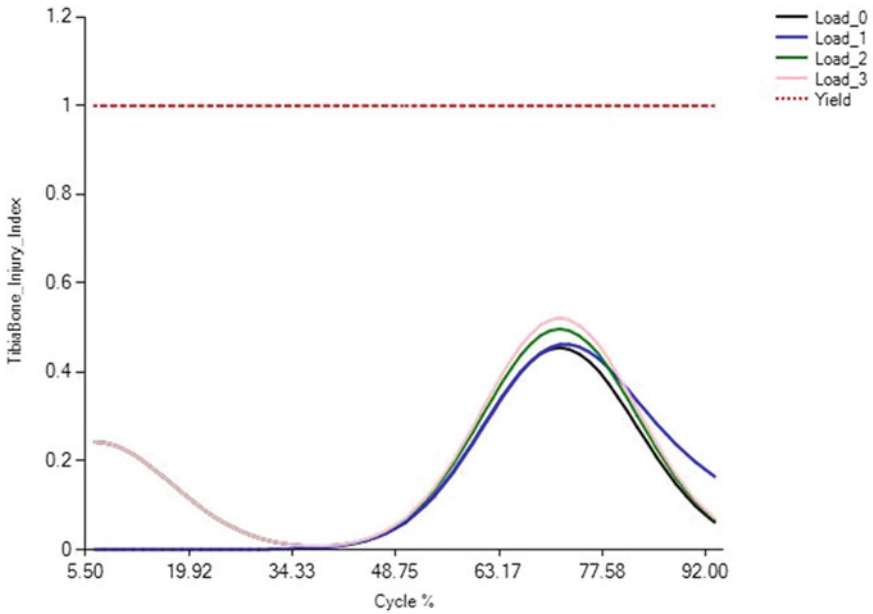


Fig. 6 Right knee tibia bone injury index in walking for different loadings

the beginning of the task cycle. The increase in the maximum injury index value for the tibia bone and the lateral meniscus due to different loadings occurred after the task cycle exceeded one third of its span.

The accuracy of the results is indicated in the form of root mean square error (RMSE) and mean absolute error (MAE). The RMSE and MAE for the right knee walking and stair ascending for the 17 kg backpack loading case are illustrated in Table 1 of Appendix 1. The values of RMSE and MAE for the walking knee are 0.031 and 0.023, respectively, and for the stair ascending knee, they are 0.044 and 0.036, respectively. This error is acceptable for the proposed model because it saves a huge amount of computation time (Fig. 7).

Table 1 RMSE and MAE values for right knee walking and stair ascending

Item	Right knee walking	Right knee stair ascending
No. of input points (no. of frames)	9	10
No. of output points	75	150
No. of variables (knee components)	14	14
RMSE	0.031	0.044
MAE	0.023	0.036

RMSE root mean square error, MAE mean absolute error

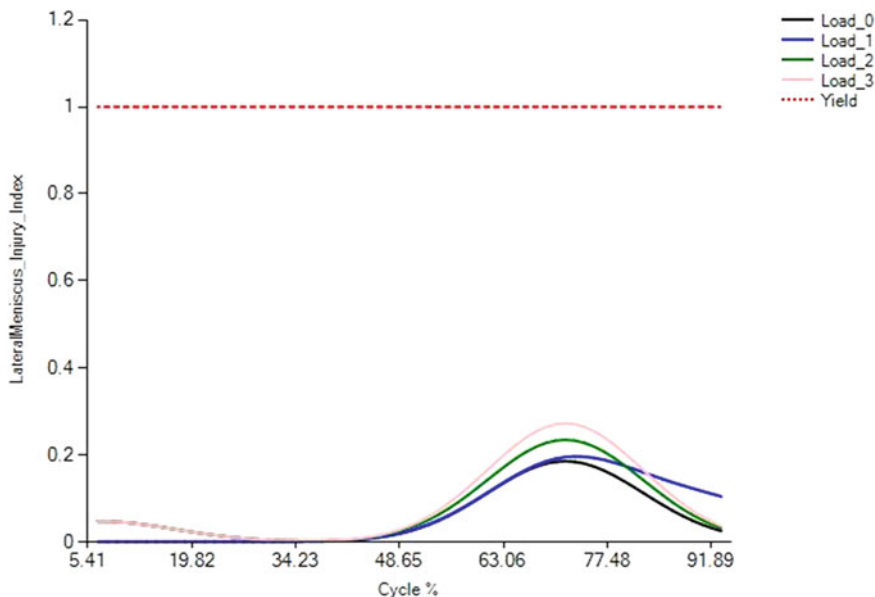


Fig. 7 Right knee lateral meniscus injury index in walking for different loadings

5 Conclusions

This work has presented a multi-scale predictive model for an injury risk assessment strategy. The predictive DHM provides dynamic prediction while considering external forces. The OpenSim software provides a model to determine the muscle force involved in the joint during the task, including external forces. The FEA model for the human knee joint provides a model for determining the stress field for selected frames of the task cycle. The neural network program (NNT) provides regressed data of the stress field covering the whole task cycle. The computational program predicts and assesses the propensity for injury in a quantitative measure through an injury index scale. The injury index model is a powerful new approach and can provide a quantitative measure of injury propensity for bones and soft tissues of the joint. It also saves a huge amount of computational time while showing acceptable accuracy. The proposed approach predicts a scale of joint risk, which can indicate the proper action for prevention.

Acknowledgments We thank the Department of Orthopaedics at the University of Iowa and in particular Dr. Donald D. Anderson, the director of the Orthopaedic Biomechanics Laboratory, for providing us the knee joint data. We also thank Dr. Mohammad Bataineh for use of the NNT program that he developed in the VSR laboratory.

Appendix 1

For the ankle joint, the compression (A_{comp}) and shear (A_{shear}) forces are computed as shown in the following equations [8]:

$$A_{comp} = f_{c-sol} + f_{c-medgas} + f_{c-tibant} + f_{c-tibpost} + GRF_z \cos(\theta_{ankle}) - GRF_y \sin(\theta_{ankle}) - mg_{foot} \cos(\theta_{ankle})$$

$$A_{shear} = f_{s-sol} + f_{s-medgas} + f_{s-tibant} + f_{s-tibpost} + GRF_z \sin(\theta_{ankle}) - GRF_y \cos(\theta_{ankle}) - mg_{foot} \sin(\theta_{ankle})$$

For the knee joint, the muscle compression (M_{comp}) and muscle shear (M_{shear}) forces are computed as shown in the following equations:

$$M_{comp} = f_{c-recfem} + f_{c-vasint} + f_{c-sar} + f_{c-tfl} + f_{c-bifemlh} + f_{c-bifemsh} + f_{c-grac} - mg_{tibia} \cos(\lambda)$$

$$M_{shear} = f_{s-recfem} + f_{s-vasint} + f_{s-sar} + f_{s-tfl} + f_{s-bifemlh} + f_{s-bifemsh} + f_{s-grac} - mg_{tibia} \sin(\lambda)$$

where $f_{c-sol}, f_{c-medgas}, f_{c-tibant}, f_{c-tibpost}$ are the compression components of the ankle muscles, $f_{s-sol}, f_{s-medgas}, f_{s-tibant}, f_{s-tibpost}$ are the shear components of the ankle muscles, $f_{c-recfem}, f_{c-vasint}, f_{c-sar}, f_{c-tfl}, f_{c-bifemlh}, f_{c-bifemsh}, f_{c-grac}$ are the compression components of the knee muscles, and mg_{tibia}, mg_{foot} are the shin and foot weight, respectively.

$f_{s-recfem}, f_{s-vasint}, f_{s-sar}, f_{s-tfl}, f_{s-bifemlh}, f_{s-bifemsh}, f_{s-grac}$ are the shear components of knee muscles, GRF_z, GRF_y are the z and y components of the ground reaction force, and λ, θ_{ankle} are the knee and ankle angles, respectively (Fig. 8 and Table 1).

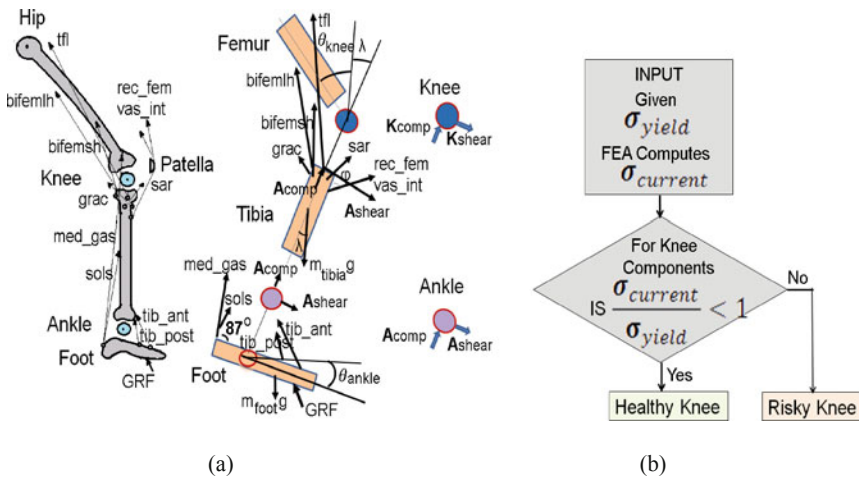


Fig. 8 a Muscle force analysis [2, 8], b injury prediction algorithm [2, 8]

Appendix 2

See Tables 2 and 3.

Table 2 Injury index for knee joint components at 17 kg backpack loading

Joint component	Right knee at 71.6 % of walking cycle	Right knee at 66.4 % of stair ascending cycle
ACL	0.105	0.145
FB	0.057	0.158
FC	0.019	0.036
LCL	0.115	0.217
LM	0.234	0.093
MCL	0.110	0.159
MM	0.128	0.206
PB	0.107	0.065
PC	0.001	0.001
PT	0.119	0.264
PCL	0.023	0.076
QT	0.072	0.095
TB	0.497	0.490
TC	0.027	0.038

ACL anterior cruciate ligament, *Fb* femur bone, *FC* femur cartilage, *LCL* lateral collateral ligament, *LM* lateral meniscus, *MCL* medial collateral ligament, *MM* medial meniscus, *PB* patella bone, *PC* patella cartilage, *PCL* posterior cruciate ligament, *QT* quadriceps tendon, *TB* tibia bone, *TC* tibia cartilage

Table 3 Comparison of injury index at different loadings for tibia bone and lateral meniscus in walking

Cycle (%)	Tibia bone			Lateral meniscus		
	Load-0	Load-2	Load-3	Load-0	Load-2	Load-3
6.7	0.242	0.242	0.242	0.047	0.047	0.047
20.3	0.111	0.111	0.111	0.021	0.021	0.021
33.6	0.011	0.011	0.011	0.011	0.011	0.002
48.6	0.047	0.052	0.054	0.019	0.024	0.028
63.5	0.343	0.375	0.393	0.140	0.207	0.240
77.1	0.401	0.439	0.460	0.163	0.439	0.460
91.9	0.078	0.085	0.089	0.032	0.040	0.047

Load-0 = no backpack, Load-1 = 10 kg backpack, Load-2 = 17 kg backpack, Load-3 = 33 kg backpack

References

1. Renstrom, P.A.F.H., Konradsen, L.: Ankle ligament injuries. *Br. J. Sports Med.* **31**(1), 1–20 (1997)
2. Sultan, S., Marler, R.T.: Multi-scale predictive human model for preventing injuries in the ankle and knee. In: 6th International Conference on Applied Digital Human Modeling, July, Los Vegas (2015)
3. Ruscio, B.A., Jones, B.H., Bullock, S.H., Burnham, B.R., Canham-Chervak, M., Rennix, C.P., Wells, T.S., Smith, J.W.: A process to identify military injury prevention priorities based on injury type and limited duty days. *Am. J. Prev. Med.* **38**, S19–S33 (2010)
4. Zambraski, E.J., Yancosek, K.E.: Prevention and rehabilitation of Musculoskeletal Injuries during military operations on training. *J. Strength Conditioning Res.* (2012 National Strength and Conditioning Association), **26**(7), 101 (2012)
5. Hauret, K.G., Bruce H., Jones, B.H., Bullock, S.H., Canham-Chervak, M., Canada, S.: Musculoskeletal Injuries Description of an Under-Recognized Injury Problem Among Military Personnel. US Army Report (2006)
6. Danny, L.T., Hollingsworth, J.: The prevalence and impact of musculoskeletal injuries during a pre-deployment workup cycle: survey of a Marine Corps special operations company. *J. Spec. Oper. Med.* **9**(4), 11–15 (2009)
7. Army Report TB MED 592: Prevention and control of musculoskeletal injuries associated with physical training. Technical Bulletin, May 2011
8. Sultan, S., Marler, R.T.: Multi-scale human modeling for injury prevention. In: 2nd International Conference on Applied Digital Human Modeling, July, San Francisco (2012)
9. Abdel-Malek, K., Yang, J., Kim, J., Marler, R.T., Beck, S., Nebel, K.: Santos: a virtual human environment for human factors assessment. In: 24th Army Science Conference, November, FL, Assistant Secretary of the Army (Research, Development and Acquisition), Department of the Army, Washington, DC (2004)
10. Denavit, J., Hartenberg, R.S.: A kinematic notation for lower-pair mechanisms based on matrices. *J. Appl. Mech.* **77**, 215–221 (1995)
11. Liu, Q., Marler, T., Yang, J., Kim, J., Harrison, C.: Posture prediction with external loads—a pilot study. In: SAE 2009 World Congress, April, Detroit, MI, Society of Automotive Engineers, Warrendale, PA (2009)
12. Marler, T., Knake, L., Johnson, R.: Optimization-based posture prediction for analysis of box-lifting tasks. In: 3rd International Conference on Digital Human Modeling, July, Orlando, FL (2011)
13. Marler, R.T.: A study of multi-objective optimization methods for engineering applications. Ph.D. Dissertation, University of Iowa, Iowa City, IA (2005)
14. Kubiček, M., Florian, Z.: Stress and strain analysis of the knee joint. In: Engineering MECHANICS, vol. 16(5), pp. 315–322 (2009)

Identifying the Factors Affecting Automotive Driving Posture and Their Perceived Importance for Seat and Steering Wheel Adjustment

Xuguang Wang and Jeanne Bulle

Abstract The aim of the present study was to identify the factors affecting the driving posture and their order of importance for the postural prediction when using a digital human modelling tool. An experiment was carried out with 35 volunteers testing 5 different vehicles with a clutch pedal, covering a large range of European drivers and passenger vehicle types. The seat and steering wheel positions for each vehicle were first adjusted in a lab condition without riding. Then subjects were asked to drive the vehicle on road for about 5 min. Afterwards, they were asked to fill in a questionnaire in order to know the use of available vehicle interior adjustments and to identify the order of priority of the factors affecting the adjustment of vehicle interior dimensions. Results show that 47 out of 175 person-vehicle combinations (27 %) made at least one re-adjustment during the road driving session, suggesting the stationary lab condition could not fully represent road driving. For 55 of 175 volunteers-vehicle combinations (31.4 %), at least one adjustment was judged too restrictive. As expected, short volunteers complained more frequently than others did. The most important factor considered for adjusting the seat and steering wheel positions was the accessibility of the pedals for all participants. The second most important factor depended on stature group. For tall volunteers, the accessibility of the steering wheel was classified as the second most important, while it was the road visibility for short and average height volunteers. These observations could be helpful not only for identifying possible vehicle interior design issues but also for identifying task priority for driving posture prediction when using a DHM tool.

Keywords Driving posture · Anthropometry · Vehicle interior dimension · Automotive

X. Wang (✉) · J. Bulle

LBMC, UMR_T9406, IFSTTAR, Univ Lyon, Université Claude Bernard Lyon 1,
69622 Lyon, France

e-mail: xuguang.wang@ifsttar.fr

1 Introduction

Digital human models (DHM) are used for ergonomic assessment of a product/workplace in its early phase of design (see [1] for a state-of-art of DHMs). This is particularly true for automotive industries [2]. One of key features required for car interior design is its capacity of driving posture prediction. A vehicle should be designed so that a driver can be positioned for a good visibility of external environment and a good manipulability of the controls such as steering wheel and the pedals. In order to accommodate a large population with a high variation of anthropometric dimensions, today's vehicles are designed with a large range of seat and steering wheel adjustments while all other controls are fixed. However, in some extreme cases, it is possible that a driver cannot find his/her optimum position. This may be the case especially for small and tall drivers. Meanwhile, a digital human modelling tool such as RAMSIS is now used for virtually testing a vehicle in its early stage of design. Many geometric constraints, such as vision line, foot and hand positions, head room, etc., have to be appropriately defined to predict a driving posture by an optimisation approach. However, there is no guarantee that all task constraints can be satisfied at the same time. Once conflicts happen, it is important to know which constraints are of higher priority. A good algorithm for predicting driving posture should also be able to take into account the priority of constraints and ensure that the high priority constraints are always satisfied [3]. Therefore there is a need for identifying the factors which affect the driving posture and their order of importance considering driver's anthropometry and vehicle characteristics.

In the present work, an experiment was carried out in collaboration with Toyota Motor Europe NV/SA, with 35 volunteers testing 5 different vehicles with a clutch pedal, covering a large range of European drivers and passenger vehicle types. After having tested in both lab and real road conditions, driving postures were measured by a motion capture system. Moreover, a questionnaire was designed to know the use of available vehicle interior adjustments and to identify the order of priority of the factors affecting the adjustment of vehicle interior dimensions. Results of the questionnaire analysis are reported in the present paper.

2 Materials and Methods

2.1 Participants

35 volunteers, aged from 20 to 45 years old, participated in the experiment. They were recruited according to their stature, in order to obtain a representative sample of the European driver population. The following groups were defined:

- Short volunteers: stature ≤ 165 cm (mainly females)
- Average volunteers: stature between 166 and 180 cm (males and females)
- Tall volunteers: stature ≥ 180 cm (mainly males).

Table 1 Main characteristics of participants

Group	N	Age (years)	Stature (cm)	Weight (kg)
Short	12(1M/11F)	27 ± 9	158 ± 5	58 ± 7
Average	14(9M/5F)	26 ± 6	172 ± 4	64 ± 7
Tall	9(9M/0F)	25 ± 6	187 ± 5	80 ± 17

All participants were regular drivers with one year minimum driving license. The main characteristics are summarized in Table 1. They were informed consent and paid for their participation in the experiment.

2.2 Vehicles

Five real vehicles were selected (Table 2) and rented based on seat height and field of view (visibility out). The seat height (H30) for the five vehicles was ranged from 231 mm to 387 mm. In order to have a test vehicle with a medium seat height, a 30 mm mat was added to the seat of Vehicle 3. Seating Reference Point (SgRP) is a particular point on the seat travel path, defined by the seat H-point (SAE J826). SgRP can be located in different ways depending on car manufacturers. In this study, it was defined as the H-point location when the seat was placed at its rearmost and mid-height position. The field of view (FOV) is characterized by the relative position of SgRP and the resulted eye point, with respect to the lowest point of windshield in the side view, called ceramic point of the vehicle. For two vehicles with a similar SgRP, the vehicle with a higher and more forward ceramic point is considered having more restrictive FOV. All vehicles had at least the following adjustments:

- Seat vertical and longitudinal position
- Seat back inclination
- Steering wheel vertical (tilt angle) and longitudinal (telescopic) position.

Table 2 Criterion for selecting test vehicles

Seat height (H30)	Field of view		
	Good	Average	Limited
Low (~245 mm)	V1		V2
Medium (~280 mm)		V3 (+30 mm mat)	
High (~330 mm)	V4		V5

2.3 *Experimental Conditions and Procedure*

For each vehicle, four conditions were tested. At first, an experimenter adjusted the seat and the steering wheel to three initial positions (Table 3), in a random order. For each initial configuration, volunteers were asked to adjust the seat and the steering wheel until reaching a comfortable driving posture. After having tested all three configurations without road riding, subjects were asked to drive the vehicle outside for a 5-min circuit. During the road driving, they were allowed to re-adjust the seat and steering wheel positions. For each test condition, three postures were measured depending on the left foot position: rest, beginning of clutching and end of clutching, using a Vicon motion capture system. The right foot was asked to keep in contact with the accelerator pedal and the hands on the steering wheel in 10-to-2 position. Test order of the five vehicles was also randomized.

Prior to the experiment, more than 20 anthropometric dimensions were measured for each participant and then after markers were attached to the body.

2.4 *Questionnaire*

In order to know how adjustments were used, participants were asked to fill-in a questionnaire after having tested each vehicle. The questionnaire was composed of three questions (Appendix):

- Q1. Among the available interior adjustments, which ones are modified after the road driving session?
- Q2. Among the available interior adjustments, which ones do not provide enough range of adjustment?
- Q3. Order the factors listed hereafter according to their priority when adjusting the vehicle interior for driving
 - Accessibility of the pedals
 - Accessibility of the steering wheel
 - Accessibility of the controls
 - Panel visibility
 - Road visibility
 - Room between the head and car roof
 - Others.

Table 3 Three initial adjustment configurations (*S* seat, *SW* steering wheel)

	Rear-low (RL)	Forward-high (FH)	Middle (MI)
S height	Lowest	Highest	Mid
S fore-aft	Rearmost	Foremost	Mid
S Back angle	Most reclined	Least reclined	Mid
SW height	Lowest	Highest	Mid
SW fore-aft	Rearmost	Foremost	Mid

In the present paper, only the results from questionnaire analysis are presented. Detailed analysis of inter and intra variability in in-vehicle driving postures can be found in Bulle’s Ph.D. thesis [4].

3 Results

Q1 aims to know if a driver could choose his/her adjustments without a road driving session. Results are summarized in Tables 4 and 5. Compared to the initial adjustments when a vehicle is stationary, the vision constraints during road driving should be stronger. 47 over 175 person-vehicle pairs (27 %) made at least one change during the road driving session (Table 4), showing the need of real road driving practice for ensuring appropriate driving posture. The need of re-adjustment mainly concerned seat position, 25 times for seat fore-aft position, 17 for seat back inclination, 13 for seat height over 175 trials in total (Table 5). For the steering wheel, re-adjustment mainly concerned the two vehicles with a low seat height, V1 and V2. V4 had the smallest number of re-adjustments. Proportionally, tall participants needed less re-adjustments (13.3 %) than short and average height drivers.

Table 4 Number of times that volunteers changed at least one adjustment during the road driving session

Group	V1	V2	V3	V4	V5	Total	%
Short	4	4	3	3	4	18	30.0
Average	4	6	6	3	4	23	32.9
Tall	1	2	3	0	0	6	13.3
Total	9	12	12	6	8	47	26.9

Table 5 Number of times that an adjustment was changed during the road driving

Vehicle/group	Seat height	Seat fore-aft	Back inclination	SW height	SW fore-aft	Total
V1	1	4	5		3	13
V2	3	6	3	3		15
V3	4	9	3			16
V4	2	2	3			7
V5	3	4	3		1	11
Short	5	11	8		3	27
Average	7	10	8	2	1	28
Tall	1	4	1	1		7
Total	13	25	17	3	4	62

Results are presented by vehicle and group of stature

Table 6 Number of times that at least one adjustment was considered as too restrictive

Group	V1	V2	V3	V4	V5	Total	%
Short	6	6	9	4	4	29	48.3
Average	5	1	5	2	1	14	20.0
Tall	2	3	5	0	2	12	26.7
Total	13	10	19	6	7	55	31.4

Q2 was designed to know if the ranges of available seat and steering wheel adjustments were large enough. Responses of Q2 are summarized in Tables 6 and 7. For 55 over 175 person-vehicle pairs (31.4 %), at least one adjustment was judged too restrictive. The percentages of the number of times with at least one unsatisfying adjustment were respectively 48, 20 and 26.7 % respectively for the short (S), average-height (A), and tall (T) participants. More short participants complained than other two groups. When looking at which adjustments were unsatisfying, seat height was reported the most frequently, followed by the steering wheel fore-aft and height adjustments. Note that V3 had the highest number of times that an adjustment was considered as unsatisfying. This may be due to the modification in seat height by adding a mat of 30 mm.

Q3 was designed to know the order of priority (importance) of the six factors when adjusting the seat and steering-wheel position. Results (Table 8) clearly show that for all volunteers, the most important factor for the adjustment of seat and steering wheel positions is the accessibility of the pedals for 76 % of the trials. The second factor depended on group of stature. For short and average volunteers, the road visibility was ranked as the second most important factor, followed by the accessibility of the steering wheel. For tall volunteers, the accessibility of the steering wheel was classified as more important than road visibility. It is interesting to note that for short and average volunteers there is a clear difference between the first factor (accessibility of the pedals) and the second (visibility of the road). However, for tall volunteers, the difference between first and second factors is not so clear.

Table 7 Number of times that an adjustment was considered too restrictive

Vehicle/Group	Seat Height	Seat fore-aft	Back inclination	SW Height	SW fore-aft	Total
V1	7	2	1	6	5	21
V2	6	2		5	3	16
V3	10	2		3	12	27
V4	3			2	2	7
V5	4			2	2	8
Short	20	2		6	13	41
Average	5	1	1	6	6	19
Tall	5	3		6	5	19
Total	30	6	1	18	24	79

Results are presented by vehicle and group of stature

Table 8 Cumulative percentages of the number of times one of the six factors was classed (from 1 for the most important to 7 for the least important)

	Factor	Order of importance for adjusting seat and SW position						
		1	2	3	4	5	6	7
Short	Acc. of the pedals	84.3	98.6	98.6	98.6	98.6	100	100
	Acc. of SW	0.0	40.0	90.0	92.9	92.9	100	100
	Acc. of other controls	0.0	1.4	1.4	14.3	80.0	92.9	100
	Control panel visibility	0.0	0.0	8.6	75.7	85.7	98.6	100
	Road visibility	14.3	57.1	85.7	95.7	100	100	100
	Head clearance	1.4	1.4	7.1	14.3	34.3	92.9	100
Average	Acc. of the pedals	88.3	100	100	100	100	100	100
	Acc. of SW	0.0	26.7	73.3	83.3	98.3	100	100
	Acc. of other controls	0.0	0.0	8.3	68.3	100	100	100
	Control panel visibility	0.0	1.7	18.3	40.0	91.7	100	100
	Road visibility	11.7	70.0	93.3	100	100	100	100
	Head clearance	0.0	1.7	6.7	8.3	10.0	100	100
Tall	Acc. of the pedals	46.7	82.2	88.9	91.1	93.3	100	100
	Acc. of SW	35.6	60.0	80.0	93.3	100	100	100
	Acc. of other controls	0.0	13.3	26.7	57.8	84.4	100	100
	Control panel visibility	0.0	13.3	17.8	37.8	93.3	100	100
	Road visibility	15.6	26.7	68.9	97.8	100	100	100
	Head clearance	2.2	4.4	17.8	22.2	28.9	100	100
All	Acc. of the pedals	76.0	94.9	96.6	97.1	97.7	100	100
	Acc. of SW	9.1	40.6	81.7	89.7	96.6	100	100
	Acc. of other controls	0.0	4.0	10.3	44.0	88.0	97.1	100
	Control panel visibility	0.0	4.0	14.3	53.7	89.7	99.4	100
	Road visibility	13.7	53.7	84.0	97.7	100	100	100
	Head clearance	1.1	2.3	9.7	14.3	24.6	97.1	100

Surprisingly, head clearance was ranked as the least important factor, even for tall volunteers. The visibility of control panel was not considered as an important factor affecting the adjustments.

4 Discussion and Conclusion

In the present study, the use of seat and steering wheel adjustments was investigated for identifying the factors affecting automotive driving posture and their perceived importance. The main observations are summarized as follows:

- For 47 out of 175 person-vehicle combinations (27 %), at least one adjustment during the road driving session was modified. Seat adjustments were mainly concerned. Proportionally, tall participants (13.3 %) needed fewer changes in vehicle interior dimension than short and average height drivers did.
- For 55 of 175 person-vehicle combinations (31.4 %), at least one adjustment was judged too restrictive. Proportionally, short participants (48.3 %) complained much more than other two groups (20 % and 26.7 for average and tall groups).
- The accessibility of the pedals was considered as the most important factor when adjusting vehicle interior dimensions for all participants. The second most important factor depended on stature group. For tall volunteers, the accessibility of the steering wheel was classified as the second most important factor, while it was the road visibility for short and average height volunteers.

Results show that the in-vehicle driving posture adopted in a stationary lab condition was not representative of road driving position for more than 30 % of trials. This is probably due to the road vision requirement that cannot be well apprehended in a stationary lab condition. This is particularly true for shorter drivers, for whom the road visibility was classified as the second most important factor affecting the seat and steering wheel position. This is in agreement with the observation that shorter drivers made more changes in seat and steering wheel position than taller drivers during the road driving session. However, in currently existing digital human modeling tools such as RAMSIS, eye position and vision line need to be specified by users for posture prediction. For instance, concerning vision constraints, it is recommended in the RAMSIS Application Guide [5] that the eyes should be above the lowest vision bounding plane with a tangent of vision line of 6° downwards. Results of the present study strongly suggest that vision constraints should be specified depending on stature group, in agreement with the results of comparison between RAMSIS prediction and experimental observations by our earlier studies [6].

It should be noted that few studies have been investigated on effects of the road vision on driving posture. For instance, in Reed's cascade prediction model (CPM) [7], only seat height (H30), cushion angle and steering wheel position were considered as vehicle dimensions. There is a need for future investigation on effects of both vehicle interior and exterior dimensions on driving posture.

In the present study, it was observed that short participants complained that the range of at least one adjustment was too restrictive, much more than other two groups did proportionally, suggesting that currently existing vehicles may not be well designed for short drivers.

Appendix: Questionnaire

Q1: Among the following adjustments available in the vehicle, which ones were modified during the road driving session? Explain why you made these changes.

Adjustments	Modified during the driving session?		Why
	Yes <input type="checkbox"/>	No <input type="checkbox"/>	
Seat height	Yes <input type="checkbox"/>	No <input type="checkbox"/>	
Seat fore aft position	Yes <input type="checkbox"/>	No <input type="checkbox"/>	
Seat back inclination	Yes <input type="checkbox"/>	No <input type="checkbox"/>	
SW height	Yes <input type="checkbox"/>	No <input type="checkbox"/>	
SW fore aft position	Yes <input type="checkbox"/>	No <input type="checkbox"/>	
Lumbar support	Yes <input type="checkbox"/>	No <input type="checkbox"/>	
Other	-		

Q2: Among the following adjustments available in the vehicle, which ones were too restrictive in their range of adjustment?

Adjustments			If yes, in which direction?	
	Yes <input type="checkbox"/>	No <input type="checkbox"/>	Upwards <input type="checkbox"/>	Downwards <input type="checkbox"/>
Seat height	Yes <input type="checkbox"/>	No <input type="checkbox"/>	Upwards <input type="checkbox"/>	Downwards <input type="checkbox"/>
Seat fore aft position	Yes <input type="checkbox"/>	No <input type="checkbox"/>	Forwards <input type="checkbox"/>	Rearwards <input type="checkbox"/>
Seat back inclination	Yes <input type="checkbox"/>	No <input type="checkbox"/>	Forwards <input type="checkbox"/>	Rearwards <input type="checkbox"/>
SW height	Yes <input type="checkbox"/>	No <input type="checkbox"/>	Upwards <input type="checkbox"/>	Rearwards <input type="checkbox"/>
SW fore aft position	Yes <input type="checkbox"/>	No <input type="checkbox"/>	Forwards <input type="checkbox"/>	Downwards <input type="checkbox"/>
Lumbar support	Yes <input type="checkbox"/>	No <input type="checkbox"/>	Forwards <input type="checkbox"/>	Rearwards <input type="checkbox"/>
Other				

Q3: Classify the factors listed hereafter by their priority required for adjusting the seat and steering wheel position (1 the most important, 6 the least important):

Accessibility of the pedals
Accessibility of the steering wheel
Accessibility of other controls
Control panel visibility
Road visibility
Free room between head and roof
Other (———)

References

1. Duffy, V.G.: Handbook of digital human modeling: research for applied ergonomics and human factors engineering. CRC Press, Taylor and Francis Group, Boca Raton, FL (2009)
2. Chaffin, D.B.: Improving digital human modeling for proactive ergonomics in design. *Ergonomics* **48**(5), 478–491 (2005)
3. Peng, J., Wang, X., Denninger, L.: An iterative tasks-priority optimization-based method for predicting driving posture. In: 2nd International Symposium on Digital Human Modelling, Ann Arbor, Michigan, USA, 11–14 June 2013
4. Bulle, J.: Experimental investigation on intra- and inter-individual variability in automotive driving postures for their prediction using a digital human model. Doctorat Thesis, Génie mécanique [physics.class-ph]. Université Claude Bernard—Lyon I (2013). <https://tel.archives-ouvertes.fr/tel-00948391>
5. Speyer, H.J., Pruett, C., Rothaug, H.: RAMSIS: a step-by-step instruction guide for working on evaluation tasks. Human Solutions GmbH, Kaiserslautern (2005)
6. Bulle, J., Caccia Dominioni, G., Wang, X., Compigne, S.: Comparing RAMSIS driving posture predictions with experimental observations for defining optimum task constraints. In: 2nd International Symposium on digital human modelling, Ann Arbor, Michigan, USA, 11–14 June 2013
7. Reed, M.P., Manary, M.A., Flannagan, C.A.C., Schneider, L.W.: A statistical method for predicting automobile driving posture. *Hum Factors: J. Hum. Factors Ergon. Soc.* **44**(4), 557–568 (2002)

Optimization-Based Prediction of the Motion of a Soldier Performing the ‘Going Prone’ and ‘Get Up from Prone’ Military Tasks

Mahdiar Hariri

Abstract In this work, an optimization based 3-D motion prediction of the motion of a soldier transitioning between a “Standing” posture and a “Prone” posture is presented. Based on the time discretization strategy between these two postures, a set of motion frames are defined such that they include important moments of time during the motion (such as moments when the parts of soldier’s body that touch the ground alter). Then every frame of the motion is analyzed, predicted and certified to be both feasible and optimal considering all dynamic properties of a motion frame such as velocities, accelerations and all higher derivatives of the human’s position. The digital human model is a full-body, three dimensional model with 55° of freedom. Six degrees of freedom specify the global position and orientation of the coordinate frame attached to the pelvic point of the digital human and 49° of freedom represent the revolute joints which model the human joints and determine the kinematics of the entire digital human. Motion is generated by a multi-objective optimization approach minimizing the mechanical energy and joint discomfort simultaneously. The optimization problem is subject to constraints which represent the limitations of the environment, the digital human model and the motion task. Design variables are the joint angle profiles. All the forces, inertial, gravitational as well as external, are known, except the ground reaction forces. The feasibility of the generation of that arbitrary motion by using the given ground contact areas is ensured by using the well-known Zero Moment Point (ZMP) constraint. During the kneeling motion, different parts of the body come in contact and lose contact with the ground which is modeled using a general approach. The ground reaction force on each transient ground contact area is determined using the equations of motion. Using these ground reaction forces, the required torques at all joints are calculated by the recursive Lagrangian formulation. This simulation is able to predict feasible and optimal motions that vary when loading (such as backpack, etc.) or the equipment that the human model carries change as or when the human model’s strength, size or weight is altered.

M. Hariri (✉)

Faculty at Wichita State University, 1845 Fairmount St, Wichita, KS 67260, USA
e-mail: Mahdiar.Hariri@wichita.edu

Keywords Digital human · Robotics · Going prone · Get up · Predictive dynamics · Kinematics · Dynamics · Virtual reality

1 Introduction

The need for representing simulated soldiers has been primarily driven by military requirements. These requirements appeared very early in the beginning stages of the digital human modeling field [1, 2].

Despite this need, there have been very few samples of basic military tasks (such as aiming, kneeling or going prone) simulated by simplified or whole body digital human models. This has been due to the complexity of these tasks. This complexity arises from the complex combination of joint angle variables that are required to achieve these motions or postures. As a result, most of the efforts have been focused on the playback of a recorded motion on a digital human model without actually simulating these motions. Therefore the results will need to be recorded again when inputs of the problem (environment conditions, soldier anthropometry or loading on the soldier) are modified. Such efforts have appeared in the literature as early as 1995. Granieri et al. [3] from the University of Pennsylvania uses postures and motions of a human and maps them on a digital human called “Jack” with a lower number of degrees of freedom. These motions include: standing, kneeling, firing, crawling, going prone, running, walking. They store them for later playback in digital environments.

Alexander and Conradi [4] has recently tested the existing digital human models for performing more complex motions. This complex motion is a stand to kneeling motion. In that work, several digital human models are used. The report indicates that: “Modeling of complex motions with the digital human models was complex and intensive. None of them allowed a realistic simulation of specific movements. Although modeling was possible, it was very complex to model the movement and it required manual actions”.

There is also some other less relevant work, using over-simplified models to calculate some specific parameters in question. For example, Macko et al. [5] tries to determine the significant points on a shooter’s body to compare the computed and measured shooter movements in standing, kneeling and prone firing positions.

2 The “Going Prone” and “Getting Up from Prone” Tasks

“Marksmanship” refers to the art or skill of using a firearm, such as a rifle or a pistol. In this research, we use the “Rifle Marksmanship” instructions from the “U.S. Marine Corps Reference Publication (MCRP)” [6] as the major references for definition of terms and procedures.

The “Going Prone” task can be performed in several ways with or without using the rifle stock as support. In this research we model the method presented in [7]

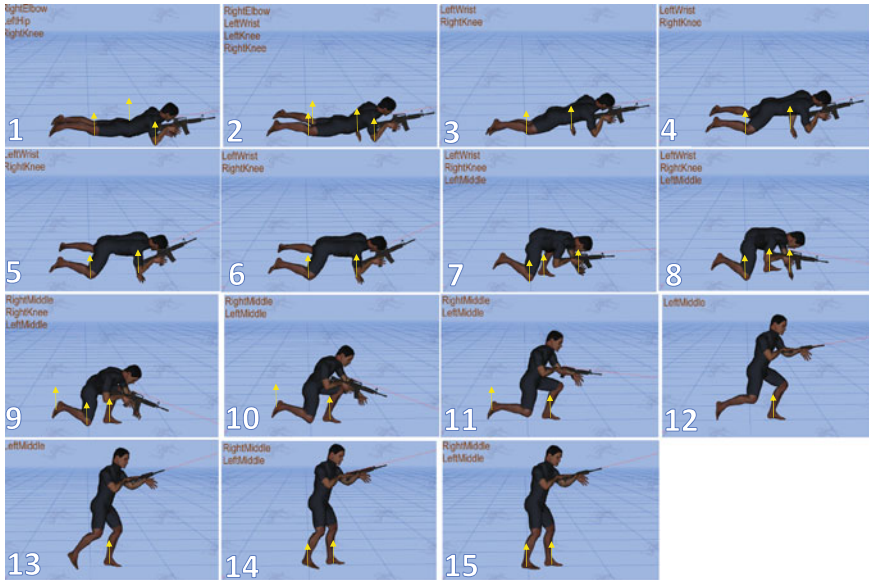


Fig. 1 Fifteen stages for performing the “get up from prone” task and the ground reaction force points

(without using the rifle stock). In a different paper that was previously published by the same author, the “Going Prone” task was modeled using the rifle stock as pivot point. According to [6] (Page 52 or part 5005, Sect. 5–8), the stages for this task are:

1. Stand erect facing the target, keeping the feet a distance of shoulder width apart.
2. Lower yourself into position by dropping to both knees.
3. Shift the weight forward to lower the upper body to the ground using the left hand to break the forward motion.

However, regarding the “Get up from Prone” task, no specific procedure was found. Regarding the “Get up from Prone” task, 15 stages were assumed to be required for performing this task. These 15 stages are shown by the 15 motion slides in Fig. 1. Each motion slide represents a change in the contact condition of the human with the environment.

3 Modeling the Motion Tasks in Predictive Dynamics

In this work, the two tasks (“Going Prone” and “Get up from Prone”) are modeled using the predictive dynamics method. Predictive dynamics, developed recently [8, 9], is a novel approach for simulating human motion in the digital human modeling field. It is a term that is coined to characterize the prediction of human motion in a

physics-based world. Most of the known information for modeling a human motion task such as walking, running, aiming, kneeling, going prone, etc. usually appears as inequality constraints. These constraints represent the limitations of the environment (e.g. non-adhesive contact areas), the limitations of the digital human model (e.g. joint angle or torque limits) and the limitations of the motion task (e.g. those requirements that differentiate crawling from walking).

The non-contact external forces are all assumed to be known during the motion. Design variables are the joint angle profiles. An arbitrary motion (a set of joint angle profiles for all joint angles) of the avatar (humanoid robot) is used as an initial guess. Based on the value of design variables, the kinematic analysis of the model is carried out using the Denavit–Hartenberg method. It is assumed that the digital human has several non-adhesive contact areas with only the horizontal ground. All the forces except the ground reaction forces are known, which are the inertial, gravitational and external forces.

The possibility of generation of the arbitrary motion by using the given ground contact areas is ensured by using the ZMP constraint. When ZMP constraint is satisfied, we are sure that it is possible to find unilateral distributed contact forces on those contact areas to satisfy dynamic equilibrium equations [10]. In other words, neglecting the limitations of the digital human and the motion task, when ZMP constraint is satisfied, we are sure that it is possible to generate the arbitrary motion using the given contact areas if enough friction exists on them.

Based on this motion, the required external contact forces and moments that should act on each separate contact area are calculated such that dynamic equilibrium equations hold. Using these contact forces and moments, the required torques at all joints are calculated. Physical constraints such as constraints on joint angles and torques are imposed. This renders a feasible (realistic and possible) motion. Best motions are selected (motion is optimized) based on human performance measures, such as speed, energy and comfort which act as objective functions in the optimization formulation. Predicting motion in this way allows one to use avatars to study how and why humans move the way they do, given a specific scenario.

4 Ground Contact Modeling

Table 1 lists the stages of changes of GRF points, ZMP areas for the “Going Prone” task. A more complicated list is required for the ground contact modeling of the “Get up from Prone” task (because “Get up from Prone” needs 15 stages of GRF changes as seen in Fig. 1 compared to 7 stages for “Going Prone” as seen in Fig. 2). The contact areas of the avatar with the ground in the predictive dynamics method are assumed to be flat, rigid and non-adhesive. These ground contact areas affect the dynamics of the system in three different ways:

1. For the digital human, the possibility of motion (ZMP constraint) and the dynamic stability of motion (ZMP stability margin) depend on these contact

Table 1 Stages of changes of GRF points, ZMP areas corresponding to Fig. 2

Figure part	GRF points (points that can take ground reaction forces)		Points defining the ZMP convex hull	
	(A)	Left mid foot	Right mid foot	Right heel outer
			Left toe outer	Left heel outer
(B)	Left mid foot	Right mid foot	Right mid foot outer	Right toe outer
			Left toe outer	Left mid foot outer
(C)	Left mid foot	Right mid foot	Right mid foot outer	Right toe outer
	Left knee	Right knee	Right knee	Left knee
			Left toe outer	Left mid foot outer
(D)	Left knee	Right knee	Left knee	Right knee
	Left wrist		Left wrist	
(E)	Left knee	Right knee	Left knee	Right knee
	Left wrist	Right elbow	Right elbow	Left wrist
	Left wrist	Right elbow	Right elbow	Left wrist
(F), (G)	Left knee	Right knee	Left knee	Right knee
	Right elbow	Left pelvis	Right elbow	Left pelvis

areas [10]. The ZMP constraint and the ZMP stability margins depend on the convex hull of the ground contact areas. The shape and size of this convex hull is variable during the motion and depends on the contact areas of the digital human with the ground at each moment during the motion.

- The values of the ground reaction forces and moments exerted on the digital human by each individual contact area will be used in the calculation of actuation torques at the joints of the digital human. The distributed ground reaction forces acting on each individual contact area are replaced by an equivalent concentrated force and moment acting at a point on that contact area. We call them the GRF (Ground reaction force) points. They are the points on the digital human which can take ground reaction forces and moments during the motion whenever those contact areas come in contact with the ground.

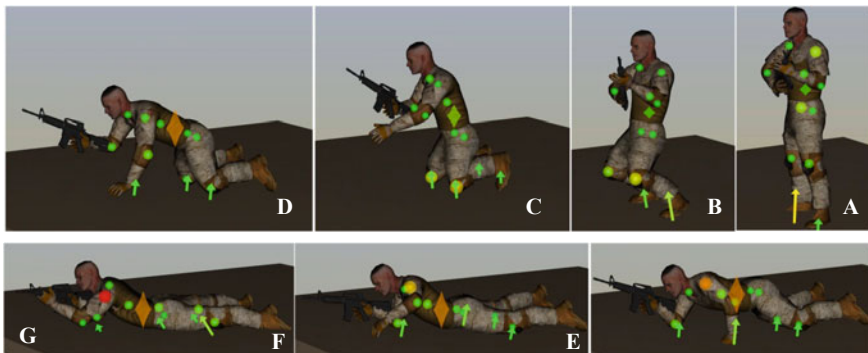


Fig. 2 Slides of going prone simulation for the human model

3. The points that are in contact with the ground receive frictional force from the ground and as long as the frictional force is large enough, those points will not slide (slip) on the ground (no slip condition). Therefore the ground contact points have zero velocity as long as they remain in contact with the ground.

5 Results for the “Going Prone” Task

The simulation is able to predict the results for different inputs. In general, the inputs are:

- Environment properties
- Soldier properties (such as soldier’s anthropometry, strength, size or weight)
- External masses attached to the soldier (such as backpack or the equipment that the soldier carries)
- External forces acting on the soldier (such as wind)

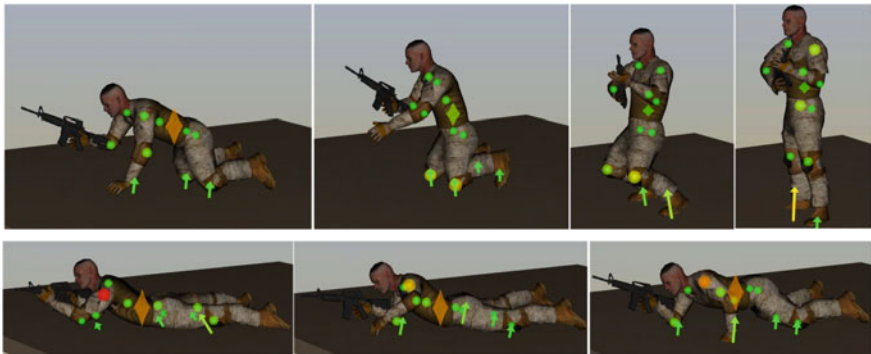


Fig. 3 Slides of going prone simulation for the human model without backpack

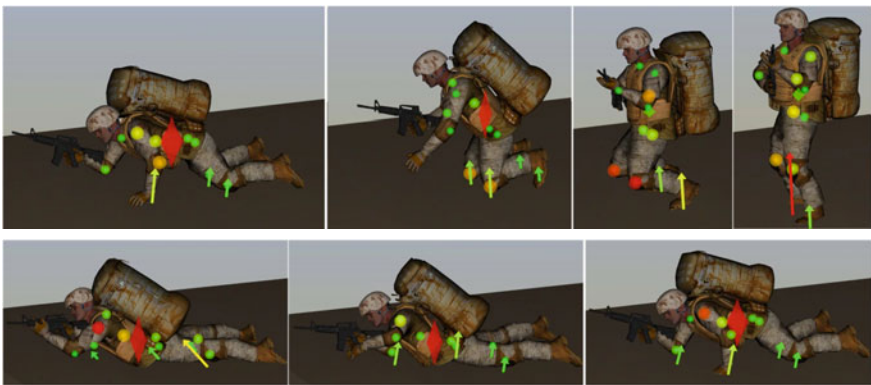


Fig. 4 Slides of going prone simulation for the human model with backpack

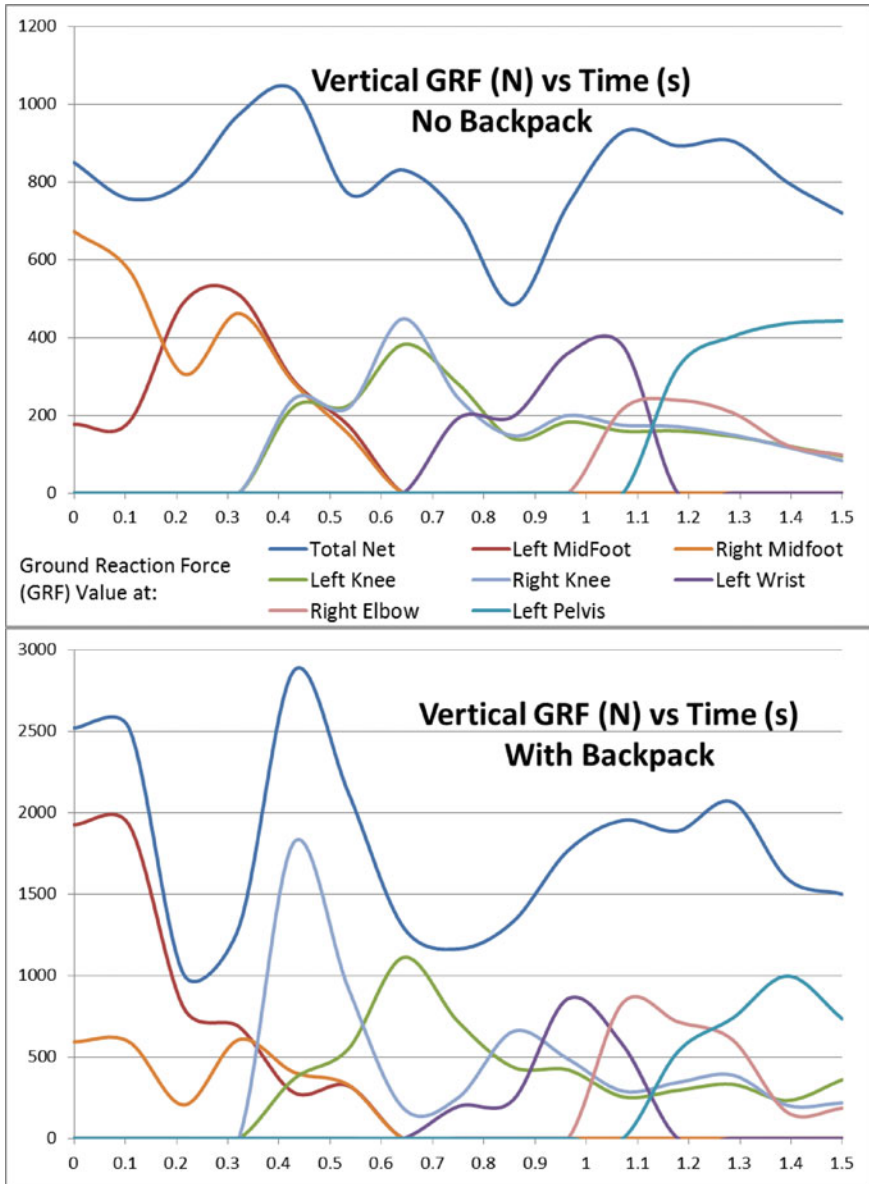


Fig. 5 Comparison of the values of ground reaction forces (vertical component, not frictional) for the going prone motion cases: ‘with backpack’ (Fig. 4) and ‘without backpack’ (Fig. 3). The total value of GRF as well as its value tolerated by different body parts that come in contact with the ground at different instances during the motion is plotted

As an example, slides of motion simulation results for two sets of input for the “Going Prone” task are shown in Figs. 3, 4, 5. The effect of the backpack in the kinematics as well as in dynamics (increasing the value of ground reaction forces and joint torques) can be seen in these figures (Joint torque values are depicted at some human joint locations where green shows a low value and red shows a high value of torque.).

6 Results for the “Get up from Prone” Task

Similar to the “Going Prone” task, this simulation is also able to predict the results for different inputs. As an example, slides of motion simulation results for two sets of input for the “Get up from Prone” task are shown in Figs. 6 and 7. The effect of the backpack in the kinematics as well as in dynamics (increasing the value of

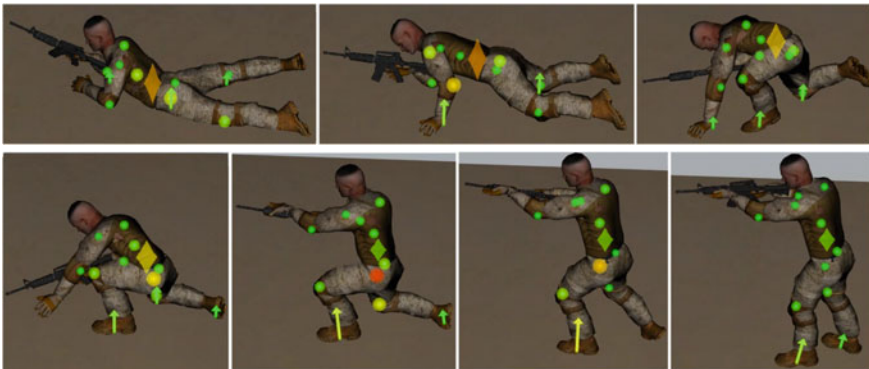


Fig. 6 Slides of get up from prone simulation for the human model without backpack

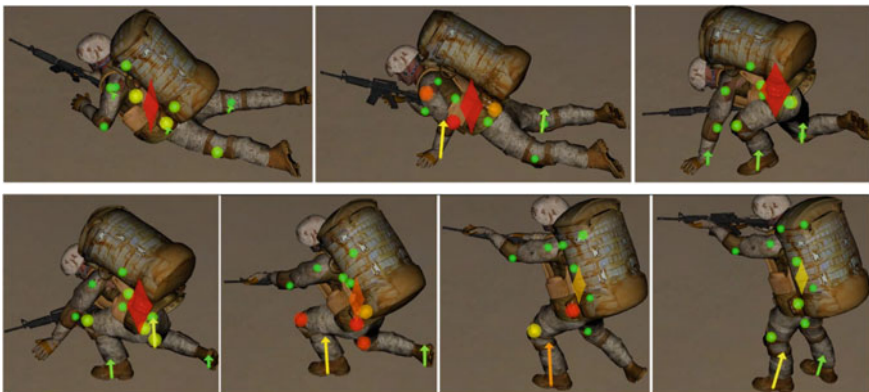


Fig. 7 Slides of get up from prone simulation for the human model with backpack

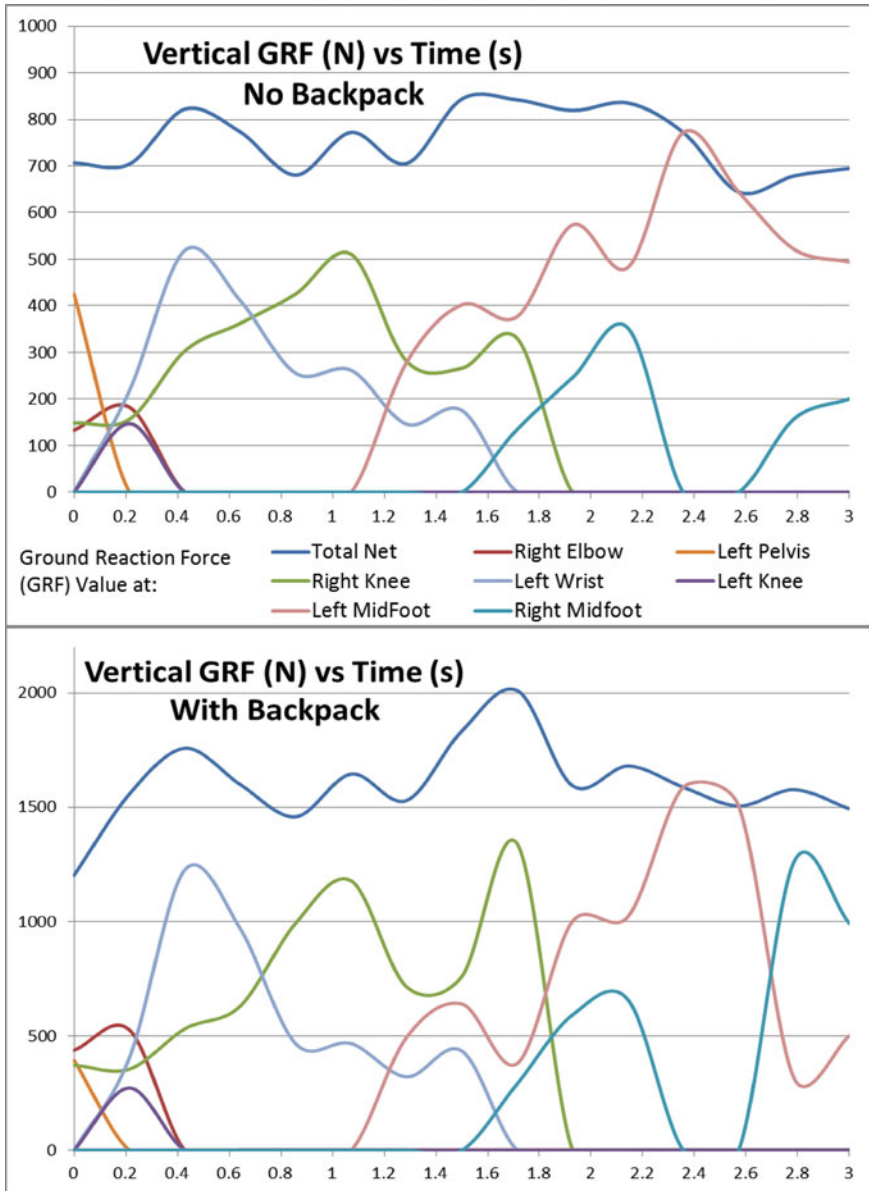


Fig. 8 Comparison of the values of ground reaction forces (vertical component, not frictional) for the get up from prone motion cases: ‘with backpack’ (Fig. 7) and ‘without backpack’ (Fig. 6). The total value of GRF as well as its value tolerated by different body parts that come in contact with the ground at different instances during the motion is plotted

ground reaction forces and joint torques) can be seen in Figs. 6, 7 and 8 (Joint torque values are depicted at some human joint locations where green shows a low value and red shows a high value of torque.).

References

1. Wysocki, F., Fowlkes, D.: Team target engagement simulator advanced technology demonstration. In: Proceedings of the Individual Combatant Simulation Symposium (1994)
2. Pratt, D.R., Barham, P.T., Locke, J., Zyda, M.J., Eastman, B., Moore, T., Biggers, K., Douglass, R., Jacobsen, S., Hollick, M.: Insertion of an articulated human into a networked virtual environment. In: Proceedings of the Fifth Annual Conference on AI, Simulation, and Planning in High Autonomy Systems (1994)
3. Granieri, J.P., Crabtree, J., Badler, N.I.: Production and playback of human figure motion for 3D virtual environments. In: Proceedings of Virtual Reality Annual International Symposium (1995)
4. Alexander, T., Conradi, J.: On the Applicability of Digital Human Models for Personal Equipment Design. HCI International, San Diego (2011)
5. Macko, M., Racek, F., Balaz, T.: A determination of the significant points on sporting shooter body for comparison of the computing and measuring shooter movement. In: Proceedings of the WSEAS Applied Computing Conference, Athens, Greece (2009)
6. Corps, U.S.M.: Rifle Marksmanship (Marine Corps Reference Publication, MCRP 3-01A), Albany, GA. Department of the Navy Headquarters, Washington, DC (2001)
7. Army, U.S.: Rifle Marksmanship (Field Manual 23-8); Fort Benning, GA. Department of the Army Headquarters, Washington, DC (1974)
8. Xiang, Y., Chung, H.J., Mathai, A., Rahmatalla, S., Kim, J., Marler, T., Beck, S., Yang, J., Arora, J.S., Abdel-Malek, K.: Optimization-based Dynamic Human Walking Prediction, SAE Digital Human Modeling Conference, June 2007, Seattle, WA (2007)
9. Hariri, M., Arora, J., Abdel-Malek, K.: Optimization-Based Prediction of Aiming and Kneeling Military Tasks performed by a Soldier. ASME 2012 IDETC: Human Modeling and Simulation for Engineering, Chicago, IL, USA, 12–15 August 2012
10. Hariri, M.: A study of optimization-based predictive dynamics method for digital human modeling. (2012). PhD Dissertation, The University of Iowa

Part II
Virtual Reality and Simulation

FCA Ergonomics Proactive Approach in Developing New Cars: Virtual Simulations and Physical Validation

Spada Stefania, Germanà Danila, Sessa Fabrizio and Lidia Ghibardo

Abstract Cars' manufacturing is subject to radical change because of market continuous request of new models developed in few years. Original Equipment Manufacturer and suppliers have to develop more flexible assembly chains, manufacturing services and methods for job planning. And this requires new concepts for process design and for production: the human centered approach to improve manual assembly. In Fiat Chrysler Automobiles, during process design “Digital Manufacturing” and immersive virtual reality have been used in design phase. Holistic ergonomics assessment method as EAWS and ErgoUAS Methods have been used for ergonomic optimization of assembly tasks and for optimal line balancing. Parallel to virtual phase physical assessment on prototypes runs in order to have a physical validation of design/virtual solutions.

Keywords Digital human modeling · Virtual simulations · Postural assessment

1 Introduction

Cars' manufacturing is subject to radical change because of market continuous request of new models developed in fewer and fewer years. Original equipment manufacturer and suppliers have to develop more flexible assembly chains, manufacturing services and methods for job planning. And this new approach requires new concepts of process design and of production that can be summarized as ‘human centered approach to improve manual assembly’. Fiat Chrysler Automobiles, during process design, has used “Digital Manufacturing” and

S. Stefania · G. Danila · L. Ghibardo (✉)
Fiat Chrysler Automobiles—Manufacturing Engineering—Ergonomics,
Torino, Italy
e-mail: Lidia.ghibardo@fcagroup.com

S. Fabrizio
Fiat Chrysler Automobiles—Manufacturing Engineering Southern
Italy—Digital Manufacturing and Ergonomics, Pomigliano d’Arco (NA), Italy

immersive virtual reality to support the realization of a flexible assembly lines. In fact, virtual simulations allow to create different scenarios to carry on an assembly task and to make improvements and changes almost without any costs optimizing the proactive ergonomics. These different simulated scenarios are evaluated and compared, from different points of view, by a working team made up of occupational doctors, designers, ergonomics specialist and blue collars. The deep application of virtual simulation techniques allows to point out ergonomics critical issues such as reachability and visibility problems and the engagement of incongruous postures or anomalous application of forces. Virtual simulations give as output the behavior of a static mannequin and, of course, it does not take into account the versatility and adaptability of ‘flesh and blood’ operator that often optimized postures and task performance. So a physical assessment on prototypes is needed in order to fully understand critical issues and to prioritize improvements. More over this phase allows blue collars to choose, with designers and occupational doctors, the better solution among the proposed ones. To maximize the physical assessment effectiveness, simulations were performed in an ergonomics laboratory where all facilities of assembly line are duplicated. In this way, assembly line space and working conditions are available and simulations were performed without interfering with plant’s activities and using different set up. In the industrialization step, holistic ergonomics assessment method as EAWS and ErgoUAS system have been used for ergonomic optimization of assembly tasks and for optimal line balancing. Physical assessment on prototypes runs parallel to virtual phase in order to have a physical validation of design/virtual solutions. A case study of this approach will be presented in this paper to focus on the importance of physical assessment performed parallel to virtual simulation phase. A detailed description of two different scenarios coming from the virtual simulation, in design phase, will be given together with the physical assessment carried out with blue collars to choose the better solution in the task execution. The task implies ergonomics criticism because of the complexity of the tasks and the high quality and esthetics requirements.

2 Digital Manufacturing

One of the most important aspects of the DM project, is the information’s “active management” that allows designers and engineers to make detailed virtual simulations in order to improve the car’s manufacturing process. This concept has requested an important development on the methods used by FCA Manufacturing Engineering to manage all the information related to the production process: technological data are available in an unique simulation environment that contains virtual models of the car components and of the production plant (robots, tools, equipment, etc.). The key factor to improve DM simulations has been to insert digital human models and “human centred” simulation methods in the virtual environment in order to perform certified simulations for all the manual operations that are designed for the production process in the future plant (Fig. 1).

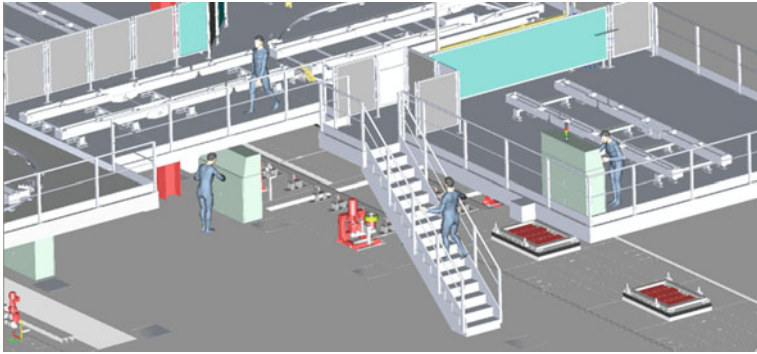


Fig. 1 A virtual model of a production plant

Digital Human Models are nowadays a standard in simulations software and many commercial products, like “Jack” by Siemens, are available on the market [1]. The Digital Manufacturing allows to create a virtual plant where virtual mannequins interact with digital models of car’s components, equipment, containers, etc. in order to simulate and improve working conditions with many benefits on ergonomics, safety, final product quality, work organization and general production costs (Fig. 2).

3 3D Immersive Virtual Reality

Mathematics of object can be used to create a 3D image of car and components. The operator wearing adequate glasses can be set in the immersive environment and interact to objects and tools. This system enables operators and designers to simulate all assembly operations, giving a realistic perception of size and space. In this way it is possible to highlight critical issues related to visibility and accessibility at

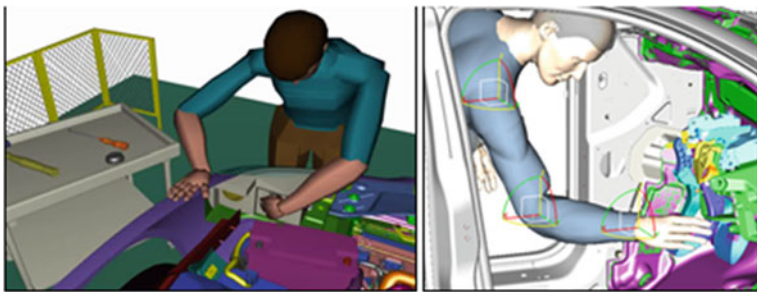


Fig. 2 An example of assembly tasks

Fig. 3 An example of a working team using 3d immersive reality and an operator using the system



the working point, while ergonomics specialists can check the possible risks related to the workstation directly with the operator or using the information provided by the dummy virtual system (Fig. 3).

4 Ergonomics Method

The fundamental development on which FCA has based the Digital Manufacturing project for human simulations, has been the effort to improve standard digital human modeling software in order to let them be compliant to FGA's design standards (based on international technical norms—ISO/EN norms) and FGA's production standards that are based on European/Italian legal specifications on safety and ergonomics. In this way, designers have not only a virtual representation of the future plant but also the virtual tools to validate design solutions. Reference frames on these mannequins have been created in order to have specific points on which evaluate body angles, distances, etc. according to the most important ergonomics methods requested by ISO/EN standards (ISO 11226) and by FGA's standards (like OCRA NIOSH, Snook and Ciriello, EAWS).

EAWS especially is the ergonomics risk assessment method applied in design phase as an ergonomic screening tool. It links corrective and proactive ergonomics, points out ergonomic problems and offers design solutions to overcome them. The EAWS consists of four sections for the evaluation of

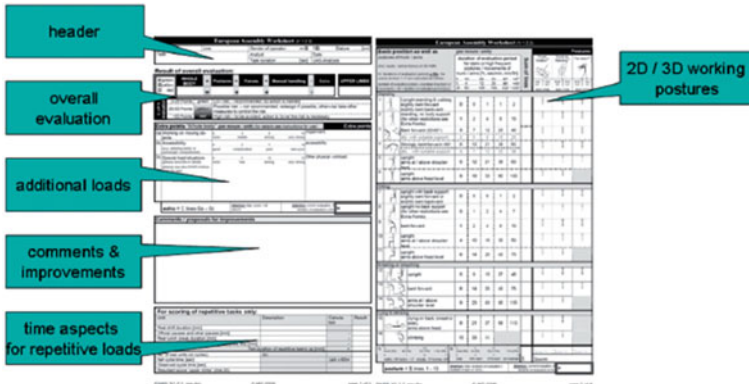


Fig. 4 EAWS structure and sections (pp. 1, 2)

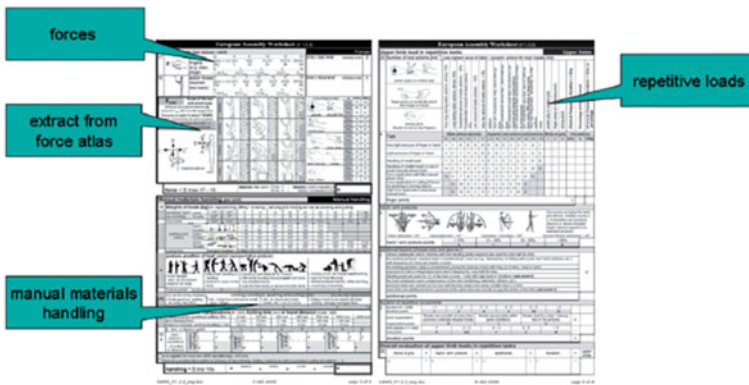


Fig. 5 EAWS structure and sections (pp. 3, 4)

- working postures and movements with low additional physical efforts
- action forces of the whole body or hand-finger system,
- manual materials handling and
- repetitive loads of the upper limbs (Figs. 4 and 5).

The evaluation, of mechanical load request by the workplace (considering product and process together) also in design phase, has to be carried out by the measurement of some physical parameters on prototypes or similar models.

5 Physical Assessment

To assess physical parameters used in ergonomics risk assessment methods and tools choice was created at Mirafiori Plant, in the Manufacturing Engineering area the new ergonomic laboratory, ErgoLab. The main analysis conducted concerning postural aspects and efforts exerted by operators during working tasks as well as experimental measurement of physical parameters involved in equipment and tools use. In ErgoLab, the workplace of production units have recreated: Assembly and Painting are provided by car hook that can accommodate car models of different segments, Body in White is provided by welding system and a dedicated preparation workbench, Handling is provided by different container types, LCA systems and Ro-Ro; a mechanic workshop is provided by adaptive workbench to simulate preparation workstations. The laboratory is grounded on the consistent experience gained over years from the collaboration with FCA Research Center, on different issues: the physical parameters measurement, the ergonomic design of workplace and, generally, the support during the design phase, selection and training in correct use of pieces of equipment according to national and international legislation requirements. The aim of ErgoLab creation is supporting plants, the Manufacturing Engineering area and designers with reliable information and data to design

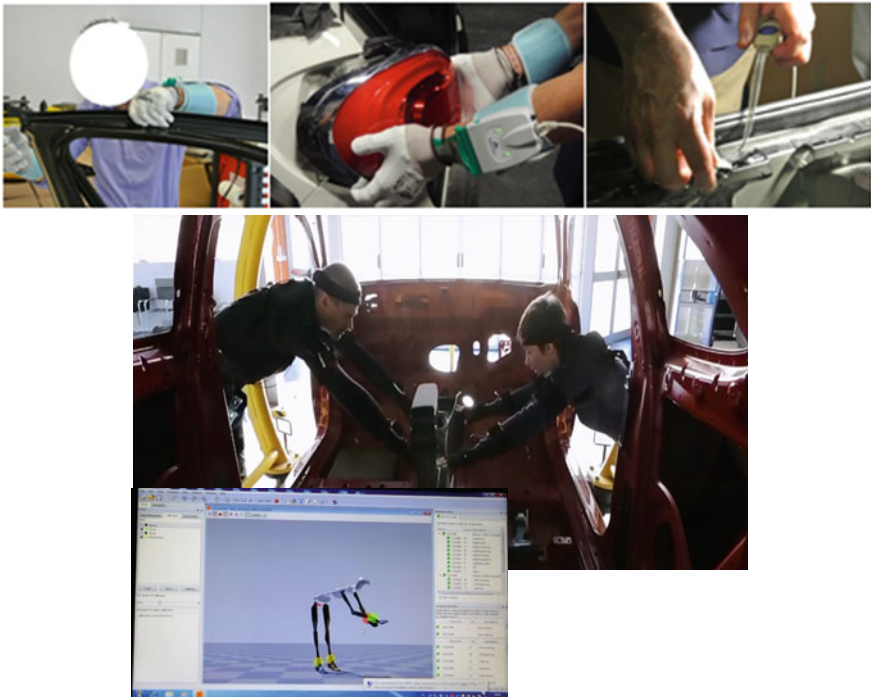


Fig. 6 Example of physical measurement

technological systems and ergonomic workstations. The main purpose is to make measurement procedures more accessible and to recreate working conditions without interfering with the working process.

The main field of laboratory activities concern:

- measurement of force, localized and distributed pressure, reaction force couple, hand/tool interaction
- acceleration
- angles assumed by the main joints

All measurements focus on the physical characterization of the following three main areas: Tools, Equipments and Work methods. The acquisitions are made using the most advanced commercial instruments and sensors and the experimental procedures are well defined, documented and repeatable (Fig. 6)

6 Conclusions

In this paper, the authors have shown the approach used in FCA based on simulation methods and experimental facilities to analyse ergonomics aspects of future workcells.

The approach is based on virtual and physical methods that can be quickly used by project designers and plant ergonomics experts. Using these tools it becomes also possible to do a preliminary ergonomic analysis of the future workcell according to the most important ergonomics indexes (like OCRA and EAWS) in order to get a preliminary ergonomics optimization of workcells during the initial phases of a new product/process.

Reference

1. Stephens, A., Godin, C.: The truck that jack built: digital human models and their role in the design of work cells and product design, SAE Paper n. 2006-01-2314 (2006)

Virtual Human Motion Design and Ergonomics Analysis in Maintenance Simulation

Fuyang Yu, Qing Xue and Minxia Liu

Abstract Maintainability is one of the main targets of product development. Through simulating the actual maintenance process, maintainability problems can be identified by virtual reality technology. Most virtual reality softwares provide virtual human motion simulation functions, but the virtual human motion control methods of them are defective. In order to enhance virtual human motion control, maintenance task model was established in this paper, virtual human motion model was designed. Then a virtual human motion database based on Jack was developed by Tcl/Tk Python language, and it was applied to a real maintenance process. Furthermore, the maintenance process was simulated in Jack and the ergonomics of it were analyzed. The result showed that the motion database can be effectively applied to virtual maintenance simulation and make the maintenance process-related ergonomics analysis conveniently.

Keywords Ergonomics · Motion database · Virtual human · Virtual maintenance

1 Introduction

Maintainability is the probability of successfully performing and completing a specified corrective maintenance action, or a specified preventive maintenance action or both with specified conditions, time, procedure and methods [1]. Traditional maintainability testing is after production. With the development of computer technology, virtual human maintenance simulation (VHMS) has become a feasible method. This method can detect product maintainability at the design stage of product. A general method for virtual maintenance application is to replace physical prototypes with digital prototypes, and replace the real personnel with

F. Yu · Q. Xue (✉) · M. Liu

School of Mechanical Engineering, Beijing Institute of Technology, Beijing
100081, China

e-mail: yufuyoung@qq.com

virtual human. Then virtual maintenance scenery is constructed, and disassembly or assembly activities can be animated.

There are two methods for VHMS, one is on the desktop of the computer, the virtual human is controlled by software, and another is through virtual reality hardware such as data glove or data suit. In this paper, we just discuss VHMS through software. Jack and DELMIA are two mature softwares supporting VHMS and analysis, but these softwares are all low-level virtual human body control with varying the angles of virtual human body joints or a kinematic chain. On the one hand, this control method efficiency is relatively low; on the other hand, the accuracy of virtual human motion is not high. Some improved virtual human motion control methods (such as Key Frames, Forward Kinematics and Inverse Kinematics) are proposed to for virtual human motion modeling [2, 3]. Moreover, path planning of virtual human can solve this problem [4, 5].

Before VHMS, maintenance task needs to be decomposed into motions to support simulation software. Currently human action classification and decomposition methods mainly in the field of ergonomics, such as Sabu Rick Therblig, MODAPTS (Modular Arrangement of Predetermined Time Standard), MTM (Methods-Time Measurement), however, those motion classification methods focus on the analysis of motion and does not apply to VHMS.

In this paper, we proposed a maintenance task decomposition model and virtual human maintenance motion database (VHMMD) to achieve a high-level virtual human motion control and reuse those maintenance motions. The VHMMD was developed in Jack with Python and Tck/Tk language. Then an oxygenation wrench assembly and disassembly process was simulated in Jack based on this model. Finally, some ergonomics factors that affecting maintenance were analyzed, which include reachability, visibility and fatigue.

2 Virtual Human Motion Design

2.1 Maintenance Task Decomposition

Maintenance task decomposition is first proposed by Vujoservic of the University of Iowa [6]. According to his idea, maintenance task can generally be decomposed into four levels, they are maintenance level, maintenance task level, maintenance operations level and basic maintenance operation level. This maintenance task decomposition method focus on maintenance tools and maintenance objects and do not consider the maintenance process of human motion, which is not beneficial to VHMS. Therefore, this paper proposed a method of decomposing maintenance task for virtual human. The basic maintenance operation level was further decomposed into maintenance motion unit. Maintenance motion unit refers to a continuous movement of several joints of human, it do not have specific maintenance semantics.

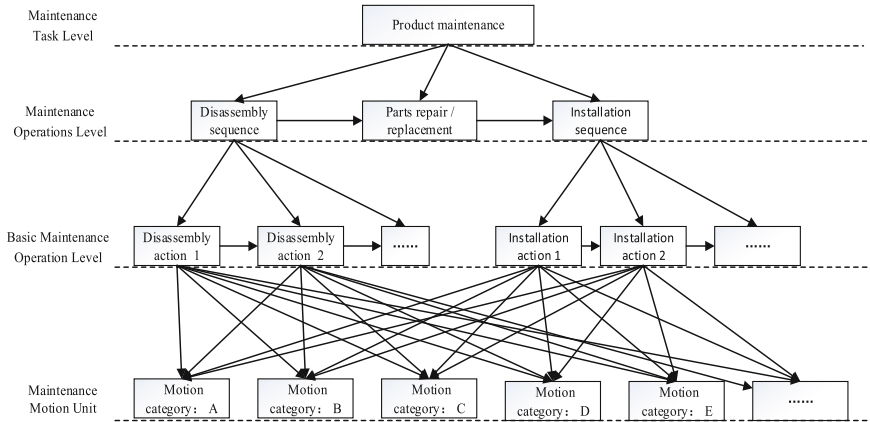


Fig. 1 Hierarchical virtual human motion models

Based on layered maintenance task decomposition, we decomposed the maintenance process by human activity-centered, classified virtual human motion and established hierarchical virtual human motion models (Fig. 1).

2.2 Virtual Human Maintenance Motion Classification

In a human activity-centered maintenance process, the maintenance process can be further divided into two stages:

- (A) maintenance preparation stage: virtual human moves to the repair location and prepares tools. It can be divided into:
 1. Tool preparation: virtual human fetches maintenance tools in the initial position.
 2. Virtual human movement: virtual human moves from the initial position to the target position. According to the different work environment, the virtual human body is in different postures.
- (B) maintenance stage: virtual human adjusts posture and completes the maintenance operations using tools or without the use of tools. It can be divided into:
 1. Posture adjustment: depending on the failure site of maintenance object, virtual human changes the relative position with maintenance object and enter maintenance observation or maintenance work posture.
 2. Maintenance operation process: virtual human starts maintenance work with tools or without tools.

According to separate maintenance process stages and commonly used motions in VHMS, we divided virtual human maintenance motion into four categories, they are movement motions, posture adjustment motions, hand operation motions and tools operation motions. Table 1 shows details of the virtual maintenance motions of the four categories.

Table 1 virtual human maintenance motion description

Movement motions		Posture adjustment motions	
Name	Description	Name	Description
Walk	Alternately move left and right foot and swing arms	Stand	Natural standing, hands down
BendWalk	Move with waist bending at an angle	Bend	Bend forward a certain degree
Sidle	Move sideways	Sit	Rest weight on bottom with back vertical
Climb	Up and down stairs or steps	Squat	Crouch or sitting with knees bent
Creep	Move with the body closed to the ground	Kneel	Hit the ground with knee
Crawl	Move forward on the hands and knees with body dragged along the ground	SingleKneel	Hit the ground with left or right knee
Wriggle	Move with the back on the ground	LieDown	Lie down with abdomen closed to the ground
Carry	Move with objects	LieUp	Lie down with back closed to the ground
		LieSide	Lie down with one's side closed to the ground
Hand operation motions		Tools operation motions	
Name	Description	Name	Description
ArmMove	Arm move a distance	PryOut	Use small tools to pry
ArmLift	Arm move up	AwlTurn	Use tools to screw
ArmLower	Arm move down	Clamp	Clamp
ArmPush	Arm push forward	Peening	Peen
ArmTurn	Screw	Wrench	Wrench
ArmGrasp	Seize with finger	Impact	Use tools to hit with force
ArmRelease	Loosen one's grip		
ArmHold	Hold something firmly		

2.3 VHMMD Development

Jack is an ergonomic professional evaluation software, but there are some defects in the VHMS. It is poor control of the virtual human. Therefore, we redevelop Jack and establish VHMMD to suit various maintenance tasks.

Jack is programmed based on C language, the interface and operating platform are developed by Tcl/Tk. And Python language is utilized to write a JackScript for model motion controlling and analysis, so we use JackScript to develop VHMMD and control function, and we use Tcl/Tk language to develop control interface. Jack secondary development process is shown in Fig. 2.

JackScript provides a number of motion control functions such as Move, Walk, Rotate and MoveShoulder, JackScript can be viewed in the help document of Jack. By calling and integrating those functions in python, we can implement the required motions. The following example introduces how to call functions for virtual human motions.

```
from js import *
def t():
    h=CreateHuman()
    posture_1=h.Pose(name="stand_working")
    posture_2=h.Pose(name="squat")
    M=DoInOrder(a1,a2, duration=2, Start=0)
    M.Start()
```

For the above program, we define two postures for the created human. They are respectively stand_working and squat. Then we use DoInOrder function to realize movement from a standing posture to squat posture. The movement duration is 2 s.

By the same method, we realize virtual human motions that defined in Table 1, and those motions can be called in Jack. Figure 3 gives the VHMMD interface,

Fig. 2 Jack secondary development process

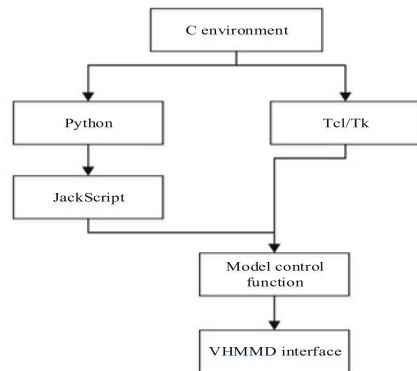
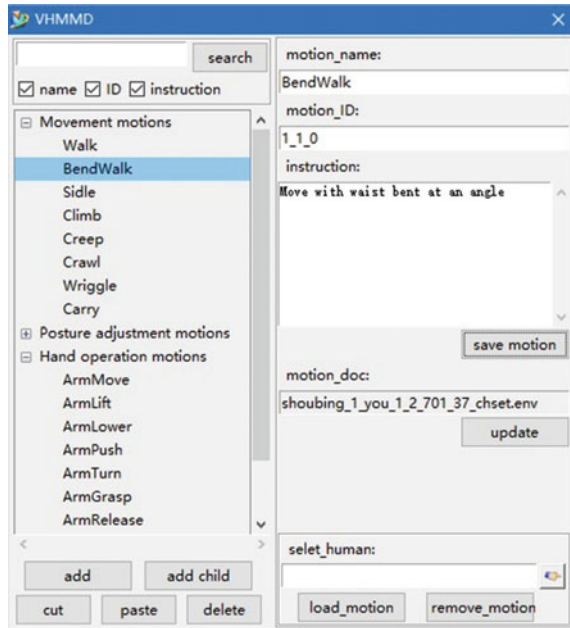


Fig. 3 Virtual human maintenance motion database



which is developed by Tcl/Tk. In VHMS process, we can load different motions for virtual human by selection. In addition to, we can also add motions to VHMMD according to the actual demand.

3 Virtual Human Maintenance Simulation

In this part, we apply VHMMD to a real maintenance process.

Oxygenation wrench is the key equipment for environmental control and life support subsystem of spacecraft, which is installed manually on an oxygenation valve. Return module is between the 2nd to the 3rd floor of assembly platform, and oxygenation valve is located on the wall of it. The installation of oxygenation wrench is given in Fig. 4.

After establishing virtual environment, the whole installation process was simulated in Jack. Figure 5 is simulation screenshots.

4 Virtual Maintenance Ergonomics Analysis

Many ergonomic factors affect maintenance. Analysis based on VHMS mainly includes reachability, visibility and fatigue [7].

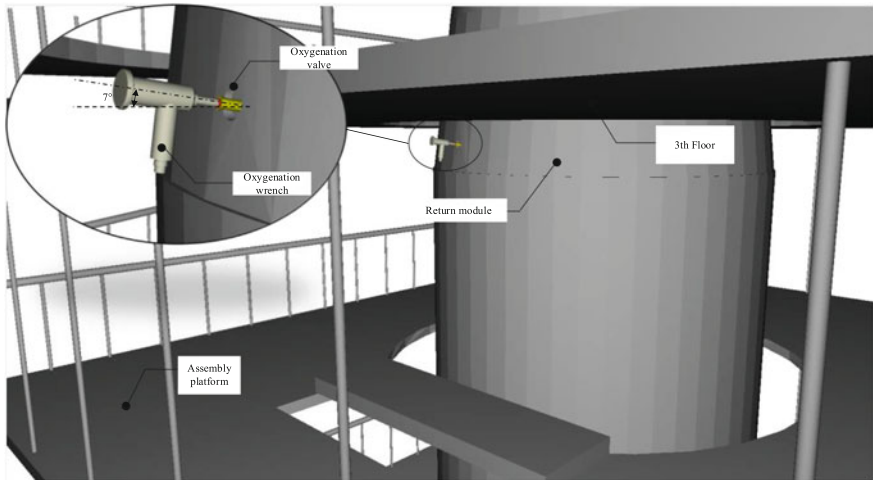


Fig. 4 The installation of oxygenation wrench in virtual environment

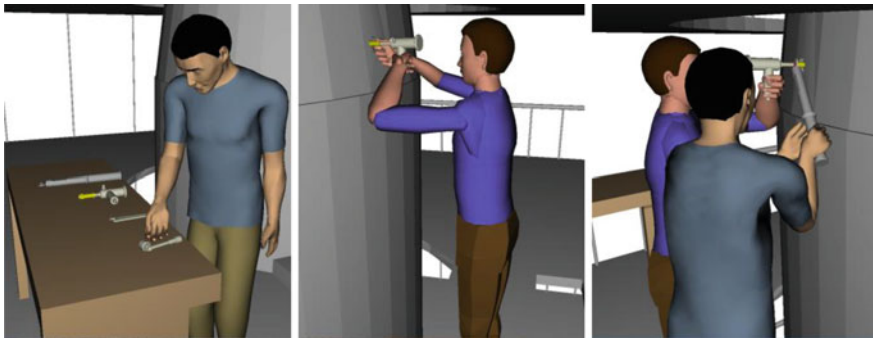


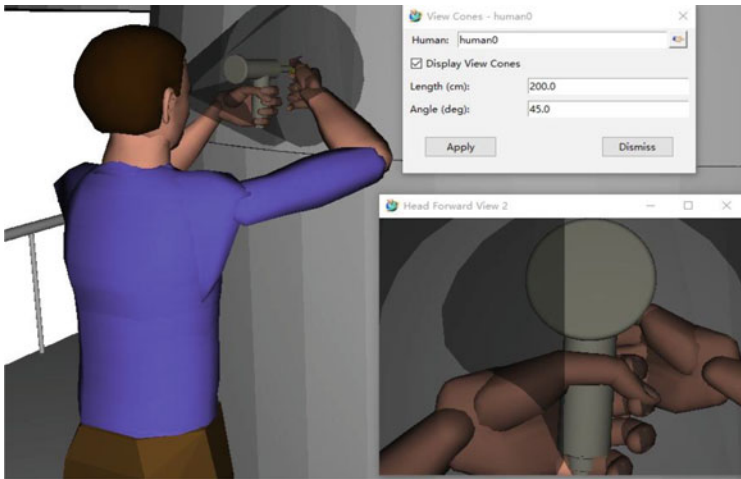
Fig. 5 Oxygenation wrench installation Simulation

Reachability reflects the impact of working space and parts layout of maintenance work. In VHMS, we can use Reach Zones to detect whether virtual human can approach the maintenance parts. Workspace is an important factor of reachability that needed to considerate. Using Collision Detection can find if the operation space for personal and tools is enough. By importing 95 % Chinese virtual human, collision detection algorithm provided in Jack was utilized to check the process of oxygenation wrench installation. The result is shown in Table 2.

Visibility is to determine whether maintenance parts are in the observation fields. According to Chinese control center ergonomic design guidelines, when personal is standing, the best view is 15° to 45° under the horizontal line. The View Cones of Jack can show virtual human view by parameter setting (Fig. 6).

Table 2 The collision detection results of entities in installation

Entity_1	Entity_2	Collision detection (yes/no)
Virtual human head	3rd floor	No
Virtual human arm	Return model sidewall	No
Socket wrench	Return model sidewall	No
Torque wrenches	Return model sidewall	No

**Fig. 6** Visible area with a 45° “view cone”

Fatigue is a complicated physiological and psychological feeling. Fast upper evaluation (RULA) is the most widely used method for evaluation of the risk of human upper limb currently [8]. We can select the key posture to make RULA analysis. Figure 7 shows the work posture analysis interface in JACK.

5 Conclusion and Discussion

For the process of oxygenation wrench installation in a virtual environment, the workspace is satisfactory, there is no collision between the virtual human and other parts, and the operating space for tools is sufficient. For the visibility detection, since the installation position is too high, we found that virtual human can't observe the installation position from the front (Fig. 7), which affects quality of oxygenation wrench installation. The RULA (Fig. 7) result shows that the posture is acceptable if not maintained or repeat for long periods, and it is also acceptable for other postures in the installation process.

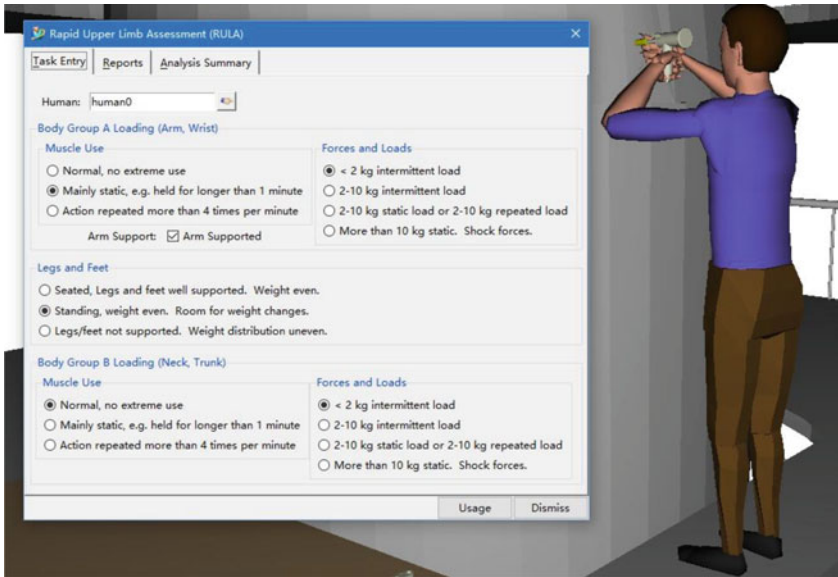


Fig. 7 RULA analysis for oxygenation wrench installation

For the virtual human motion design and ergonomics analysis mentioned above, we draw the following conclusions.

- (a) Maintenance task decomposition is useful for virtual human motion design. We gain the most motions in a specific maintenance process according to this method.
- (b) VHMD can be applied to virtual human maintenance simulation, and Table 1 is just an example for typical maintenance motions, more detailed maintenance motions may be added if needed.
- (c) There are also other ergonomics analysis method for human task in Jack, such as NIOSH analysis [9], for different aims, we can select different methods.
- (d) After ergonomics analysis, some improvement measures should be provided according to the result, we do not discuss how to improve the maintenance process because of length constraint.
- (e) Hand shape is also important for virtual human control in VHMS, it will be researched in the future.

Acknowledgments At the point of finishing this paper, I would like to express my sincere thanks to my supervisor, Ms. Xue Qing, who has given me so much useful advices on my writing, and has tried her best to improve my paper. Then, I would like express my gratitude to Mrs. Liu Minxia, who provided me much information regarding maintenance simulation. Without their help, it would be much harder for me to finish my study and this paper.

References

1. Kececioglu, D.: Maintainability, Availability, and Operational Readiness Engineering Handbook. DEStech Publications Inc., Lancaster (2003)
2. Chen, Z., Chen, J., Xu, C.Y.: Motion control for virtual human based on IK by two phases and key frames. *Comput. Eng. Des.* **33**(7), 2760–2765 (2012)
3. Drumwright, E.: A fast and stable penalty method for rigid body simulation. *IEEE Trans. Vis. Comput. Graph.* **14**(1), 231–240 (2008)
4. Yao, J., Lin, C., Xie, X., et al.: Path planning for virtual human motion using improved A* star algorithm[C]. In: 2010 Seventh International Conference on Information Technology: New Generations (ITNG). IEEE, pp. 1154–1158 (2010)
5. Peng, Fei, Zhao, Yao, Zhu, Zhijie, Yan, Fuyu: Sub-space decomposition-based incremental sampling path planning of virtual human. *Comput. Simul.* **05**, 423–427 (2014)
6. Vujosevic, R.: Maintainability analysis in concurrent engineering of mechanical systems. *Concurrent Eng.* **3**(1), 61–73 (1995)
7. Yu, F., Xue, Q., Meng, W., Liu, M.: Ergonomics evaluation of virtual maintenance process based on fuzzy and AHP method. In: Proceedings of the 22nd International Conference on Industrial Engineering and Engineering Management 2015. Atlantis Press, pp. 751–762 (2016)
8. Qiu, S., Yang, Y., Fan, X., He, Q.: Human factors automatic evaluation for entire maintenance processes in virtual environment. *Assembly Autom.* **34**(4), 357–369 (2014)
9. Dempsey, P.G.: Usability of the revised NIOSH lifting equation. *Ergonomics* **45**(12), 817–828 (2002)

Virtual Reality for Safety, Entertainment or Education: The Mars Mission Test

Irene Lia Schlacht, Antonio Del Mastro and Salman Nazir

Abstract A Virtual reality (VR) has many applications; the main ones are related to safety and performance, entertainment, and education. To increase safety and performance, VR may use, for example, simulation for training purposes or for improving the performance of the operator; in entertainment, it can be used to experience for fun new realities that are possible only virtually; and finally, in education, VR can be used to let the user learn in an immersive environment. This paper wants to open a debate on how to increase the trustworthiness of virtual reality in order to increase the number of possible applications in the field of safety.

Keywords Human factors · Human-systems integration · Virtual reality · Space mission

1 Introduction: Safety and Simulation

“The entertainment industry is one of the most enthusiastic advocates of virtual reality, most noticeably in games and virtual worlds. But other equally popular areas include:

I.L. Schlacht (✉)

Design Department, Politecnico di Milano, Extreme-Design Research Group,
Via Durando 38-a, 20100 Milan, Italy
e-mail: irene.schlacht@mail.polimi.it

I.L. Schlacht

Karlsruhe Institute of Technology, IFAB Institut für Arbeitswissenschaft und Betriebsorganisation, Kaiserstraße 12, 76131 Karlsruhe, Germany

A. Del Mastro

Italian Mars Society, Via Dalmine, 10/A, 24035 Curno, BG, Italy
e-mail: segreteria@marsociety.it

S. Nazir

Training and Assessment Research Group (TARG), University College of Southeast Norway (HSN), Notodden, Norway
e-mail: Salman.Nazir@hbv.no

- Virtual Museums, e.g. interactive exhibitions
- Galleries
- Theatre, e.g. interactive performances
- Virtual theme parks
- Discovery centres

Many of these areas fall into the category ‘edutainment’ in which the aim is to educate as well as entertain” [1]. However, there are also many possible scientific and educational applications, in areas such as training, testing of procedures, medical devices, and rehabilitation [2, 3]. One problem of scientific application of VR is that the context of the application may be confused with that of entertainment, decreasing the trust of the user and, as a consequence, negatively affecting the results. For example, if a doctor performs remote surgery on a patient, virtual reality may be used to increase performance and reduce the risk of failure. In the same way, VR can also help the patient to train their motor performance during rehabilitation. In both cases, trust in the system is very important to achieve an increase in safety and performance. Deutsche Bank created a simulation environment in Second Life where the user was able to interact with the bank as an avatar to learn about new credit opportunities and get consulting. But how ready are we to make investments in Second Life? How much trust do we have in virtual reality systems? How much might it be perceived as an application used just for fun?

2 The Case Study

This problem has been shared by the Italian Mars Society, which has developed a virtual reality scenario to help test and develop technologies for a human Mars mission. The Italian Mars Society [4] states: “The international space community is contemplating long-duration crewed missions to Mars in the near future. In this regard, human space mission simulators play an important role in developing and testing hardware and software technologies required for such missions. Simulators also provide an ideal platform for conducting research in psychology, physiology, medicine, mission operations, human factors and habitability. These research areas are critical in ensuring crew well-being and performance for long term space missions.”

A Mars surface and a Mars base mission have been reproduced virtually on the basis of the real Martian surface. “As operational test beds, the stations serve as a central element in support of parallel studies of the technologies, strategies, architectural design, and human factors involved in crewed missions to Mars. The facilities also feature field laboratories in which data analysis can begin before scientists leave the field site and return to their home institutions” [4].

The virtual interaction is done with immersive visual and audio environment using the Oculus Rift technology.

2.1 Test Procedures and Result

To verify the interaction and the trust in the system, the Mars scenario was proposed to 17 testers. The test was performed during the event “Bergamo Scienza” in Italy in 2015 and during a mission simulation in Madonna di Campiglio, Italy, in 2014.

2.2 Open Access Test

During the “Bergamo Scienza” event, to motivate the testers to use the virtual reality environment, a scenario was provided with several tasks within a questionnaire.

The scenario was a rescue mission: “*G1 Emergency Mission: The Mars 2035* V-eras station is contaminated by a toxic Martian fungus. You’re safe with your crew in a rescue module 2 km from the station, but there remain only a few hours of oxygen available to live in the module.

There is a solution: in the greenhouse of the station, the presence of a substance that immunizes against the effect of the fungus has been identified. To save the mission, you have to enter the lab. The mission depends on your help. Fulfill the tasks and save the mission.” (Figs. 1, 2 and 3).



Fig. 1 Italian Mars Society VR system at “Bergamo Scienza” (© Italian Mars Society 2015)



Fig. 2 Italian Mars Society VR system at “Bergamo Scienza” (© Italian Mars Society 2015)

In this paper, the most important observations from this test are reported. The persons who volunteered for the test were mostly younger, under 35 years of age. Of the 17 tests, only 2 were incomplete and not valid. The other 15 subjects completed the entire test.


The first task was described as follows: “Enter the station, try to orient yourself as quickly as possible to get to the greenhouse where the immunizing substance is located. Check how long it takes; if you can get there within 60 s, you will not get contaminated.”

Only 1/5 of the testers found the task difficult; among the persons who found this difficult, only one was under the age of 35, which demonstrated that the first approach with the software was quite intuitive at least for persons under 35 years of age.

The second task was described as follows: “Now you have the immunizing substance and you have to reach the crew as soon as possible. Exit the station; the sand outside is contaminated by the fungus, so be careful not to stir it up! EXIT FROM THE STATION AND MOVE AWAY as quickly as possible to the emergency module.”

A little more than $\frac{1}{4}$ found this task difficult; in this case, a decrease in performance was also seen among younger testers. However, the majority of the people still found the first and the second task easy, showing that the system may be intuitive for most people.

Bergamo Scienza
3-17 October 2015 The Italian Mars Society



Welcome to Mars! Please answer the following questions and begin the mission:

- *If you participate in the mission, you agree that your answers will be used anonymously for the development of other missions. O I agree; O I do not agree*
- *You are aware that your contribution is voluntary and you can stop the simulation at any time. O yes O no*
- *Your age is 0-18 years: O 18-25; O 25-35; 35-50 O; O >50*
- *You are: O student; O professional O professional from the field*

G1 Emergency Mission

The Mars 2035 V-eras station is contaminated by a toxic Martian fungus. You're safe with your crew in a rescue module 2km from the station, but there remain only a few hours of oxygen available to live in the module.

There is a solution: in the greenhouse of the station, the presence of a substance that immunize against the effect of the fungus has been identified. To save the mission, you have to enter the lab. The mission depends on your help. Fulfill the task and save the mission.”

Task 1

Enter the station, try to orient yourself as quickly as possible to get to the greenhouse where the immunizing substance is located. Check how long it takes; if you can get there within 60 seconds, you will not get contaminated.

Time O <60 sec. O > 60 sec.

Level O difficult O ok O easy

Task 2

Now you have the immunizing substance and you have to reach the crew as soon as possible. EXIT the station; the sand outside is contaminated by the fungus, so be careful not to stir it up! EXIT FROM THE STATION AND MOVE AWAY as quickly as possible to the emergency module.

Your rover is turned upside down O yes O no

Level O difficult O ok O easy

Task 3

The crew has caught up with you and is safe, but the mission is not finished; Earth awaits communication. Answer the 6 questions and end the mission. If you want to, you can also leave your suggestions.

1. Tasks 1 and 2 were completed successfully without stress. O yes O no Suggestions:
2. The mission is realistic and I identified myself with the context. O yes O no Suggestions:
3. The Martian terrain has a very realistic effect. O yes O no Suggestions:
4. The simulation is optimal. O yes O no Suggestions:
5. The mission is useful for increasing my knowledge and can be used in education. O yes O no

What field: Tips:

(Optional) Other suggestions are welcome:

Mission Support sends thanks from Earth if you want to leave the simulation team. Add your contact details to the mailing list of the Mars Society to get information about the next mission.

Mission Over.

Fig. 3 The questionnaire, Italian Mars Society VR system at “Bergamo Scienza”

Table 1 OBSERVATIONS
 V-ERAS: MISSION G1
 (Italian Mars Society,
 17.10.2015, Bergamo
 Scienza)

Observations:
• Increase the graphics
• 3 toilets needed inside the station
• Plants will make it prettier
• Need to be improved
• Support audio
• It is more for entertainment
• Is just a game; make it more scientific and useful
• Avoid having to close the door
• The knowledge was increased by the tutorial
• Graphical mistakes: door too small and wall that became transparent
• You can walk through the wall

As a conclusion of the experiment, five questions were asked to understand how the system was perceived.

Of the 15 testers, two thirds reported the tasks as stressful, which also shows that these persons were actually involved in the tasks. Also, the majority reported that they had been able to identify themselves with the scenario, in particular, the subjects under the age of 35; on the other hand, of the 4 subjects over the age of 50, only 1 managed to identify himself with the virtual environment. The overall quality was evaluated positively by the majority of the testers. Regarding possible applications of the mission, such as with regard to learning features or educational application, the system was associated more with entertainment than with education or training like from the observations reported (Tables 1 and 2).

2.3 Test with Selected Persons

During the mission in Madonna di Campiglio, a mission simulation was also performed with a more complex task over a period of one week. The team had some problems related to the low level of comfort of the equipment. However, there was no observation or comment or doubt about the main scientific purpose of the system with regard to scientifically testing procedures, equipment, and overall mission aspects. More information is reported in “Space Missions a safety model” [5] (Figs. 4 and 5).

Table 2 RESULT V-ERAS: MISSION G1 (Italian Mars Society, 17.10.2015, Bergamo Scienza)

Age		0-18			18-25				25-35			35-50		50+			Total			
17 subjects, 2 tests not valid		A	B	C	D	E	F	G	H	I	L	M		N	O	P	Q	15		
Interaction Easy: V; Ok: 0; Difficult: X																	V	0	X	
T1	Station	V	0	0	0	X	0	0	0	V	V	V		X	V	V	X	6	6	3
T2	Rover	X	X	0	V	V	0	X	V	0	V	0		V	0	V	X	6	5	4
Tot																	12	11	7	
Qualities Yes: V; No: X																				
T3.1	Stress	X	V	X	X	V	V	X	X	V	V	V		V	V	V	V	10		5
T3.2	Identification in the avatar	X	V	V	V	V	V	X	V	V	X	X		V	X	X	X	8		7
T3.3	Terrain	V	V	X	V	V	V	-	V	X	X	X		V	X	X	X	7		7
T3.4	Simulation	V	V	V	X	V	V	X	V	V	X	X		V	X	V	X	9		6
T3.5	Application: knowledge and education	V	V	V	X	V	X	X	V	X	X	X		V	X	X	V	7		8
Tot	V	3	5	3	2	5	4	-	4	3	1	1		5	1	2	2	41		-
Tot	X	2	-	2	3	-	1	4	1	2	4	4		-	4	3	3	-		33

Blue subject from the field

Fig. 4 Simulation on the motivity virtual dimension station



Fig. 5 Visualization of the avatar on Mars (© Schlacht 2014)



3 Conclusion

The Italian Mars Society developed a VR system to test possible missions to Mars, including rescue procedures.

With 17 testers, we studied how people would react and how much the program may be trusted to act as training and testing facility. The VR system attracted mostly young people. The majority of the people did not see a strong purpose in terms of acquiring knowledge or using it as an educational application, leading us to conclude that the entertainment aspect is stronger. To increase the level of trust and improve scientific application, the persons involved need to be selected and trained as in the tests performed with selected persons. If the VR system is open to the public, it will attract mostly young people, who will emphasize the entertainment aspect. If the system is used in a restricted environment with selected and trained persons, the purpose and the results could be scientific.

Acknowledgments Thanks to all the person & institutions involved. For the images: Italian Mars Society.

References

1. Virtual Reality Blog.: Virtual Reality in Entertainment. <http://www.vrs.org.uk/virtual-reality-applications/entertainment.html> (2015)
2. Schultheis, M.T., Rizzo, A.A.: The application of virtual reality technology in rehabilitation. *Rehabil. Psychol.* **46**(3), 296–311. <http://dx.doi.org/10.1037/0090-5550.46.3.296> (2001)
3. Kaufmann, H., Dünser, A.: Virtual reality. In: Summary of Usability Evaluations of an Educational Augmented Reality Application, Lecture Notes in Computer Science, vol. 4563, pp. 660–669 (2007)
4. Italian Space Society.: Project Overview. <http://erasproject.org/project-overview/> (2015)
5. Schlacht, I.L.: Space Mission as Safety Model. *Ergonomics and Human Factors in Safety Management* (2016)

The Argument for Simulation-Based Training in Dietetic Clinical Education: A Review of the Research

Farhood Basiri

Abstract Simulation methodology has been successfully incorporated into a multitude of health care education disciplines with demonstrated efficacy through validated evaluation and research. Similarly, health education programs have increasingly implemented modeling and simulation methodologies into their curricula. At this time, however, there is comparatively little research of simulation-based tools or methodologies used in dietetic clinical education. Does simulation-based health education produce positive learning outcomes? Is there evidence-based research to substantiate adoption of simulation-based methodologies and tools in clinical dietetic education? This article focuses on the qualitative and quantitative research currently available in this arena.

Keywords Modeling and simulation · Dietetics simulation · Simulation-based instruction · Clinical training · Medical simulation training · Health care education

1 Introduction

Schools of Nursing and related fields in health care education are undergoing radical change as once-traditional methods of instruction are criticized for failing to effectively deliver content and training based on real-world expectations [1]. Health education programs have increasingly implemented modeling and simulation tools in effort to provide learners opportunities to train and rehearse clinical activities in low-risk, simulated environments prior to their transition into industry practice. Do simulation-based education strategies produce positive learning outcomes in health care fields similar to dietetics? Specifically, is there evidence-based research to substantiate adoption of simulation-based methodologies and tools into clinical

F. Basiri (✉)

Institute for Simulation and Training, University of Central Florida,
3100 Technology Parkway, Orlando, FL 32826, USA
e-mail: fbasiri@knights.ucf.edu

dietetic education? This discussion will look at several studies and attempt to answer these questions.

1.1 Simulation Methodology in Health Care Education

Although simulation often incorporates new and interactive technologies as a delivery vehicle, it is not a technology [2]. Simulation is defined as the instructional techniques and methodologies used to replace or imitate real experiences through guided, participative scenarios [2]. Simulation for the purpose of health care education began decades ago with the use of low-fidelity simulations and has evolved at an unprecedented pace [3].

Now, in 2016, Simulation methodologies have been successfully incorporated into a multitude of health care education disciplines with demonstrated outcomes through validated evaluation and research. West, et al. state “the focus of nursing education has changed from a didactic teaching approach to an interactive learning approach” [1], one where greater emphasis is placed on learner competency, critical thinking and decision-making skills, and enhanced interdisciplinary interactions which result in reduced practitioner mistakes as well as improved patient safety [4]. While many critical texts advocate for health care education to incorporate interactive, immersive, or simulation-based instructional methodologies (and transition away from didactic or traditional instruction), few acknowledge the potential benefits to dietetics education [5, 6].

1.2 Transferability of Simulation-Based Tools and Methods

The American Association of Colleges of Nursing (AACN) state simulation experiences provide learners a safe and effective environment to apply the cognitive and performance skills necessary for professional practice [7], and presently, simulation methodologies are integrated into many nursing education programs [8]. Aside from teaching practitioner skills, the AACN has found simulation-based educational strategies capable of measuring proficiency of learners’ clinical skills and applied knowledge [9]. As both nursing and dietetics are competency-based disciplines, they can both benefit from simulation-based educational methodologies [9].

Thompson and Gutschall, in their *Blueprint for Simulation in Dietetics Education*, support the transferability of simulation methodology in nursing education settings to dietetics education via the premise that existing nursing literature related to simulation-based education can be extrapolated to formulate the framework for the design, development, and implementation of simulation-based tools and methodologies for dietetics education [4]. Transferability appears to be an obvious, natural fit, based on their comparison of the AACN’s defined list of

Essentials of Baccalaureate Education for Professional Nursing Practice [9] and the *Selected Core Competencies for Registered Dietitians* skills [10].

2 Educator Challenges

Dietetics education programs suffer comparable challenges and are arguably under greater pressures when reliant upon resources often shared by nursing education programs. Dietetics educators are also faced with a dwindling number of clinical sites for training dietetics students and interns in clinical preparedness [10, 11]. While evidence supports the efficacy and benefits of simulation methodologies in health care education, few instructors possess the skills to immediately integrate simulation into their curricula, first needing guidance to effectively incorporate such technologies and methods into their programs of study [10]. According to Arthur et al., “academic staff who are responsible for simulation activities require a range of skills and may need additional training in new technologies [10].” Further studies have shown growing interest in simulation-based health care training, and its associated pedagogical research can also be attributed to the increased pressures facing health care educators; chiefly a shortage of health care faculty, the growing complexity of the health care industry, climbing financial penalties associated with practitioner mistakes, growing industry-wide demand for care, and an overall reduction in the availability of health care educational resources—specifically clinical training placements for students [12, 13]. Yet the health care industry calls on educators to do a better job preparing students for professional practice despite the inadequacy of educational resources, as industry employers can no longer offer resource-intensive programs designed to transition recent nursing graduates into independently functioning caregivers [13].

This industry demand, coupled with responsibilities inherent to dietetics instruction alongside many other pressures facing dietetics education programs create an opportunity—and urgent need—to develop sustainable and efficient educational tools for dietetics clinical instruction. A limited number of dietetics programs have implemented simulation-based strategies to address rotation site shortages, but further search is needed to analyze the efficacy of these efforts [5, 14, 15].

2.1 *Resources for Simulation Development in Dietetics Education*

A complex instructional methodology, simulation should be carefully and deliberately phased into existing dietetics curricula in a manner that allows for careful evaluation to ensure no deterioration in program quality [4]. Readily available

nursing simulation frameworks can be modified and incorporated into dietetics-focused frameworks. Evaluation tools have been developed to ensure stringent quality benchmarks in nursing simulation methodologies in both low- and high-fidelity tools [16–18]. Although these tools were designed for a variety of health care education fields, they may serve as useful models for the development of dietetics-specific instruments [18].

In 2015, the International Nursing Association for Clinical Simulation and Learning (INACSL) published their updated *INACSL Standards of Best Practice: SimulationSM*, a set of performance standards addressing nine key simulation areas for nursing education [19]. Jeffries' proposed framework and evaluation tools such as the Simulation Design Scale (SDS) and Educational Practice in Simulation Scale (EPSS) provide dietetics educators a foundation of conceptual tools and models on which to base their simulation frameworks [10, 13, 20].

3 Justifications for Adoption of Simulation Methodologies in Dietetics Education

3.1 Reduced Practitioner Errors

The *Evidence-Based Handbook for Nurses* published by the U.S. Agency for Healthcare Research and Quality contends it unrealistic to assume recent graduates of nursing education programs have received the full and complete practitioner training necessary when transitioning to industry practice [21]. The handbook further asserts, “orientation programs for new graduates and continuing education for nurses are essential tools to help practitioners improve their knowledge, skills, and expertise so that quality patient care is provided and outcomes are optimized while errors are minimized [21]. In the past, educators aimed to produce competent practitioners by providing learners a variety of clinical experiences to which students could apply classroom content [13]. With limited educational resources, however, today’s students are found to lack the critical skills vital for professional clinical practice. Simulation-based tools provide for efficient methods of teaching clinical content and practitioner skills without fear of causing harm to real patients [13, 15, 18].

3.2 Improved Patient Safety and Wellbeing

Over the past 17 years, scholars have increasingly recognized the painful consequences of practitioner errors. Research by Durham and Alden suggest an “alarming rise in morbidity and mortality among hospitalized patients throughout the United States heightens concerns about professional competency [21].” Raising

similar alarms, a major study in the Institute of Medicine's 2000 report, *To Err is Human: Building a Safer Health System*, suggests nearly 100,000 preventable deaths can be attributed annually as a result of medical error [22]. The report goes on to urge improvements in patient safety by "establishing a national focus to create leadership, research, tools, and protocols to enhance the knowledge base about safety [22]. Following the report's release, the US Agency for Healthcare Research and Quality supported the development of new technologies to reduce medical errors, conducted large-scale projects to test safety intervention strategies, and provided funding for researchers to develop and demonstrate new approaches for improving provider education [22].

3.3 Learner Access to Repeatable Lessons

Effective simulation-based education tools normally allow for learners to repeat scenarios in order to become proficient in skills and procedures [21]. Without simulation tools, learners may be limited by clinical site and/or instructor availability in order to practice lessons, gain confidence, or obtain knowledge beyond their minimum proficiency levels [4, 6, 13, 20]. The combination of interactive technologies and simulation methodologies allow for learners and practitioners to complete a variety of low-risk simulated scenarios, with or without an instructor's presence, in or outside of a real clinical environment. And although current technology limits the realism and fidelity of simulated experiences, they nonetheless allow students to experience a variety of critical events before they are responsible for one in a working, real world environment [23].

3.4 Improved Quality of Education

Simulated scenarios allow for greater depth of student learning experiences. Dietetics students participating in a clinical rotation may not experience a particular type of patient scenario, whereas with simulation many things become possible. Simulation can provide learning tools for clinical scenarios which, although important, may be difficult for some health care educational programs to present in an effective model or ideal framework. In these cases, applicable simulation methodologies could be incorporated instead to provide educational scenarios to the benefit of program learners, and by extension, to the future patients they aim to serve. Reduced dependency on clinical site resources may also allow for instructors to focus more on student learning outcomes than pure facilitation of instruction.

Acknowledgments The author wishes to acknowledge his instructors and colleagues from Florida State University and the University of Central Florida for their many years of mentorship and support.

References

1. West, C., Usher, K., & Delaney, L.: Unfolding case studies in pre-registration nursing education: Lessons learned. *Nurse Educ. Today* **32**(5), 576–580 (2012, 2011). doi:[10.1016/j.nedt.2011.07.002](https://doi.org/10.1016/j.nedt.2011.07.002)
2. Gaba, D.: The future vision of simulation in health care. *Qual Safety Health Care* **13**(suppl_1), I2–I10 (2004) doi:[10.1136/qshc.2004.009878](https://doi.org/10.1136/qshc.2004.009878)
3. Lapkin, S., Levett-Jones, T., Gilligan, C.: A systematic review of the effectiveness of interprofessional education in health professional programs. *Nurse Educ. Today* **33**(2), 90–102 (2013). doi:[10.1016/j.nedt.2011.11.006](https://doi.org/10.1016/j.nedt.2011.11.006)
4. Thompson, K., Gutschall, M.: The time is now: A blueprint for simulation in dietetics education. *J Acad Nutr Dietetics* **115**(2), 183–194 (2015). doi:[10.1016/j.jand.2014.12.001](https://doi.org/10.1016/j.jand.2014.12.001)
5. Turner, R.E., Evers, W.D., Wood, O.B., Lehman, J.D., Peck, L.W.: Computer-based simulations enhance clinical experience of dietetics interns. *J. Am. Diet. Assoc.* **100**(2), 183–190 (2000). doi:[10.1016/S0002-8223\(00\)00059-6](https://doi.org/10.1016/S0002-8223(00)00059-6)
6. Safaii-Fabiano, S.J., Ramsay, S.A.: The effect of classroom simulation on dietetics students' self-efficacy related to medical nutrition therapy. *J. Am. Diet. Assoc.* **111**(9), A57–A57 (2011). doi:[10.1016/j.jada.2011.06.207](https://doi.org/10.1016/j.jada.2011.06.207)
7. Academy of Nutrition and Dietetics Education. (2012, April 10). Update for the 2012 NDEP Area Meetings. Retrieved from <http://www.indiana.edu/~nutrvmg/DEP2012.html>
8. Forrest, K., McKimm, J., Edgar, S.: *Essential simulation in clinical education*. Wiley, Chichester, West Sussex (2013)
9. American Association of Colleges of Nursing. *The essentials of baccalaureate education for professional nursing practice*. (October, 20, 2008)
10. Kable, A.K., Arthur, C., Levett-Jones, T., Reid-Searl, K.: Student evaluation of simulation in undergraduate nursing programs in Australia using quality indicators. *Nursing Health Sci.* **15** (2), 235–243 (2013). doi:[10.1111/nhs.12025](https://doi.org/10.1111/nhs.12025)
11. Hampl, J.S., Herbold, N.H., Schneider, M.A., Sheeley, A.E.: Using standardized patients to train and evaluate dietetics students. *J. Am. Diet. Assoc.* **99**(9), 1094–1097 (1999). doi:[10.1016/S0002-8223\(99\)00261-8](https://doi.org/10.1016/S0002-8223(99)00261-8)
12. Reising, D.L., Carr, D.E., Shea, R.A., King, J.M.: Comparison of communication outcomes in traditional versus simulation strategies in nursing and medical students. *Nur Edu Perspect.* **32** (5), 323 (2011)
13. Jeffries, P.R.: A framework for designing, implementing, and evaluating simulations used as teaching strategies in nursing. *Nur Educ. Perspect.* **26**(2), 96 (2005)
14. Evers, W.D., Turner, R.E., Bell, C.T.: Use of multimedia simulations for developing clinical reasoning skills may affect scores on the registration examination for dietitians. *J. Am. Diet. Assoc.* **104**(8), 39 (2004). doi:[10.1016/j.jada.2004.05.105](https://doi.org/10.1016/j.jada.2004.05.105)
15. Turner, R.E., Evers, W.D., Bell, C.T.: Multimedia patient simulations in the undergraduate dietetics medical nutrition therapy course improve clinical reasoning skills of the dietetics intern. *J. Am. Diet. Assoc.* **104**(8), 39 (2004). doi:[10.1016/j.jada.2004.05.106](https://doi.org/10.1016/j.jada.2004.05.106)
16. Sando, C., Faragher, J., Boese, T., Decker, S.: Simulation standards development: An idea inspires. *Clin. Simul. Nurs.* **7**(3), e73–e74 (2011). doi:[10.1016/j.ecns.2010.12.004](https://doi.org/10.1016/j.ecns.2010.12.004)
17. Adamson, K.A., Kardong-Edgren, S.: A method and resources for assessing the reliability of simulation evaluation instruments. *Nurs. Educ. Perspec.* **33**(5), 334 (2012)
18. Arthur, C., Leyett-Jones, T., Kable, A.: Quality indicators for the design and implementation of simulation experiences: a delphi study. *Nurse Educ. Today* **33**(11), 1357–1361 (2013). doi:[10.1016/j.nedt.2012.07.012](https://doi.org/10.1016/j.nedt.2012.07.012)
19. The International Nursing Association for Clinical Simulation and Learning: *INACSL Standards of Best Practice: Simulation* (June, 2015). Retrieved from <http://www.inacsl.org/i4a/pages/index.cfm?pageID=3407>

20. Tosterud, R.: Karlstad University, Faculty of Health, Nature, and Engineering (from 2013), & Department of Health Services (in Swedish). Simulation used as a learning approach in nursing education, Students' experiences and validation of evaluation questionnaires (2015)
21. Hughes, R.G. (ed.): Patient safety and quality: an evidence-based handbook for nurses (Prepared with support from the Robert Wood Johnson Foundation). AHRQ Publication No. 08-0043. Rockville, MD: Agency for Health care Research and Quality (March 2008)
22. Kohn, L.T., Corrigan, J., Donaldson, M.S.: To err is human: building a safer health system. National Academy Press, Washington, D.C (2000)
23. Sanford, P.G.: Simulation in nursing education: a review of the research. Qual. Rep. **15**(4), 1006–1011 (2010). Retrieved from <http://www.nova.edu/ssss/QR/QR15-4/sanford.pdf>

The Working Posture Controller— Automated Assessment and Optimisation of the Working Posture During the Process

The Duy Nguyen, Carla Pilz and Jörg Krüger

Abstract We present the Working Posture Controller (WPC), a novel technology to help workers preventing posture-related Musculo-skeletal disorders. The innovation lies in the fact that the system does not require tedious work place design or process planning, since it automatises these steps. We discuss this technology from different views including a first technical evaluation, discussions concerning use cases, safety and economic and legal challenges when integrating such a technology into the production line.

Keywords Human centred automation · Musculo-skeletal disorders · Assistance system

1 Introduction

Except elaborated automation technology, the human worker is still a vital component in the production line. Human workers become especially indispensable when the production is characterised by low lot sizes or the tasks require high senso-motoric skills. Unfortunately, enterprises and their work force often face the problem of Work-related Musculo-skeletal Disorders (WMSDs) reducing productivity and resulting in high health expenses. WMSDs are one of the most significant reasons for worker absenteeism in companies. In the EU the costs related to WMSDs are estimated at upto 2 % of the GDP, which translates to around € 240 bn [1].

Human Centred Automation (HCA) [2] denotes the shift of paradigm in manufacturing through turning away from fully automated production lines to tightly

T.D. Nguyen (✉) · J. Krüger
Technische Universität Berlin, Chair for Automation Technology,
Pascalstr. 8-9, 10587 Berlin, Germany
e-mail: theduy.nguyen@iat.tu-berlin.de

C. Pilz
INPRO Innovationsgesellschaft mbH Berlin, Steinplatz 2, 10623 Berlin, Germany
e-mail: Carla.Pilz@inpro.de

coupled human-machine systems. The human represents the core of such manufacturing systems and the machine's task becomes to assist the human by compensating weaknesses and providing additional capabilities. HCA aims to increase the flexibility and productivity combining the adaptivity of the human worker with the strength and precision of the machinery. Through its capabilities to perform forceful tasks, there is potential to significantly reduce the physical load and, thus, ease the problem of WMSDs.

We present a novel system, the "Working Posture Controller" (WPC) [3], which aims at reducing the posture related MSD risk. Unlike solutions proposed so far, this equipment operates immediately in the process instead of requiring manual planning effort. The significance of this work lies in the development of a novel form of MSD prevention equipment, which is able to operate in the process without human involvement. The system consists of an intelligent sensory system to monitor the working posture and an actuator system, which holds the work piece and is able to manipulate its pose. After an automatic assessment of the worker's posture, the actuator automatically adjusts the work piece pose to enable adopting a natural working posture. The adjustment of the work piece takes only a few seconds after an ergonomically unfavourable posture has been detected. The system does not need human expertise for the work place design and can adapt to individual anthropometry. In past works, we have intensively described the technical details. Since we believe that developing such a new solution requires a holistic approach including technical and social aspects, this paper concentrates on the aspects besides the core technology, namely use cases of such a technology and economic and legal challenges when introducing into the factory line.

2 Related Work

According to Punnett and Wegman [4], MSDs include a wide range of inflammatory and degenerative conditions affecting the muscles, tendons, ligaments, joints, peripheral nerves, and supporting blood vessels. Most commonly affected body regions are low back, neck, shoulder, forearm and hands.

Putz-Anderson et al. [5] identify the most dominant risk factors for MSDs as force exertion, monotonous strain through repetitive movement and awkward static posture over a long time. The risk factor force is defined either as an external load e.g. in material handling or as an internal force on a body structure. The risk factor repetition characterises monotonous strain originating from cyclical work, which involves repetitive movement. Repetition shall not be considered as primary factor, but always in combination with posture or force. The risk factor posture is often caused by adopting an awkward static posture for many hours a day—sometimes in combination with forceful work and highly repetitive actions.

2.1 Traditional WMSD Prevention

There has been extensive research and proposed measures from different scientific disciplines, including human factors, medicine and engineering to prevent WMSDs. In order to help work place designers and ergonomists to choose the appropriate approach out of the myriad of solutions, Goggins et al. [6] propose an effectiveness scale for ergonomic interventions. The most effective measures are the ones, which completely eliminate the exposure (level 1). If this is not possible, level 2 measures are preferred, which reduces the exposure intensity. Afterwards, measures are recommended, which at least reduce the time of exposure (level 3), such as organisational measures. Finally, the least effective solutions are the ones, which merely rely on the worker’s behaviour (level 4). In the following, examples are listed addressing each risk factor.

The complete separation of the worker from the force or a reduction (level 1–2) is mostly achieved by automation of mechanisation of the process through introduction of equipment. Schmidler et al. [7] call such devices lifting aids or transport assistance. Exposure time (level 3) can be reduced by allowing longer breaks or introducing job rotation. Finally, ergonomic interventions have often involved the training of lifting techniques [8] (level 4).

For the risk factor repetition, Bergamasco et al. [9] propose the following level 2 methods: These are namely work place layout optimisation and the introduction of ergonomic instruments and tools reducing the use of force, awkward postures and movements. Furthermore, there are level 3 measures, such as job design or increased rest periods. Worker training (level 4) can be employed to address the correct motion while performing the task.

The key to eliminate the risk factor posture is to enable the worker to avoid awkward postures or to reduce the time the worker has to adopt it. Basically, this is done by careful anthropometric work place geometry design [10] (level 1–2). Also, job rotation schemes can reduce the exposure time (level 3). Finally, training the subject to regularly alternate between postures (level 4) e.g. sitting and standing [11] can help to reduce the risk. Additionally, alert systems [12] can be introduced, which notify the user when an awkward posture is adopted over a pre-defined period of time.

Ergonomic interventions can be distinguished by whether the measures are applied when the process is planned (e.g. work place design) or when they directly operate in the process (e.g. lifting aids) being able to quickly adapt to new situations. Table 1 depicts the best achievable level of effectiveness for each risk factor in each phase. Whereas the force risk factor can be eliminated by methods in the

Table 1 Best achievable effectiveness of measurements [6] addressing each MSD risk factor

	Planning	In process
Posture	Level 1	Level 4
Force	Level 1	Level 1
Repetition	Level 1	Level 4

planning phase as well as in the process, the factors posture and repetition lack this flexible option.

2.2 Computer Aided WMSD Prevention

With the advance of computers, researchers in manufacturing technology found new ways to support engineers and ergonomists in their task of MSD prevention. This section briefly describes the technologies which play an essential role for our system.

Digital Human Models (DHM). Digital Human Models are virtual representations of the real worker used in factory simulation tools. DHMs allow the designer to visualise and insert the human into a complex environment to simulate and perform task-related as well as ergonomics related analyses. Delleman et al. [13] state several reasons why these techniques have been created. Firstly, there is a cost motivation. Designing and producing hardware prototypes is time consuming and cost intensive. While requiring higher effort to digitise the prototypes, DHMs pay off in later stages where multiple physical alternatives have to be evaluated. Secondly, testing prototypical work places requires a large population with different anthropometrics and capabilities to verify. DHMs offer an efficient way to test the setup with different virtual individuals. Finally, the 3D representation of the DHM enables additional visualisations e.g. of the worker's field-of-view, which are hard to obtain using traditional assessment methods. Application areas lie in design, modification, visualization and analysis of virtual workplaces or product interactions [14].

DHMs offer high potential to answer questions concerning work place design by simulation. Their purpose is to simplify the usage of powerful level 1 measures in planning phase. However, programming a realistic motion for the DHM is tedious. Hence sensory has been developed to naturally capture the worker's motion. Either optical sensors [15] or acceleration/inertia-based sensors [12] have been used, so far. The acquired data can be used for further analysis by specialists, to enhance the realism of DHM motions or to implement in-process warning systems [12].

Human Robot Collaboration. Human Robot Collaboration aims at delegating the forceful parts of a task to robotic manipulators, so-called Intelligent Assist Systems (IAS) or Intelligent Automation Devices (IAD) [16]. Due to intelligent sensor systems and elaborated safety mechanisms, human and robot can share the work place combining each other's strengths. The main purpose of this type of equipment is to apply powerful manipulators which execute ergonomically critical tasks on behalf of the worker, who controls equipment and process. Examples for such devices are Collaborative Robots (Cobots) [16] or Exo-Skeletons [17]. Thus, the advantage is that the technology represents a level 1–2 measure, but without requiring effort to plan the work place in detail.

An interesting approach has been researched by Thomas et al. [18], where an assistance system consisting of multiple robots has been developed to reduce the

labour intensive manual handling of heavy parts in welding. The idea is to apply robots to hold the part in such a way that the welder can process it without the need to adopt awkward postures. Based on the shape of the work piece and the welding task, a robot motion is planned in advance, which enables a natural working posture. The planning is supported by DHMs.

3 The Working Posture Controller (WPC)

As described in the last section, there have been effective methods proposed to deal with each single WMSD risk factor. However, most of them operate in the work place planning phase. In a mass customisation scenario, where there are low product batch sizes, this means that the planning has to be done for each new product, which turns out as tedious. In contrast computing power offers a chance to automatise the effort-critical parts leading to solutions, such as Cobots or Exo-skeletons. With the WPC, we intend to close this scientific gap enabling automated, adaptive and immediate workplace design.

3.1 Work Flow

The WPC system consists of two parts: a sensor and an actuator. The sensory system is positioned at the work place and monitors the posture of the worker during the whole process. For this purpose, we have developed an algorithm to capture the motion of the worker and assess the posture-related risk according to a simplified version of the “Ergonomics Assessment Worksheet (EAWS)” tool [19]. In case it exceeds an acceptable threshold, the system notices the worker and proposes a re-adjustment of the work place to enable a more natural working posture. An awkward working posture needs to be adopted when a region of the work piece is hardly visible or not accessible. Therefore, the spatial relation between worker and work piece has to be altered, such that the requirements can be met with still adopting a natural posture. The modification of the spatial relation is achieved by attaching the work piece to an actuator, which can modify its pose. If the user accepts the proposed adjustment, the sensor initiates the actuator to move the work piece. Figure 1 schematically depicts the sequence of actions when working with the WPC. Depending on the options of an enterprise, different types of actuators (industrial robot, height-adjustable platform, tilting table) can be employed to alter the pose of the work piece. The WPC is able to consider the available degrees of freedom (DoF) of the actuator and determine the best solution within these limitations. In the following, the methods used for the WPC are briefly described. The workflow is structured into the steps “Posture Assessment” and “Posture Optimisation”.

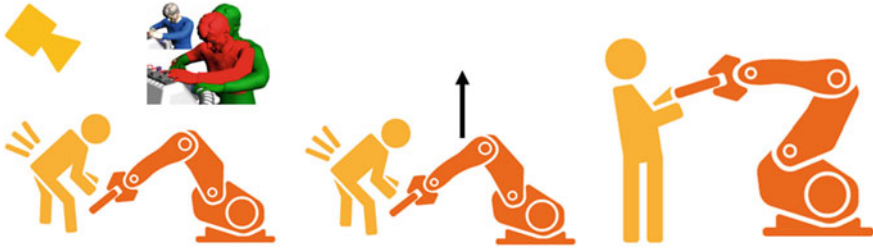


Fig. 1 Schematic description of the sequence of actions. In the *left image*, the sensor detects that the worker has performed the task in bent forward posture for a while, which affects the back. Hence, it initiates to rise the work piece (shown by the picture in the *middle*). The *right picture* then shows the worker performing the task in upright posture after adjustment

Posture Assessment. This section briefly describes how our system observes the occurring working postures during a process and computes a numerical score representing the ergonomic risk. The technical details have been intensively described in a previous work [3]. As sensory hardware, we use the Microsoft Kinect[®] sensor, which provides colour images as well as depth maps. The latter image type contains the distance of each pixel to the nearest obstacle in the scene. Hence, depth maps provide 3D information, which significantly simplifies the task of human motion analysis. The biggest advantages of the Kinect as sensor are its cost efficiency (price around 200 \$) and that the worker does not require to wear additional expensive equipment. We have chosen the hardware setup bearing in mind that will best achieve an impact when they can be widely employed. We use the EAWS [19] as the basis for assessing the risk in the postures. It is one of the most popular methods used for observation-based posture assessment. The EAWS assigns a pre-defined score for each occurring static posture in the process depending on its estimated physical load and share of time. Originally, this observational method requires a human expert to monitor the process. Automatising the EAWS requires the system to recognize the pre-defined postures in each image frame. In brief, we use a simple DHM, which we fit into the image data (the silhouette of the worker) using optimisation techniques. From the fitted DHM, we use Machine Learning algorithms to identify the posture.

Posture Optimisation. Having determined the posture, the goal is to adjust the work piece pose to enable a natural working posture. An adjustment is only triggered when the current EAWS score exceeds an acceptable threshold. We assume that the work piece is attached to an actuator. Given the input DHM determined in the Posture Assessment step, we strive to determine an actuator configuration, such that the worker is able to perform the task at least equally well compared to the situation before adjustment (goal 1) and simultaneously adopt a more natural posture (goal 2). Possibly, there is a trade-off between these two goals making it impossible to achieve both. In this case, the system shall find a configuration, which poses an acceptable compromise. Furthermore, the sought actuator configuration shall consider the available degrees of freedom meaning that the system proposes a

height value for a lift table and angular configurations for an industrial robot. As said in the name, we model this problem as a non-linear mathematical optimisation problem:

$$\begin{aligned} (\mathbf{x}, \mathbf{q}) &= \arg \min f(\mathbf{x}, \mathbf{q}) \\ \text{subject to } &g(\mathbf{x}) \leq 0, h(\mathbf{q}) \leq 0 \end{aligned} \quad (1)$$

The variable \mathbf{x} denotes the actuator configuration and \mathbf{q} represents the posture the worker will adopt after the adjustment. The objective function $f(\mathbf{x}, \mathbf{q})$ assigns low values for favourable postures \mathbf{q} and corresponding actuator configurations \mathbf{x} . The non-linear boundary conditions $g(\mathbf{x})$ and $h(\mathbf{q})$ can be defined to exclude unlikely postures or actuator configurations from the solution space. The solution to the optimisation problem (1) denotes the sought adjustment. Depending on the available degrees of freedom, f and g have to be appropriately modelled. Note that the solution \mathbf{q} is the predicted posture after adjustment based on the mathematical modelling and does not guarantee that the worker is able to fulfil the task in this way.

3.2 Use Cases

This section presents potential use cases for the WPC. Basically, they can be derived from the tasks of traditional work place design, as the works as automated work place designer. However, due to the ability to initiate an adjustment right in the process instead of afterwards, we can realise additional scenarios to support the worker.

Match the Working Height to the Task. According to the German standard DIN 33406:1988-07, the optimal working heights for work places for a standing worker depends on the task. For precision work a working height between 95 and 120 cm is recommended. Light work is best fulfilled in a height between 85 and 110 cm and heavy work in a height 65–95 cm depending on the worker’s anthropometry. These assumptions apply for smaller products. If the product is bigger, the range of working heights becomes wider, since the product dimensions have to be added to the working heights. If the system knows the severity of the task and the product size, it can incorporate these constraints into the Posture Optimisation problem. Moreover, DIN 33406 states that an optimal posture for precision work is sitting whereas heavy work is preferably performed standing. With adjusting the working height, the worker can be enabled to perform the task in the recommended posture.

Reduce Postural Load When Improving Reachability and Visibility. When regions of the work piece to be processed are not in range or not visible for inspection, the worker may have to adopt awkward postures to accomplish the task. This situation often occurs with large products when tasks are at different locations of the product. For example, modifying electric engines might require working on

top as well as at the bottom of the product. The WPC would increase reachability and visibility by changing the pose of the work piece instead of the pose of the worker.

Adjusting Force Direction. According to Schaub et al. [20] the maximum acceptable force exposure depends on the worker's posture and the direction the force is applied. When standing upright, higher force exertions are acceptable than when sitting with hands above head. Additionally, higher force exertions can be tolerated, if the force direction points downwards than upwards. Through adjustment of the work piece pose, a task that originally requires an upward force direction can be transformed into one requiring downward direction. Furthermore, by adjusting the working height, the worker can be enabled to stand or sit.

Reducing Severity of Monotonous Strain. In Sect. 2.1, it is stated that the risk factor repetition always depends on other risk factors, e.g. posture. Improving the posture for each cycle in a repetitive task also reduces the exposure intensity for the whole task. An example could be decreasing the distance between the worker and the product to be processed and thus avoid that the worker has to reach out every time.

Initiating a Dynamic Postural Change. Although upright standing postures and upright sitting postures are the most preferable ones according to the EAWS, monotonically adopting one of them leads to higher load. Hence, it is essential that the worker change the posture from time to time. Neuhaus et al. [21] encourages the worker to sit in 50 % of the time and stand in 50 %. Through the Posture Assessment component, system knows the current posture and the time the worker has remained in it. If the time exceeds a threshold, the system change the work piece pose, which then enables the worker to change his or her posture.

3.3 *Safety Mechanisms*

Since the system's actuators share a common work place with the worker and are able to create high forces, the safety mechanism are mandatory. The most current requirements for collaborative operation of robots and human are stated in the pre-standard ISO/TS 15066. Moreover, hazard scenarios have been classified. Haddadin et al. [22] mention the following possible contact scenarios to consider: unconstrained impacts, clamping in the robot structure, constrained impacts, partially constrained impacts, and resulting secondary impacts. Furthermore, there is another safety issue to be considered when the robot holds the work piece: In some circumstances, not all parts of the work piece are fixed. If the object is tilted, these parts could possibly fall out. Ideally, the safety mechanisms shall exclude all these threats. In the following, we briefly describe three mechanisms, which can enhance the safety of our system. We are aware of the fact that implementing all of them can reduce working efficiency. Therefore, the choice which one to implement depends on the specific use case.

Human Confirmation for Adjustments. Unexpected behaviour leading to injuries can be dramatically reduced when every action of the system needs to be confirmed by the human. A movement while the worker is performing a task can lead to a contact scenario in the worst case. Hence, a confirmation mechanism ensures that at least the worker expects the motion of the actuator. Alternatively, a manual mode can be integrated, where the user completely controls the actuator. In any case, the control interface should be placed outside of the manipulator's range. This guarantees doubled protection: First, the human is out of range. Second, the Posture Assessment system can confirm that the human is outside of the hazard area. Moreover, the actuator shall only move, when the human holds the confirmation button being fixed outside the range of the actuator. This dead man's switch like mechanism guarantees that the actuator stops moving as soon as the worker enters the hazard area. Finally, an explicit emergency stop is mandatory according to the DIN EN 60204-1. It should be placed near the worker in order to quickly react on potential clamping scenarios.

Reduced Degrees of Freedom. Collisions can be also avoided when the degrees of freedom can be effectively reduced, since this reduces the range of the actuator, and thus, the hazard area. For example, if the human stands in front of the work piece the chance of a collision is dramatically reduced when the actuator is only allowed to move vertically. This safety mechanism can also prevent unfixed parts from the product from falling out. The limitation of the end effector orientation can be realised in hardware as well as be incorporated into the Posture Optimisation problem as a boundary condition $g(\mathbf{x})$.

Reduced Speed. According to ISO 10218, the maximum allowed speed of the end effector in physical cooperation scenarios is 25 cm/s. This gives the worker time to react in case an unexpected situation happens. In the case of a contact, the reduced speed results in a lower force released onto the worker. If a higher speed is desired to increase efficiency, barrier mechanisms and the optical system can be used to determine the distance of the human to the manipulator. The further the worker is located the higher the execution speed can be set.

4 Technological Evaluation

We have conducted experiments to evaluate the performance of our system. In particular, we were interested how effectively can the risk be reduced? Therefore, we created a test dataset with image sequences of nine subjects performing various standing EAWS postures. The set of subjects comprises 1 female and 8 males with anthropometric heights roughly ranging between 1.5 and 2 m. The subjects performed working motions adopting the postures in a randomized order (see Fig. 2 (left) for example frames). The heights of the hands ranged from 0 cm (strongly bent) to 293 cm (hands above head). The duration of each posture was arbitrarily chosen to be between 1 and 3 s. We then determined the EAWS scores before and after adjustment by the system, which achieved a mean deviation of less than 10

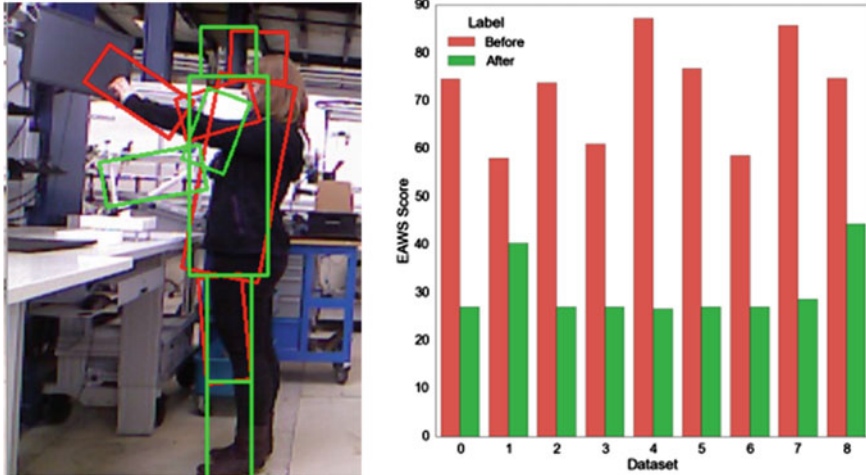


Fig. 2 Example for captured and predicted posture (*left*) and EAWS scores before and after adjustment (*right*)

points compared to human assessment in our experiments. Figure 2 (right) depicts the results.

Our system then simulated the adjustments using a lift table as an actuator and assessed the predicted posture. The EAWS [19] defines scores above 50 as critical and above 25 as considerable. Only scores below 25 points are completely acceptable. As can be seen in the results, the system manages transform all critical postures into at least partly acceptable ones. The majority of the posture sequences are fully acceptable.

5 Discussion

5.1 Technological Feasibility

Generally, the simulation results show that the system is able to significantly reduce the postural load. However, we need further experiments to verify whether the predicted postures are feasible to adopt and enable task fulfilment. The system in its current state only identifies 2D postures, since the capturing of 3D body parameters is a significantly harder problem, which cannot be solved with the approach used so far. Going from 2D to 3D dramatically increases the search space, which dramatically increases computation time. Therefore, cases, such as lateral bending or trunk torsion cannot be identified. Moreover, in its current state, the system is only able to monitor one worker in its field of view. Finally, the question of when the system should propose an adaptation of the work place, has not been considered. If it is

initiated too often, the user will be annoyed due to a frequent interruption of the work flow. As a first approach, the system could come up with an adaptation strategy, if a sequence of postures for a product is known. In this case, the first cycle can be used to observe and learn the posture sequence whereas the upcoming ones can be assisted.

5.2 Economic and Legal Challenges for Operation in Real Environment

Apart from technological challenges, there will be non-technological challenges to tackle when integrating such a new technology into the production line. In this section, we briefly discuss these issues. Since legal aspects play a fundamental role in the discussion and laws differ from country to country, we mostly focus on Germany.

Economic Challenges. The main economic challenge lies in persuading the enterprise that the benefits of using such a system will surpass the costs. Thereby, cost and benefit can be monetary as well as non-monetary, such as employee satisfaction. We distinguish between direct and indirect costs/benefits. Direct costs e.g. equipment price of acquisition, can be attributed to a specific source in the system whereas indirect costs/benefits (e.g. unsatisfied workers) are a by-product of other factors and hard to quantify. Potential benefits can be lower worker absenteeism, lower health expenses and the perception of the enterprise as a company caring for its work force. Potential costs come from maintenance, the investment into the equipment, training and operating costs (e.g. electricity). The fundamental problem here is that the costs are better measurable than potential benefits, which are hard to express in numbers. Potential arguments for benefits can come from the effects of ergonomic intervention studies (e.g. [6]) and studies about the current health expenses of the companies. The German Federal Institute for Occupational Safety and Health (BAuA) estimates the monetary costs for an absence day is around 105€ [23]. For small and medium-sized enterprises (SMEs), which are more dependent on single workers, the costs can be even higher. Another idea to tackle this problem can be done by introducing governmental incentives for prevention measurements, such as lower taxes or subsidies for such technologies.

Legal Challenges. The system operates on optical sensors. The continuous camera-based monitoring of the worker raises questions concerning privacy. Recording the work force without consent can lead to severe legal consequences. This challenge can only be solved by dialogue with employee organisations. Thereby, various questions (referring to the German data privacy law § 6 b BDSG) have to be agreed on: Can the person be identified by the recorded information? Does the person agree? Where are the recordings saved and what is their purpose? Who has access to them? How long is the retention time? There are technical solutions which can help to solve these issues. The information recorded by the

system can be discarded right after processing. Since the Ergonomics assessment is based on the silhouette images of the person, the RGB images can be completely ignored. After the extraction of the body parameters, the silhouettes can be discarded, as well. Therefore, the computer infrastructure has to ensure that the information cannot leak outside, e.g. by a lack of internet connection. These technical mechanisms can support the system to fulfil legal regulations and persuade the employee organisation.

6 Conclusions and Outlook

We have presented a novel type of equipment to help preventing posture-related WMSDs. Unlike former approaches, the solution is able to automatically adjust the work place without the necessity of a work place designer or an ergonomist significantly reducing time to integrate the measurement. Furthermore, we have provided an overview how to use such systems, make it safe and pointed out challenges to be tackled when integrating such a device in real environment. Apart from studies to verify its performance at a real work place, there has to be additional dialogue with employee organisations and the company management board. Once the technology has matured, the worker has to be incorporated into the development process, since he/she takes the final decision whether to accept to work with such an equipment or not.

Acknowledgments This research is funded by the German Research Foundation (DFG) in the Collaborative Research Centre (CRC) SFB 1026 Sustainable Manufacturing Shaping Global Value Creation at Technische Universität Berlin. The authors would like to thank Jan Kuschan for providing valuable feedback.

References

1. Fit for Work Europe: Why early management of chronic disease in the EU workforce should be a priority: a call for action for the Latvian Presidency of the EU & Member States, Riga (2015)
2. Nguyen, T.D., Kleinsorge, M., Postawa, A., Wolf, K., Scheumann, R., Krüger, J., Seliger, G.: Human centric automation: using marker-less motion capturing for ergonomics analysis and work assistance in manufacturing processes. Proceedings of the 11th Global Conference on Sustainable Manufacturing (GCSM)—Innovative Solutions, Berlin. 586–592 (2013)
3. Nguyen, T.D., Kleinsorge, M., Kruger, J.: ErgoAssist: An assistance system to maintain ergonomic guidelines at workplaces. Emerging Technology and Factory Automation (ETFA), 2014 IEEE, pp 1–4. IEEE (2014)
4. Punnett, L., Wegman, D.H.: Work-related musculoskeletal disorders: the epidemiologic evidence and the debate. *J. Electromyogr. Kinesiol.* **14**, 13–23 (2004)
5. Putz-Anderson, V., Bernard, B.P., Burt, S.E., Cole, L.L., Fairfield-Estill, C., Fine, L.J., Grant, K.A., Gjessing, C., Jenkins, L., Hurrell Jr, J.J., et al.: Musculoskeletal disorders and workplace factors. National Institute for Occupational Safety and Health (NIOSH) (1997)

6. Goggins, R.W., Spielholz, P., Nothstein, G.L.: Estimating the effectiveness of ergonomics interventions through case studies: implications for predictive cost-benefit analysis. *J Safety Res.* **39**, 339–344 (2008)
7. Schmidler, J., Hölzel, C., Knott, V., Bengler, K.: Human Centered Assistance Applications for Production. *Adv. Ergon. Manuf. Manag. Enterp. Future* **13**, 380 (2014)
8. Engels, J.A., Van der Gulden, J.W.J., Senden, T.F., Kolk, J.J., Binkhorst, R.A.: The effects of an ergonomic-educational course. *Int. Arch. Occup. Environ. Health* **71**, 336–342 (1998)
9. Bergamasco, R., Girola, C., Colombini, D.: Guidelines for designing jobs featuring repetitive tasks. *Ergonomics* **41**, 1364–1383 (1998)
10. Das, B., Grady, R.M.: Industrial workplace layout design An application of engineering anthropometry. *Ergonomics* **26**, 433–447 (1983)
11. Muggleton, J.M., Allen, R., Chappell, P.H.: Hand and arm injuries associated with repetitive manual work in industry: a review of disorders, risk factors and preventive measures. *Ergonomics* **42**, 714–739 (1999)
12. Ding, Z.Q., Luo, Z.Q., Causo, A., Chen, I.M., Yue, K.X., Yeo, S.H., Ling, K.V.: Inertia sensor-based guidance system for upperlimb posture correction. *Med. Eng. Phys.* **35**, 269–276 (2013)
13. Delleman, N.J., Haslegrave, C.M., Chaffin, D.B. (eds.): Working postures and movements: tools for evaluation and engineering. CRC Press, Boca Raton (2004)
14. Lämkuhl, D., Hanson, L.: Roland Örtengren: A comparative study of digital human modelling simulation results and their outcomes in reality: a case study within manual assembly of automobiles. *Int. J. Ind. Ergonom.* **39**, 428–441 (2009)
15. Martin, C.C., Burkert, D.C., Choi, K.R., Wieczorek, N.B., McGregor, P.M., Herrmann, R.A., Beling, P.A.: A real-time ergonomic monitoring system using the Microsoft Kinect. In: *Systems and Information Design Symposium (SIEDS), 2012 IEEE*. 50–55. IEEE (2012)
16. Krüger, J., Lien, T.K., Verl, A.: Cooperation of human and machines in assembly lines. *CIRP Ann. Manuf. Techn.* **58**, 628–646 (2009)
17. Yang, C.-J., Zhang, J.-F., Chen, Y., Dong, Y.-M., Zhang, Y.: A review of exoskeleton-type systems and their key technologies. *Proc. Inst. Mech. Eng. C J.* **222**, 1599–1612 (2008)
18. Thomas, C., Busch, F., Kühlenkoetter, B., Deuse, J.: Process and human safety in human-robot-interaction—a hybrid assistance system for welding applications. In: *Proceedings of the 4th International Conference on Intelligent Robotics and Applications—Volume Part I* (2011)
19. Schaub, K., Caragnano, G., Britzke, B., Bruder, R.: The European assembly worksheet. *TIES.* **14**, 616–639 (2013)
20. Schaub, K., Wakula, J., Berg, K., Kaiser, B., Bruder, R., Glitsch, U., Ellegast, R.-P.: The assembly specific force atlas: The assembly specific force Atlas. *Hum Factors Ergon Manuf.* **25**, 329–339 (2015)
21. Neuhaus, M., Healy, G.N., Dunstan, D.W., Owen, N., Eakin, E.G.: Workplace sitting and height-adjustable workstations. *Am. J. Prev. Med.* **46**, 30–40 (2014)
22. Haddadin, S., Albu-Schaffer, A., Hirzinger, G.: Requirements for safe robots: measurements, analysis and new insights. *Int. J. Robot. Res.* **28**, 1507–1527 (2009)
23. Bundesministerium für Arbeit und Soziales (BMAS)/Bundesanstalt für Arbeitsschutz und Arbeitsmedizin (BAuA): Sicherheit und Gesundheit bei der Arbeit 2014, Dortmund (2015)

Older Driver's Physiological Response Under Risky Driving Conditions—Overtaking, Unprotected Left Turn

Se Jin Park, Murali Subramaniyam, Seoung Eun Kim,
Seunghye Hong, Joo Hyeong Lee and Chan Min Jo

Abstract Twenty healthy elderly and twenty healthy young taxi drivers drove a car simulator through an immersive virtual environment. Two driving events were considered intersection crossing and overtaking a lead vehicle with continuous cross traffic coming from opposing direction. The physiological responses measured were electroencephalogram (EEG) from frontal (Fz) and occipital lobe (O₂), electrocardiogram (ECG), and galvanic skin response (GSR). The data were measured using Biopac MP150 system and analyzed using AcqKnowledge (ver. 4.2) software. EEG results conveyed stress and eyestrain for the elderly; the increased heart rate and GSR results expressed the nervousness and/or stress for the elderly in both driving situations. The physiological results confirm that aging causes a decrement in cognitive functions, the deficit in visual perceptual skills, and difficulty in decision-making. Therefore, research and policy improvement required for elders. For example, the shorter renewal period for a driving license, and cognitive test like in the USA.

S.J. Park (✉) · M. Subramaniyam · S.E. Kim · S. Hong · J.H. Lee · C.M. Jo
Center for Medical Metrology, Korea Research Institute of Standards and Science (KRISS),
267 Gajeong-ro, Yuseong-gu, Daejeon, Korea
e-mail: sjpark@kriss.re.kr

M. Subramaniyam
e-mail: murali.subramaniyam@gmail.com

S.E. Kim
e-mail: havocangel@kriss.re.kr

S. Hong
e-mail: seung-H@kriss.re.kr

J.H. Lee
e-mail: najoohyoung@kriss.re.kr

C.M. Jo
e-mail: jochanmin@kriss.re.kr

S.J. Park · M. Subramaniyam · S.E. Kim · S. Hong · J.H. Lee · C.M. Jo
Knowledge Converged Super Brain (KSB) Research Department,
Electronics and Telecommunications Research Institute (ETRI), Yuseong-gu, 218,
Gajeong-ro, Daejeon, Korea

Keywords Risky driving condition · Aging · Driving simulator · Physiological measure

1 Introduction

The low fertility rate and the increase in the life expectancy at birth contributed to the steady rise in median age. Aging results from increasing longevity, and most importantly, declining fertility [1]. Population aging is taking place in nearly all the countries of the world. In Korea, people over 65 years of age will account for 38.2 % of Korea's population in 2050, making it the most aged society among the 30 member economies of the Organization for Economic Cooperation and Development (OECD) [2]. As the population in the developed world is aging, so the number of older drivers is increasing [3, 4]. Age-related decline in cognitive function threatens safety and quality of life for an elder.

Road traffic accident is a major but neglected public health challenge. The World report on road traffic accident prevention has indicated that worldwide, an estimated 1.2 million people die in road traffic accident each year and as many as 50 million are being injured [5, 6]. By 2020, the road accident is expected to be the third major killer after HIV and TB [7]. In Korea, death per 100,000 population caused by transport accidents is 13.8, which is much higher than that of the United States (12.4), Japan (4.5), and Denmark (4.0) [8]. As of the end of 2014 (Fig. 1), 4762 persons were killed in the traffic accidents, in that 44.2 % were elderly age above 65 years [9].

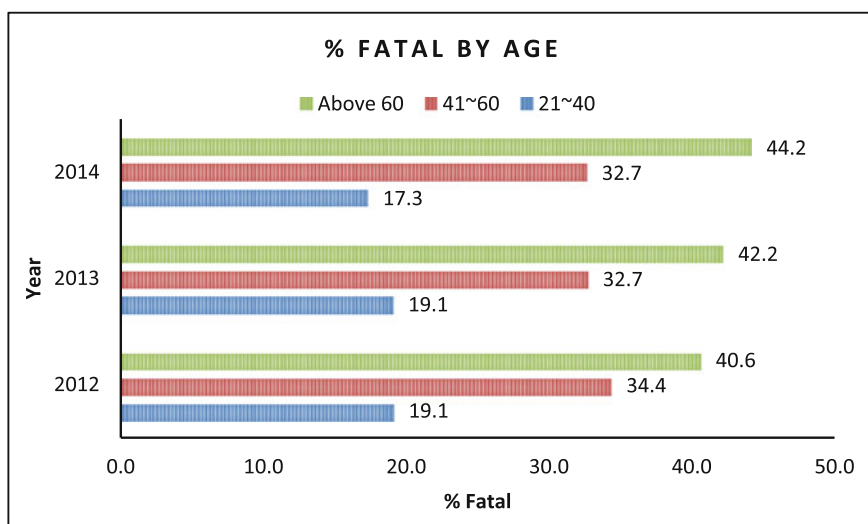


Fig. 1 Mortality rate based on age group due to traffic accidents (2012–2014) [8]

Driving is considered as a complex task which involving coordination and execution of various cognitive, physical, sensory, and psychomotor skills [10, 11]. Peden [7] highlighted that 85 % of all traffic accidents due to the human behavior. Also, many kinds of literature highlighted that the human factor is being the most prevalent contributing factor of road traffic accidents [12–14]. Risky driving behaviors were linked with an increased chance of an injury or death [15]. The risky driving situation also linked with an increased accident risk. For example, single lane overtaking maneuvers involve risk for accident and require extreme care. Unprotected left turn while driving is one of the most advanced maneuvers susceptible to accident risk for new and the most experienced drivers.

This investigation examined how the elderly and young drivers negotiate the challenging perceptual-motor problem with significant real-world implications—overtaking a vehicle in a single lane, and unprotected left turn.

2 Materials and Methods

2.1 Subjects

In this study, two groups (elderly = 20 and younger = 20) of taxi drivers were enrolled. The participants were healthy male drivers licensed to drive a motor vehicle. The elderly drivers had more than thirty years of driving experience, and the younger had more than three years of driving experience. Both groups of participants had no clinical history of mental diseases and visual problem to drive a car in the driving simulator. The average age of them was 65.6 ± 5.0 years (old), and 26.3 ± 2.0 years (younger).

2.2 Driving Simulator

A driving simulator located at Chungnam Techno Part (CTP) in Korea Automobile Technology Institute was used (Fig. 2). Notable specification of the simulator as



Fig. 2 Driving simulator used in this study

follows: VGA to QXGA (2048×1536), True SXGA + 1400×1050 resolution, and scan rates of 15 kHz to 120 Hz (horizontal) and 23.97–150 Hz (vertical). The simulator operated in the controlled environment with temperature ($25\text{ }^{\circ}\text{C}$) and relative humidity (40–50 %).

2.3 *Driving Scenario*

As mentioned earlier, this investigation examined how the elderly and young drivers negotiate the challenging perceptual-motor problem with significant real-world implications—overtaking a vehicle in a single lane (Event 1), and unprotected left turn (Event 2). In event 1, participants crossed the intersection with continuous cross traffic coming from opposing direction. In event 2, participants crossed a lead vehicle with continuous cross traffic coming from opposing direction under single lane.

2.4 *Physiological Measurement*

The physiological responses measured were electroencephalogram (EEG) from frontal (F_z) and occipital lobe (O_2), electrocardiogram (ECG), and galvanic skin response (GSR). The data were measured using Biopac MP150 system, and AcqKnowledge (ver. 4.2) software was used for data analysis. The relative beta band ratio ($\text{beta}/(\text{alpha} + \text{beta} + \text{theta} + \text{delta}) \times 100$) was calculated from the EEG analysis. Average R-R interval (sec) was calculated from the ECG analysis. Average amplitude (micro Siemens) was calculated from the GSR. The sampling frequency of measuring physiological signals was 1000 Hz. Skin impedance was under 10 k Ω . An independent t-test was performed to test statistical significance.

3 Results and Discussion

3.1 *Electroencephalogram (EEG)*

The relative beta band power ratio from the frontal lobe (F_z) significantly differed between the elder and younger when taking an unprotected left turn and higher for the elder (Fig. 3). However, there was no significant different between the elder and younger's relative beta band power ratio when overtaking a lead vehicle. The increased brain activity in the frontal lobe conveyed the increased or excessive brain load or activity required for the elderly for decision making while taking an unprotected left turn, which causes stress for the elderly.

The relative beta band power ratio from the occipital lobe (O_2) significantly differed between the elder and younger when taking an unprotected left turn and

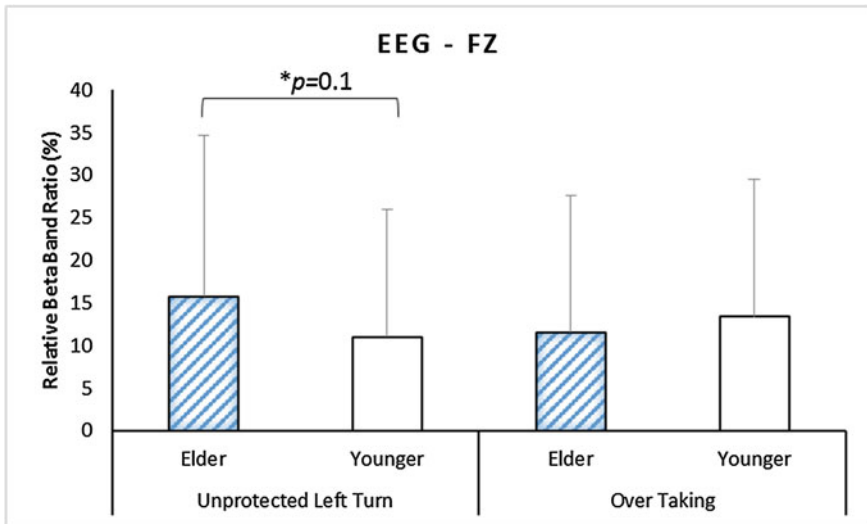


Fig. 3 Frontal lobe EEG relative beta band power ratio comparison between elder and younger when taking an unprotected left turn and overtaking a lead vehicle

higher for the elder (Fig. 4). However, there was no significant different between the elder and younger's relative beta band power ratio when overtaking a lead vehicle. The increased brain activity in the occipital lobe conveyed the increased or excessive brain load or activity required for the elderly for integrating the visual

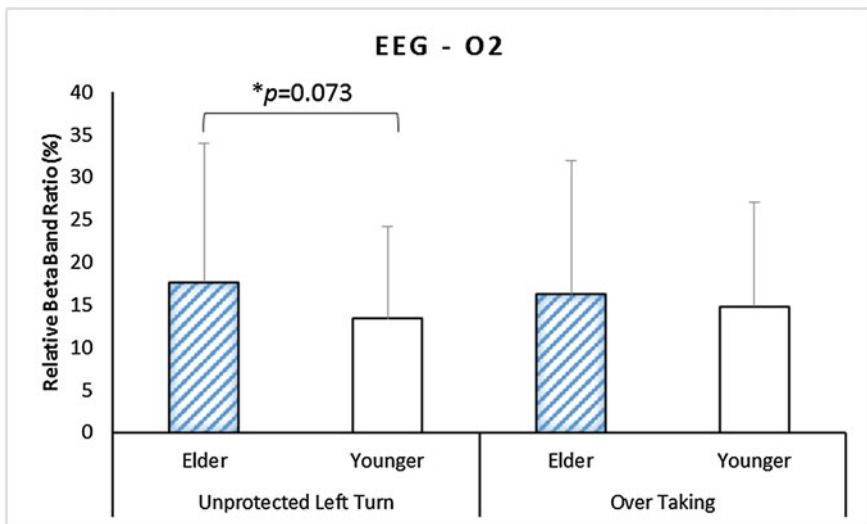


Fig. 4 Occipital lobe EEG relative beta band power ratio comparison between elder and younger when taking an unprotected left turn and overtaking a lead vehicle

information while taking an unprotected left turn, which causes eyestrain for the elderly. Even though there was no significant different in the occipital lobe EEG brain activity while overtaking a lead vehicle; greater brain activity was required for the elderly for integrating visual information.

3.2 *Electrocardiogram (ECG)*

The R-R interval significantly differed between the elder and younger, and shorter for the elderly while overtaking a lead vehicle. The decreased or shortened R-R interval conveyed the increased heart rate (Fig. 5). The increased heart rate increase the nervousness and/or stress for the elderly than the younger during the risky driving situation. Even though there was no significant different in the R-R interval while taking an unprotected left turn, the elder's R-R interval was shorter than the younger.

3.3 *Galvanic Skin Response (GSR)*

The skin conductance significantly differed between the elder and younger, and greater for the elderly (Fig. 6) in both risky driving situations. The increased skin

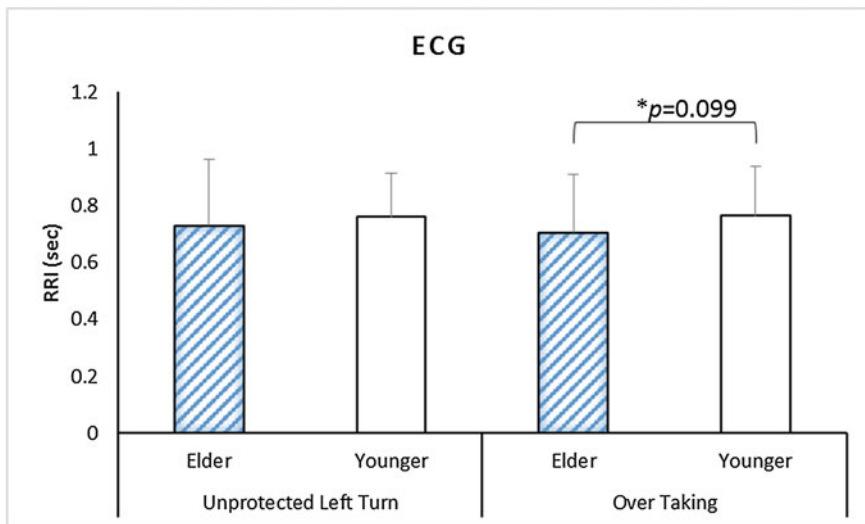


Fig. 5 ECG R-peak to R-peak (R-R interval) comparison between elder and younger when taking an unprotected left turn and overtaking a lead vehicle

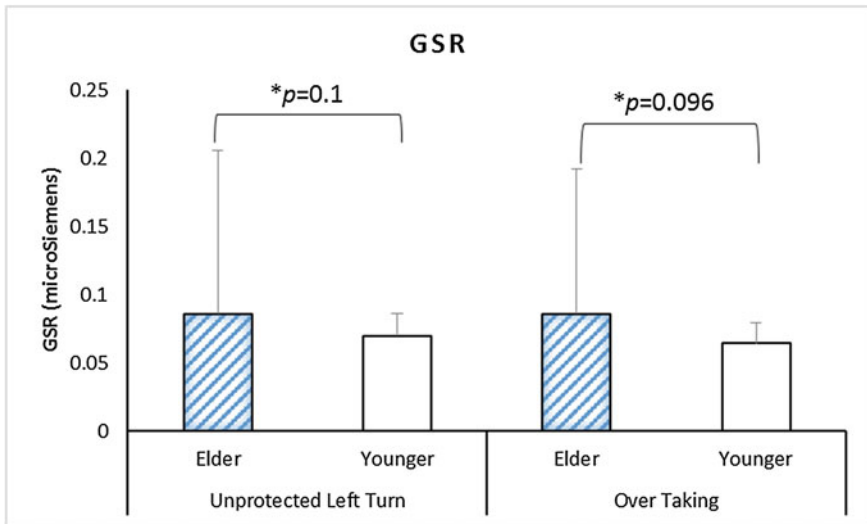


Fig. 6 Galvanic skin response comparison between elder and younger when taking an unprotected left turn and overtaking a lead vehicle

conductance conveyed the increased arousal or emotional state. The increased arousal increase the nervousness and/or stress for the elderly than the younger.

4 Conclusion

In this study, we presented the physiological characteristics of the elderly and young taxi drivers while driving under the risky situations (taking an unprotected left turn and overtaking a lead vehicle). The EEG results conveyed the increased brain load, stress, and eyestrain for the elderly. Also, the heart rate and skin conductance results expressed the increased arousal and stress for the elderly. Aging causes a decrement in cognitive functions, the deficit in visual perceptual skills, and difficulty in decision-making. With this in view, the research policy improvement required for protecting the elderly. For example, shortening the driving license period for older persons and cognitive test like in the USA.

References

1. Park, S.J., Min, S.N., Lee, H., Subramaniyam, M.: A driving simulator study: elderly and younger drivers' physiological, visual and driving behavior on intersection. In: Proceedings 19th Triennial Congress of the IEA, pp. 1–3 (2015)
2. Statistics Korea (KoSTAT): Korea's population. <http://kostat.go.kr>

3. Andrews, E.C., Westerman, S.J.: Age differences in simulated driving performance: compensatory processes. *Accid. Anal. Prev.* **45**, 660–668 (2012)
4. Cohen, J.E.: Human population: the next half century. *Science* **302**(5648), 1172–1175 (2003)
5. Hassen, A., Godessor, A., Abebe, L., Girma, E.: Risky driving behaviors for road traffic accident among drivers in Mekele city, Northern Ethiopia, *BMC Research Notes*, Vol. 4 (2011)
6. WHO: Global status report on road safety time for action, Switzerland (2009)
7. Pedan, M., Scurfield, R., Sleet, D.: World report on road traffic injury prevention (2004)
8. Hong, K., Lee, K.M., Jang, S.: Incidence and related factors of traffic accidents among the older population in a rapidly aging society. *Arch. Gerontol. Geriatr.* **60**(3), 471–477 (2015)
9. The Korea Road Traffic Authority (KoROAD):. Road traffic accidents in Korea. <http://taas.koroad.or.kr>
10. Young, K., Regan, M., Hammer, M.: Driver distraction: a review of the literature. *Distracted driving*, 379–405 (2007)
11. Hughes, G.M., Rudin-Brown, C.M., Young, K.L.: A simulator study of the effects of singing on driving performance. *Accid. Anal. Prev.* **50**, 787–792 (2013)
12. Lewin, I.: Driver training: a perceptual-motor skill approach. *Ergonomics* **25**, 917–924 (1982)
13. Farland, R.A., Moore, R.C.: Human factors in highway safety: a review and evaluation. *N. Engl. J. Med.* **256**, 792–798 (1957)
14. Nabi, H., Consoli, S.M., Chastang, J.F., Chiron, M., Lafont, S., Lagarde, E.: Type A Behavior Pattern Risky driving behaviors, and serious road traffic accidents: a prospective study of the GAZEL Cohert. *Am. J. Epidemiol.* **161**, 864–870 (2005)
15. Turner, C., McClure, R., Pirozzo, S.: Injury and risk-taking behavior—a systematic review. *Accid. Anal. Prev.* **36**, 93–101 (2004)

Part III
Applied Modeling and Simulation

Modeling Decision Flow Dynamics for the Reliable Assessment of Human Performance, Crew Size and Total Ownership Cost

Tareq Z. Ahram, Waldemar Karwowski, Serge Sala-Diakanda
and Hong Jiang

Abstract This chapter aims to demonstrate research progress and current understanding of the impact of acquisition technology selection and manning decisions on maintenance, sustainment, training and total ownership costs for the increasingly complex naval platform. The chapter demonstrates a comprehensive approach based on system dynamics modeling to model complex processes and technology insertion alternatives, with the emphasis on constructing a reliable system dynamics model of the total ownership cost (TOC) and related major human-system components categorized in two groups: human-system performance and manpower skill model to support conducting tradeoff analysis and, technology integration and insertion processes. The system dynamics models presented as the building blocks to ultimately help management determine the required skills and manpower needs in order to meet long term strategic goals of reduced manning and reduced total ownership cost, and avoiding performance risks and hazards. Along with this core model, this chapter three illustrates interaction matrices, redundancy level matrix, crew flexibility matrix and technology interaction matrix. The benefit of the models approach process is to identify the critical factors that lead to unwanted and unforeseen results or behaviors which can affect the attainment of new and/or desired capabilities and total systems readiness. In conclusion, simulated model results demonstrate the ability to track both total ownership cost and the performance of the underlying processes for enhanced decision flow models and reliable assessment.

Keywords Human performance · Decision dynamics · Total ownership cost

T.Z. Ahram (✉) · W. Karwowski · S. Sala-Diakanda · H. Jiang
Institute for Advanced Systems Engineering, University of Central Florida,
Orlando, FL, USA
e-mail: tahram@ucf.edu

W. Karwowski
e-mail: wkar@ucf.edu

1 Introduction

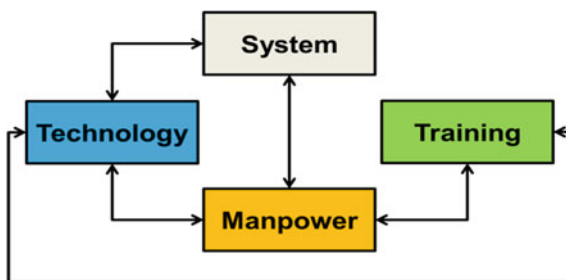
System dynamics modeling (SDM) is a powerful modeling technique that defines causal connections and relationships between the various elements of the system. Each connection is described mathematically and allowed to evolve over time. This chapter illustrates a system dynamics approach to model and simulate decision flow dynamics and variables associated with human and system performance [1]. This approach allows for the dynamic representation of complex systems through the progression of time and allow for robust life cycle model development.

SDM allows capturing the interdependencies between the various human performance and system requirements and cost elements across a given program [2–4]. The approach based on SDM is uniquely appropriate to modeling the type of decision support because it contains performance and cost representations of human performance and system processes. In this chapter a comprehensive system dynamics model introduced and built based on the data of human performance cost drivers and the results from the Visibility and Management of Operating and Support Costs (VAMOSOC) system data. [5]. This chapter demonstrates the development of the SDM and TOC model prototype which captures four interacting problem space sectors [6, 7]: System, Technology, Manpower and Training. Along with this model, researchers formulated three interaction matrices labeled, Redundancy Level Matrix (RLM), Crew Flexibility Matrix (CFM) and Technology Interaction Matrix (TIM).

2 Method

SDM and decision support model prototype was built to capturing decision metrics via causal loop diagrams, to integrate details of the Manpower-Training interactions. The prototype is expected to provide a solid framework for future model development activities, as it captures the four interacting problem space sectors previously proposed, and reproduced in Fig. 1: System, Technology, Manpower and Training. The double arrows indicate bidirectional interactions between model sectors. This section describes the methodology for developing a model prototype,

Fig. 1 Total ownership cost problem space



as well as some of its current limitations. The prototype was developed around the following question: How can the NAVY reduce the crew size of its ship, while maintaining or increasing current efficiency levels?

The main hypothesis of this model is that there are two solutions to help achieve reduced crew size:

1. To substitute crew with technology and
2. To enable crew members to perform multiple tasks through multidisciplinary training, thereby breaking silos' effects [8–10].

The following key variables were included in the model: Crew size, technology insertion, crew training and ship performance. The following description provides details of the aforementioned prototype developed in VENSIM simulation software (<http://vensim.com>).

3 Crew Size Adjustment Model Logic

Figure 2 identifies overall crew size model logic, with several key features of the system dynamics model. First is the main variable named *crew size*, since the main objective is to reduce crew size because of its impact on the Direct Unit Cost. The figure identifies also the two approaches affecting the crew size, both guided by crew reduction goals. Lastly, the model postulates that ship readiness may negatively impact the ability to reduce the size of the crew, especially if readiness is

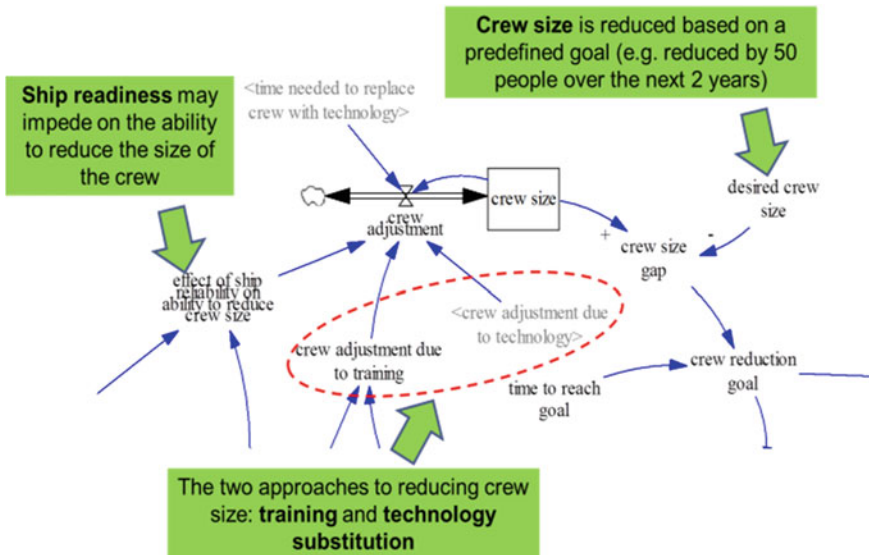


Fig. 2 Postulated total ownership cost problem space

below a minimum acceptable level. The model is composed of training strategy, technology substitution strategy, technology obsolescence, Ship capability and system behavior as discussed in the following sections.

3.1 Multidisciplinary Training Strategy Model Logic

The model logic for the multidisciplinary training strategy is shown in Fig. 3. The main variable in this area is the multidisciplinary training capacity. As shown in Fig. 3, there are several parameters and factors which will determine the ability to reduce crew size through multidisciplinary training, including (1) the crew reduction goal, (2) the training capacity and the time to adjust that capacity, (3) the bias toward increased training, and (4) the flexibility of the crew, which is a measure of the number of functions a particular team member or crew can be trained to perform.

3.2 Technology Substitution Strategy Model Logic

Figure 4 captures the technology substitution strategy approach. Likewise, several factors are considered including (1) the time required to acquire a new technology, (2) the time needed for testing and integration, (3) the number of crew functions that can be eliminated, and (4) the redundancy between the technologies present on the ship.

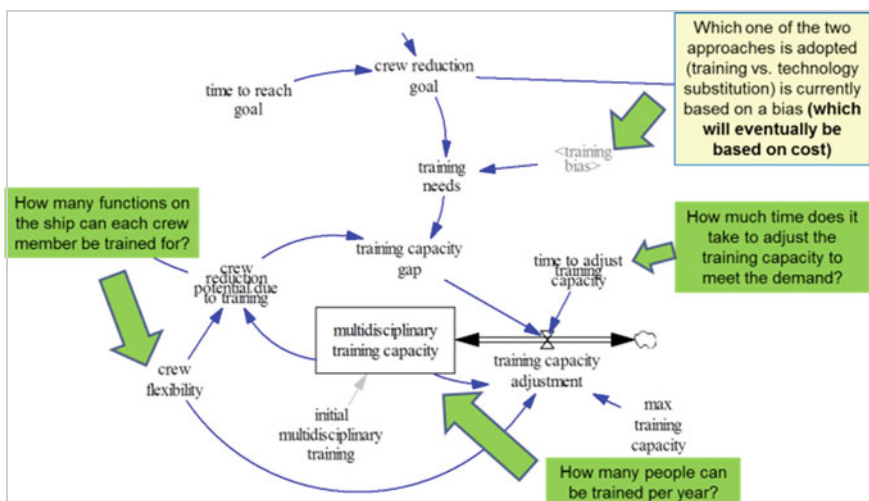


Fig. 3 Multidisciplinary training strategy model logic

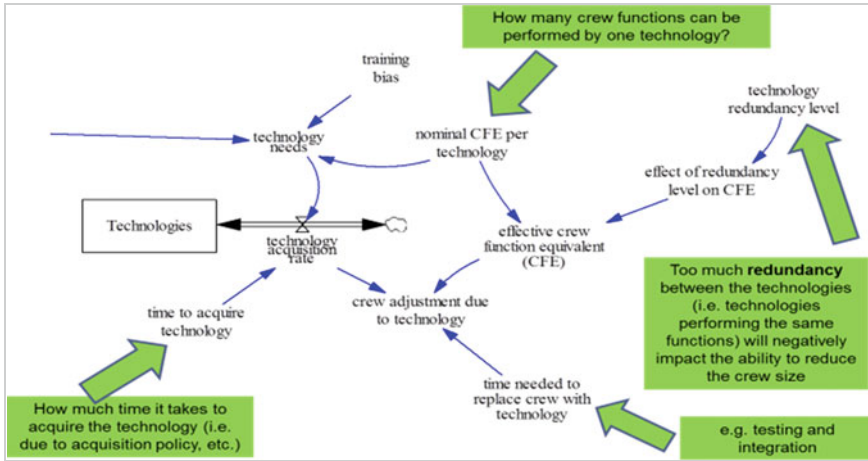


Fig. 4 Technology substitution strategy model logic

3.3 Technology Obsolescence Model Logic

The SDM prototype also captures the concept of *technology obsolescence* (Fig. 5), which is primary acting as a function of the age of the technology. The older the technology presented on the ship, the less capable the ship becomes (although the team recognizes that there are differences between ship readiness, reliability, and availability, these are aggregated, at this stage into the concept of ship capability). For example, archaic communication or out-dated on-broad training technologies may prevent the ship to participate in large scale, multi-vessels training. However,

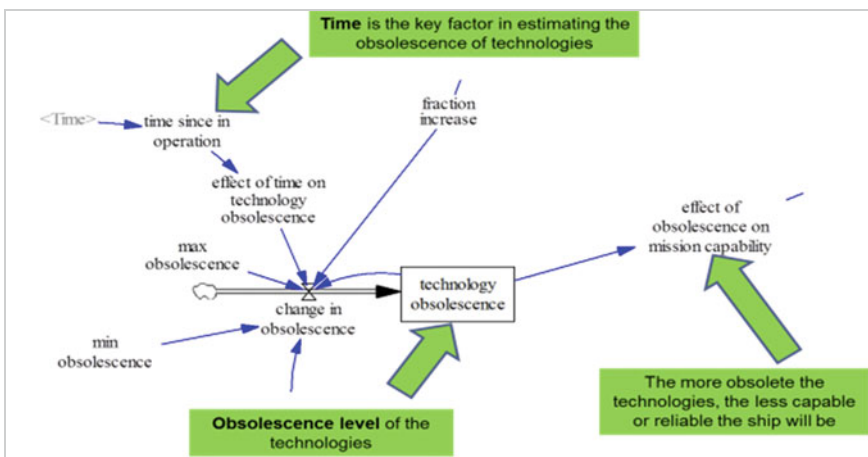


Fig. 5 Technology obsolescence as function of time, and its effect on ship capability

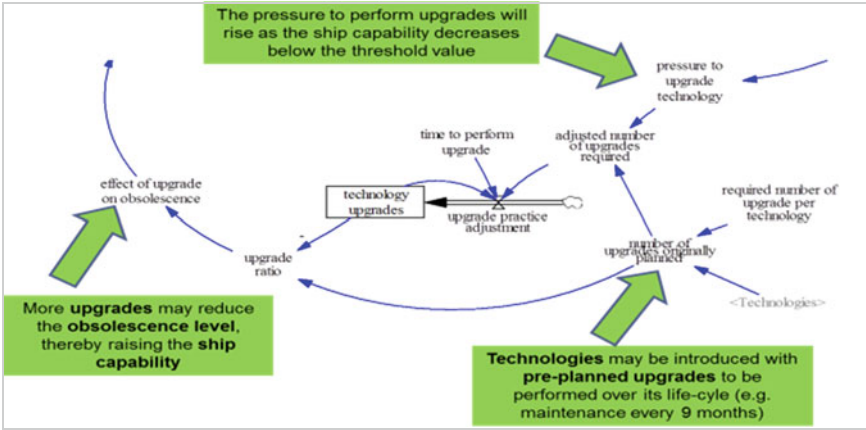


Fig. 6 Technology upgrade model logic

technology obsolescence may be reduced or avoided by performing periodic technology insertions and upgrades, the model logic is shown and described in Fig. 6.

3.4 Ship Capability Model Logic

The last model logic is the change in ship capability (Fig. 7). Currently, it is postulated to be driven primarily by the obsolescence of the technology as

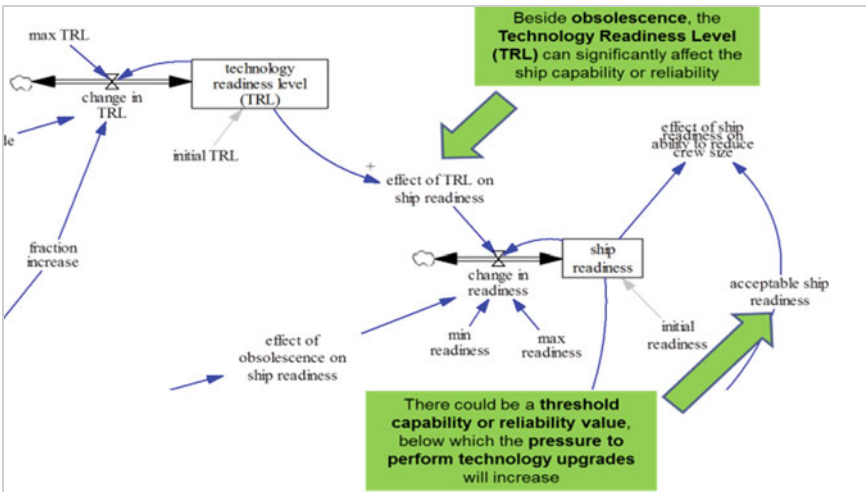


Fig. 7 Factors affecting and affected by ship capability

Table 1 Model parameters value for first scenario

• Current crew size: 300 crew members
• Desired crew size: 100 crew members
• Time to reach desired crew size: 5 years
• Initial TRL value (average): 8 (maximum is 9)
• Initial ship capability: 0.8 (maximum is 1)
• Maximum training capacity: 10 people per year
• Nominal crew function equivalent (CFE) per technology: 10 people per technology
• Time to acquire technology: 9 months
• Time to complete training: 6 months
• Redundancy level: 0 (no redundancy)
• Bias toward training: 0.5 (this meaning no bias between technology and training)

mentioned above, but also by the technology readiness level known as TRL. The lower the TRL value, the less mature the technology and therefore the less capable the ship. Although the exact nature of this relationship is not known, capturing the essence of this relationship is a critical step toward modeling the technology-system interaction depicted in the sector map of Fig. 1.

4 Results and Discussion

Two experiments were conducted to assess the prototype. The model parameters values that were selected are shown in Table 1. The behavior of selected variables are shown in Fig. 8.

5 Discussion

The model clearly shows how the pursuit of the crew reduction goal resulted in a temporary increase in multidisciplinary training, and the adoption of several new technologies. The model also highlights the interactions between some of the variables. For example, the ship capability increases over time as the Technology Readiness Level (TRL) increases. However, during that same timeframe the technology on-board the ship is becoming increasingly less effective due to normal technology obsolesce over time or compatibility with other upgraded systems, eventually leading to a significant decline in the ship capability roughly after around year 20. This decline, in turn, prompted a significant increase in technology upgrades to be performed, which eventually result in improvement in the

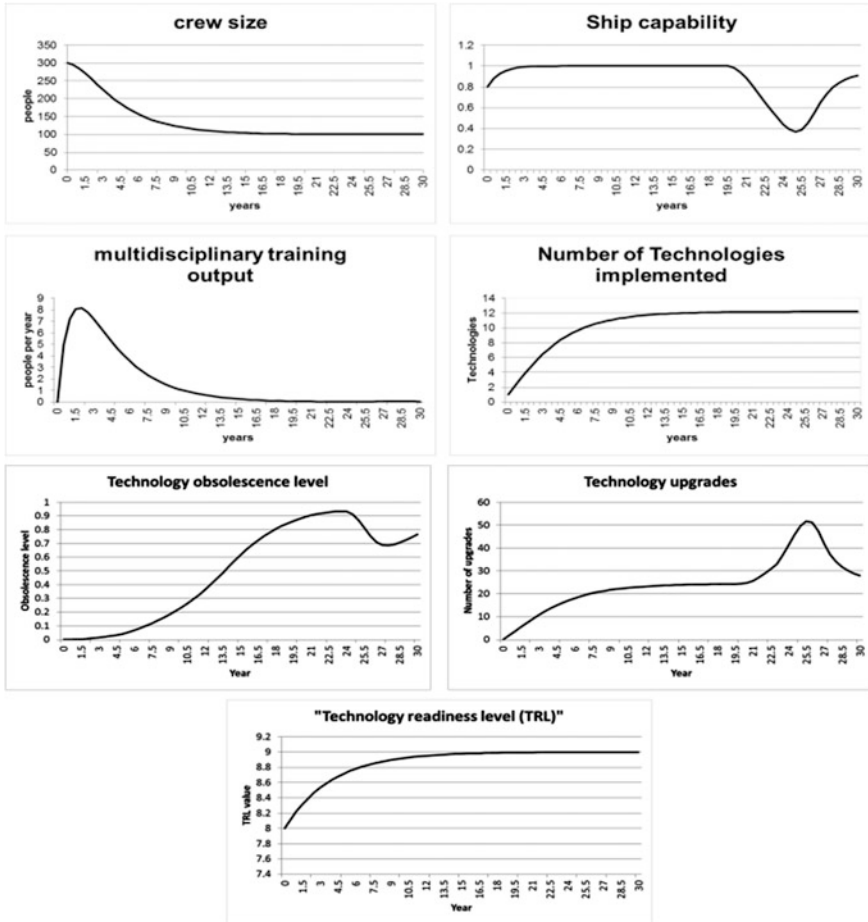


Fig. 8 Prototype behavior under first scenario

technology, and a reversal of the downward trend in ship capability and associated increased manning and maintenance cost.

A second simulated scenario investigated was an SDM model run in which both the time to acquire technology and the time to complete training were both doubled (18 months and 6 months respectively, instead of 9 and 3 months). Figure 9 shows the interesting effect of these changes in terms of the number of technology upgrades performed and the obsolescence of the technology on-board the ship over time. These significant delays resulted in the obsolescence being allowed to drop more significantly, and for technology upgrades to be more erratic (more significant changes from month-to-month) than in the original scenario. The net effect of these delays is a more severe deterioration of the ship capability.

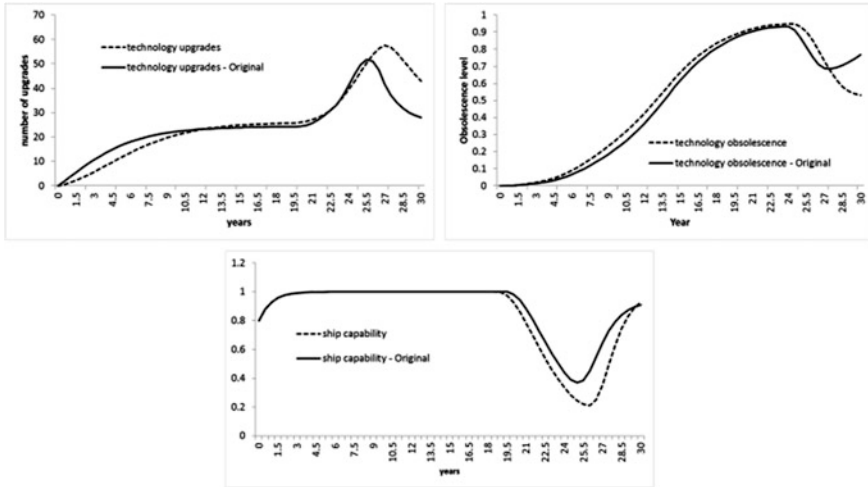


Fig. 9 Prototype behavior: scenario comparison

The system dynamics model developed and tested in this research didn't include full scale cost parameters of human performance due to the complexity of cost assessment with respect to complex human-system interaction. However, those are not expected to be the most significant challenges in the TOC model building process. Instead, it is the identification and the modeling of the drivers of those costs that are expected to present the most significant challenges. To that end, the research team will focus on providing a reasonable model which has the potential to offer significant benefits for the development of subsequent TOC models. Model results are summarized in the following sections.

6 Conclusions

The prototype model building process discussed in this study help identifying variables related to efficiently formulating and identifying appropriate trade-offs between manpower and technology insertions with the aim of reducing the total ownership cost of ships. Three matrices were formulated as Redundancy Level matrix (RLM), Crew flexibility matrix (CFM) and Technology interaction matrix (TIM).

		Destination: Crew functions			
		C ₁	C ₂	C ₃	C ₄
Source: Technology by categories	TC _A	0	1	1	0
	TC _B	1	1	0	1
	TC _C	0	1	1	1
Redundancy score =		0.67			
0		The technology TC _i will not cover that functionality			
1		The technology TC _i will cover that functionality			

Fig. 10 Redundancy level matrix

6.1 Redundancy Level Matrix (RLM)

The RLM provides a unique and concise approach for capturing the redundancy which may be present between various technology options. This redundancy is measured in terms of the number of technologies T_{ci} which can support the same crew function C_i . The higher the number of technologies (and associated technology components) capable of performing the same function, the higher the redundancy level, and the lower the ability of the newly introduced technology to reduce the crew size and associated manpower costs. Figure 10 provides an example on how to calculate the redundancy level when three technologies and four crew functions are considered. The redundancy score is a number between 0 and 1. Where 0 means that technology not able to cover new functionality while 1 indicates current technology is sufficient to add the new functionality.

6.2 Crew Flexibility Matrix (CFM)

The CFM seeks to quantify the ability of the crew to be trained to effectively perform additional functions without affecting their current task performance. Given two crew functions C_i , and C_j , the task is to specify how easily a sailor originally assigned to C_i could be trained for C_j . Assuming 3 levels of trainability (1, 2, 3) where 1 indicates that training is extremely difficult (or not practical), and 3 indicates that it would be easy, a crew flexibility score may be computed as shown in Fig. 11, once all the crew function pairs have been assigned a trainability level. Note that the pair C_iC_j may not have the same trainability level as C_jC_i . For example the training C_3C_1 is expected to be a much more difficult than the training C_1C_3 .

The flexibility score is a normalized value between 0 and 1. The higher the number, the more flexible the crew to be trained for another function in the same

Crew Flexibility Matrix (CFM)		i = 1, 2, 3			i = function i, C _i = crew performing function i	
		Destination				
		C ₁	C ₂	C ₃	Trainability levels	
Source	C ₁	3	1	3	3	Easy
	C ₂	2	3	2	2	Moderate
	C ₃	1	1	3	1	Difficult
	Flexibility score =	0.56				
	min flexibility score	0	not flexible			
	max flexibility score	1	very flexible			

Fig. 11 Crew flexibility matrix (CFM)

level of difficulty, and the higher the potential for crew reduction. This approach was not incorporated in the logic of model discussed earlier and will be tested and validated in the future. Additionally, note that the crew functions which bare the same name in the RLM and the CFM are effectively the same function, thereby providing a linking mechanism between them.

6.3 Technology Interaction Matrix (TIM)

The TIM differs from the RLM in that its focus is on the impact of the technology readiness level of a given technology on another technology through its interaction with it. Figure 12 shows the TIM involving three (3) technologies T_{CA}, T_{CB} and T_{CC}. Along with the TIM are the TRL values of each technology. The figure shows that T_{CC} is expected to provide outputs to T_{CB}, but that its readiness level is only 5, compared to 8 for T_{CB}. This should be expected to negatively impact the reliability of this interaction. Like RLM and the CFM, the TIM was not included in the prototype model presented earlier in this study and is currently under development.

Technology Interaction Matrix							
	TC _A	TC _B	TC _C				TRL value
TC _A		X					TC _A 3
TC _B			X				TC _B 8
TC _C	X	X					TC _C 5
T _{ci}	Technology Category i						

Fig. 12 Technology interaction matrix (TIM)

6.4 Manpower-Training Interactions Causal Loop Diagramming

The prototype model discussed in previous sections has some limitations in the administration of training process. While the prototype acknowledges the presence of a training capacity, it does not, for example, model the effect of training on the skill level of the crew. A causal loop diagram (CLD) shown in Fig. 13 was developed to capture the Training-Manpower sectors interactions. Revisions and additions are applied regularly to this model as more information is gained about new training strategies.

This version of the CLD contains essentially 3 loops. The need to adopt “advanced technologies” is driven by the pressure to reduce manpower cost (variable named *Manpower cost saving pressure*). This is the case we are investigating as postulated in this model, because the level of automation introduced by the state-of-the-art technology leads to the identification of crew reduction opportunities (loop B3). In addition, these technologies increase the ship’s capability (loop B1). However, they also raise the skill level required from the crew. This leads to a skill level gap which then drives the revision of current (or formulation of new) training requirements (loop B2). Because higher skill levels may result in higher pay grades, manpower cost can, in turn, increase exponentially, thereby potentially sustaining the pressure for manpower cost saving measures.

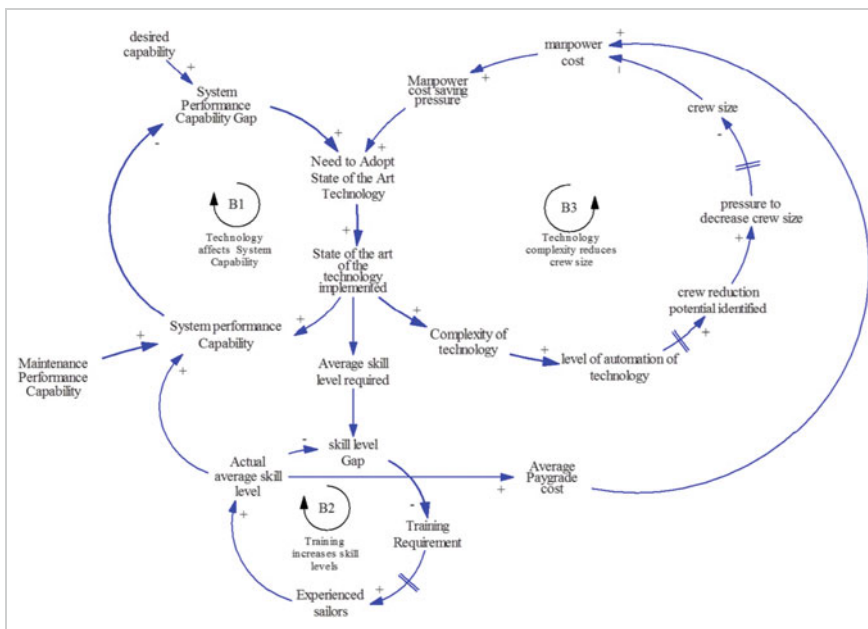


Fig. 13 Manpower-training interactions

Acknowledgements This research was sponsored by the Office of Naval Research Contract No. N00014-14-1-0777. The authors acknowledge the helpful guidance by Dr. William Krebs, ONR Program Management, and the contributions of the technical team.

References

1. Gansler, J.S.: Office of the secretary of defense. memorandum: definition of total ownership cost (TOC), life cycle cost, and the responsibilities of program managers. 13 Nov 1998
2. Bartolomei, J.: A system dynamics model of government engineering support during the development phase of a military acquisition program. In: Proceedings of the 19th International Conference of the System Dynamics Society. International System Dynamics Society, Atlanta, GA
3. Damle, P.H.: A system dynamics model of the integration of new technologies for ship systems, Master's Thesis, Virginia Tech (2003)
4. Monga, P., Triantis, K.: A dynamics model for the development of new technologies for ship systems. Submission Syst Dyn J (2002)
5. Naval visibility and management of operating and support costs (VAMOSC) 5.3 Detailed ships user manual. (2012). Website: <http://www.dtic.mil/cgibin/GetTRDoc?Location=U2&doc=GetTRDoc.pdf&AD=ADA354008>
6. Foundation For future naval fleets—The future for naval engineering—Report prepared for the committee on naval engineering in the 21st Century transportation research board—VADM, USN (Retired)
7. Department of Defense, Instruction, Operation of the Defense Acquisition System. 12 May 2003. (DoDI 5000.2). <http://www.dsto.defence.gov.au/publications>
8. Hafeez, K., Aburawi, I., Norcliffe A.: Human resource modeling using system dynamics. In 22nd International Conference on the System Dynamics Society (2004)
9. O'Rourke, R.: Navy force structure and shipbuilding plans: background and issues for congress. Congressional Research Service (2011)
10. Wang, J. (2005). A review of operations research applications in workforce planning and potential modelling of military training. DSTO Systems Science Laboratory. Retrieved from <http://dSPACE.dsto.defence.gov.au/dSPACE/handle/1947/3940> (2008)

Modeling the Perception Reaction Time and Deceleration Level for Different Surface Conditions Using Machine Learning Techniques

Mohammed Elhenawy, Ihab El-Shawarby and Hesham Rakha

Abstract The ability to model the driver's perception reaction time (PRT) and deceleration level is important for signal-timing design. The current state of practice considers PRT and the deceleration level deterministic and uses of constant values for them. The state of practice ignores the differences in PRT and deceleration level between individual drivers approaching the same intersection at the onset of yellow. The research presented in this paper uses data collected from two controlled field experiments on the Smart Road at the Virginia Tech Transportation Institute (VTTI) to model brake PRT and the deceleration level at the onset of a yellow indication for different roadway surface conditions. The paper uses many of the recent state of art machine learning to train models that can be used to predict the brake PRT and deceleration level of approaching driver.

Keywords Brake perception reaction time · Deceleration · Machine learning · Deep learning

1 Introduction

With advances in sensing, communications, and computational technologies, research in the area of safety is increasing significantly. Most new cars have active safety features including anti-lock braking and adaptive cruise control systems to reduce road accidents [1]. In the US, the Department of Transportation (DOT) reported 32,367 fatalities caused by road accidents in 2011 [2]. A significant

M. Elhenawy · I. El-Shawarby · H. Rakha (✉)
Virginia Tech Transportation Institute, Blacksburg, USA
e-mail: hrakha@vt.edu

I. El-Shawarby
Faculty of Engineering, Ain-Shams University, Cairo, Egypt

H. Rakha
Department of Civil and Environmental Engineering, Virginia Tech,
Blacksburg, USA

percentage of these road accidents occurred at signalized intersections because of the dilemma zone problem. Rear-end crash and right-angle crash are the two types of dilemma-zone-related crashes. These crashes can be avoided if the yellow time is properly designed. Driver perception reaction time (PRT) is important in the calculation of the yellow interval duration in traffic signal design [3]. So that an accurate estimation of the PRT is required for a proper design of the yellow time. PRT is a random variable, which has a distribution, and the state of practice in designing the yellow time uses the 85th percentile brake PRT that equals 1.0-s [4]. However, there are studies showed that the brake PRTs lies in the range of 1.1–1.3 s [5].

PRT is the sum of two portions. The first is the time a driver needs to perceive sensory signal and decide his response. The second portion is the time needed for executing the decided response. For example, the PRT of a driver at the onset a yellow light at a traffic signal consists of the time needed to perceive the yellow light and decide to stop plus the time needed to move his foot from the accelerator and touching the brake [6]. In general, PRT studies can be classified into three categories: simulator studies, controlled road studies, and naturalistic observation [6]. Each study type has limitations that we need to consider when generalizing its outcome to normal driving conditions. The drivers in simulator and controlled road are more alert than under normal driving conditions which may yield shorter PRT measurements. Naturalistic studies have the highest validity, however it is not possible to test effects of independent variables, place drivers in emergency or even urgent situations, measure perception and movement times separately, or control driver demographics to avoid sample bias.

Caird, et al. conducted a simulator study which included 77 drivers approaching signalized intersections at 70 km/h. The analysis of the driver's behavior showed that the PRT is significantly affected by the time to intersection (TTI) but not the age. Moreover, they demonstrated that PRT has a grand mean of 0.96 s and ranges from 0.86 s for drivers closest to the intersection stop line to 1.03 s for drivers farthest from it. In another study [7]. Rakha et al. [8] conducted a controlled road study where data was collected from 60 participants to study driver brake PRTs at the onset of the yellow indication at high-speed signalized intersection. The study demonstrated that the distribution of the brake PRT could be modeled using log-normal or beta distribution. They show that the state of practice 1.0-s, 85th percentile PRT used in the design of traffic signals is valid. El-Shawarby et al. [9] conducted controlled a road study to characterizes the impact of a wet road surface and rainy weather conditions on driver PRT at the onset of the yellow indication on the approach to a high-speed signalized intersection. The study demonstrated that driver PRT increased under conditions of a wet pavement surface and rainy weather as compared to clear weather conditions over the entire TTI range.

Transportation engineers consider driver deceleration levels in the design of yellow time as well. Traffic signal designers assumed constant driver deceleration levels equal 3 m/s^2 or 10 ft/s^2 . Moreover, driver deceleration levels are important in most traffic simulators, vehicle fuel consumption and emission models, and design

of deceleration lane lengths. Many studies done to characterize the mean and range of the deceleration level and what factors affect it.

An early study conducted at Connecticut demonstrated that the average maximum brake deceleration level was 0.95 m/s^2 (9.7 ft/s^2) for vehicles moving at speed $16.1\text{--}40.2 \text{ km/h}$ ($10\text{--}25 \text{ mph}$) [10]. Parsonson and Santiago [11] studied 54 intersection approaches in four counties in the southeastern United States and concluded that 3 m/s^2 (10 ft/s^2) is a good estimate for the brake deceleration level. Two other research effort were done at different intersections in metropolitan areas in Phoenix, Arizona, and Tucson, Arizona [12, 13] to find out the mean deceleration level at higher speeds. Both studies reported wide interval of deceleration level with upper bound greater than or equal 4 m/s^2 (13.2 ft/s^2). El-Shawarby et al. [14] conducted a controlled field test to study the impact of several factors such as age, gender, and TTI on driver deceleration levels at the onset of the yellow indication on high-speed signalized intersection approaches. This study showed that the mean deceleration level ranges from 3.6 to 4.1 m/s^2 which is significantly higher than the 3 m/s^2 deceleration level used in the state-of-the-practice traffic signal design guidelines. Moreover, the results demonstrate that at shorter TTIs at the onset of yellow the driver deceleration levels are higher. Furthermore, deceleration levels of older drivers (60 years of age or older) are greater than deceleration levels of younger (under 40 years old) and middle-aged (between 40 and 59 years old) drivers.

The deceleration level at stop-controlled intersections grabbed the attention of the researchers as well. Wang et al. [15] recommended a maximum deceleration level of 3.4 m/s^2 (11.2 ft/s^2) for passenger cars approaching stop-controlled intersection. They reported that the 3.4 m/s^2 (11.2 ft/s^2) was corresponding to the 92.5th percentile deceleration level at stop-controlled intersections. Another research done at rural stop sign-controlled intersections in southern Michigan to study the factors explaining the variation in the observed deceleration and acceleration rates. The study concluded that the initial speed, driver demographics, and time of day explained about 18, 5 and 5 % of the variation in deceleration levels respectively [16].

The past two decades have seen numerous research efforts and advances in both machine learning and computers. Many machine learning techniques require a large number of computations and are infeasible without computers. The available machine learning algorithms and computation power encourages researchers to transfer this knowledge into their fields. Transportation engineers are among people who are interested in applying these algorithms to address transportation problems. This interest increases with the availability of naturalized data sets and data sets collected from controlled experiments. Recently, some machine learning algorithms were used in the transportation field, including: classifying and counting vehicles detected by multiple inductive loop detectors [17], identifying motorway rear-end crash risks using disaggregate data [18], automatic traffic incident detection [19], real-time detection of driver distraction [20, 21], transportation mode recognition using smartphone sensor data [22], and video-based highway asset segmentation and recognition [23]. Modeling driver stop/run behavior at signalized intersections is very important and is ideal for applying machine learning techniques [24, 25].

The modeling of brake PRT and deceleration levels seems to be a good candidate for application of machine learning algorithms. Observations of the stopping driver from naturalized datasets or from controlled field experiments, datasets can be used to train machine learning algorithms. The trained models could then be used to predict future driver brake PRT time and deceleration level at the onset of yellow light.

In this paper, we adopted the state of art machine learning techniques to model the brake PRT and deceleration levels of the driver at the onset of the yellow signal. We demonstrate that models built using machine learning algorithms give better prediction than the traditional multiple linear regression.

2 Methods

In this section, we briefly describe the feature selection algorithm and the classifiers used in this paper as building blocks in the proposed hierarchal classifier.

2.1 *Decision Tree*

Decision tree method is a greedy and recursive algorithm starts from a root where the entire data is in one node. Subsequently, a tree is grown by splitting the data using binary splitting approach. The chunk of the data at the parent node is portioned between the resultant leaves to minimize the objective function. In order to predict the response for a new unseen test observation, it pushed down by going through the tree from the root to a leaf. The final leaf determines the response of the test observation [26]. While growing the tree, the data is divided by employing a criterion in several steps or nodes. In practice, Gini index, and Cross-Entropy are used for classification and mean-square error (MSE) of the responses is used for regression.

2.2 *Random Forest*

Random forest method, as proposed in 2001 [27], creates an ensemble of decision trees. For each tree, a subset of features is randomly selected to grow the tree. Also, adding more trees does not lead to over-fitting but at some point not much benefit is gained by including more trees [28]. The response of a test observation is obtained by averaging the predictions from all the individual regression trees on this unseen test observation.

2.3 Adaptive Boosting Algorithm

The Adaptive Boosting (AdaBoost) is a machine learning algorithm that is based on the idea of incremental contribution [29]. AdaBoost was introduced as an answer to the question of whether a group of “weak” learner algorithms that each has low accuracy can be grouped together and boosted into an arbitrarily accurate “strong” learning algorithm. In this paper we used the LSBoost (least squares boosting) which fits regression tree ensembles. LSBoost minimizes the mean-squared error, at each iteration, by adding a new-trained tree. The algorithm fits a new tree to the difference between the observed response and the ensemble prediction, which includes all trees trained in the previous iterations.

2.4 Artificial Neural Networks

In machine learning, artificial neural networks (ANN) are used to estimate or approximate unknown linear and non-linear functions that depend on a large number of inputs. Artificial neural networks can compute values or return labels using inputs. An ANN consists of several processing units, called neurons, which are arranged in layers. ANN can use learning algorithm such as back propagation to learn the weights and biases for each single neuron [30]. This kind of network its performance get worse as the number of hidden layers increases because of the vanishing of the gradient. In this paper we used the autoencoder which is proposed by Hinton and Salakhutdinov [31] to build deep network. An autoencoder can discover interesting structure in the data by setting its inputs and outputs equal and using backpropagation to learn its weights and biases.

3 Data Description

The data used in this paper was collected from two different field experiments. The field experiments done at the Virginia Department of Transportation’s (VDOT) Smart Road facility, located at the Virginia Tech Transportation Institute (VTII). The length of the Smart Road is a 3.5 km (2.2 mile). It is a two-lane road with one four-way signalized intersection. The horizontal layout of the test section is fairly straight, and the vertical layout has a substantial grade of 3 % [32]. The two field data collection efforts were conducted to characterize driver behavior at the onset of a yellow indication as a function of various driver and traffic stream characteristics under different weather conditions.

Two vehicles were used in each study, one was driven by test participant (accompanied by the in-vehicle experimenter) and the other vehicle was driven by a trained research assistant to simulate real-world conditions by crossing the

intersection from the side street when the signal was red for the test vehicle. The test vehicle was equipped with a real-time data acquisition system (DAS), differential Global Positioning System (GPS) unit, a longitudinal accelerometer, sensors for accelerator position and brake application, and a computer to run the different experimental scenarios. The vehicle data stream was synchronized with changes in the traffic signal controller by the communication channel that links the data recording equipment to the inter-section signal control box. The phase changes was triggered by the test vehicle using the GPS unit to determine the distance from the intersection. The two vehicles were equipped with a communications system between them, operated by the research assistants, and with the Smart Road control room.

In both studies, participants drove loops on the Smart Road, crossing a four-way signalized intersection where the data were collected. Exclusive of practice trials, the participant drove the entire test course 24 times for a total of 48 trials, where a trial consists of one approach to the intersection. Each participant was tested individually. Among the 48 trials, there were 24 trials in which each yellow trigger time to stop-line occurred four times. For the remaining 24 trials, the signal indication remained green.

3.1 Dry Roadway Surface Field Experiment

In this study, twenty-four licensed drivers were recruited in three equal age groups (under 40-years-old, 40 to 59-years-old, and 60-years-old or older); equal number of male and female participants were assigned to each group [33]. The data collection effort was conducted under clear weather conditions. The test conditions were based on two instructed vehicle speeds of 72.4 km/h (45 mi/h) and 88.5 km/h (55 mi/h). Each participant was assigned to the two test conditions (sessions), one test condition per day, taking approximately 1.5 h per session to complete. A 4-s yellow interval at the 72.4 km/h instructed speed and a 4.5-s yellow interval at the 88.5 km/h instructed speed were triggered for a total of 24 times (four repetitions at six distances). The yellow indications were triggered when the front of the test vehicle was 40.2, 54.3, 62.5, 70.4, 76.5, and 82.6 m (132, 178, 205, 231, 251, and 271 ft) from the intersection for the 72.4 km/h instructed speed and 56.7, 76.2, 86, 93.6, 101, and 113 m (186, 250, 282, 307, 331, and 371 ft) for the 88.5 km/h instructed speed.

3.2 Rainy/Wet Roadway Surface Field Experiment

In this study, twenty-six drivers were recruited in three age groups (under 40-years-old, 40 to 59-years-old, and 60 years of age or older), each group is male-female balanced [34]. The major differences of this study than the previous one were: (a) all runs were conducted under rainy weather conditions with wet

pavement surfaces and (b) all runs were executed at only one instructed speed of 72.4 km/h (45 mi/h). A 4-s yellow interval at the 72.4 km/h instructed speed was triggered for a total of 24 times (four repetitions at six distances). The yellow indications were triggered when the front of the test vehicle was 54.3, 62.5, 70.4, 76.5, 82.6, and 92.7 m (178, 205, 231, 251, 271, and 304 ft).

4 Results

This section presents the regression results of the machine learning algorithms. There are six predictors used to predict the PRT and deceleration level of the driver:

- Ge is the gender (1 = female, 0 = male)
- Gr is the grade (1 = downhill, 0 = uphill)
- A is the age (years)
- TTI is the time-to-intersection
- V is the approach speed (km/h) divided by the instructed speed
- SC is the roadway surface condition (0 = rainy/wet surface, 1 = dry)

The machine learning models are evaluated using relative and absolute prediction errors. The relative error is computed as the mean absolute percentage error (MAPE) using Eq. (1). This error is the average absolute percentage change between the predicted and the true values. The corresponding absolute error is presented by the mean absolute error MAE using Eq. (2). This error is the absolute difference between the predicted and the true values.

$$\text{MAPE} = \frac{100}{J} \sum_{j=1}^J \frac{|y_j - \hat{y}_j|}{y_j} \quad (1)$$

$$\text{MAE} = \frac{1}{J} \sum_{j=1}^J |y_j - \hat{y}_j| \quad (2)$$

where

J total number of observations in the testing data set,

y ground truth traffic state, and

\hat{y} predicted traffic state.

For each machine learning algorithm, the average of MAE and MAPE are calculated using the 10-fold-cross-validation method. In the 10-fold-cross-validation method approach, the data set is divided into 10 chunks of data (folds). Then, the regression model is built using 9 folds and the unused fold. This driver is used to test the model. The entire process is repeated where each fold is used once as a test and the average MAE and MAPE are calculated across all folds.

4.1 Classification and Regression Tree

The Classification and Regression Tree (CART) model was implemented using Matlab. Pruning was applied to prune the tree at different levels. The MAE and MAPE obtained from a 10-fold Cross-Validation at different Pruning are used to find the best tree.

Figure 1 shows the regression trees that model the PRT and deceleration level. The CART that model the PRT has an average MAE equals 0.1212 s. As shown Fig. 1 all the predictors appear in the tree and the root of the tree is the grade. Figure 2 shows the tree that model the deceleration level. This tree uses the TTI, Ge, and SC and find the other three predictors are not necessary to predict the deceleration level. The CART that model the deceleration level has an average MAE equals 0.3586 m/s².

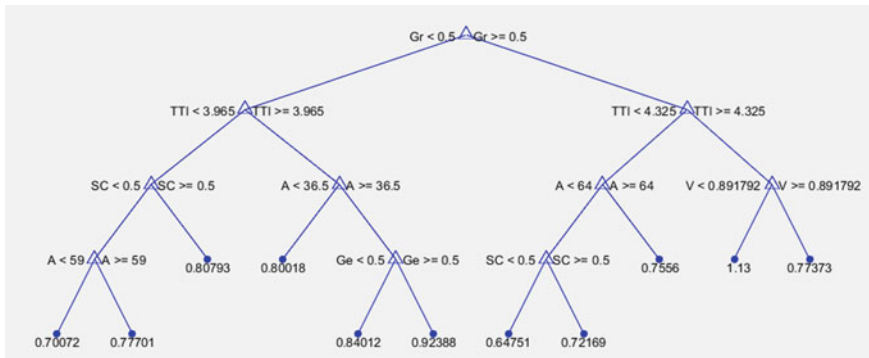


Fig. 1 The CART model for the PRT

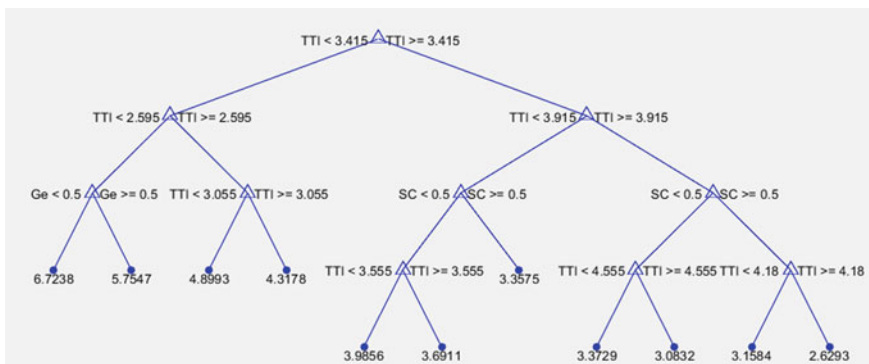


Fig. 2 The CART model for the deceleration level

4.2 *Random Forests*

The Random Forest (RF) model was implemented using Matlab. In order to find the sufficient number of trees that gives the best result we did sensitivity analysis. We grow the forest from 5 to 50, using 50 trees step. After approximately 30 trees, no benefit is gained by including more trees. Thus, to apply RF to model the PRT and deceleration level, 50 trees were used, which is a sufficiently large number. The RF that model the deceleration level has an average MAE equals 0.1070 s for the PRT and 0.3406 m/s² for the deceleration level.

4.3 *Ensemble of Deep Networks*

The Ensemble of deep networks model was implemented using Matlab. In general, deep learning needs large data to avoid overfitting and give good performance. In order to overcome this problem we used an ensemble of deep network each on has two hidden layers and the number of neurons in the first and second hidden layers changed from 2 to 12 and from 5 to 20 respectively. The total number of deep networks in the ensemble is 167, which gives an average MAE equals 0.1070 s for the PRT and 0.3406 m/s² for the deceleration level.

4.4 *Adaptive Boosting*

The Adaptive Boosting Adaboost model was implemented using Matlab. We did sensitivity analysis to find best number of weak learner. We found Adaboost using 50 trees is sufficient to model our dataset. The Adaboost has an average MAE equals 0.1141 s for the PRT and 0.3314 m/s² for the deceleration level.

4.5 *Models Comparison*

In this section, we show the tables which compare between the different machine learning algorithms we used to model the PRT and the deceleration level. For the sake of completeness, we include the MAE and MAPE when using the multiple linear regression (MLR). As shown in Table 1 the machine learning algorithms give better PRT prediction than MLR except CART. It is also shown that RF is the best algorithm. Table 2 shows the predictions error for the deceleration level and all machine learning algorithms has lower errors than the MLR. Table 2 shows that the ensemble of deep networks gives the best prediction.

Table 1 The mean of MAPE (%) and MAE (sec) for PRT

Algorithm	Mean MAPE	Mean MAE
MLR	16.1140	0.1180
CART	16.5435	0.1212
Random forest	14.5782	0.1070
Ensemble of deep networks	15.5386	0.1141
Adaboost	14.6113	0.1074

Table 2 The mean of MAPE (%) and MAE (m/s²) for deceleration level

Algorithm	Mean MAPE	Mean MAE
MLR	10.8734	0.3802
CART	10.2287	0.3586
Random forest	9.6866	0.3406
Ensemble of deep networks	9.3650	0.3314
Adaboost	9.6074	0.3397

5 Conclusions

In this paper, we adopt several machine learning algorithms to model the brake PRT and the deceleration level. The built models could be used to predict PRT and the deceleration level at good accuracy. The adopted algorithms have the advantage of being non-parametric algorithms and they avoid many of the MLR assumptions such as normality and equal variance. The results obtained by modeling data set collected from two controlled experiments done at the smart road at VTTI show that machine learning algorithms are promising techniques in modeling PRT and deceleration level. We compared the adopted machine learning techniques and MLR using the prediction errors. For the PRT, all adopted machine learning techniques are better than the MLR except the CART, besides the RF gives the best prediction. For the deceleration level, MLR gave the worst predictions while the ensemble of deep networks gives the best prediction. In the near future when vehicle to infrastructure communication will be deployed, the signal controllers at intersections could use the developed machine learning models in conjunction with classification algorithms to detect the behavior of the driver if the signal is turned into yellow. Then it predicts the PRT and deceleration levels for the expected stopping drivers. Based on the prediction of these two quantities it could decide to extend the green to avoid any potential crashes at the intersection.

Acknowledgments The authors acknowledge the support of Ahmed Amer, Huan Li, and the other research assistants at the Center for Sustainable Mobility, VTTI for running the tests, and to the Center for Technology Development and the Smart Road Operations Group at VTTI. This work was supported in part by grants from the Virginia Transportation Research Council (VTRC), the Mid-Atlantic Universities Transportation Center (MAUTC), and SAFETEA-LU funding.

References

1. Jones, W.D.: Keeping cars from crashing. *IEEE Spectr.* **38**(9), 40–45 (2001)
2. Hastie, T., Tibshirani, R., Friedman, J.: *The Elements of Statistical Learning Data Mining, Inference, and Prediction*. In: Springer Series in Statistics (ed.), Springer, Berlin (2009)
3. Thompson, B.A.: *Determining Vehicle Signal Change and Clearance Intervals*. Institute of Transportation Engineers, Washington, DC (1994)
4. Milazzo, J., et al.: The effect of dilemma zones on red light running enforcement tolerances. In: Transportation Research Board 81st Annual Meeting, Washington, DC (2002)
5. Taoka, G.T.: Brake reaction times of unalerted drivers. *ITE J.* **59**(3), 19–21 (1989)
6. Green, M.: “How long does it take to stop?” methodological analysis of driver perception-brake times. *Transp. Hum. Factors* **2**(3), 195–216 (2000)
7. Caird, J.K., et al.: The effect of yellow light onset time on older and younger drivers’ perception response time (PRT) and intersection behavior. *Transp. Res. Part F: Traffic Psychol. Behav.* **10**(5), 383–396 (2007)
8. Rakha, H., El-Shawarby, I., Setti, J.R.: Characterizing driver behavior on signalized intersection approaches at the onset of a yellow-phase trigger. *IEEE Trans. Intell. Transp. Syst.* **8**(4), 630–640 (2007)
9. El-Shawarby, I., Abdel-Salam, A.-S., Rakha, H.: Evaluation of driver perception-reaction time under rainy or wet roadway conditions at onset of yellow indication. *Transp. Res. Rec. J. Transp. Res. Board* **2384**, 18–24 (2013)
10. Williams, W.L.: Driver behavior during the yellow interval. *Transp. Res. Rec.* **644**, 75–78 (1977)
11. Parsonson, P.S., Santiago, A.: Design standards for timing the traffic signal clearance period must be improved to avoid liability. In: *ITE Compendium Technical Papers*, pp. 67–71 (1980)
12. Wortman, R.H., Matthias, J.S., Transportation, A.: *An Evaluation of Driver Behavior at Signalized Intersections*. Arizona Department of Transportation, Phoenix Arizona (1983)
13. Wortman, R.H., Witkowski, J.M., Fox, T.C.: *Traffic characteristics during signal change intervals (Abridgment)* (1985)
14. El-Shawarby, I., et al.: Impact of driver and surrounding traffic on vehicle deceleration behavior at onset of yellow indication. *Transp. Res. Rec. J. Transp. Res. Board* **2248**, 10–20 (2011)
15. Wang, J., et al.: Normal deceleration behavior of passenger vehicles at stop sign-controlled intersections evaluated with in-vehicle global positioning system data. *Transp. Res. Rec. J. Transp. Res. Board* **1937**, 120–127 (2005)
16. Haas, R., et al.: Use of intelligent transportation system data to determine driver deceleration and acceleration behavior. *Transp. Res. Rec. J. Transp. Res. Board* **1899**, 3–10 (2004)
17. Ali, S.S.M., et al.: Application of random forest algorithm to classify vehicles detected by a multiple inductive loop system. In: *2012 15th International IEEE Conference on Intelligent Transportation Systems (Itsc)*, pp. 491–495 (2012)
18. M.-H. Pham, et al.: Random forest models for identifying motorway rear-end crash risks using disaggregate data. In: *13th International IEEE Annual Conference on Intelligent Transportation Systems*, Madeira Island, Portugal (2010)
19. Liu, Q., Lu, J., Chen, S.: Traffic incident detection using random forest. In: *Transportation Research Board 92nd Annual Meeting*, Washington DC
20. Yulan, L., Reyes, M.L., Lee, J.D.: Real-time detection of driver cognitive distraction using support vector machines. *IEEE Trans. Intell. Transp. Syst.* **8**(2), 340–350 (2007)
21. Tango, F., Botta, M.: Real-time detection system of driver distraction using machine learning. *IEEE Trans. Intell. Transp. Syst.* **14**(2), 894–905 (2013)
22. Jahangiri, A., Rakha, H.: Developing a support vector machine (SVM) classifier for transportation mode identification by using mobile phone sensor data. In: *Transportation Research Board 93rd Annual Meeting* (2014)

23. Balali, V., Golparvar-Fard, M.: Scalable nonparametric parsing for segmentation and recognition of high-quantity, low-cost highway assets from car-mounted video streams. In: Construction Research Congress 2014@ Construction in a Global Network. ASCE (2014)
24. Machiani, S.G., Abbas, M.: Predicting drivers decision in dilemma zone in a driving simulator environment using canonical discriminant analysis. In: The 93rd Annual Meeting of the Transportation Research Board, Washington, DC (2014)
25. Elhenawy, M., et al.: Classification of driver stop/run behavior at the onset of a yellow indication for different vehicles and roadway surface conditions using historical behavior. *Procedia Manufact.* **3**, 858–865 (2015)
26. Breiman, L., et al.: *Classification and Regression Trees*. CRC press, Boca Raton (1984)
27. Breiman, L.: Random forests. *Mach. Learn.* **45**(1), 5–32 (2001)
28. Hastie, T., et al.: *The Elements of Statistical Learning*, vol. 2. Springer, Berlin (2009)
29. Freund, Y., Schapire, R.: A short introduction to boosting. *Japanese Soc. Artif. Intell.* **14**(5), 771–780 (1999)
30. Rumelhart, D.E., Hinton, G.E., Williams, R.J.: Learning representations by back-propagating errors. *Cogn. Model.* **5**(1)
31. Hinton, G.E., Salakhutdinov, R.R.: Reducing the dimensionality of data with neural networks. *Science* **313**(5786), 504–507 (2006)
32. Rakha, H., et al.: Vehicle dynamics model for predicting maximum truck acceleration levels. *J. Transp. Eng.* **127**(5), 418–425 (2001)
33. Amer, A.M.M., Rakha, H.A., El-Shawarby, I.: A behavioral modeling framework of driver behavior at onset of yellow a indication at signalized intersections. In: Transportation Research Board 89th Annual Meeting, Washington DC (2010)
34. El-Shawarby, I., et al.: Driver behavior at the onset of yellow indication for rainy/wet roadway surface conditions. In: Transportation Research Board 91st Annual Meeting (2012)

3D Scanning of Clothing Using a RGB-D Sensor with Application in a Virtual Dressing Room

Michael B. Holte

Abstract This paper presents an approach for creating digital clothing with application in a virtual dressing room. The clothes are made digital by scanning real clothes using a RGB-D sensor. While creating digital clothing using specialized programs, e.g. Marvelous Designer 2, is a time consuming process, the 3D scanning process is relatively fast. The model is acquired via registration of different views while rotating on a platform; a complete rotation is performed in approximately 60 s, however, we have achieved satisfactory results even with rotations of 15 s. The surface is textured using the RGB images acquired during the scanning process, and the color of the occluded parts is approximated via K-Nearest Neighbors (KNN). We show early results of creating digital clothing of high quality by scanning real clothes.

Keywords Cloth scanning · Virtual dressing room · 3D reconstruction · RGB-D sensor · Computer graphics

1 Introduction

Today people are increasingly shopping online; most of them are satisfied buying certain types of goods online like books, electronics, tickets etc. However, when it comes to buying clothes online, they are not entirely satisfied [1]. A report shows that there is approximately a 25 % return rate of the ordered goods in the online clothing industry in Denmark. The reason for the returns at this moment can be speculated as, the clothes do not fit the customers properly, or the customers simply dislike the cloth when they actually wear it. As a result, there is an increase in the costs for the online retailers and dissatisfaction among the consumers. Apparently, the consumers are looking for more reliable solutions for buying clothes online.

M.B. Holte (✉)

Department of Architecture, Design and Media Technology,
Aalborg University, Niels Bohrs Vej 8, 6700 Esbjerg, Denmark
e-mail: mbh@create.aau.dk

The industry is beginning to recognize that new technologies like virtual-reality and 3D camera-based systems have great potential to solve this problem. Hence, the virtual dressing room addresses this problem by enabling the consumers to, e.g., try on the virtual version of the clothes on their virtual 3D avatar/profile before buying the real clothes, from the convenience of their home computers, TV or hand-held devices.

1.1 The Virtual Dressing Room

The current state-of-the-art solutions use 3D/range cameras or lasers technologies to acquire 3D information of the costumer, enabling estimation of the body shape and measurements. One such solution is Bodymetrics [2], which uses a rig setup of multiple Microsoft Kinect sensors to measure the user's body proportions, followed by an expert in the shop floor guiding the customer to find the right fit. This is a costly and time-consuming process. Hence, this is not a real-time interactive virtual dressing room, but serves solely for measuring the proportions of the costumer. In contrast, Fitnect [3] is a real-time interactive system, which employs the Microsoft Kinect sensor to acquire input video and depth/3D information of the user. The 3D information of the body facilitates automatic fitting of the clothes to the body, which follows the user's movements.

At the company interface, a major challenge of developing a virtual dressing room is how to design and produce digital clothing for augmentation. Creating digital clothing using specialized programs, e.g. Marvelous Designer 2 [4] (see Fig. 1), is a time consuming process, hence it might be difficult to convince the manufactures of an investment in digital clothing. In this paper, we suggest another option, where digital clothing is produced by 3D scanning of real clothes.

1.2 Data Acquisition and 3D Reconstruction

Several different kinds of sensors are available for 3D data acquisition: marker-based systems [5], stereo vision [6, 7], structured light [8], laser-range scanners [9], Time-of-Flight (ToF) sensors [10, 11], the Microsoft Kinect sensor [12] and multi-camera systems [13]. The downside of the marker-based systems is that one has to use markers (or a special suit with markers), while stereo vision, multi-camera systems and structured light suffer from the need of careful calibration of multiple cameras and/or projectors. In contrast, the Microsoft Kinect and ToF sensors do not suffer from these requirements. However, these sensors only capture the depth values from one viewpoint of a surface, while, a multi-camera system with a sufficient number of cameras is able to capture the entire 3D surface from 360°. To overcome this problem Izadi et al. [14] propose an approach for fusion of

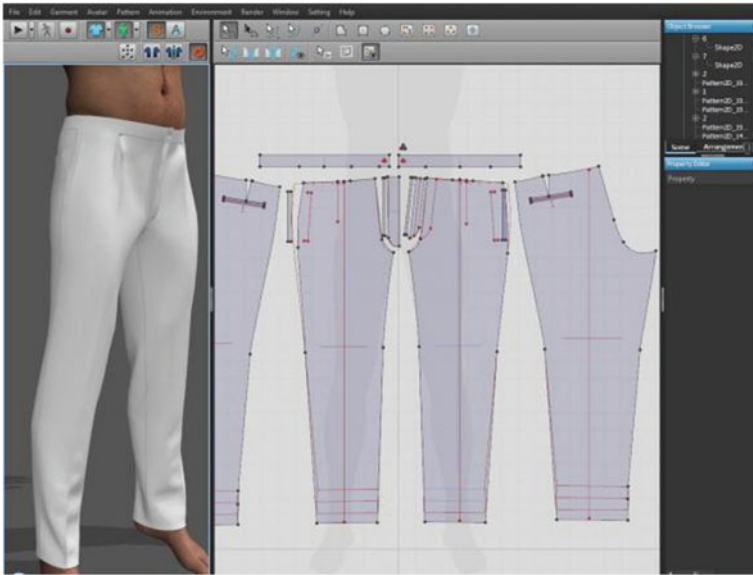


Fig. 1 An example image showing the design of clothing using Marvelous Designer 2 [4]

depth information captured by a moving Kinect sensor. This allows for fusion of surfaces captured from multiple viewpoints.

The captured depth information and thereby the reconstructed 3D surface is often affected by noise, due to nature of the sensor and the capturing process. This results in errors like incomplete surfaces (holes) and smaller noise components. Several techniques have been proposed to filter and correct these errors, e.g., Bilateral filters [15, 16] and Laplacian smoothing. Starck and Hilton propose a global optimization method for reconstruction and filtering of 3D surfaces [17], and Liepa propose a method for filling holes in unstructured triangular meshes [18].

1.3 Our Approach and Contributions

In this paper, we present an approach for creating digital clothing with application in a virtual dressing room. The clothes is made digital by scanning real clothes using a single RGB-D sensor (Sect. 2). We employ the Microsoft Kinect for this purpose, which facilitates easy integration with the most promising virtual dressing room solutions, like Fitnect [3]. While creating digital clothing using specialized programs, e.g. Marvelous Designer 2 [4] (see Fig. 1), is a time consuming process, the 3D scanning process is relatively fast. We adopt the *KinectFusion* approach proposed by Izadi et al. [14]; however, instead of moving the sensor we rotate the object. Concretely, the model is acquired via registration of different views while

rotating on a platform; a complete rotation is performed in approximately 60 s, however we have achieved satisfactory results even with rotations of 15 s. Before registration a series of Bilateral filters [15, 16] are applied to each Point Cloud (PC). Then the PC is registered using Iterative Closest Point (ICP) [19] and the resulting PC is stored in a Voxel Grid [20]. When a sufficient number of PCs have been acquired, the surface is reconstructed using Marching Cubes [21]. Outliers caused by noise are removed and the surface, if non-manifold, is transformed into a manifold one. Next, the surface is smoothed via Laplacian smoothing and holes filled with the algorithm proposed by Leipa [18]. Finally, the number of Polygons is reduced via Quadric Edge Collapse Decimation [22]. The surface is textured using the RGB images acquired during the scanning process, and the color of the occluded parts is approximated via K-Nearest Neighbors (KNN). In Sect. 3 we show early results of creating digital clothing of high quality by scanning real clothes, and in Sect. 4 we give concluding remarks and discuss future work.

2 The 3D Scanning Process

In this section, we give a step-by-step description of our approach for creating digital clothing by scanning real clothes using a single Microsoft Kinect sensor.

2.1 The Setup

The cloth scanning setup consists of a mannequin doll mounted on top of a rotating platform, enabling 360° rotation. A Microsoft Kinect sensor captures the RGB and depth information of the mannequin wearing the clothes, as shown in Figs. 2 and



Fig. 2 The 3D cloth scanning setup using a mannequin doll and a Microsoft Kinect sensor

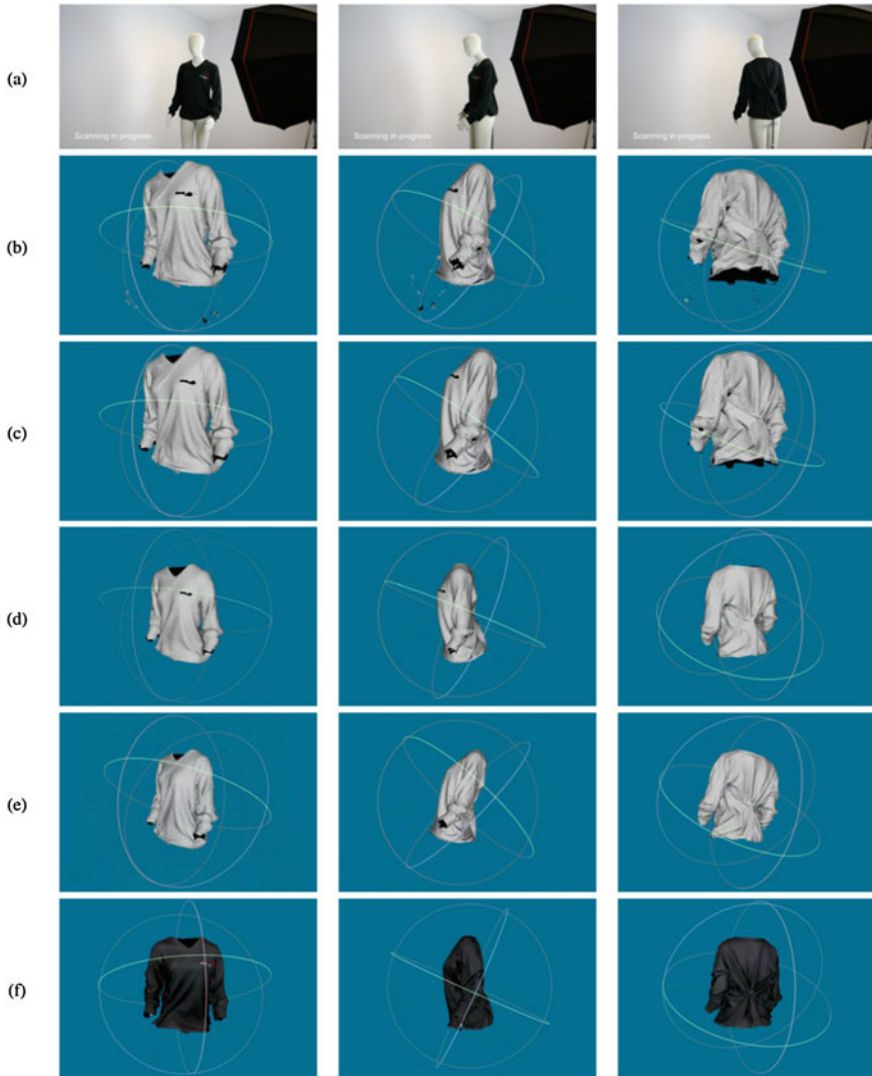


Fig. 3 Intermediate results of the cloth scanning process seen from three different viewpoints (columns): **a** the setup and data acquisition, **b** the reconstructed mesh, **c** noise reduction, **d** filling holes, **e** polygon reduction and **f** texturing

3a. The model is acquired via registration of different views while rotating on the platform. The results shown in Figs. 3, 6 and 7 have been made with a complete rotation performed in approximately 60 s; however, we have achieved satisfactory results even with rotations down to 15 s.

2.2 Data Acquisition

The acquired depth map is converted from image coordinates into 3D points (vertices) and normals in the coordinate space of the sensor. Given the intrinsic calibration matrix \mathbf{K} of the Kinect sensor, at time i , a specific depth measurement $\mathbf{D}_i(x, y)$ is reprojected as a 3D vertex in the camera's coordinate space as follows: $\mathbf{v}_i(x, y) = \mathbf{D}_i(x, y)\mathbf{K}^{-1}[x, y, 1]$. Corresponding normal vectors for each vertex are computed using neighboring reprojected points: $\mathbf{n}_i(x, y) = (\mathbf{v}_i(x+1, y) - \mathbf{v}_i(x, y)) \times (\mathbf{v}_i(x, y+1) - \mathbf{v}_i(x, y))$ (normalized to unit length $\mathbf{n}_i/||\mathbf{n}_i||$). The 6DOF camera pose at time i is a rigid body transform matrix $\mathbf{T}_i = [\mathbf{R}_i|\mathbf{t}_i]$ containing a 3×3 rotation matrix \mathbf{R}_i and 3D translation vector \mathbf{t}_i . Given this transform, a vertex and a normal can be converted into global coordinates $\mathbf{v}_i^g(x, y) = \mathbf{T}_i\mathbf{v}_i(x, y)$ and $\mathbf{n}_i^g(x, y) = \mathbf{R}_i\mathbf{n}_i(x, y)$, respectively [14].

2.3 Registration

Before registration a series of Bilateral filters [15, 16] are applied to each Point Cloud (PC), which reduce noise by smoothing while preserving details. Then, the PC is registered using Iterative Closest Point (ICP) [19]. ICP is applied to track the camera pose for each depth frame, by estimating a single 6DOF transform that closely aligns the current oriented points with those of the previous frame. This gives a relative 6DOF transform which can be incrementally applied together to give the single global camera pose \mathbf{T}_i . The first step of ICP is to find correspondences between the current oriented points at time i with the previous at $i - 1$ using projective data association [14, 19]. Given this set of corresponding oriented points, the output of each ICP iteration is a single transformation matrix \mathbf{T} that minimizes the point-to-plane error metric [23], defined as the sum of squared distances between each point in the current frame and the tangent plane at its corresponding point in the previous frame [14]:

$$\arg \min \sum_{\substack{(x,y) \\ \mathbf{D}_i(x,y) > 0}} \left\| (\mathbf{T}\mathbf{v}_i(x, y) - \mathbf{v}_{i-1}^g(x, y)) \cdot \mathbf{n}_{i-1}^g(x, y) \right\|^2. \quad (1)$$

We use a linear approximation to solve this system, by assuming only an incremental transformation occurs between frames [23, 24].

2.4 3D Reconstruction

Instead of fusing point clouds before reconstructing the mesh, we first use a volumetric surface representation based on [20]. By predicting the global pose of the camera using ICP, any depth measurement can be converted from image coordinates into a single consistent global coordinate space. A 3D volume of fixed resolution is predefined and updated, which maps to specific dimensions of a 3D physical space. This volume is subdivided uniformly into a 3D grid of voxels. When a sufficient number of PCs have been acquired and stored in the voxel grid, the surface is reconstructed using Marching Cubes [21]. The resulting mesh is shown in Fig. 3b.

2.5 Filtering and Enhancement

After 3D reconstruction, outliers caused by noise are removed and the surface, if non-manifold, is transformed into a manifold one. Figure 4 shows examples of noise and holes in the reconstructed mesh. The surface is refined via Laplacian smoothing (Fig. 3c) and holes filled (Fig. 3d). We use the algorithm described in [18], which effectively fills holes in unstructured triangular meshes. The resulting patching meshes interpolate the shape and density of the surrounding mesh, and works with arbitrary holes in oriented connected manifold meshes. The steps in filling a hole include boundary identification, hole triangulation, refinement, and fairing (see [18] for further details).

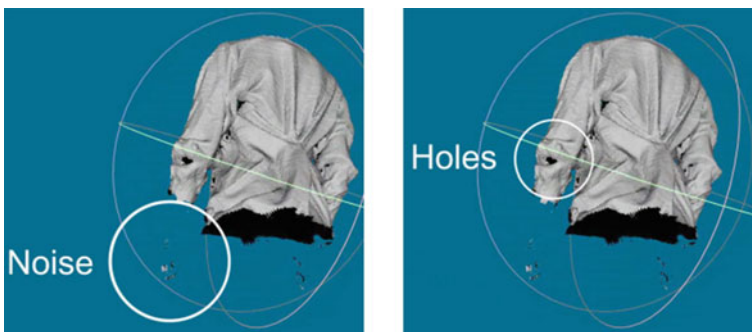


Fig. 4 Examples of noise and holes in the reconstructed mesh

2.6 Polygon Reduction

The number of polygons are reduced via Quadric Edge Collapse Decimation [22]. An example is shown in Figs. 3e and 5, where the number of polygons for a shirt is reduced from 288.620 to 9.976 polygons, while still preserving a satisfactory level of detail.

2.7 Texturing

The surface is textured using the color information from the RGB images acquired during the scanning process. The mapping is performed using a trivial projection from camera space to object space. While this works well for non-occluded surfaces, color information is not available for occluded surfaces. For the occluded parts, the color is approximated via K-Nearest Neighbors (KNN). An example of a textured digital piece of cloth is shown in Figs. 3f and 6.

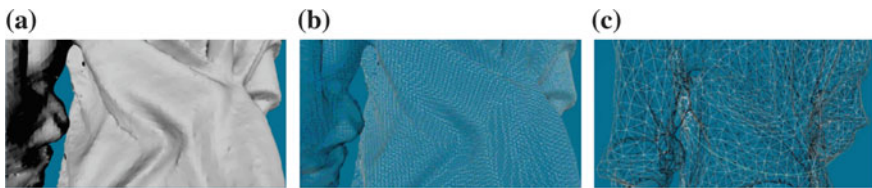


Fig. 5 Polygon reduction from 288.620 to 9.976 polygons. **a** High density surface, **b** high density mesh (288.620 polygons), **c** polygons reduced to 9976 polygons

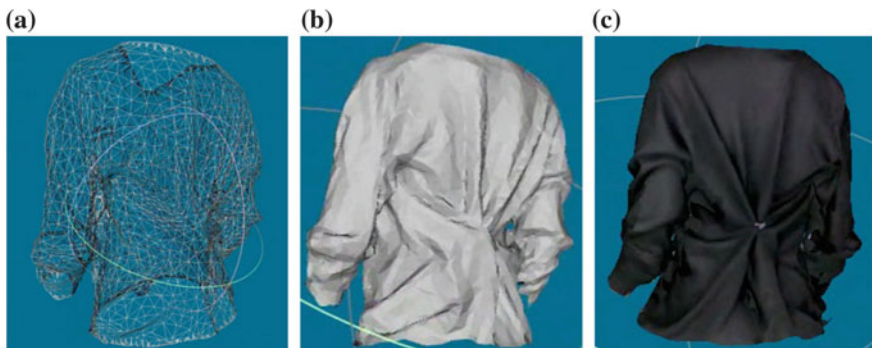


Fig. 6 The resulting textured digital shirt by 3D scanning of a real shirt. **a** Mesh, **b** surface, **c** texturing

3 Experimental Results

In this section, we show early experimental results of scanning different kinds of clothes using the presented 3D scanning setup and data processing pipeline. Figure 7 shows the results of scanning a shirt, a T-shirt and a pair of pants. As can be seen, the quality and detail level of the resulting digital clothes are good. Obviously, the appearance of the digital clothes depends on how the mannequin has



Fig. 7 Experimental results of scanning three different kinds of clothes (a shirt, a pair of pants and a T-shirt) displayed from multiple viewpoints

been dressed up in the real clothes. However, when animating the clothes with respect to the movements of the body, in a virtual dressing room setting like Fitnect [3], the digital clothes can be transformed accordingly.

4 Conclusion

At the company interface, a major concern of developing a virtual dressing room is how to design and produce digital clothing. Creating digital clothing using specialized programs, like Marvelous Designer 2, is a time consuming process, hence, it might be difficult to convince the manufactures of an investment in digital clothing. In this paper we have proposed a significant faster approach for creating digital clothing by 3D scanning of real clothes using a single RGB-D sensor (Microsoft Kinect) for application in a virtual dressing room. We employ a mannequin doll mounted on a rotating platform, which is wearing the clothes to be scanned. A full scan (a complete rotation) is performed in approximately 60 s; however, we have achieved satisfactory results even with rotations of 15 s. Hence, the 3D cloth scanning is a much faster alternative to create digital clothing than having a graphical designer produce the clothes.

In future work, we want to animate the digital clothes using non-rigid transformation [25], and integrate it with a gesture-based graphical user interface similar to Fitnect [3].

Acknowledgments The research leading to these results has been conducted in collaboration with Virtual Lab ApS and has received funding from The Danish National Advanced Technology Foundation under the research project “The Virtual Dressing Room”.

References

1. Schaupp, L.C., Belanger, F.: A conjoint analysis of online consumer satisfaction. *J. Electron. Commer. Res.* **6**(2), 95–111 (2005)
2. Bodymetrics, <http://www.bodymetrics.com>
3. Fitnect Interactive Kft, <http://www.fitnect.hu>
4. Marvelous Designer, <http://www.marvelousdesigner.com>
5. Neumann, T., Wacker, M., Varanasi, K., Theobalt, C., Magnor, M.: High detail marker based 3D reconstruction by enforcing multiview constraints. In: *Proceedings of SIGGRAPH (2012)*
6. De-Maeztu, L., Mattoccia, S., Villanueva, A., Cabeza, R.: Linear Stereo Matching. In: *ICCV (2011)*
7. Scharstein, D., Szeliski, R.: A taxonomy and evaluation of dense two-frame stereo correspondence algorithms. *IJCV* **47**(1–3), 7–42 (2002)
8. Fof, D., Sliwa, T., Voisin, Y.: A comparative survey on invisible structured light. *Proc. SPIE* **5303**, 90–98 (2004)
9. Werghe, N.: Segmentation and modeling of full human body shape from 3-D scan data: a survey. *TSMC-C* **37**(6), 1122–1136 (2007)

10. Kolb, A., Barth, E., Koch, R., Larsen, R.: Time-of-flight sensors in computer graphics. In: Eurographics—State of the Art Reports (2009)
11. Stoykova, E., Alatan, A.A., Benzie, P., Grammalidis, N., Malasitis, S., Ostermann, J., Piekh, S., Sainov, V., Theobalt, C., Thevar, T., Zabulis, X.: 3-D time-varying scene capture technologies: a survey. *IEEE Trans. Circuits Syst. Video Technol.* **17**(11), 1568–1586 (2007)
12. Shotton, J., Fitzgibbon, A., Cook, M., Sharp, T., Finocchio, M., Moore, R., Kipman, A., Blake, A.: Real-time human pose recognition in parts from single depth images. In: CVPR (2011)
13. Gkalelis, N., Kim, H., Hilton, A., Nikolaidis, N., Pitas, I.: The i3DPost multi-view and 3D human action/interaction database. In: CVMP (2009)
14. Izadi, S., Kim, D., Hilliges, O., Molyneaux, D., Newcombe, R., Kohli, P., Shotton, J., Hodges, S., Freeman, D., Davison, A., Fitzgibbon, A.: KinectFusion: real-time 3D reconstruction and interaction using a moving depth camera. In: ACM Symposium on UIST (2011)
15. Porikli, F.: Constant time $O(1)$ bilateral filtering. In: CVPR (2008)
16. Tomasi, C., Manduchi, R.: Bilateral filtering for gray and color images. In: ICCV (1998)
17. Starck, J., Hilton, A.: Surface capture for performance based animation. *IEEE Comput. Graphics Appl.* **27**(3), 21–31 (2007)
18. Liepa, P.: Filling holes in meshes. In: Eurographics/ACM SIGGRAPH Symposium on Geometry Processing (2003)
19. Rusinkiewicz, S., Levoy, M.: Efficient variants of the ICP algorithm. In: 3DIM (2001)
20. Curless, B., Levoy, M.: A volumetric method for building complex models from range images. In: Proceedings of SIGGRAPH (1996)
21. Lorensen, W.E., Cline, H.E.: Marching cubes: a high resolution 3D surface construction algorithm. *SIGGRAPH Comput. Graphics* **21**(4), 163–169 (1987)
22. Garland, M., Heckbert, P.S.: Surface simplification using quadric error metrics. In: Proceedings of SIGGRAPH (1997)
23. Chen, Y., Medioni, G.: Object modeling by registration of multiple range images. *ICV* **10**(3), 145–155 (1992)
24. Low, K.: Linear least-squares optimization for point-to-plane ICP surface registration. In: Technical Report, TR04-004, University of North Carolina (2004)
25. Guan, P., Reiss, L., Hirshberg, D., Weiss, A., Black, M.J.: Drape: DRessnig any person. *ACM Trans. Graph.* **31**(4), 1–10 (2012)

Application of Strength Requirements to Complex Loading Scenarios

Scott England and Sudhakar Rajulu

Abstract NASA's endeavors in human spaceflight rely on extensive volumes of human-systems integration requirements to ensure mission success. These requirements protect space hardware accommodation for the full range of potential crewmembers, but cannot cover every possible action and contingency in detail. This study was undertaken in response to questions from various strength requirement users who were unclear how to apply idealized strength requirements that did not map well to the complex loading scenarios that crewmembers would encounter. Three of the most commonly occurring questions from stakeholders were selected to be investigated by human testing and human modeling. Preliminary findings indicate that deviation from nominal postures can affect compliance with strength requirements positively or negatively, depending on the nature of the deviation. Human modeling offers some avenues for quickly addressing requirement verification questions, but is limited by the fidelity of the model and environment.

Keywords NASA · Strength · Requirements · Biomechanics · Ergonomics · Human-systems integration · Spacesuits



1 Introduction

NASA programs involving human spaceflight usually design operations and hardware around human performance capabilities. In general, these capabilities are defined to protect task completion by the majority of potential crewmembers, who

S. England (✉)
MEI Technologies Inc., 2525 Bay Area Blvd. Suite 300,
Houston, TX 77058, USA
e-mail: scott.a.england@nasa.gov

S. Rajulu
NASA Johnson Space Center, 2101 NASA Parkway,
Houston, TX 77058, USA

Table 1 Example of idealized strength exertions from typical NASA strength requirements

Type of strength	Minimum crew operation loads [N (Lbf)]			Maximum crew operational loads [N(Lbf)]	
	Crit 1 operations	Crit 2 operations	Other operations		
One handed pulls	One handed pulls				
Seated horizontal pull In ² [Subject in a seated position pulls towards his/her body. Unilateral/Isometric measurement]		111 (25)	147 (33)	276 (62)	449 (101)
Seated vertical pull down ² [Subject in a seated position pulls downwards. Unilateral/Isometric measurement]		125 (28)	165 (37)	311 (70)	587 (132)

may be weak, injured, or deconditioned by extended time in microgravity. Currently the primary references for questions about crew strength abilities are the strength tables present in the various program-level requirements documents, including the Human Systems Integration Requirements [1] and the ISS Crew Transportation and Services Requirements Document [2]. These tables present 34 uniaxial exertions for the whole body. Table 1 illustrates the format of typical NASA strength requirement tables. These tables are repeated for each suit configuration, typically unsuited, suited-unpressurized, and suited pressurized. Unfortunately, tasks required of crewmembers are not always easily represented as an isometric exertion in a single direction.

The Anthropometry and Biomechanics Facility (ABF) maintains Subject Matter Expert (SME) status over NASA’s strength requirements and frequently fields questions about how to interpret and apply the strength requirements. These questions usually focus on one or more of several confounding factors that are often encountered when mapping uniaxial exertions to functional tasks. They include

- How to handle multiple joint exertions?
- How to deal with a subject bracing against their environment?
- How to interpret off-nominal exertions?

Potential solutions include task modification, biomechanical analyses, modeling, and human strength testing. This study sought to improve the utility of existing strength requirements by providing a consistent response for dealing with situations containing complex loading scenarios and by beginning to lay the groundwork for more comprehensive strength requirements in the future. Phase I of this study

investigated differences in strength performance between nominal and complex loading scenarios with human subjects and with human models. Phase II will build on lessons learned from Phase I and expand to include suited testing and additional loading scenarios.

The foundation of strength requirements applied to human spaceflight are the 34 strength exertions presented in the primary program-level requirements documents, the HSIR and the ICTSR. These 34 exertions, while extensive, are not fully comprehensive of all possible exertions that could be expected of a crewmember in the completion of mission objectives. This study documents the process of how strength requirements should be used and what to do when a task does not easily fall under the supplied strength requirements.

2 Method

Stakeholders and users of NASA's strength requirements were polled about commonly occurring issues in mapping tasks from NASA missions and hardware development to strength requirements provided in the program human factors requirements documents. Feedback from strength requirement users could be placed into three major categories:

1. How does one combine multiple-joint exertions?
2. How does one deal with braced exertions?
3. How does one deal with off-nominal position exertions?

2.1 Test Scenarios and Setup

The applications of these confounding factors were diverse, potentially expanding to include any exertion or combination of exertions from the strength requirement tables. Several down-selection criteria were deployed to constrain the problem further, including criticality of the task, frequency of the task, and ability of the task to be replicated in a 1 g environment. Specific tasks were chosen and reconstructed in a biomechanics laboratory environment as well as in a commercially available strength-modeling package, 3D Static Strength Predictor Program (3DSSPP). 3DSSPP was developed at the Center for Ergonomics at the University of Michigan for the purpose of predicting static strength capabilities of various segments of the population [3]. Human data were collected using a PrimusRS strength dynamometer (BTE Technologies, Hanover, Maryland) setup to simulate the problematic tasks to the greatest degree possible. An initial run of two unsuited pilot subjects was conducted to verify the test technique in Phase I of this study before a later full run of six to eight suited test subjects was conducted in Phase II.

Fig. 1 Multi-joint exertion of wrist and elbow



Multiple-Joint Exertions. A multiple-joint exertion involves situations where a control is operated with a combination of two joints, for example, concurrent motion of the elbow and wrist (Fig. 1). This situation may arise when a seated crewmember needs to perform a maximal reach from a restrained position to actuate a piece of hardware. Here either the wrist or the elbow could be flexed to actuate the hardware. Primary questions involve which type of exertion to use and whether more than one exertion can be added together simultaneously.

Human strength data were collected by positioning the head of the PrimusRS at a height even with the subject's shoulder and installing a handle attachment to measure a vertical force. Subjects were instructed to grip the Primus attachment with the shoulder flexed to 90° and elbow straight while applying a maximal exertion in the upward vertical direction with just the wrist in one set of trials and just the elbow in another. Each set was repeated three times or until the coefficient of variation was below 10 % for three trials. This test setup was modeled in 3DSSPP by placing the simulated subject in the same posture as the human subjects and applying a load to the center of the right hand. The model does not possess the

option of selecting which muscle set to activate, so the load at the hand was set to the wrist flexion strength requirement load of 17 lb. in one run, and the elbow flexion strength requirement load of 8 lb. in another. This setup was run with models possessing 50th-percentile male, 95th-percentile male, and 5th-percentile female anthropometries.

Braced Exertions. Braced exertions involve a confounding factor such that only one arm may be used to actuate the hardware of interest, but the second arm is available for bracing, as illustrated in Fig. 2. While not present in the 34 exertions from the NASA strength tables, this is potentially a desirable approach to increase the ability of the free arm to react opposite to the bracing.

Human strength data were collected in this posture by positioning the PrimusRS so that force could be exerted into the long axis of the forearm with the subject's elbows bent to 90° of flexion. Maximal exertions of horizontal force were collected with the subject in each of two postures. These postures were an unbraced stance, supported by only the soles of their feet and the grip of their dominant hand, and a braced stance in which the subject's non-dominant arm could firmly react against a rigid, anchored surface. This test setup was modeled in 3DSSPP by placing the simulated subject in the postures shown in Fig. 2 and applying a load to the center of the right hand and the left hand. The load in the right hand was the arm pull strength requirement load of 24 lbs. For braced exertions, the left hand received the arm push strength requirement load of 22 lbs. This setup was run with models possessing 50th-percentile male, 95th-percentile male, and 5th-percentile female anthropometries.

Off-Nominal Exertions. Off-nominal exertions involve a situation where a piece of hardware requires rotational motion that must be decomposed into simpler, unidirectional motions (Fig. 3). Additionally, these motions may be required to take place outside of the nominal posture presented in the strength tables.

Human strength data were collected in this posture by positioning the PrimusRS such that the subject's dominant hand could grasp the handle attachment of the dynamometer with the elbow flexed to 90° for the nominal position and with the

Fig. 2 Unbraced versus braced exertions

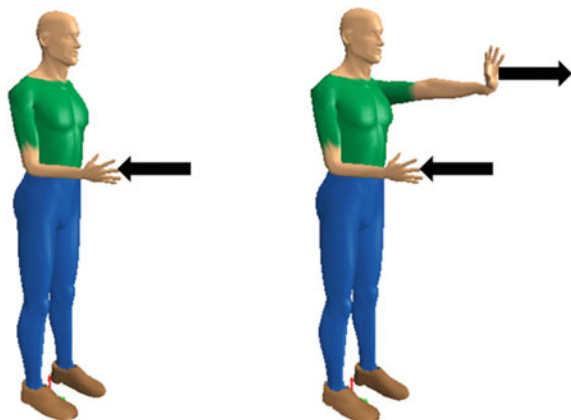


Fig. 3 Off-nominal exertions

handle at approximately eye level for the off-nominal position. Subjects performed four maximal exertions in each posture: pushing away, pulling toward, pulling medially, and pulling laterally. These four maximal exertions were performed in both the nominal and off-nominal postures. This test setup was modeled in 3DSSPP by placing the simulated subject in the postures shown in Fig. 3 and applying a load to the center of the right hand. The load in the right hand was iterated through the strength requirement load corresponding to a push load of 22 lbs., a pull load of 24 lbs., a medial load of 13 lbs., and a lateral load of 8 lbs. This setup was run with models possessing 50th-percentile male, 95th-percentile male, and 5th-percentile female anthropometries.

2.2 *Unsuited Human Strength Testing*

Human strength data were collected using the Caldwell method [4]. The core concepts of this method are

- Strength is assessed with a steady exertion sustained for 4 s
- Effort should be gradually and steadily increased to maximum without jerking within approximately 1 s
- No instantaneous feedback is provided to the subject during testing

- No goal setting, reward, or competition is permitted during testing
- A minimum of 1 min of rest is provided between trials

One-handed tasks were completed with the subject's dominant hand alone. Each task was repeated at least three times, and the coefficient of variation (COV) was calculated after three repetitions. Whenever the COV was above 10 %, additional repetitions were completed until three exertions had a COV below 10 %. Pilot testing was completed with two unsuited subjects to verify the test setup and identify issues not immediately obvious from human strength modeling. Full human testing will be completed with suited and unsuited subjects early in Phase II of the study in 2016.

2.3 Human Strength Modeling

Human strength modeling was performed using the 3D Static Strength Predictor Program (3DSSPP). Its primary output is the percentage of the population capable of completing an input task, according to the NIOSH lifting equation [3, 5] and empirical calculations on population strength. 3DSSPP is not capable of definitively saying whether a task could be completed for a single actuation. Rather, it provides feedback on what percentage of the population is capable of generating the required moments to resist the input forces, and if this task could be done for 8 h without elevated risk of injury. It is fair to estimate, however, that if a task could be safely completed regularly for a duration of 8 h, a weak subject could complete it a single time. It is important to note that human modeling should not be used alone in determining success of task completion. The input capabilities of 3DSSPP are somewhat limited, so not all possible human capabilities are available in the software.

The primary results of interest from 3DSSPP are the strength percentage capable calculations. The joint moments necessary to solve the modeled setup statically are calculated and compared to an equation for distribution of population strength. The percentage of the population with the capability to generate loads greater than the required loads is then reported. The population strength capabilities are determined from empirical mean strength equations developed from numerous sources and documented in relevant literature.

3 Results and Discussion

Results of human strength testing and human strength modeling are presented and analyzed below. They are paired by task being completed to highlight the differences between modeling and human testing. Human strength testing values are presented in pounds-force, which can be directly compared to the strength

requirement value for the task being simulated. Human modeling results are presented in terms of the percentage of the population accommodated at each relevant joint, that is, the percentage of the population possessing the strength to successfully complete the task being modeled. These percentages are determined through a combination of subject anthropometry and the output of the biomechanical models used by 3DSSPP.

3.1 Multiple Joint Exertion

Results from the multiple joint exertion analysis are presented in Table 2. Percentages of the population possessing the strength needed to successfully complete the task are presented on the right side of the table. The average loads across test subjects are in the bottom rows of the tables, as labeled.

Variable joint selection as a confounding factor was not well addressed with the modeling package chosen. This requirement was identified as a confounding factor

Table 2 Multiple joint exertion results

Subject	Hand load source	Load at hand (lbs)	Minimum % accommodated	% Accommodated at		
				Shoulder	Elbow	Wrist
50th percentile male model	Wrist flex requirement load	17	82	86	97	82
	Elbow flex requirement load	8	98	99	100	98
95th percentile male model	Wrist flex requirement load	17	69	69	95	76
	Elbow flex requirement load	8	97	97	100	97
5th percentile female model	Wrist flex requirement load	17	42	42	80	83
	Elbow flex requirement load	8	95	95	99	98
Pilot test subject average	Wrist flex measured load	13.7	–	–	–	–
	Elbow flex measured load	14.7	–	–	–	–

when multiple joints could provide the motion required by hardware designers. The model indicated a success rate of less than 50 % for the loads required by the anthropometry of a 5th-percentile female. That is supported by subjective feedback from the human test subjects, who reported that this posture was uncomfortable and not how they would prefer to perform the task. It was observed that subjects could generate slightly more force at the dynamometer head when attempting to flex at the elbow rather than the wrist. Neither the model nor the human testing seemed to reflect the system predicted by the strength requirements, where the wrist flexion strength should have been much higher than the elbow flexion strength. The wrist flexion strength requirement is likely much higher than experimental results because of a difference in posture, with strength requirements showing a braced forearm whereas the forearm was unsupported in this testing to combine wrist and elbow flexion. This example makes the case for human-in-the-loop testing when hardware designers need to determine, out of several options, how a task should be done.

3.2 Braced Exertion Results

Results from the braced exertion analysis are presented in Table 3. Percentages of the population with the strength to complete the task and average strength from the human test subjects are again presented on the right side and in the last two lines of the table, respectively. 3DSSPP offered another metric here in the form of coefficient of friction necessary for the system to exist statically without slippage given the posture and forces on the body. Coefficient of friction is calculated as the ratio of the sum of horizontal forces to the sum of body weight and external vertical forces.

Bracing as a confounding factor was not well addressed by the analyzed modeling package, chiefly because of the limitations of the model's inputs and the complexity of the human system. 3DSSPP relies on externally applied forces and the weight of the body to calculate joint torques, whereas the act of bracing creates a more complex load scenario than can be modeled with limited inputs. Human testing did indicate significant strength gains in the presence of bracing. This represents a conundrum for strength requirements, as bracing presents a possible means for increasing human strength applied into a system, but it also makes the system more difficult to address with even a robust set of strength requirement values. In general, strength gains due to bracing should not be counted on when protecting for the weakest crewmembers, but should be addressed when protecting hardware failure loads.

Table 3 Braced exertion results

Model anthropometry	Posture	Load at right hand (lbs)	Loa at left hand (lbs)	Minimum % accommodated	% Accommodated at			Balance	Coefficient of friction
					Shoulder	Elbow	Wrist		
50th percentile male	Unbraced	24	0	99	99	100	100	Acceptable	0.382
	Braced	24	22	99	99	100	100	Acceptable	0.494
95th percentile male	Unbraced	24	0	99	99	100	100	Acceptable	0.253
	Braced	24	22	99	99	100	100	Acceptable	0.326
5th percentile female	Unbraced	24	0	90	90	100	100	Unacceptable	-
	Braced	24	22	90	90	100	100	Acceptable	0.518
Pilot test subject average	Unbraced	28.8	-	-	-	-	-	-	-
	Braced	49.5	-	-	-	-	-	-	-

3.3 Off-Nominal Exertion Results

Results from the off-nominal exertion analysis are presented in Table 4. Percentages of the population with the strength to complete the task and average human test subject strength are again presented as labeled, for tasks performed in the nominal posture present in the strength requirements, and tasks performed at an elevated posture more representative of actual hardware placement.

Table 4 Off-nominal exertions

Model posture and anthropometry	Hand load	Right hand load (lbs)	Minimum % accommodated	% Accommodated at		
				Shoulder	Elbow	Wrist
Nominal elevation 50th percentile male	Push	22	98	98	100	100
	Medial	13	94	100	100	94
	Pull	24	99	99	100	100
	Lateral	8	97	100	100	97
High elevation 50th percentile male	Push	22	87	100	98	87
	Medial	13	94	100	100	94
	Pull	24	88	100	99	88
	Lateral	8	97	100	100	97
Nominal elevation 95th percentile male	Push	22	95	95	100	100
	Medial	13	92	100	100	92
	Pull	24	99	99	100	100
	Lateral	8	97	100	100	97
High elevation 95th percentile male	Push	22	85	100	98	85
	Medial	13	92	100	100	92
	Pull	24	84	99	99	84
	Lateral	8	97	100	100	97
Nominal elevation 5th percentile female	Push	22	83	83	100	100
	Medial	13	85	85	100	94
	Pull	24	90	90	100	100
	Lateral	8	97	99	100	97
High elevation 5th percentile female	Push	22	60	99	60	85
	Medial	13	85	85	100	94
	Pull	24	87	100	94	87
	Lateral	8	97	98	100	97
Nominal elevation pilot test subject average	Push	21.6	–	–	–	–
	Medial	16.2	–	–	–	–
	Pull	32.1	–	–	–	–
	Lateral	18.3	–	–	–	–
High elevation pilot test subject average	Push	19.7	–	–	–	–
	Medial	13.3	–	–	–	–
	Pull	25.5	–	–	–	–
	Lateral	14.6	–	–	–	–

Table 5 Percentage change in arm strength from nominal to off-nominal arm posture

Model posture and anthropometry	Hand load	Change in reported strength (%)
Delta Accommodation 50th percentile male	Push	-11
	Medial	0
	Pull	-11
	Lateral	0
Delta accommodation 95th percentile male	Push	-10
	Medial	0
	Pull	-15
	Lateral	0
Delta accommodation 5th percentile female	Push	-23
	Medial	0
	Pull	-3
	Lateral	0
Delta strength—pilot test subject average	Push	-9
	Medial	-18
	Pull	-20
	Lateral	-20

As a confounding factor to the deployment of strength requirements, the off-nominal exertion exercise was probably the most indicative of a common issue facing space vehicle design. Hardware and controls are more likely to be on the periphery of the habitable volume, requiring reaches outside of the nominal postures for which strength requirements were created. A decrease in strength capacity of crewmembers at the limits of their reach could result in a failure to actuate hardware that strength requirements would indicate should be operable when the operator is in a nominal posture. The 3DSSPP models showed a decrease in the percentage of the population accommodated that ranged from 0 to 23 %, while the human test subjects showed a decrease in strength capabilities from 9 to 21 % in the elevated, off-nominal posture (Table 5). This suggests that strength modeling is best suited to accounting for changes that only affect the physics of the system, such as off-nominal reach zones, and is less effective when there is a cognitive component, such as a choice of joint selection or complex bracing scenario.

3.4 Discussion

Human modeling and human testing were applied to three commonly occurring situations where strength requirements did not map well to operational realities. The human modeling package that was used, 3DSSPP, cannot definitively state whether a task passes or fails because of the different objective of the software, but it can give some insight into whether or not a task is likely to be problematic for the

weakest potential crewmember to complete. Human testing can offer numerous useful insights about task completion, but it is difficult to state definitively whether a task protects for the weakest crewmember when one is testing with a finite number of test subjects.

While strength requirements are a ubiquitous part of space human factors, their practical application to hardware design has long been a source of confusion. This manuscript sought to clear up some common questions about the application of NASA's strength requirements to various confounding factors. The Human Integration Design Handbook [6] mentions numerous factors to consider when using human-centered design; however, it does not describe actionable advice to answer questions about specific loading profiles. If the loading scenario is decomposed into its most simplistic form and it still does not perfectly fit the strength requirement tables, the primary remaining options to determine if the loading profile is acceptable involve either human modeling or human testing. The results of this study suggest that human-in-the-loop testing should be involved for all verification scenarios of space hardware accommodation, while human modeling may offer some insight and cost savings early in the design process.

4 Conclusions

This study sought to demonstrate potential approaches for strength requirement use. The examples included here are not fully comprehensive. The presence of a spacesuit adds a significant confounding factor that was not addressed in this manuscript. Part II of this study aims to better understand the influence of spacesuits on subject strength, include additional human testing, and expand the depth of data included in the strength database. When in doubt about how to use the strength requirement tables, a safe approach often involves asking the subject matter experts for feedback.

Strength requirements are important for human-centric design, but difficult to define for every conceivable operation. When a new operation or piece of hardware is being designed that does not map well to strength requirements, human modeling and human testing remain the two best options to determine whether the required loads can be accommodated. Modeling offers several benefits in terms of cost and speed of analysis but is often constrained by the assumptions and variables of the modeling program. Human testing typically offers the most flexibility for test setup, though test hardware can be expensive to maintain. Future work is necessary to expand findings for other complex loading scenarios including the influence of spacesuits on the application of strength requirements.

References

1. Human System Integration Requirement Document (Rev E), Constellation Program 70024. National Aeronautics and Space Administration (2010)
2. ISS Crew Transportation Services Requirements Document (Rev C), Commercial Crew Program 1130. National Aeronautics and Space Administration (2013)
3. University of Michigan Center for Ergonomics, 3D Static Strength Prediction Program User's Manual. Retrieved from http://umich.edu/~ioe/3DSSPP/Manual_606.pdf (2014)
4. Kroemer, K.H.E., Kroemer, H.B., Kroemer-Elbert, K.E.: Ergonomics: How to Design for Ease and Efficiency, 2nd edn. Prentice Hall, Upper Saddle River (2001)
5. Chaffin, D.B., Andersson, G.B., Martin, B.J.: Occupational Biomechanics, 3rd edn. Wiley, New York (1999)
6. Human Integration Design Handbook, NASA/SP 2010-3407. National Aeronautics and Space Administration (2010)

Movement Variability and Digital Human Models: Development of a Demonstrator Taking the Effects of Muscular Fatigue into Account

Jonathan Savin, Martine Gilles, Clarisse Gaudetz, Vincent Padois and Philippe Bidaud

Abstract Movement variability is an essential characteristic of human movement. However, despite its prevalence, it is almost completely ignored in workstation design. Neglecting this variability can lead to skip over parts of the future operator's movements, thus bring to incomplete assessment of biomechanical risk factors. This paper starts with a focus on movement variability in occupational activities. Then, as an example of feasibility, it describes a Digital Human Model framework intended to simulate the movement variability induced by muscle fatigue. The demonstrator is based on several simulation environments, namely (1) XDE, a virtual human simulation software tool previously used for ergonomics analyses, (2) a dynamic three-compartment model of muscle fatigue and recovery, and (3) OpenSim, a dynamic musculoskeletal simulation software. The demonstrator is a first step towards tools to assist designers in considering movement variability for improved ergonomics at the workstation.

Keywords Movement variability · Digital human models · Ergonomics assessment · Workstation design · Muscle fatigue

J. Savin (✉) · M. Gilles · C. Gaudetz
INRS, 1 rue du Morvan—CS60027, 54519 Vandœuvre-lès-Nancy cedex, France
e-mail: jonathan.savin@inrs.fr

M. Gilles
e-mail: martine.gilles@inrs.fr

C. Gaudetz
e-mail: clarisse.gaudetz@inrs.fr

V. Padois · P. Bidaud
Institut des Systèmes Intelligents et de Robotique (ISIR), Sorbonne Universités,
UPMC Univ Paris 06, CNRS, 4 Place Jussieu, 75252 Paris cedex 05, France
e-mail: padois@isir.upmc.fr

P. Bidaud
e-mail: bidaud@isir.upmc.fr

1 Introduction

Movement variability (MV) is a characteristic of human movement: whether for a given person at different times, or for different people, a prescribed movement is never performed in exactly the same way twice. MV exists in all situations, and particularly in occupational activities. It is an essential element to ensure flexibility and adaptability of the sensorimotor system to the constraints related to the person, to the task and to the environment in which a task is performed. MV may also help protect the locomotor system, for instance by delaying the appearance of fatigue which is reported to be involved in the onset of work-related musculoskeletal disorders. However, the scientific community has long neglected MV, considering it to be non-significant noise or interference while also being difficult to quantify and analyse. Thus, in the field of workstation design, MV is still almost completely ignored. Indeed, the requirements of methods such as “lean manufacturing” or “total quality management” drive workstation designers to favour standardisation of operators’ activity to avoid non-conformities and errors. Actually, neglecting MV at the design stage can lead to poor planning for the future activity performed by operators, leading to incomplete assessment of biomechanical risk factors. Thus, it seems necessary to take operators’ MV into account from the stage of workstation design to more precisely apprehend their real activity.

The objective of our study is to propose a software tool based on Digital Human Models (DHM) allowing workstation designers to simulate not only the trajectories, postures and efforts linked to a given task, but also the envelope of those trajectories, postures and efforts associated with foreseeable MV from the earliest stages of design. As a first step towards this general goal, this paper presents a feasibility study on a proposed DHM architecture simulating MV induced by muscle fatigue.

The first section of this paper presents what is currently known about movement variability. The second section deals with modelling a source of MV, namely muscle fatigue. The software elements used to perform simulation are described in the third section, and future validation experiments and further uses of this DHM for movement analysis and ergonomics are discussed in the final section.

2 What Is Movement Variability?

The study of MV is at the interface between several scientific domains: neuroscience, biomechanics, ergonomics, physiology, motor control, etc. These communities address various aspects of movement and each has their own terminology. Thus, in the literature, notions such as natural variations [1], inherent variability [2], motor variability [3] or MV [4] are encountered. In this paper, we define MV as differences in body segment movements and/or muscle activities between repeats of a task, with cyclic or intermittent task repetitiveness throughout the day. MV is linked to motor control, i.e., the constant interactions between a subject, the

environment in which they act and the task to be performed. A comprehensive presentation of MV can be found in Gaudez et al. [4] and Srinivasan and Mathiassen [5].

2.1 MV and Motor Control

Movement is planned by the central nervous system (CNS) based on sensory information related to the environment in which the task is performed, and on the subject's capacity to interpret this multifaceted information. But redundancy in the degrees of freedom of the human locomotor system make an infinite number of solutions possible when performing a movement or task. Consider, for example, the number of combinations possible thanks to joint redundancy, involvement of different muscles for the same joint, different muscle fascicles in the same muscle, different motor units in the same fascicle, application of different electrical activation patterns to motor units, existence of different control levels and strategies, etc.

Taking all the necessary information on board to plan and generate a movement comes at a considerable cost for the CNS and motor control theories try to understand the underlying rules. In the 1960s, Bernstein proposed an initial model for motor control based on reduction of the human system's complexity: muscular synergies and segmental strategies chosen through afferent information would be used to decrease the number of degrees of freedom required to efficiently control the system. Other models have then been proposed: minimum jerk, minimal effort, minimum torque change, optimal feedback control, the muscle equilibrium-point model, etc. Some of these models have been used to simulate human movement: for instance, De Magistris [6] used Fitt's law, Todorov's speed profiles model, minimum jerk optimisation, and minimum exertion to model an industrial assembly task. Those models, which lead to an "optimal" movement, assume that some signal-dependant noise appears alongside neuro-muscular activation, which is responsible for the variability observed. Churchland et al. [7] also showed that significant MV arises in the motor preparation stage. Recently, an additional approach was introduced, derived from Bernstein and based on the principle of abundance [8]. Abundance would make it possible to adapt movements to the main constraints (the task's objective) and to the secondary environmental constraints (perturbations or parallel tasks) cropping up as the movement is performed. Thus, any task would not have a single optimal solution, but a family of equivalent solutions.

It is most likely that motor control is achieved through mechanisms compatible with several of these models, depending on the situation. Applying these models and theories to the field of occupational activities, workers may have a large panel of possible movements, leading to the observed MV.

2.2 *Factors Influencing MV*

The literature presents many experiments highlighting movement variability, particularly during upper limb movements. This MV depends on various factors related either to the characteristics of the task, or of the person. In the field of occupational activities, task characteristics include pace, cognitive demand, geometry of the workstation, physical characteristics of the tools used (weight, size), job organization, etc. Designers can influence all those parameters. In contrast, designers have no influence on individual characteristics, such as gender, age, learning and experience, pain or fatigue. We call the MV due to the differing characteristics of each *individual* observed during repeats of a task *intrinsic movement variability*.

2.3 *Accounting for MV as Part of Occupational Risk Prevention*

In terms of workstation design, prevention relies on the identification, assessment and avoidance of risks. Indeed, inadequate design choices may adversely affect future operators' health and safety: operators working at an unsuitable workstation may suffer from muscle fatigue and musculoskeletal discomfort, potentially leading to work-related musculoskeletal disorders. Hence, designers should account for operators' real activity as early as possible in the design process. In Europe, regulatory requirements in this direction have been formalised in the "Directive on Machinery" 2006/42/CE [9] with which designers must comply. Thus, designers are required to ensure that any operator can work at his/her workstation, whatever his/her characteristics.

Common ergonomic assessment tools used in workstation design rely on the operators' posture (joint angles), the efforts exerted (joint torques and/or forces applied to or exerted by the operator) and the cycle time for the task. This information can be obtained by analysing operators' activity on a comparable workstation, if it exists, or with the help of simulation tools such as virtual reality (VR) [10] and DHM [6]. Unfortunately, as MV is almost completely ignored in workstation design, design tools include no feature to address it. Prevention of occupational biomechanical risk factors could be improved by developing simulation tools to calculate all possible movements likely to be performed and postures likely to be adopted by operators while completing a task, without distinguishing individual characteristics.

3 Integrating a Source of MV into a DHM: The Example of Muscle Fatigue

The previous section showed that movement variability is a complex and multi-factorial phenomenon, while also being an essential feature of human movement. MV should therefore be considered in workstation design tools such as DHM. As a feasibility study, we chose to integrate a source of intrinsic MV, namely muscle fatigue, into a DHM control. Indeed, studies show that the kinematics of movement can be modified due to fatigue. For instance, during repeated sawing movements, the amplitude of the elbow angle decreases. This decrease is compensated for by alterations to shoulder, wrist and torso movement amplitudes over time [11]. In static working conditions, similar compensatory strategies have also been observed [12].

3.1 *What Is Muscle Fatigue?*

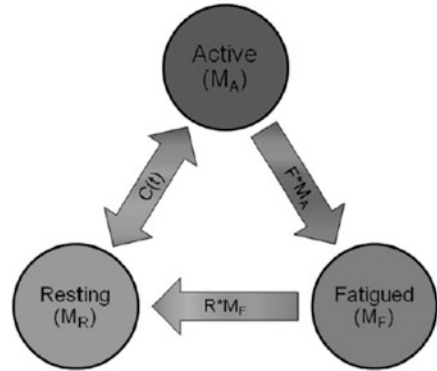
Muscle fatigue is linked to repeated muscle contractions. It is defined as a reduction in the maximum force-production or motor power capacity, linked to the execution of a task or an exercise [13]. The opposite phenomenon to fatigue is recovery, during which the locomotor system may retrieve its performance after a certain amount of time.

Because of the complexity of the phenomena involved, the literature most often deals with specific situations (isometric, isotonic or isokinetic contraction, etc.) and studies aiming to predict fatigue have long been limited to the static analysis of the relationships between the intensity of an effort and the maximum endurance time (MET). These data are very dependent on the task studied and the subjects involved, and they are not good models for occupational activity, where we are seeking to avoid exhaustion and where the muscular efforts exerted are dynamic.

3.2 *Modelling Muscle Fatigue*

For a long time, studies compared the intensity of the effort and the MET when attempting to predict muscular fatigue. Since the work of Rohmert in the 1960s up until the early part of this century, adjustments to these methods were proposed, but the advances were limited. Since the start of this century, this field of research has undergone a revival and new models have now been published. For example, Ding et al. [14] use a biochemical approach, Bül et al. [15] apply a “finite elements” approach, and a biophysical approach is developed by Liu et al. [16] in their three-compartment model. Of all these approaches, the three-compartment model appears the best adapted to integration into DHM-type tools, and the literature

Fig. 1 States and state-transitions diagram for the 3-compartment muscle fatigue model (from Frey-Law et al. [18])



presents several studies of this type of model with virtual humans in specific conditions (static effort, estimation of MET) [12, 17, 18].

For this work, we retain the model of fatigue proposed by Frey-Law et al. [17]. This model takes phenomena related to fatigue and recovery into account by considering the whole force-generation chain, from the CNS to the various muscle fibres. The muscle is modelled by a limited and constant number of fibres, M_0 . At rest, all the fibres are in an inactive state. At any time point, a proportion of the resting fibres can become active under the influence of an order from the CNS. Similarly, due to fatigue and recovery, a proportion of the activated fibres can enter the fatigued state and a proportion of the fatigued fibres can return to the resting state. The passage from one state to another is defined by three coefficients noted C , F , and R (Command, Fatigue, Recovery, respectively, see Fig. 1).

The sum of the number of active fibres, M_A , of fatigued fibres, M_F , and resting fibres, M_R , is constant. The model assumes that only active fibres produce force. For a muscle containing an adequate number of motor units, the model makes the approximation that each of them contributes through a similar elementary effort, u_0 , which is constant while activated. The F and R parameters are assumed to be constant. Parameter C is bidirectional and non-linear, depending on the expected effort (Target Load— TL) and on the current level of fatigue. For a comprehensive description of this model, see [17].

An application of this model is illustrated in Fig. 2 for a constant isometric exertion equal to 70 % of the maximum voluntary exertion. Exerted force increases rapidly because muscle is not fatigued. The expected exertion is reached and can be maintained as long as resting fibres can replace fatigued on. Since recovery is slower than fatigue, the current maximum exerable force decreases thus limiting the exerted force.

Our demonstrator is based on the simulation engine XDE which has been used in several studies to generate human movement and assess the ergonomics of occupational tasks [6, 19]. XDE manages the physical simulation of a virtual human and its environment as a whole, practically in real-time, including accurate and robust constraint-based methods for contact and collision resolution [20].

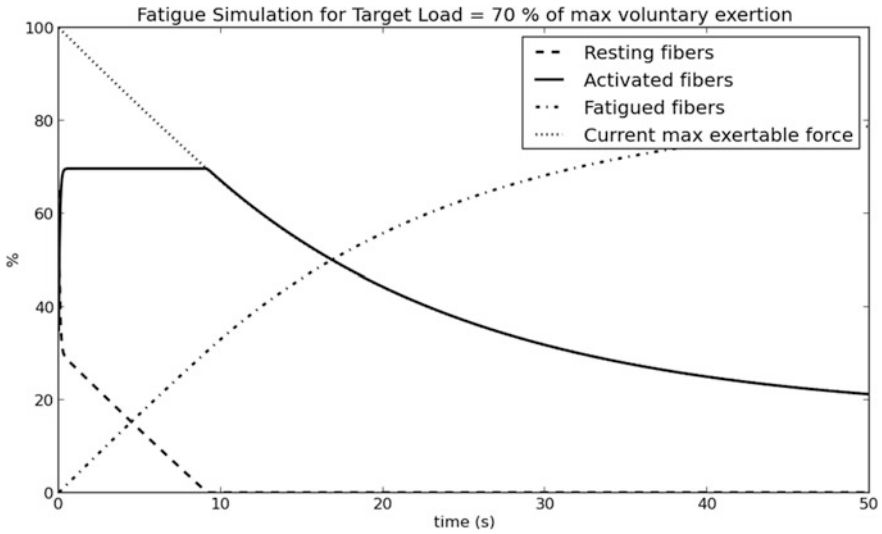


Fig. 2 Time evolution of muscle fibres state with fatigue for a target load equal to 70 % of the maximum voluntary exertion

A comprehensive description of the DHM and its optimization-based control can be found in [21].

The DHM is driven by a multi-objective linear-quadratic programming (LQP) controller, which manages the tasks to be performed such as balance, reference posture, ground contact, interaction forces, trajectory tracking, and the physical constraints of the system, such as joint angles bounds, maximum torques, etc. At each simulation step, usually 0.01 s, current state parameters are updated so that the tasks’ cost functions are optimized subject to equality and inequality constraints: equation of motion; joint range of motion, bounded velocities, accelerations or torques, contact conditions, etc. as described in Eq. (1):

$$\min_{\mathbf{X}} \sum_i \omega_i E_i(\mathbf{X}) \text{ subject to } \begin{cases} M\ddot{q} + C(q, \dot{q}) + g = S\mathbf{t} + W \\ G\mathbf{X} \leq h \\ \mathbf{X} = [t, w_C, \ddot{q}]^T \end{cases} \quad (1)$$

where E_i is the error between the current state of the system and the goal of the task T_i , ω_i is the associated weight, M is the inertia matrix, C stands for centripetal and Coriolis forces, g the gravity forces, S the actuation selection matrix and W the external and contacts wrenches.

In our proposed framework, control constraints parameters may vary as fatigue sets in. As a first step, let us consider joint torques. At each simulation step, a “dummy” controller first calculates the desired actuation torques, τ^{des} , which optimize the defined tasks subject to the defined constraints (this controller doesn’t

modify the current state of the system). In the meanwhile, Γ_{max} , the maximum voluntary joint torques are computed thanks to the OpenSim musculoskeletal simulation software [22]. Γ_{max} is computed for the current posture and velocities of the DHM, so the demonstrator can manage dynamic movements, and not only isometric activities. τ^{des} and Γ_{max} are then used as input to update the fatigue model, yielding $\tau_{max}(f)$, the *current maximum exertable* joint torques, subject to fatigue. Finally $\tau_{max}(f)$ is imposed as a constraint to the actual DHM controller, yielding to potentially new state postures, trajectories and torques if $\tau_{max}(f) < \tau^{des}$.

3.3 First Implementation

As we are at the first stage of our work, the whole architecture is currently not fully implemented. As a first-stage application, we describe hereafter a simulation for a fictional experiment where an operator must maintain his hand's position while undergoing a perturbation force. In this fictional static experiment, operator's upper limb fatigue performances are not simulated but obey the evolution described in Fig. 3.

The manikin is standing, his right elbow is flexed at about 90°. The controller's most weighted tasks are to maintain the positions of the right hand and of the center of mass, as well as contact points with the floor. An horizontal perturbation force of

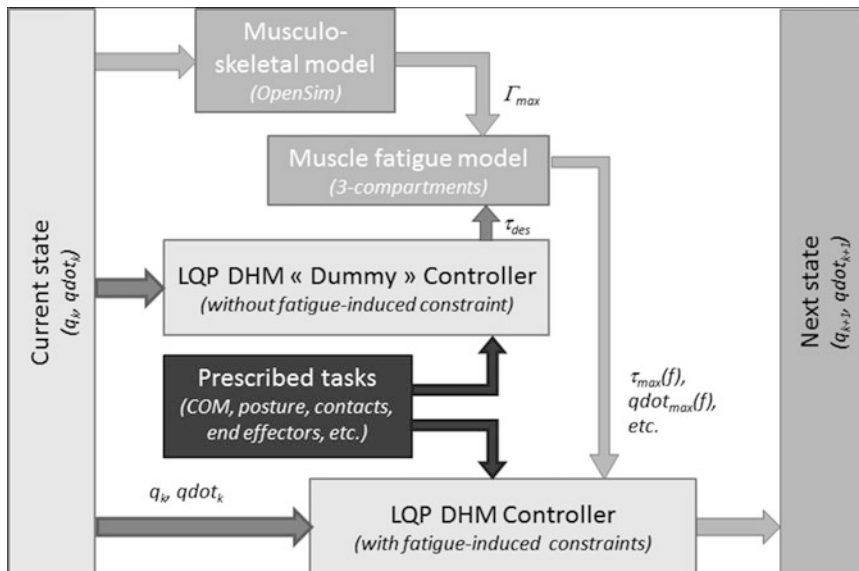


Fig. 3 Proposed framework for the demonstrator described here. *Light grey* elements correspond to the existing control. *Darker grey* elements represent new computations related to muscle fatigue. The *black* element indicates the control parameters prescribed for the motion (center of mass control, reference posture, contact forces, end-effector trajectories, etc.)

15 N is applied, pushing the manikin's right hand to the right. Fatigue is applied on the right shoulder abduction and rotation joints when the manikin is stabilized. As fatigue grows, maximum shoulder abduction joint torque decreases slowly. The manikin adapts its posture (right elbow joint angles) and the upper-trunk generates torques to compensate the loss of performance induced by fatigue, as shown in Figs. 4 and 5.

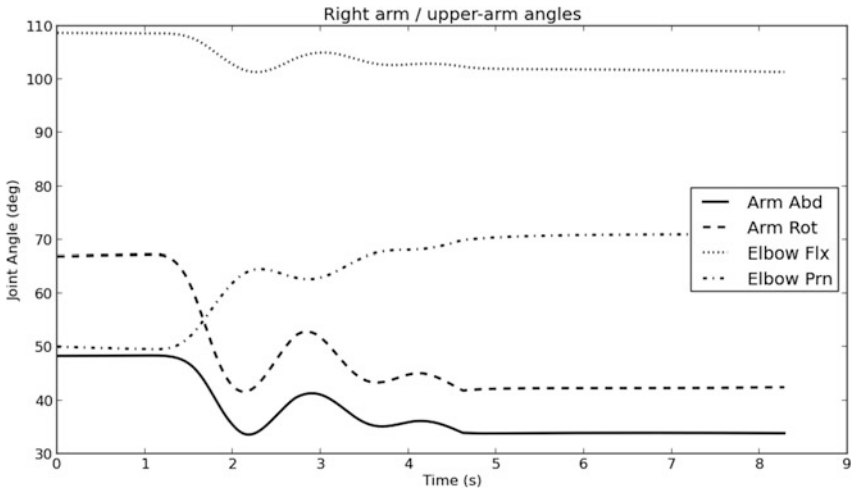


Fig. 4 Joint angle evolution of the upper limb with fatigue: right arm abduction and rotation, right elbow flexion and pronation joint angles

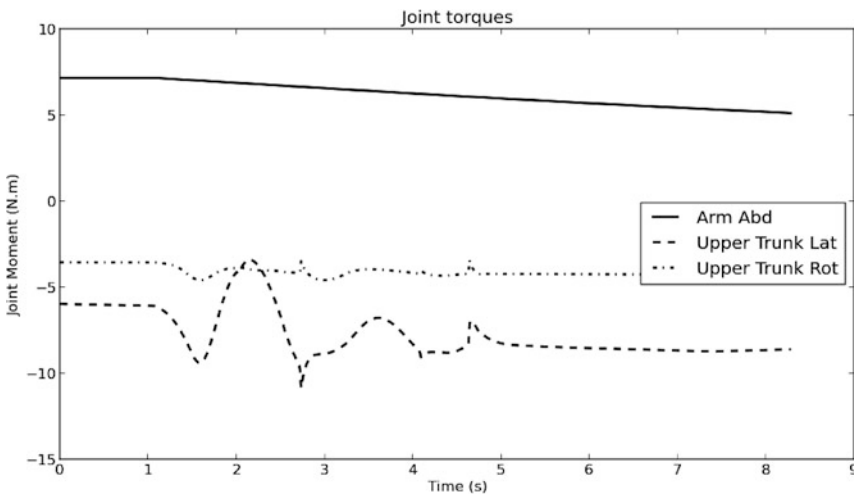


Fig. 5 Joint torques evolution with fatigue: right arm abduction torque decreases, generating changes in upper-trunk lateral tilt and axial rotation joint torques

4 Discussion

In this paper, we described a framework intended to account for fatigue-induced movement variability at the first stage of workstation design. Our demonstrator is expected to generate various simulated MV indicators such as range of postures, trajectories envelopes, range of joint moments, etc. As we are only at the very first stage of its software implementation, no validation simulation is available yet.

Scheduled validation steps are focused on the upper limbs, based on literature and laboratory experiments. Firstly, we plan to simulate the repetitive reaching task described by Fuller et al. [23]. As in the fictional simulation described in Sect. 3.3, we expect our demonstrator to mimic the compensatory behaviour described (shoulder elevation, decreased average shoulder abduction angle, lateral shift of the body's center of mass towards the non-reaching arm). Secondly, we plan to simulate a task combining movement and external forces exertion phases. At this stage, time is not considered as a quantitative parameter (the aim is not to simulate precisely *when* fatigue induces a given posture or movement, but rather to ensure that variants of postures or movements induced by fatigue can effectively be accounted for during the ergonomic assessment of the task in its entirety).

If these two experiments are properly simulated, further model adjustments may be explored. Our demonstrator could be enriched with other models of MV sources in its controller, for instance, some statistical characteristics of MV, as described in the literature [24, 25].

Ultimately, this demonstrator could be integrated into workstation design tools such as commercial DHM in order to yield simulated indicators of movement variability to workstation designers. These physical quantities, for instance range of postures, trajectories envelopes or range of joint moments are expected to better describe the operator's future activity and improve biomechanical risk factors assessment at the first stage of workstation design.

References

1. Luger, T., Bosch, T., Veeger, D., de Looze, M.: The influence of task variation on manifestation of fatigue is ambiguous—a literature review. *Ergonomics* **57**, 162–174 (2014)
2. Samani, A., Pontonnier, C., Dumont, G., Madeleine, P.: Kinematic synergy in a real and a virtual simulated assembly task. In: Proceedings 19 th Triennial Congress of the IEA. p. 8, Melbourne (Australy) (2015)
3. Latash, M.L., Scholz, J.P., Schoner, G.: Motor control strategies revealed in the structure of motor variability. *Exerc. Sport Sci. Rev.* **30**, 26–31 (2002)
4. Gaudes, C., Gilles, M.A., Savin, J.: Intrinsic movement variability at work. How long is the path from motor control to design engineering? *Appl. Ergon.* **53**(Part A), 71–78 (2016)
5. Srinivasan, D., Mathiassen, S.E.: Motor variability—an important issue in occupational life. *Work* **41**, 2527–2534 (2012)
6. De Magistris, G., Micaelli, A., Evrard, P., Andriot, C., Savin, J., Gaudes, C., Marsot, J.: Dynamic control of DHM for ergonomic assessments. *Int. J. Ind. Ergon.* **43**, 170–180 (2013)

7. Churchland, M.M., Afshar, A., Shenoy, K.V.: A central source of movement variability. *Neuron* **52**, 1085–1096 (2006)
8. Latash, M.L.: The bliss (not the problem) of motor abundance (not redundancy). *Exp. Brain Res.* **217**, 1–5 (2012)
9. Directive of the European Parliament and of the council on machinery (2006)
10. Pontonnier, C., Samani, A., Badawi, M., Madeleine, P., Dumont, G.: Assessing the ability of a VR-based assembly task simulation to evaluate physical risk factors. In: Presented at the IEEE Transactions on Visualization and Computer Graphics, Institute of Electrical and Electronics Engineers (IEEE) (2013)
11. Côté, J.N., Mathieu, P.A., Levin, M.F., Feldman, A.G.: Movement reorganization to compensate for fatigue during sawing. *Exp. Brain Res.* **146**, 394–398 (2002)
12. Ma, L., Zhang, W., Hu, B., Chablat, D., Bennis, F., Guillaume, F.: Determination of subject-specific muscle fatigue rates under static fatiguing operations. *Ergonomics* **56**, 1889–1900 (2013)
13. Vøllestad, N.K.: Measurement of human muscle fatigue. *J. Neurosci. Meth.* **74**, 219–227 (1997)
14. Ding, J., Wexler, A.S., Binder-Macleod, S.A.: A predictive model of fatigue in human skeletal muscles. *J. Appl. Physiol.* **89**, 1322–1332 (2000)
15. Böl, M., Stark, H., Schilling, N.: On a phenomenological model for fatigue effects in skeletal muscles. *J. Theor. Biol.* **281**, 122–132 (2011)
16. Liu, J.Z., Brown, R.W., Yue, G.H.: A dynamical model of muscle activation, fatigue, and recovery. *Biophys. J.* **82**, 2344–2359 (2002)
17. Frey-Law, L.A., Looft, J.M., Heitsman, J.: A three-compartment muscle fatigue model accurately predicts joint-specific maximum endurance times for sustained isometric tasks. *J. Biomech.* **45**, 1803–1808 (2012)
18. Brouillette, D., Thivierge, G., Marchand, D., Charland, J.: Preparative study regarding the implementation of a muscular fatigue model in a virtual task simulator. *Work-a J. Prev. Assess. Rehabil.* **41**, 2216–2225 (2012)
19. Maurice, P., Measson, Y., Padois, V., Bidaud, P.: Assessment of physical exposure to musculoskeletal risks in collaborative robotics using dynamic simulation. In: Padois, V., Bidaud, P., Khatib, O. (eds.) *Romansy 19—Robot Design, Dynamics and Control: Proceedings of the 19th CISM-Iftomm Symposium*, pp. 325–332. Springer, Vienna (2013)
20. Merlhiot, X., Le Garrec, J., Saupin, G., Andriot, C.: The xde mechanical kernel: efficient and robust simulation of multibody dynamics with intermittent nonsmooth contacts. In: *The 2nd Joint International Conference on Multibody System Dynamics* (2012)
21. Maurice, P., Padois, V., Measson, Y., Bidaud, P.: Sensitivity analysis of human motion for the automatic improvement of gestures. Presented at the (2015)
22. Delp, S.L., Anderson, F.C., Arnold, A.S., Loan, P., Habib, A., John, C.T., Guendelman, E., Thelen, D.G.: OpenSim: open-source software to create and analyze dynamic simulations of movement. *IEEE Trans. Biomed. Eng.* **54**, 1940–1950 (2007)
23. Fuller, J.R., Lomond, K.V., Fung, J., Côté, J.N.: Posture-movement changes following repetitive motion-induced shoulder muscle fatigue. *J. Electromyogr. Kinesiol.* **19**, 1043–1052 (2009)
24. Faraway, J., Hu, J.: Modeling variability in reaching motions. In: *SAE 2001 Transactions Journal of Passenger Cars—Mechanical Systems—V110-6*, p. 11, Arlington (VA) (2001)
25. Schmidt, R.A., Zelaznik, H., Hawkins, B., Frank, J.S., Quinn, J.T.J.: Motor-output variability: a theory for the accuracy of rapid motor acts. *Psychol. Rev.* **47**, 415–451 (1979)

Climate Variability, Opposition Group Formation and Conflict Onset

Zining Yang and Piotr M. Zagorowski

Abstract Political Science has a rich heritage of trying to understand how time-invariant geo-physical and geo-political features impact the calculus of peace and war, within and among societies. The growing body of climate change evidence has encouraged the re-examination of such questions yielding a variety of hypotheses which attempt to explain how weather variations can trigger societal and civil conflict. We develop an agent-based, predictive analytic model for sub-national conflict onset. We model the preferences and influence of citizens in geophysical space and capture the emergence of groups and the diffusion of support and opposition across society using cooperative game theory. We then model the interaction of groups and the government utilizing non-cooperative game theory to ascertain conflict onset. Such a method empowers us to ascertain the duration and magnitude of environmental shocks which would most prominently lead to conflict within societies with specific demographic and wealth characteristics.

Keywords Civil war onset · Environmental degradation · Community based organizations · Agent-based modeling · Game theory

1 Introduction

Dating back to the end of the cold war the number of armed conflicts has steadily decreased [1]. Furthermore, the severity of conflict measured as the number of battle related deaths has fallen even more dramatically since the conclusion of the Second World War [2]. Concurrently, there have been steady advances in

Z. Yang (✉) · P.M. Zagorowski
Claremont Graduate University, Claremont, CA 91711, USA
e-mail: zining.yang@cgu.edu

P.M. Zagorowski
e-mail: piotr.zagorowski@cgu.edu

Z. Yang
La Sierra University, Riverside, CA 92505, USA

democracy, development, economic integration, international cooperation, and trade. To a casual observer humanity appears to be entering a period of increasingly entrenched and potentially protracted peace [3].

Those same advancements in democracy and development have coincided with a burgeoning middle class, enhanced standards of living, and increased consumption. This rapid expansion has contributed to what many scientists call human induced climate change [4]. According to an increasingly accepted view, perhaps the greatest threat to the expansion of peace, is protracted climate change. This view has been expressed by, e.g., the United Nations Security Council, US Defense Department, and US President Barack Obama. Despite the shared rhetoric and calls for robust contingency planning there remains little systematic scientific evidence that short-term climate variability, such as changes in rainfall and temperature patterns, has any impact on the general pattern of conflict at the subnational level in modern times [5].

The Environmental Conflict Onset Review (ECOR) models demographic, economic, environmental, political and social constraints on the emergence of civil conflict in an agent-based predictive analytics model of a geophysical country with a single climate zone. Agents are individual citizens, political organizations, the political elite and others with an interest in the political orientation of the government against the backdrop of changing political allegiances, emergent community organizations, preferences of a local populace, and a changing climate. The agents' preferences are fed directly into the model which utilizes bargaining dynamics, game theory, and network theory to track satisfaction and utility to gain insight into subsequent reactions in a single dimensional policy space.

ECOR provides insights into the conditions that facilitate peace and war in a variety of political societies. Methodologically it achieves this by employing both cooperative and non-cooperative game theory in conjunction with social networking to track changes in citizens, groups, and government capabilities, preference, and salience. Theoretically, we borrow extensively from a variety of social science theories. We find increased climate variability dramatically increases the potential for conflict.

2 Literature Review

ECOR was developed using a range of relevant social science theories that are grouped into four broad categories.

The environmental conflict literature serves as the impetus for the models development. Homer-Dixon [6] argues resource scarcity contributes to the onset of conflicts through direct, indirect, or both causal pathways. Theisen et al. [5] identify changes in precipitation, temperature, rising sea levels and natural disasters as the primary triggers of resource scarcities.¹ These changes contributes to a loss of

¹Interstate conflict over these distinct climate variations is generally theorized to be a remote possibility [6:5].

livelihood, economic decline, and increased insecurity. When these forces impact societies that are dependent on agriculture, are economically poor, poses corrupt and/or weak governments, or are otherwise fractionalized, they facilitate economic and or political instability. These pressures percolate drawing the country into a vicious cycle where physical crises persist and new scarcities emerge and the state's ability to marshal resources diminishes.² This erosion of state capacity diminishes the state's moral and coercive authority, increasing the incentives for violence, while reducing the costs associated with mobilization.

To date roughly a third of the empirical studies conducted have explored civil war onset through the lens of changes in precipitation.³ Miguel et al. [7] utilized negative rainfall growth as an instrument for economic growth and concludes that drier periods increase the probability of conflict in Africa.⁴ Hendrix and Salehyan [8] find a curvilinear relationship between conflict onset and rainfall deviations. Koubi et al. [9] use rainfall deviations as an instrument for economic growth and fail to find a relationship between weather and economic performance globally. Furthermore, they find weak support that weather driven climate shocks are capable of inducing conflict in autocratic regimes. Gizelis and Wooden [10] find governance to be a key intermediary and that in its absence environmental variables are unable to predict conflict onset. Theisen et al. [5] perform a comprehensive literature review regarding climate factors and civil conflict onset; only 4 out of 10 studies support the notion that short term deficiencies increase the risk of civil conflict.

The fragility of these findings can be attributed to two factors. First, an inconsistent and evolutionary approach to operationalization of precipitation. Second, are perhaps more fundamentally is the continued reliance on the state-year as the unit of analysis.

The second is the communication literature and it is used to develop agent interactions. Specifically how people communicate with their neighbors and how that communication influences individual preferences. The ability to communicate, however, is moderated by physical distance despite increased access to electronic communication [11]. We therefore use talkspan, the theoretical distance people can reach, as a means to moderate the number of potential partners any agent can reach [12].

The frequency of communication is not a guarantee of comprehension or understanding [13]. Just because two or more people are talking does not mean they are actively or effectively communicating. A person can communicate a message to a peer that has limited impact because it is not sufficiently different enough to cause

²Homer-Dixon [6:5] contends states face "increasingly complex, fast moving, and interacting environmental scarcities" which can overwhelm a society's efforts to mitigate such scarcities through economic growth and innovation.

³Theisen et al. [5] identify 32 studies that have utilized climate factors to account for civil conflict. Ten of those studies have utilized precipitation as the primary climate factor.

⁴Ciccione challenges Miguel et al. [7] use of precipitation growth measured as the annual percentage change in rainfall.

a change i.e., speaking to the choir, is very different and is either ignored or rejected as non-sense, or the message falls between these two extremes and therefore has the potential to moderate the original position [11]. Corman et al. [14] contends, messages that are received from multiple people also increases the likelihood of acceptance.

Rogers and Bhowmik [15] research suggests people exhibit homophily, the tendency to interact more with people that share similar characteristics. Shared characteristics makes message acceptance more likely because similar individuals associate more frequently and on a more persistent basis. The acceptance of a message then is contingent on content, frequency, origin and intended recipient [13].

The third batch of literature comes from expected utility and game theory to govern the dynamics of community based organization (CBO) formation and coalition formation. Agents interact through cooperative game theory [16]. They join CBOs if two conditions are satisfied. First, membership increases their ability to influence the position of others. Second, membership requires at most the moderation of their initial policy position not sacrifice [17].

The fourth and final batch comes from the power transition tradition to account for conflict onset. Organski and Kugler [18] argue two factors drive the probability of conflict between two states: the distribution of power and the challengers' satisfaction with the status quo. Fundamentally, states that are satisfied with the status quo have no reason to fight; inversely those that are dissatisfied have reason to fight. The desire to fight, however, does not automatically facilitate conflict; rather the challenger must possess to capability to challenge the status quo.

The incorporation of power transition theory provides three benefits. First, it provides a clear definition of when two states or, for our purposes, groups are likely to engage in conflict. Second, climate variability is assumed to impact the calculus of conflict onset through manipulation of domestic satisfaction and government capacity. Third, power transition theory lends itself to the prediction of future conflicts, enabling us to ascertain the probabilistic impact of climate variability on civil conflict onset.

3 Model, Entities, and Variables

The model is substantiated in NetLogo [19]. ECOR contains a variety of entities, state variables and scales. Entities include the geophysical environment as well as a number of agents including: individual citizens, CBOs, coalitions and the government. State variables include rainfall, production efficiency, selectorate size, talkspan (the maximum distance that agents can effectively communicate), messages and political preference.

The most prominent variable in our analysis is climate variability. To maintain consistency with the current iteration of social science literature we proxy climate variability by examining the deviation in rainfall [9]. Zero indicates no change from the historical average while increasing negative or positive numbers correspond to

an absolute deviation from the historical average. Over a period of time a new local average will emerge.

The first entity is the geophysical environment. This environment represents a fictional country that is fixed in a two dimension space that is 101 by 101 square patches and does not wrap horizontally or vertically. The country is divided into rural and urban areas. The urban area is malleable in size, as a percentage of total patches, but remains geographically centered. Each patch receives precipitation independently, however, the mean and standard deviations are fixed across all patches. It is prudent then to think of the country as having a singular climate zone.

Second, individual citizen agents are randomly generated and placed within the country. Individuals are endowed with the following static characteristics: education (1–5 randomly assigned based upon a normal distribution), political affiliation, selectorate membership (dichotomously not to exceed a set percent of the population) and proximity to urban center. Citizens are also characterized by four dynamic variables: ideology (liberal-conservative score ranging from 0 to 100) which is tempered by membership or lack thereof in the society's selectorate, power (education * wealth, normalized between 0 and 1), preference (wealth * wealth trend * ideology) and wealth (rain * efficiency * proximity * education * selectorate * random term ± 0.2). An emergent class of entities are the community bargaining organizations (potentially including opposition groups) that form when a citizens coalesce around shared interests.

Both individual citizens and CBOs have attributes that are calculated by state variables. The calculation of citizen preference and power is described in the previous paragraph; CBO preference is calculated as the weighted preference of all members in that group, and CBO power is calculated as $1.5 * \text{sum of citizen power in the group}$ [12]. Both agent types have utility as one of their main attributes, the logic of which follows Bilateral Shapley Values that will be used in bargaining process. Citizen utility is a function of preference and power. When citizen A stays alone, $\text{utilityA} = (100 - \text{ABS}(\text{prefA} - \text{prefA})) * \text{powerA}$; when A and B form a CBO, $\text{utilityAB} = (\text{powerA} + \text{powerB}) * 1.5 * (100 - \text{ABS}(\text{prefA} - \text{prefB}))$. For the individual agent A in this AB coalition, utility is calculated as $\text{utilityA}(\text{AB}) = 0.5 * (V(A) + V(\text{AB})\text{utilityA} + \text{utilityAB})$ [12].

Third, the government is endowed with a variety of characteristics: ideology (liberal-conservative score ranging from 0 to 100 which is decided randomly). Individual citizen agents that are members of the selectorate continually adopt their ideological position to that of the government. The government also possesses the power to tax the citizenry and does so through the adoption of a flat tax mechanism which ranges from 1 to 70 % of the wealth generated each time step. Prior to the first time step, the governments' total revenue is simulated ten times to create a baseline revenue. During subsequent iterations the current period's revenue is compared to the simulated revenue. Surpluses constitute a discretionary fund, which is used to engage in clientelism. The number of groups to which the government can provide such private goods is limited by the government's capacity to interact with multiple groups. This capacity to negotiate ranges from 1 to 20.

Each time step corresponds to a temporal advancement of a single calendar year. Simulations are then carried out for a maximum period of twenty years. If at any point the conditions for civil war onset are satisfied, the simulation comes to an end. Therefore it is possible for a simulation run to end in the first simulated year.

4 Architecture and Modules

The ECOR model builds upon Yeung et al. [20] and Abdollahian et al. [12] and has four sequential submodels: Citizen and CBO module; Clientelism; Stakeholder Bargaining module; and Conflict Onset. Agents react to changes in rainfall that impact economic production informing their wealth, satisfaction and their attempts to influence the ideological position of their fellow agents. These efforts result in the possible formation of CBOs that are ideologically similar or distinct from the position of the government and the ruling selectorate. Against this landscape of political formation the government attempts to patronize emergent CBO groups earning their temporary loyalty through the distribution of private goods. Remaining CBOs and the government then engage in rounds of negotiations where all parties attempt to maximize their interests. Finally, remaining CBOs are compared to the government selectorate. Those that are dissatisfied, control a significant part of the overall societies wealth, and are ideologically different from the government are identified as groups that can engage in civil war to change the status quo. Actionable policy levers for deferring the emergence of opposition groups include talkspan, tax rate, electorate size and the allocation of private goods.

In Citizen and CBO module, agents are assigned initial attributes of location, ideology, education, selectorate membership, wealth, and power, which gets rescaled at each time step. They evaluate their utility using preference and power. Then the model captures CBO emergence based upon individual attributes and local social interactions. An individual citizen agent will compare his utility of staying alone and the utility of participating in a CBO. Using Bilateral Shapley Values (BSVs) from cooperative game theory, we model coalition formation, assume agents are autonomous with bounded rationality, and maximize their utility subject to the geophysical and social constraints of the environment [17, 20]. Since BSV takes into account all possible coalitions that citizens can join that maximize citizen utility, each individual citizen agent compares all possible utilities and decides whether to join or form a larger CBO. If $utilityA(AB) > utilityA$, agent A will choose to form the coalition with B; if not, then it remains as an individual. As to agent B, if $utilityB(AB) > utilityB$, it also decide to form coalition AB. Each agent does the same calculation with all other individual citizen agents N within a local neighborhood. In other words, if $utilityA(AC) > utilityA(AB)$, even if $utilityA(AB) > utilityA$, A will only choose C but do nothing to B. Only when both agents consent to grouping a coalition be created. This is to satisfy the super-additivity requirement that all players in a grand coalition are collectively rational [12]. After a citizen agent joins a CBO, their preference changes to the CBO preference.

In the second phase, government agent first gets wealth by imposes a tax upon the population. Then they will decide the number of CBOs to target as potential clients based on the targets wealth level. If a CBO is “bought” by the government agent, it will not participate in the stakeholder bargaining process in that time step, as it will not join any coalition against the government. However, their loyalty can be purchased for a single time step.

In the third phase where stakeholders bargain with each other, we introduce a non-cooperative bargaining model to reflect competing interests during the process. CBOs formed in the first phase decide whether to stay alone or get together with other CBOs to form larger coalitions. When two CBO agents decide to form a coalition, the coalition preference is calculated by the weighted individual CBO preference:

$$\text{prefAB} = (\text{prefA} * \text{powerA} + \text{prefB} * \text{powerB}) / (\text{powerA} + \text{powerB}) \quad (1)$$

Coalition power is calculated as the sum of individual CBO power:

$$\text{powerAB} = \text{powerA} + \text{powerB} \quad (2)$$

For each individual stakeholder, their coalition utility is calculated as the distance of preference multiplied by power:

$$\text{utilityA(AB)} = (100 - \text{ABS}(\text{prefA} - \text{prefAB})) * (\text{powerA} + (\text{powerAB} - \text{powerA}) * (\text{powerA} / \text{powerAB})) \quad (3)$$

The first half of the equation represents the distance between the coalition preference and agent A’s own preference. The latter half of the equation shows that power is calculated as A’s own power plus the weighted coalitional power gain. Similar to the Citizen and CBO module, after each stakeholder agent calculates their utility and makes a decision in the first round, coalitions form with preferences weighted by power and a subsequent power is calculated as the sum of the coalition members. Then each individual stakeholder and each citizen agent in CBOs participating in the stakeholder module, updates their preference according to the coalition preference. In the second round, coalitions calculates their utility based on their new preferences to decide if additional utility gains can be achieve by joining a new coalition. Simultaneously, each individual calculates the utility of separating from the current coalition and forming a new coalition with someone else. All coalitions and individual stakeholder agents perform the same process each round, until no coalition can provide higher utilities for joining agents.

In the last phase, CBO coalitions decide whether to challenge the government. If the CBO coalition’s power is greater than the a predetermined threshold and the ideological distance between the government agent is larger than 30 they will deterministically challenge the status quo.

5 Simulation Experiments and Results

We instantiate the model in NetLogo [19]. As is shown in Fig. 1. The middle of the interface shows the place where agents interact with each other. The urban area is centered in the geophysical environment and is shaded brown. The surrounding rural patches are shaded green or yellow. Green signifies an above average rainfall for the individual patch while yellow indicates the inverse. The color pattern of green and yellow refreshes every tick. Agents are randomly placed upon the geophysical environment and represented with a white dot. The grey lines that connect agents represent the emergence of coalitions.

On the far left are a series of buttons and sliders. Each slider represents a different input variable. These variables include: initial population size, mean rainfall across all patches, standard deviation of rainfall across all patches, size of urban area, government ideology, tax rate, number of parties, selectorate rate, talkspan, capacity to engage in clientelism, and the threshold for power transition theory. Outputs are located on the right-hand side. To capture the dynamic of preference and power change, we created histograms and phase portraits. On these plots the distribution of preference, satisfaction, wealth of citizens, as well as the relationship between rainfall and satisfaction, citizen power vs. government power and graphed. Aggregated variables are shown in monitors, including average rainfall of patches, number of conflicts, ratio of patches with bad rainfall over total patches, urban wealth, rural wealth, and average satisfaction.

We conducted a sensitivity analysis by varying the input parameters for a maximum of twenty time steps, this process resulted in 325,570 simulated runs. In every run all state variables and model attributes were recorded. The analytic

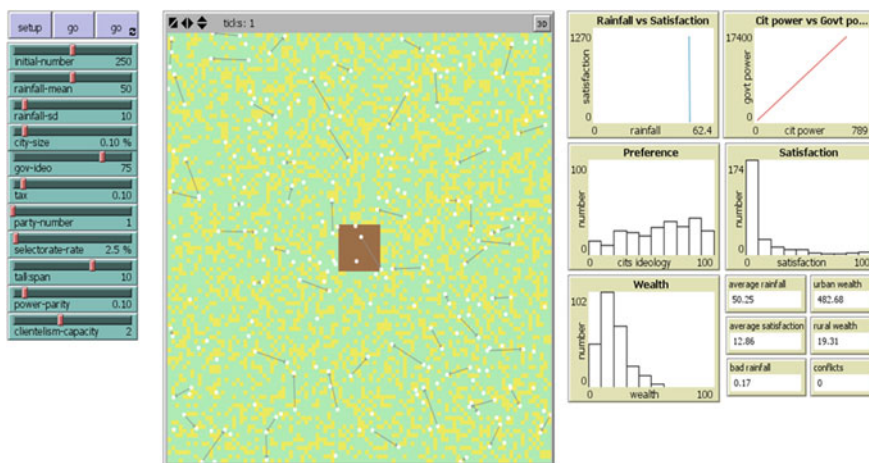


Fig. 1 NetLogo simulation interface

Table 1 Simulation input permutations

Variable	Input values		
Rainfall mean	40	50	60
Government ideology	25	50	75
Rainfall standard deviation	10		30
Talkspan	2	5	10
Power transition point	0.1	...	0.9
Selectorate rate	2.5	5	7.5
Tax rate	0.1	0.15	0.2
Clientelism	1	3	
Party number	1	2	3

method applied to the data is random effects panel logistic regression, where the dependent variable is conflict onset and the unit of analysis is country year (Table 1).

Below we detail the results from the quasi-global sensitivity analysis for civil conflict onset. In Table 2 the impact of inputs: mean rainfall, the standard deviation of rainfall, government ideology, talkspan, government wealth, government power, clientelism, the number of political parties, and selectorate rate are examined. Across all models the environmental-political input parameters are significant while the policy-levers are mixed in terms of their significance.

The environmental variables: standard deviation of rainfall and the rainfall mean are both statistically significant, however, the direction of their impacts is contrary to each other. Rainfall Mean is negatively ($\beta = -0.04$) associated with conflict onset, suggesting regions that have higher average rainfall are less susceptible to the outbreak of civil conflicts. The Standard Deviation in Rainfall, on the other hand, has a small positive ($\beta = 0.02$) effect on the emergence of conflict.

The political variables: Government Ideology, Talkspan, Government Power, and Government Wealth are consistent across all models and remain statistically significant and all are positively correlated with the emergence of civil war with the exception of Government Power. Government Power has a strong and negative ($\beta = -0.39$) impact on the occurrence of conflict. Counterintuitively, Government Wealth, is very modestly positively ($\beta = 0.01$) associated with conflict onset. Government Ideology is also positively ($\beta = 0.03$) correlated with conflict. Government Ideology, however, is crafted as a linear left-right extrapolation. While our model suggest liberal is on the right and autocratic is on the left the two could be juxtaposed. Therefore, it is prudent to reach the following conclusion as government reaches either extreme of the political spectrum the possibility of conflict increases while movements towards the center mediate the emergence of conflict. Finally, Talkspan has a strong and positive ($\beta = 0.35$) impact on the emergence of conflict.

Table 2 Environmental-conflict nexus

Variables	Model 1	Model 2	Model 3	Model 4
Mean rainfall	-0.0358*** (-0.0039)	-0.0358*** (-0.0039)	-0.0358*** (-0.0039)	-0.0360*** (-0.0039)
StdDev rainfall	0.0191*** (-0.00294)	0.0191*** (-0.00294)	0.0191*** (-0.00294)	0.0191*** (-0.00294)
Govt ideology	0.0298*** (-0.00141)	0.0298*** (-0.00141)	0.0298*** (-0.00141)	0.0298*** (-0.00141)
Talkspan	0.349*** (-0.0102)	0.349*** (-0.0102)	0.349*** (-0.0102)	0.349*** (-0.0102)
Govt Power	-0.387*** (-0.0171)	-0.387*** (-0.0171)	-0.387*** (-0.0171)	-0.391*** (-0.0172)
Govt Wealth	0.00620*** (-0.00033)	0.00620*** (-0.00033)	0.00621*** (-0.00033)	0.00627*** (-0.00033)
# Parties		0.00501 (-0.0314)		
Selectorate			-0.024 (-0.0205)	
Clientelism				-0.0459* (-0.0259)
Constant	-8.322*** (-0.229)	-8.332*** (-0.238)	-8.232*** (-0.241)	-8.222*** (-0.235)
Observations	325,570	325,570	325,570	325,570
Pseudo log likelihood	-11101.977	-11101.964	-11101.295	-11100.41
Wald chi ²	1748.47	1748.44	1749.11	1754.25
Prob > chi ²	0.00	0.00	0.00	0.00

Standard errors in parentheses. * $p < 0.05$, ** $p < 0.01$, *** $p < 0.001$

The policy levers: Selectorate Rate, Number of Political Parties, and Clientelism all have coefficients in the anticipated direction, however, none are statistically significant at the 0.05 level. As the Selectorate Size increases the occurrence of conflict decreases yielding support for the democratization thesis. But, this weak support is undermined by the fact that increases in the number of political parties are positively correlated with conflict onset, while single party states are more robust. Finally, Clientelism, has a small yet negative ($\beta = -0.05$) statistically significant relationship conflict onset. Governments that have the capacity to negotiate with opposition groups and have the wealth necessary to provide such groups with privatized goods are more likely to coopt fringe groups than weaker, poorer, and less sophisticated regimes.

6 Discussion

Our simulation has a series of implications. First, increasing deviation from the historical mean rainfall increases the frequency of civil war conflict. Additionally, the rainfall mean is statistically significant and has a negative relationship with conflict onset. Regions that are inherently drier are more apt to face environmental crises than wetter regions. It is important to note that the amount of rainfall is the more dominant of the two variables. States that have low levels of rain with increasing variation are most vulnerable while wet states with stable rainfall patterns are most resilient.

The impact of climate shifts is moderated by political and social variables. Governments that are strong in terms of power, capacity, and are centrist are the most resilient. Wealth, and by extension economic development does not reduce the incidence of conflict, rather it makes states targets for opposition groups.

Talkspan, which determines the range of each individual citizen's social interaction, proves to be very influential. At talkspan of 1, citizens only interact with direct neighbors; at 20 citizens can reach a large segment of the population. This element accounts for both traditional word of mouth communication inherent in lesser developed societies and sophisticated telecommunication techniques in advanced economies. The ability to communicate makes it easier to share the victories and defeats of everyday life. Societies that limit talkspan via censorship, firewalls, and checkpoints are taking a calculated risk and attempting to forestall or prevent the emergence of civil conflict as they deny potential adversaries the ability to coordinate.

The above research design suffers from a variety of operationalization, simulation, and methodological shortcomings. We test multiple power transition points ranging from 0.1 to 0.9 of the selectorate's total power. Power Transition theorists, however, identify 0.8 to 1.2 as the optimal range. We, however, believe civil conflict differs from interstate conflict in that conflict onset distinguishes a group as a potential challenger that would have gone unnoticed otherwise. Only by self-identifying can a group hope to draw support from diaspora's and other third parties. Secondly, the Malthusian argument is dependent on increasing population densities as a means of increasing stress. We keep the population within our society stable because of limitations in computing power. Additionally, we readily acknowledge our suppositions that a single climate-zone society does not exist within reality, however, it was necessary to abstract otherwise there would exist an infinite number of permutations.

The Homer-Dixon approach also hypothesizes the existence of feedback loops, which can exasperate resource and population pressures. This correlates with the notion that there exist simultaneous interactions between variables, and we attempted to model them accordingly, however, omissions and simplifications cannot be avoided.

This paper aims to test the hypothesis that climate variability can lead to conflict. To achieve this we developed an agent-based model that draws from a wide variety

of social science theories. We then simulated the existence of 17,496 countries for a period of twenty-years. This yields 325,570 simulated years' worth of data. We find support for the environmental-conflict narrative. This approach provides several advancements over previous research. First, it looks towards subnational causes of conflict rather than the aggregation of state variables. Secondly, we attempt to look to the future and predict rather than postdict. In terms of policy, governments should take note that climate variability can and does lead to conflict. Conflict, however, is not a foregone conclusion as there are many things a government can do to reduce its level of vulnerability. Some of these policy remedies have been hailed as silver bullets to an array of state problems for many years while others appear to have no substantive impact.

References

1. Themmer, L., Wallensteen, P.: Patterns of major armed conflicts, pp. 2001–2010 (2011)
2. Lacina, B., Gleditsch, N.P.: Monitoring trends in global combat: a new dataset of battle deaths. *Eur. J. Population* **21**(2–3), 145–166 (2005)
3. Pinker, S.: *The Better Angels of Our Nature: Why Violence has Declined*. Penguin, City of Westminster (2011)
4. Donat, M.G., Alexander, L.V., Yang, H., Durre, I., Vose, R., Dunn, R.J.H., Willett, K.M., Aguilar, E., Brunet, M., Caesar, J., Hewitson, B.: Updated analyses of temperature and precipitation extreme indices since the beginning of the twentieth century: the HadEX2 dataset. *J. Geophys. Res. Atmos.* **118**(5), 2098–2118 (2013)
5. Theisen, O.M., Gleditsch, N.P., Buhaug, H.: Is climate change a driver of armed conflict? *Clim. Change* **117**(3), 613–625 (2013)
6. Homer-Dixon, T.: *Environment, Scarcity and Violence*. Princeton University Press, Princeton (1999)
7. Miguel, E., Satyanath, S., Sergenti, E.: Economic shocks and civil conflict: an instrumental variables approach. *J. Polit. Econ.* **112**(4), 725–753 (2004)
8. Hendrix, C.S., Salehyan, I.: Climate change, rainfall, and social conflict in Africa. *J. Peace Res.* **49**(1), 35–50 (2012)
9. Koubi, V., Bernauer, T., Kalbhenn, A., Spilker, G.: Climate variability, economic growth, and civil conflict. *J. Peace Res.* **49**(1), 113–127 (2012)
10. Gizelis, T.I., Wooden, A.E.: Water resources, institutions, and intrastate conflict. *Polit. Geogr.* **29**(8), 444–453 (2010)
11. Siero, F.W., Doosje, B.J.: Attitude change following persuasive communication: integrating social judgment theory and the elaboration likelihood model. *Eur. J. Soc. Psychol.* **23**(5), 541–554 (1993)
12. Abdollahian, M., Yang, Z., Nelson, H.: Techno-social energy infrastructure siting: sustainable energy modeling programming (SEMPPro). *J. Artif. Soc. Soc. Simul.* **16**(3), 6 (2013)
13. Berlo, D.K., Lemert, J.B., Mertz, R.J.: Dimensions for evaluating the acceptability of message sources. *Pub. Opin. Q.* **33**(4), 563–576 (1969)
14. Corman, S.R., Tretheway, A., Goodall, B.: A 21st century model for communication in the global war of ideas. In: Consortium for Strategic Communication, Report, 701 (2007)
15. Rogers, E.M., Bhowmik, D.K.: Homophily-heterophily: relational concepts for communication research. *Publ. Opin. Q.* **34**(4), 523–538 (1970)
16. Suijs, J., Borm, P., De Waegenare, A., Tijs, S.: Cooperative games with stochastic payoffs. *Eur. J. Oper. Res.* **113**(1), 193–205 (1999)

17. Ketchpel, S.: Coalition formation among autonomous agents. *Lect. Notes Comput. Sci.* **957**, 73–88 (1995)
18. Organski, A.F.K., Kugler, J.: *The war ledger* Chicago (1980)
19. Wilensky, U.: *NetLogo*. Evanston, IL. Center for Connected Learning and Computer-Based Modeling. Northwestern University, Evanston (1999)
20. Yeung, C.S., Poon, A.S., Wu, F.F.: Game theoretical multi-agent modelling of coalition formation for multilateral trades. *IEEE Trans. Power Syst.* **14**(3), 929–934 (1999)

Towards a Comprehensive Simulator for Public Speaking Anxiety Treatment

Esin Söyler, Chathika Gunaratne and Mustafa İlhan Akbaş

Abstract Public speaking anxiety (PSA) is often cited as the most common social phobia. Virtual reality enables us to overcome PSA with life-like scenarios. This paper first reviews the state-of-the-art in virtual environments as an emerging treatment for public speaking anxiety and presents a comprehensive Virtual Environment (VE). In most of the studies there is a lack in the inclusion of physical and vocal cues. Physical and vocal cues generated by the audience are crucial contributors to PSA. We design a virtual auditorium with an audience exhibiting these physical and vocal cues; a comprehensive VE, helping overcome PSA. Additionally, participants are subjected to the three phases of speech: Anticipation, Performance and Recovery [Cornwell et al. in *Biol Psychiatry* 59(7):664–666, 2006 1]. The resulting simulator can then be used for training and eventual treatment of PSA in addition to being used as a tool for identifying cues to which speakers are more sensitive to.

Keywords Public speaking anxiety · Virtual environments · Physical cues · Vocal cues · Virtual audience

1 Introduction

Public speaking anxiety (PSA) is often cited as the most common social phobia among the general populace. In Diagnostic and Statistical Manual of Mental Disorders (DSM V) [2], anxiety disorders are categorized as a group characterized by anxiety and fear. The definition of anxiety is: “an unpleasant emotional state or

E. Söyler · C. Gunaratne (✉)

Institute for Simulation and Training, University of Central Florida, Orlando, FL, USA
e-mail: chathika.gunaratne@ucf.edu

E. Söyler
e-mail: esin.soyler@knights.ucf.edu

M.İ. Akbaş
Complex Adaptive Systems Laboratory, University of Central Florida, Orlando, FL, USA
e-mail: miakbas@ucf.edu

condition that is characterized by subjective feelings of tension, apprehension, and worry, and by activation or arousal of the autonomous system” [3]. Anxiety disorders prevent people from performing a variety of daily activities such as: interacting with an unknown individual or staying in crowded places [4]. According to DSM V [2] there are four types of anxiety disorders; (1) panic disorder, (2) obsessive-compulsive disorder, (3) agoraphobia (specific phobia) and (4) social phobia. Public speaking anxiety is a type of social phobia. To understand public speaking anxiety better we need to first define social phobia. Pertaub et al. [5] stated that people with social phobia usually suffer from a strong fear of social performance and fear that they will act in a way that is humiliating or embarrassing such that others will judge them negatively.

According to Burnley et al. [6], 85 % of the general population experiences some level of anxiety while delivering a public speech. People with public speaking anxiety reported that they are concerned that they will: (1) feel embarrassed after making mistakes that make them look “stupid” in front of others, (2) feel uncomfortable at the thought of being in the center of attention, and (3) believe that no one will show interest about what they have to say [7]. Public speaking anxiety has physical, verbal and non-verbal symptoms. These symptoms can be listed as trembling/shaking, cold hands, rapid heartbeats, sweating, blushing, dizziness, digestive discomfort, shaky voice, stuttering, speaking fast or slow, fidgeting, inability to stand still, avoiding eye contact and wiping hands [8].

Public speaking anxiety is intensified through to physical and vocal cues generated by the audience and the environment. These cues range from simple opening and closing of stage curtains, to distraction of individuals in the audience and even applause. Cues have been shown to cause public speaking anxiety, yet consistence of the individual contribution of cues demands further study.

Allen et al. [9] performed a meta-analysis for public speaking anxiety treatment types. They have identified seven different basic treatment/therapy types for reduction of this anxiety. These methods are: systematic desensitization, cognitive modification, skills through education, cognitive modification with skills training, and systematic desensitization with cognitive modification.

Addition to basic public speaking anxiety treatment types, virtual reality is a new treatment type. Virtual reality has been used since the late 1960s in various application areas. Computer based virtual reality environments, 3D Virtual Environments (VE) and autonomous characters have been increasingly important over the last several decades [10]. For treating anxiety disorders, one of the most effective ways is to use exposure therapy [4]. The exposure therapy can be done by actual exposure, by visualization, by imagination and by using virtual reality [4]. Using virtual reality in exposure therapy provides computer simulated environments and 3D graphical environments, which users can interact within [4]. A longitudinal study, conducted by Anderson et al. [11] showed that virtual reality exposure therapy had a long term improvement on participants’ reduction in public speaking anxiety level. Creating a VE enables experimenting in specific, re-created scenarios, under a controlled environment [12]. There are studies addressing the treatment of social anxiety disorders with virtual reality environments. However, to

the best of our knowledge, there are only a few public speaking anxiety specific virtual reality treatments [13] in the literature.

In this paper, we present a comprehensive VE for treating public speaking anxiety. The VE includes major physical and vocal cues experienced by a speaker addressing a crowd in an auditorium. The VE includes a reactive virtual audience of avatars and stage objects such as curtains and a podium. This VE acts as both a safe practice environment for those with public speaking anxiety and also importantly, as a diagnostic tool through which the consistency of physical and vocal cues throughout different participants can be analyzed. This information will help design focused treatments which directly address the actual causes of the individual's public speaking anxiety disorder.

The first part of the paper focuses on a literature review on the existing research studies on virtual reality usage in anxiety disorders and public speaking anxiety. The second part of the paper focuses on the created VE, physical and vocal cues, and benefits.

2 Existing Virtual Reality Usage in Anxiety Disorders

The first study for public speaking and VE was conducted in 1999 by Slater et al. [14]. They studied the reactions of public speakers delivering a speech to an audience of computer-generated avatars. Correspondence of the speakers' positive evaluations to the actual intended reactions of the virtual audience was measured. Level of expressed anxiety was compared against the speaker's evaluation of his performance; a better performance should correlate to lower signs of anxiety [14]. In their design they have used Distributive Interactive Virtual Environment where they created a seminar room with 8 avatars with dynamic behaviors such as: twitches, blinks, and nods. However, the avatars had no hands and their facial expressions were not clear. Ten participants in the study were recruited from postgraduate students and the results show that public speaking anxiety reduces with higher perceived positive reactions from the audience.

Later studies also showed the usage of a similar virtual reality environment. Most of the studies created a virtual conference room environment [5, 15–17]. The advantages of using the state of the art in interactive virtual human have been demonstrated [18]. In the study by Pertaub et al. [5] the experiments took place in a simulated conference room where there is a table with 6–8 avatars around it. Although the room settings remain the same, the audience reactions were tweaked to experiment on the speaker's reactions. The first scenario used a static audience, the second scenario used a positive audience and the third had negative audience characteristics. Lee et al. [16] replaced avatars in the VE with image-based rendering and moving pictures creating a higher fidelity visual representation of the actual environment, yet lacking the immersion brought about by the previous studies.

In [19], Chollet et al. report that participants found it a pleasurable experience interacting in the VE used for PSA treatment. Moreover, they found that the participants' eye contact skills with the audience was improved and that they used less pause fillers in their speech. Gupta et al., have described a video and audio capturing system which use the participant's feedback to the responses of a virtual audience member. This system uses a computer display to render the virtual audience and creates a live feedback loop between the speaker and the audience member [20].

Previous studies aiming to reduce PSA, measured the participant's anxiety level through self-reported anxiety tests [5, 15, 17, 21, 22]. While recruiting the subjects, Pertaub et al. [5] chose to give Fear of Negative Evaluation and SCL-90-R scales to determine the anxiety levels of the participants. In most of the studies Personal Report of Confidence as a self-reported speaker scale was used to identify the participants' anxiety level [5, 15, 17, 22]. Although self-reporting is a strong data collection technique, there are disadvantages in using them [23] such as: anchoring effects, primacy and recency effects, time pressure, consistency motivation and credibility of self-reports [23]. In existing virtual reality treatments, the participants in the study grade themselves against these scales through pre- and post-tests. According to the results of these scales, it was found that after the virtual reality therapy, participants were feeling less anxious about performing in public [24]. Although results show that there was a decrease on the anxiety, we cannot attribute the VE as the causation of this decrease as it could have been a placebo effect causing the answers of the participants to be biased. We can expect participants to evaluate themselves better in the post-test. The one year follow-up study of Safir et al. [24] showed that participants who evaluated themselves as less anxious following the training retained their lowered level of anxiety even one year after. In our proposed prototype, to measure the anxiety level a heart rate monitor [25] and skin conductivity sensor will be used in addition to self-reporting scales. This will enable us to validate the consistency of the results of the self-reported tests.

In this prototype it is aimed to provide training for speakers' to train with crowded large audience in an auditorium with vocal and physical cues. In our study, we provide a comprehensive design of a virtual auditorium with diversity of the audience's responses, or physical and vocal cues. Curtain opening/closing [1], ambient audience noise [1, 14], conversations within the audience [14], sleeping individuals [14], facial expressions [14, 15], visible exiting/entering [1, 14] and applause [1, 14]. Lee et al. and Anderson et al. [15, 16] use live streaming of individuals (therapists) to fill the audience. Despite the high fidelity of the simulated audience this would be highly resource consuming and impractical when training is aimed for very large audiences. However, existing research studies on public speaking focused on the small crowd of a conference room and did not usually involve facing a larger crowd such as an auditorium full of people.

3 A Comprehensive Virtual Training Environment

This section discusses the development of a comprehensive training simulator for overcoming public speaking anxiety. The previous sections showed the benefits of immersion in a simulated auditorium with avatars, capable of demonstrating real reactions of audience towards this end. Practicing speech in such simulated environments is already proven to help lowering the public speaking anxiety levels of participants [21]. We have also emphasized the importance of including important physical and vocal cues of the audience as observed by the speaker while delivering the speech.

The literature emphasizes the need to systematically combine the different types of cues used in these studies to build a comprehensive training VE. The advantage of our simulator is its capability of being used as a tool to analyze the speaker's sensitivity to different physical and vocal cues. This information can then be used to help speakers with PSA overcome their specific phobias through treatments targeting these specific cues, instead of undergoing general PSA therapy.

Additionally, through this comprehensive simulator we intend to provide a safe environment for participants to: (1) gain control over their anxiety by subjecting themselves to a similar environment prior to an actual speech, (2) practice their speech before presenting in real life events and (3) understand what it feels to be in the center of attention.

The virtual reality environment scenario was created according to the causes of PSA reported by Katz in [7]. These include verbal and facial reactions, body language, head movement and focus. It is expected that the combination of the factors, which have been studied individually in the literature, will provide a stronger environment to achieve PSA reduction.

3.1 *Virtual Environment (VE)*

Our simulator simulates a large auditorium capable of hosting a large audience of autonomous avatars (Fig. 1). The auditorium features a stage with two flights of steps, a podium and curtain, several levels of seating, each level consisting of several rows of chairs. The rows are separated by a central aisle and bordered by two aisles on the sides.

3.2 *Virtual Humans*

The opportunity to be in a realistic auditorium with avatars, which are capable of demonstrating real reactions of audience, will be beneficial to decrease the anxiety levels of the speakers. Research indicates that conference room scenarios with



Fig. 1 Speaker approaches the podium to address an audience capable of hosting a large audience



Fig. 2 Autonomous virtual audience reacting to the speaker through physical and vocal cues

avatars responding in real-time to their delivery have proven helpful to lower the public speaking anxiety levels of participants [21].

The VE includes animated 3D characters. These characters simulate automated behavior and respond to the speaker's arrival, delivery, pauses and exit. The simulator has been developed using Unity and models of virtual humans from the Unity Assets store have been used. Physical and vocal cues have been scripted into these avatars. The avatars have the ability to react to the speaker at varying levels of attention (Fig. 2); i.e. they may act fully interested, mildly interested, distracted or bored.

Figure 3 shows a screenshot of the speaker's perspective of the virtual audience as seen from the stage. The avatars are performing a variety of behaviors simultaneously from entering, to being seated to asking questions.

Fig. 3 Speaker's perspective of the virtual audience as seen from the stage



3.3 *Physical and Vocal Cues*

In addition to the participant's delivery of speech, physical and vocal cues generated from the audience have a crucial impact on the anxiety level of the participant. As shown in the literature [7], being in the center of attention and the belief that no one will be interested in one's speech are the top causes of anxiety. Correct variation of physical cues from the autonomous audience can help to decrease speakers' anxiety levels when they are faced with those kinds of situations. The physical cues used in this study are:

- Opening and closing of curtains
- Avatars entering and leaving the auditorium
- Avatar gaze shifts when talking with each other instead of listening to the speaker
- Avatar facial expressions (boredom, excitement)
- Visual applause (clapping, standing)
- Level of avatar eye contact with speaker

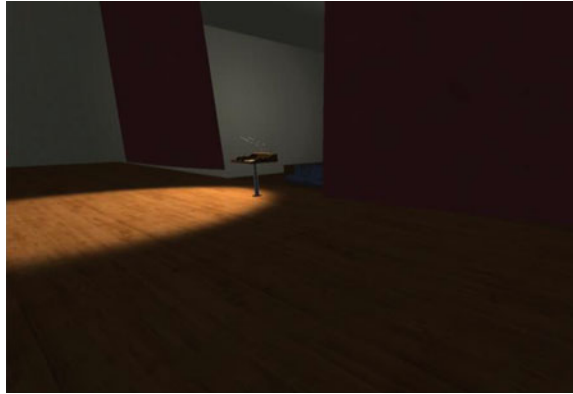
Another factor that affects anxiety is sound, which is referred to as vocal cues. For vocal cues we used sound-proof headphones, which provided the audios that we present. The vocal cues used in this project are:

- Noise of walking, entry and exit of audience members
- Introduction of the speaker
- Ambient auditorium noise
- Distractions from audience (such as phone ringing noise)
- Applause

3.4 *Experimental Procedure*

Within this VE participants can perform their speech as if addressing a real life assembly. Waiting for curtains to open, starting their speech and the reactions of

Fig. 4 Speaker awaiting his turn at the backstage behind curtains



avatars can help detecting the participants' anxiety level at each step. This will help us figure out which cue contribute most to the participant's anxiousness. Here we discuss the workflow expected to be performed by the speaker within the simulation.

Participants' are subjected to the full event flow encountered during the delivery of a speech, which consists of three phases: (1) Anticipation, (2) Performance and (3) Recovery as defined in [1]. Thus, several real-life actions are systematically performed before and after a speech are simulated.

During the anticipation phase, the participant must walk past the audience onto the stage. The participant starts walking from the back of the auditorium and is required to walk up to the stage using the aisles and passing the audience. The participant ascends the stairs and walks backstage. Then the participant must await his turn to speak behind closed curtains (Fig. 4), while he is being introduced briefly to the crowd.

Next, the participant is subjected to the performance phase of the speech. This begins with the opening of the curtains. The participant must walk up to the podium at the middle of the stage and will be highlighted by the spotlight. They then greet the audience, await applause and begin delivery of a prepared speech. During this stage the participant is subjected to the many physical and vocal cues generated by the autonomous avatars in the audience.

Finally, during the recovery phase, the participant thanks the audience and the curtains close. The participant then descends using the stairs at which point the simulation will end.

Anxiety measurements will be conducted throughout the three phases, using skin conductivity sensor [26] and heart-rate measures [16, 26]. The simulation was developed using Unity, with scripts for virtual humans and behaviors for the audience. Immersion was improved by exporting the simulation into an android application for 3D Google cardboard, an inexpensive (\$15.00 as at March 2016) [27] head-mounted display device. Therefore, the application was deployed on an android smart-phone which was paired with the Google cardboard display.

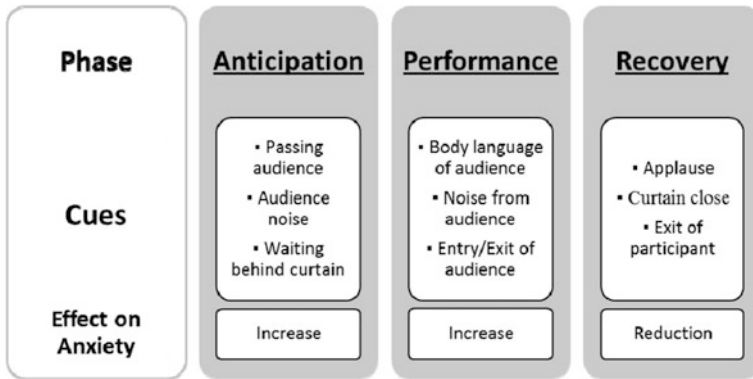


Fig. 5 Expected effects on anxiety level caused by physical and vocal cues during each phase of the experimental procedure

4 Expected Results and Benefits

The simulated training environment aims to help lower the anxiety levels of participants who suffer from public speaking anxiety. By immersing the participant in a VE of reactive avatars, we re-create a controllable stressful situation for the participant to practice in. This simulator may be considered as a speech therapy application or a diagnostic tool. The anxiety level of the participant is measured throughout the experiment procedure described above in order to facilitate these actions.

Figure 5 illustrates the effects of the physical and vocal cues on the anxiety level. The anticipation and performance phases contribute to the speaker’s anxiety level, while the recovery phase will cause a drop in the speaker’s anxiety causing them to exhibit a feeling of relief.

Through repeated exposure, this VE can be used a treatment tool. Gradual increase in the difficulty of maintaining audience attention, length of exposure and size of audience will improve the speaker’s confidence over time and improve their performance in public speaking.

Importantly, by using varying levels of intensity in each physical and vocal cues expressed by the audience during the delivery of the speech, it is possible to pinpoint the major contributors to the participant’s PSA. This information can then be used to give a detailed diagnosis of the participant’s public speaking anxiety disorder, allowing treatments to be focused and more effective.

5 Conclusion and Future Work

This paper emphasizes the need for a more comprehensive VE for training people to overcome public speaking anxiety. Existing treatment plans using VE are reviewed and a lack of literature focusing specifically on this problem is identified. Most of the studies used rather small audiences despite aiming for higher fidelity and displayed a lack in diversity of physical and vocal cues generated by the audience.

A comprehensive VE inclusive of the three phases of public speaking and the many physical and vocal cues generated by the audience could fill the gap in this method of training. The design of such a VE has been discussed. This simulator both acts as a tool for treating public speaking anxiety as well as diagnostic tool identifying the root causes of the participant's public speaking anxiety disorder.

Future work will involve the evaluation of this VE against a significant number of participants and analysis of correlations between physical/vocal cues and speaker's level of anxiety. Further, the VE must be tested and compared with the traditional techniques for model verification.

References

1. Cornwell, B.R., Johnson, L., Berardi, L., Grillon, C.: Anticipation of public speaking in virtual reality reveals a relationship between trait social anxiety and startle reactivity. *Biol. Psychiatry* **59**(7), 664–666 (2006)
2. DSM-5 American Psychiatric Association. *Diagnostic and Statistical Manual of Mental Disorders*. American Psychiatric Publishing, Arlington (2013)
3. Schwarzer, R., Quast, H.-H., Jerusalem, M.: The impact of anxiety and self-consciousness on cognitive appraisals in the achievement process. In: Zuckerman, M., Spielberger, C. (eds.) *Test Anxiety Res.* LEA, USA (1976)
4. Gorini, A., Riva, G.: Virtual reality in anxiety disorders: the past and the future. *Expert Rev. Neurotherapeutics* **8**(2), 215–233 (2008)
5. Pertaub, D.P., Slater, M., Barker, C.: An experiment on public speaking anxiety in response to three different types of virtual audience. *Presence Teleoperators Virtual Environ.* **11**, 68–78 (2002)
6. Burnley, M., Cross, P., Spanos, N.: The effects of stress inoculation training and skills training on the treatment of speech anxiety. *Imagination Cogn. Pers.* **12**, 355–366 (1993)
7. Katz, L.: *Public Speaking Anxiety*. University of Tennessee at Martin Counselling Center (2000)
8. North, M., Rives, J.: Virtual reality therapy in aid of public speaking. *Int. J. Virtual Reality* **3**, 2–7 (2001)
9. Allen, M., Hunter, J.E., Donohue, W.A.: Meta-analysis of self-report data on the effectiveness on public speaking anxiety treatment techniques. *Commun. Edu.* **38**(1), 54–76 (1989)
10. Onyesolu, M.O., Eze, F.U.: Understanding virtual reality technology: advances and applications. *Adv. Comput. Sci. Eng.* 53–70 (2011)
11. Anderson, P.L., Price, M., Edwards, S.M., Obasaju, M.A., Schmertz, S.K., Zimand, E., Calamaras, M.R.: Virtual reality exposure therapy for social anxiety disorder: a randomized controlled trial. *J. Consult. Clin. Psychol.* **81**(5), 751 (2013)

12. Nagendran, A., Pillat, R., Kavanaugh, A., Welch, G., Hughes, C.: AMITIES: avatar-mediated interactive training and individualized experience system. In: Proceedings of the 19th ACM Symposium on Virtual Reality Software and Technology, pp. 143–152 (2013)
13. Vanni, E., Conversano, C., Debbio, D.A., Landi, P., Carlini, M., Fanciullacci, C., Bergamasco, M., Fiorino, A., Dell’osso, L.: A survey on virtual environment applications to fear of public speaking. *Eur. Rev. Med. Pharmacol. Sci.* **17**, 1561–1568 (2013)
14. Slater, M., Pertaub, D.P., Steed, A.: Public speaking in virtual reality: facing an audience of avatars. *Comput. Graph. Appl. IEEE* **19**(2), 6–9 (1999)
15. Anderson, P.L., Zimand, E., Hodges, L.F., Rothbaum, O.B.: Cognitive behavioral therapy for public-speaking anxiety using virtual reality for exposure. *Depress. Anxiety* **22**, 156–158 (2005)
16. Lee, J.M., Ku, J.H., Jang, D.P., Kim, D.H., Choi, Y.H., Kim, I.Y., Kim, S.I.: Virtual reality system for treatment of the fear of public speaking using image-based rendering and moving pictures. *CyberPsychol. Behav.* **5**(3), 191–195 (2002)
17. Slater, M., Pertaub, D.P., Barker, C., Clark, D.M.: An experimental study on fear of public speaking using a virtual environment. *CyberPsychol. Behav.* **9**(5), 627–633 (2006)
18. Mykoniatis, K., Angelopoulou, A., Proctor, M.D., Karwowski, W.: Virtual humans for interpersonal and communication skills’ training in crime investigations. In: *Virtual, Augmented and Mixed Reality. Designing and Developing Virtual and Augmented Environments*. Springer, Berlin, pp. 282–292 (2014)
19. Chollet, M., Wörtwein, T., Morency, L.P., Shapiro, A., Scherer, S.: Exploring feedback strategies to improve public speaking: an interactive virtual audience framework. In: *Proceedings of the 2015 ACM International Joint Conference on Pervasive and Ubiquitous Computing*. ACM, pp. 1143–1154 (2015)
20. Gupta, A., Makhboroda, Y., Story, B.H.: U.S. Patent No. 20,160,049,094. Washington, DC: U.S. Patent and Trademark Office (2016)
21. Wallach, H.S., Safir, M.P., Bar-Zvi, M.: Virtual reality cognitive behavior therapy for public speaking anxiety: a randomized clinical trial. *Behav. Modif.* **33**(3), 314–339 (2009)
22. Harris, S., Kemmerling, R.L., North, M.M.: Brief virtual reality therapy for public speaking anxiety. *CyberPsychol. Behav.* **5**(6), 543–550 (2002)
23. Paulhus, D.L., Vazire, S.: The self-report method. In: Robins, R.W., Fraley, R.C., Krueger, R. F. (eds.) *Handbook of research methods in personality*, pp. 224–239. Guilford, London (2007)
24. Safir, M.P., Wallach, H.S., Bar-Zvi, M.: Virtual reality cognitive-behavior therapy for public speaking anxiety: one-year follow-up. *Behav. Modif.* 1–12 (2012)
25. Ling, Y., Brinkman, W.P., Nefs, H.T., Qu, C., Heynderickx, I.: Effects of stereoscopic viewing on presence, anxiety, and cybersickness in a virtual reality environment for public speaking. *Presence Teleoperators Virtual Environ.* **21**(3), 254–267 (2012)
26. Diemer, J., Alpers, G.W., Peperkorn, H.M., Shibani, Y., Mühlberger, A.: The impact of perception and presence on emotional reactions: a review of research in virtual reality. *Frontiers Psychol.* **6** (2015)
27. Google Store.: Retrieved from https://store.google.com/product/google_cardboard (2016)

The Research on VR-Based of Technology Generating Equipment and Interaction Equipment

Yan Liu and Fan Wang

Abstract The technology of VR (Virtual Reality) is the result of the progress of science and technology since the 20th century, it embodied the computer technology, computer graphics, multimedia technology, sensor technology, display technology, human body engineering, human-computer interaction theory, the latest achievements of artificial intelligence, and other fields, has become the latest achievements after relay information field of multimedia technology and network technology is widely attention and research, development and application of hot spots, is currently the fastest growing a multi-disciplinary comprehensive technology. Rapid generating equipment and interaction changed in the past, between people and computer dull, stiff, passive way of communication, make the man-machine interaction between become more humanized, blazed a new research field of human-computer interaction interface, which provides a new interface for the application of intelligent engineering tools, for all kinds of engineering provides a new description method of large-scale data visualization, but also changed the way people work and lifestyle and ideology.

Keywords Virtual reality technology · Generate equipment · Interaction equipment · Immersion · Interactive · Imaginative

1 Introduction

The Virtual reality technology as an effectively simulated creatures in their natural environments, listen to and dynamic behavior of the interactive technology, its ideas, concepts, inoculation and appear can be traced back to ancient China during

Y. Liu (✉)

Wuhan University of Technology School of Design, Wuhan, Hubei, China
e-mail: 453752020@qq.com

F. Wang (✉)

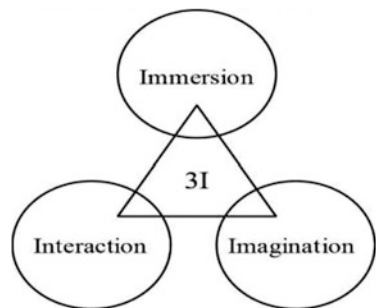
Hubei Urban Construction Vocational and Technological College, Wuhan, Hubei, China
e-mail: 56786968@qq.com

the warring states period (468–376 BC). According to “mozi. Lu asked” records, “states cut bamboo think magpie, and fly, no fewer than three days”, its raw material is very thin wood or bamboo. People later on the kite tied on bamboo whistle and use of bamboo wind whistle, sound, such as zheng, therefore calls “the kite”. Analog audio kite flying animals invention, this is the earliest records about ancient Chinese test vehicle model. When people in a kite, which looked from a distance lifelike simulation flight interaction between animal and human nature scenes with sweet and pure and fresh, the zheng from the verisimilitude, onomatopoeia, interactive behavior is the application of virtual reality technology in people’s life. This process has a long history. Later this technology spread to the west, west they called kite craft, and by using the principle of kite invented the airplane. Inventor Edwin a. ink flight simulator was invented in 1929, makes a person feel and sit on the plane is the same, really people got inspiration from the behavior of animal flight, has a rich imagination, creates more inventions, the virtual reality technology to the ground to take root, have extensive social cognitive basis.

2 Characteristics of Virtual Reality Technology

American scientists Burdea G in 1993 annual meeting of the world electronic published an article called “Virtual Reality Systems and Applications” (Virtual Reality) system and application of the article, for the first time in this article puts forward the three characteristics of Virtual Reality technology, i.e., the Immersion (based), interactive (Interaction) and imaginative (Imagination). These three features are not isolated, between them is mutual influence, each feature implementation depends on two other features. So, we can take these three features expressed as shown in Fig. 1 of the triangle, they also referred to as the “3I characteristic of virtual reality”.

Fig. 1 3I characteristic of virtual reality



2.1 *Immersion*

The immersion refers to the user feel is surrounded by a virtual world, like completely into the virtual world. Is the most important characteristic of virtual reality technology, make the user feel part of the virtual world, users become participants by the observer, the immersion and participate in the activities of the virtual world. Ideal virtual world should reach the level of the user to distinguish true and false, virtual reality technology based on physical or psychological characteristics of human visual, auditory, lifelike three-dimensional image generated by the computer, the user wear the helmet mounted display and data gloves and other interactive devices, become a member of the virtual environment.

Multi-perceptual. The Immersion is derived from the Multi-perceptual in the virtual world, in addition to common visual perception, force sensing and auditory perception, perception, tactile perception, motion perception, perception of taste perception, smell, etc. Ideal virtual reality should have people have many kinds of awareness. The establishment of the visual immersion depends on the user and the integration of virtual world. So, the virtual reality system must provide the user with three-dimensional images and wide field of vision, along with the people at the same time, the movement of the resulting scene images should also be real-time change subsequently. In order to achieve the auditory immersion, virtual reality system mainly make users feel is a virtual sound in three-dimensional space. Which are different from ordinary stereo. Ordinary stereo sound can make the person feel comes from a plane, and 3D virtual sound can make the listener feel voice came from a spherical space anywhere around ears. In the virtual world, people can by means of various interactive equipment, experience, grasp operations such as feeling. Now, however, the technical level also cannot achieve the same as the real world completely tactile immersion effect, just can realize simple force feedback effect.

Autonomy. The Virtual objects in the independent activity, or interaction with the user interaction, the dynamic should have certain performance, the performance shall be subject to the provisions of the law of nature or the designer. Autonomy refers to objects in the virtual environment based on the extent to which the laws of physics to make action. When driven by external forces, for example, the object will move towards the direction of the force, overturned or falling, etc.

2.2 *Interactivity*

The Interactivity mainly refers to the natural interaction, virtual reality system emphasizes the nature of the interaction between people and the virtual world, such as people move, movement of the rotation of the head, hands, etc. To this end, mainly by means of special hardware equipment (such as data glove and force feedback device, etc.) to complete the interaction. These devices the user can

through the way of nature, having the feeling in the real world. For example, the user can directly with the hand grasping objects in the virtual world, then hand a sense of touch, and can feel the weight of the object, can distinguish with stone or sponge, and by grasping objects in the scene can be immediately with the mobile movement. For example, in the virtual Forbidden City tour system, users can feel new feelings brought by the interaction of virtual reality system. When a user roaming in the virtual environment, visitors to the stereoscopic image by wearing the helmet mounted display in the user's field of view, and as the user's head movement, the new viewpoint of constantly updated scene real-time display to visitors.

2.3 *Imaginative*

The Imaginative refers to the user according to the access to a variety of information in the virtual world and their own behavior in the system through logic and reasoning and thought processes, such as associate as the running state of the system to its ability to imagine the future progress. It helps human to obtain more knowledge, the mechanism and regularity of deep understanding complex systems. Mankind is facing more and more in many fields, and break through the problem to be settled urgently, such as manned space flight, medical surgery simulation and training, large product design research and forecast weather and natural disasters and multiple joint military exercises, etc. If, in accordance with the traditional method to solve these problems, not only to invest huge human and material resources, spent a long time, even to bear the risk of casualties. And the emergence and development of virtual reality technology, which provides a new way to solve these problems and the new way. Virtual reality can make human from qualitative and quantitative integrated virtual environment to get the understanding of the perceptual and the rational, deepen the concept, generate new ideas and conceptions, and actively seek and explore information. Therefore, the appropriate application object and virtual reality of creativity and imagination, can greatly improve the production efficiency, reduce labor intensity, improve the quality of the product development.

3 The Generating Equipment of Virtual Reality

The Generating Equipment of virtual reality is mainly refers to create a virtual scene, real-time response to the user a variety of computer equipment operation, the virtual reality system performance depends largely on the performance of computer equipment, according to the speed of the CPU and the image processing ability, the formation of virtual reality devices can be divided into high performance, graphics workstations, personal computer mainframe computers and distributed computer network.

3.1 High-Performance PC

The Virtual reality development of the economy and the most basic computer configuration requirements is equipped with a graphics accelerator card in high-grade computer platform, can stable operation is based on the 3D drawing language open virtual simulation system, and with a CRT display or external projector to show the main means. In high-performance PC system, its core is computer graphics accelerator card, in order to accelerate the speed of image processing, system can configure multiple graphics accelerator card.

3.2 Graphic Workstation

The Graphics workstations (static) is a kind of graphics, image, image (dynamic) and the floorboard of the high grade special purpose computer video work. From the perspective of the purpose of the workstation, the three dimensional animation, data visualization processing and CAD, CAM and EDA, requires the system have strong ability of graphics processing. Graphic workstation has been widely used in professional graphic design, such as advertising, media design, architecture, interior design, such as architectural renderings and roaming animation, CAD, CAM, CAE (e.g., machinery, mold design and manufacturing), video editing, such as nonlinear editing, film and television animation (e.g., 3D video effects), video monitoring, testing (e.g., product of the visual inspection), virtual reality (such as ships, aircraft simulation driving), military simulation (such as 3D battle environment simulation).

3.3 Super-Computer

With the development of virtual reality technology, the computing power is more and more complex, the calculation amount of data is very huge, so need the support of super computer, super computer, often referred to as consisting of hundreds of thousands or more processors, can calculate the ordinary computer and the server cannot complete computer large, complex subject. People can use super computer by numerical simulation to predict and explain couldn't get through the experiment of natural phenomena.

3.4 Distributed Computer Network

The Distributed virtual environment refers to it resides in two or more than two network computers, these computers to share the entire simulation calculation of

load. If in distributed virtual environment two (or more) user called cooperation, refers to the simulation tasks they perform given in turn, only one user at a time with a given virtual object interaction, on the contrary, called a collaboration, referring to them at the same time with a given virtual object interaction.

4 The Interaction Equipment of Virtual Reality

The Virtual reality has set up a virtual world, interaction between people and systems in the virtual world, mutual influence, and to produce the immersion virtual reality, common keyboard, mouse and other interactive equipment cannot completely meet the need, must have the corresponding interaction device support. At present virtual reality interactive devices according to the function different, can be divided into visual display devices, auditory perception, virtual objects, motion capture equipment operating equipment.

4.1 *Visual Display Device*

The Visual display of the equipment is mainly to provide customers with stereo vision, according to the scene and this kind of scenario will change in real time. The key technology of such devices is stereo display, mainly adopt two methods to implement, a show at the same time around the two images, called display technology at the same time, it is to make the two images there are subtle differences that make the eyes can only see the image, this technology is mainly used in helmet mounted display. Another technique is to display technology, at a certain frequency alternate displays two images, in order to ensure that each eye can only see their corresponding image, by the user with the same frequency synchronous switching active or passive 3D glasses to see images, this technology is mainly used in 3D glasses.

Head-Mounted Display. The Helmet display is widely used in virtual reality system of stereo display device, is usually fixed on the user's head, as the movement of the head and movement, and is equipped with position tracking, real time measure the position and facing Angle of the head, and entered into the computer. Computer generated the data reflects the current position and facing the scene images, and then by two LCD or CRT display to offer two eyes images respectively.

Binocular Omni-Orientation Monitor. The Binocular omni-directional monitor is a portable display, display device is a special kind of head. Use BOOM is similar to using a telescope, he put the two independent CRT monitors bundled together, is supported by two mutually vertical mechanical arm, this not only allows the user to within the radius of 2 m sphere space free to manipulate the monitor position with the hand, also can display the weight of the balance to be clever and

always maintain level, is not affected by platform motion, every node on the bracket position tracking, can carry out real-time observation and interaction.

Large-Screen Projection, LCD Shutter Glasses. The Cavernous VR system is a kind of based on projection screen surrounded Cave Automatic Virtual Environment (Cave Automatic Virtual Environment, Cave). CAVE system is a cube structure, usually in the CAVE system is also equipped with 3D stereo system, users can achieve immersion feel. User wired or wireless type stereoscopic glasses, can feel themselves in a virtual world, annulus is very similar to the 3D movie, the whole system can real-time interaction with the user and respond, system can not only produce three-dimensional panoramic images, but also the head tracking function, can accurately measure the head position, and know in which direction the user is viewing. Describe system can follow the line of sight of real-time virtual scenes, in this way, users don't have to like on ordinary computer 3D graphics applications, to press the keyboard to convert the Angle of view, the user can very naturally, by turning the head to transform perspective, the CAVE of virtual reality is much greater than those who only have stereo image system is more superior.

4.2 Auditory Perception Devices

The Auditory information is second only to human visual information of the second sensing channels, it receives the user and virtual environment of voice input on the one hand, on the other hand also generation of 3D virtual environment, 3D is not the concept of stereo sound, but generated by a computer, can be manually set sound source in the three-dimensional space position of a synthetic voice. The sound technology not only consider the man's head and torso to the impact of sound reflection, real-time tracking, also to the person's head can make virtual sound as the person's head movement change accordingly, so that they can get a realistic 3D sound effects. At present, the technology of the virtual reality of auditory perception equipment mainly has two kinds of headphones and speakers.

Headphones. Based on the head of auditory perception devices will follow participants moving head, and can provide a completely isolated environment. Acoustic characteristics of different headphones have different weight, size and the way the parts installed in the ear. A headset is protective ear headphones, its volume is relatively large and heavy, and protective ear pads cover on the ear. Another set of headphones is earplugs, voice through it to a specific point in a ear. Earplugs volume is small, and closed in the compressible plug.

The Speaker. The speaker is a commonly used electro-acoustic devices, it is a kind of fixed position of auditory perception. In most cases it can provide people with sound, can also be based on the head of visual reality equipment used in the speaker.

4.3 Virtual Object Operating Equipment

Data Glove. The Data glove is a kind of wear on the user's hand, used to detect the user hand sensing device, and sends a corresponding electrical signal to the computer so as to drive the virtual simulation real hand movements. In actual use, the data glove itself does not provide information related to the spatial location, must match the position tracking device application. Data glove not only convey hand gesture accurately in real time to a virtual environment, and is able to contact with the virtual object information feedback to the operator. Provide operators with a more direct, more natural, more effective way to interact with the virtual world, greatly enhance the interactive and immersion. And provides the operator with a common, direct way of human-computer interaction, especially suitable for hand need more degrees of freedom model of virtual objects in a complex operation of virtual reality system.

Tactile Feedback Device. The Tactile feedback is also called contact feedback refers to a touch from the sensors in the skin surface sensitive nerve, including contact surface geometry, degree of hardness, smooth surface and temperature real-time information, such as in a VR system without tactile feedback, when the user access to the virtual world of when an object is easy to make a hand through the object, so as to lose their sense of reality. The effective method to solve this problem is increasing tactile feedback in user interaction equipment. This feedback information is mainly based on the sense of vision, air pressure, vibration tactility, electronic touch and neuromuscular simulation method.

Force Feedback Device. The Force sensing feedback is by using the advanced technology and the space of the virtual object movement into the surrounding mechanical movement of physical devices, allowing users to experience the real strength of feeling and sense of direction, its main principle is through the force feedback system by computer for the user's hand, wrist, arm, such as motion resistance, thus the user feel the size and the direction of the force.

4.4 Motion Capture Equipment

In VR systems in order to realize the interaction with the VR system, participants must be determined the direction of the position such as head, hands, body, accurate tracking measure the movement, these movements in real-time monitoring, so that the data feedback to display and control system. The work of VR system is indispensable, which is the motion capture technology research content.

The Sensor. The Sensors in the motion capture device is fixed in certain parts of the moving objects tracking device. Through physical sensors provide information, motion capture device can obtain the information such as position, velocity of moving object. Different motion capture the number of sensor task requires different, character to capture, for example, if the people of the whole trajectory

capture, need sensor quantity is less, if capture local information such as the face and hands of the body, because of the joints and detail more, you will need to increase the number of sensors.

Signal Capture Equipment. Because now the widely used optical motion capture system, often with a high resolution infrared camera signal capture and access. For before mechanical motion capture system, electrical signals are collected through a piece of circuit board.

Data Transmission Equipment. The data transmission equipment is mainly responsible to obtain the motion capture information in real time into the computer, and then through the computer for real-time analysis and processing information.

Data Processing Equipment. Motion capture device to capture the data needs to be revised and processed in combination with 3D model, with the help of computer, the data of high-speed computing power to complete the processing of data.

5 Conclusion

In order To do a good job, must first sharpen It, perfect virtual reality can not do without the collaborative operation and support of computer hardware and software, only clear the characteristics of the virtual reality and hardware requirements, we can according to different types of virtual reality system to select the most appropriate equipment to achieve the purpose of our generation and interaction, and fill the gap between information processing system can obtain, look forward to in the near future, become a kind of virtual reality system of multidimensional a powerful information processing system, become people to thinking and creating aides and the concept of the people have a powerful tool for deepening and acquire new concept.

Assessing Hazard Identification in Surface Stone Mines in a Virtual Environment

Jennica L. Bellanca, Timothy J. Orr, William Helfrich,
Brendan Macdonald, Jason Navoyski and Brianna Eiter

Abstract Mine workers are expected to remain vigilant and successfully identify and mitigate hazards in both routine and non-routine locations. The goal of the current research project is to better understand how workers search and identify hazards. NIOSH researchers developed a data collection setup to measure a subject's gaze, head position, and reaction time while examining 360° 2D-panoramic images at a surface mine. The data is integrated in semi real-time to determine region of interest (ROI) hit accuracy for hazards within the images. The purpose of this paper is to discuss the development and implementation of the hardware and software. The following aspects of the setup will be explored in the paper: (1) environment selection, (2) image creation, (3) stimulus display, (4) synchronization, (5) gaze mapping, and (6) region of interest (ROI) hit calculation.

Keywords Eye tracking · Hazard recognition · Virtual reality

J.L. Bellanca (✉) · T.J. Orr · W. Helfrich · B. Macdonald · J. Navoyski · B. Eiter
Pittsburgh Mining Research Division, National Institute for Occupational Safety
and Health, Centers for Disease Control and Prevention, Pittsburgh, PA, USA
e-mail: JBellanca@cdc.gov

T.J. Orr
e-mail: TOrr@cdc.gov

W. Helfrich
e-mail: WHelfrich@cdc.gov

B. Macdonald
e-mail: BMacdonald@cdc.gov

J. Navoyski
e-mail: JNavoyski@cdc.gov

B. Eiter
e-mail: BEiter@cdc.gov

1 Background

The metal/non-metal mining industry saw a spike in fatalities between October 2013 and January 2015. Thirty-seven mine workers were fatally injured in accidents, which is a significant increase relative to the record low number of fatalities in the two years prior—16 fatalities in both 2012 and 2011 [1]. In an effort to address this increase in fatalities, during the summer of 2015 the Mine Safety and Health Administration (MSHA) put forth new guidance on “working place” examinations. The goal of this guidance is to increase attention on mine workers’ ability to identify hazards at a mine site [2]. Mining is a major undertaking that involves the use of complex heavy machinery, equipment, and processes, as well as numerous and diverse worker activities that take place in a dynamic, challenging environment [3]. In order to safely perform their duties, mine workers are expected to remain vigilant and successfully identify and mitigate hazards in both routine and non-routine locations. The goal of the current research project at the National Institute for Occupational Safety and Health (NIOSH) Pittsburgh Mining Research Division (PMRD) is to better understand the process of hazard recognition and to identify differences across various groups of participants (e.g., mine workers employed at stone, sand and gravel operations, safety professionals, and students). The long-term goal of this work is to develop training materials to help mine workers recognize and mitigate hazards.

PMRD researchers developed a virtual reality setup to examine participants’ ability to search and identify hazards. Researchers developed a set of 360° 2D-panoramic images of locations at a surface stone mine that are displayed while collecting each subject’s eye position, body position, and reaction time data. This data collection setup involves stimulus presentation and review in a single visit using two different virtual reality environments. The stimulus setup involves the integration of true-size panoramic images, millisecond accurate synchronization of image timing, motion capture data, scan path data, reaction time data, and high-speed video where subjects are allowed to move freely within the viewing area of the 360° cylindrical display. The gaze, motion capture, and reaction time data is integrated in semi real-time in order to determine region of interest (ROI) hit accuracy for researcher-identified hazards within the images. The review setup displays the fixation and hazard identification data to the subjects immediately following the panoramic data collection on a powerwall screen during a researcher-guided review session. The purpose of this paper is to discuss the development and implementation of the hardware and software. The following aspects of the setup will be explored in later sections of the paper: (1) environment selection, (2) image creation, (3) stimulus display, (4) synchronization, (5) gaze mapping, and (6) region of interest (ROI) hit calculation.

2 Simulation Environments

2.1 *Stimulus Environment*

Because of the impracticality of staging hazards and collecting gaze and reaction time data in the field, researchers were required to turn to the development of a virtual environment. It has been shown, especially for complex search tasks, that environments that are more realistic produce improved training transfer and performance results [4]. However, the cost of environment development and the end goal of developing distributable training materials made a full stereoscopic 3D environment impractical. This study was explicitly interested in hazard search and identification in surface stone facilitates. While these operations are very dynamic, the large scale of the locations and equipment generally requires the hazard identification to be completed at a distance to avoid entering into a dangerous location. Furthermore, a large room diameter would give the participant a more open experience that more closely mimics actual working place examinations.

From a technical perspective, stereoscopic stimulus presentation has been shown to provide significant improvements in only close task performance [5]. A static, monoscopic scene is sufficient because the large distance scale reduces the necessity of scene movement and perspective changes. Projection on larger screens offers a wider field of view that may increase peripheral awareness; this, while often linked to movement, allows us to understand scene context and is an important aspect of immersive environments that can play a role in search tasks [5, 6]. Furthermore, large screens have been shown to be just as effective as head-mounted displays and do not incur the technological restrictions [7]. Nevertheless, the importance of realism with respect to the task complexity and transfer still plays a key role [8]. Higher-resolution imagery has also been shown to increase search task performance; for this reason, high fidelity images were selected [9]. Finally, panoramic images are more deployable as they can be easily integrated into possible training products without extensive software development or hardware requirements. These factors make a large display of static 360° panorama images an appropriate choice.

The stimulus environment consists of a 360° panoramic theater roughly 10 m in diameter with a screen height of three meters. The screen is a polyvinyl material stretched over a steel tubular frame creating a parabolic toroid, where the mid-screen distortion is about 14 cm pulling inward toward the center of the space. The screen is coated with a silver, high-gain, retroreflective material to maintain polarization of incident light so that it can be used for passive stereoscopic viewing. Imagery is front-projected onto the surface from six 1920 × 1080 pixel projectors (Titian 1080p 3D, Digital Projection, Kennesaw, GA) mounted above the screen. The projected images are configured with a 10 % overlap. The setup also includes an array of 10 motion capture cameras (T20, Vicon, Oxford, UK) to provide real-time tracking and precise motion capture capabilities. Eye tracking is

accomplished using SensoMotoric Instruments' (SMI) Eye Tracking Glasses (ETG) 2.0 (Teltow, Germany). Scenery for the system is rendered from a single workstation using in-house applications developed with Unity (Unity Technologies, San Francisco, CA).

2.2 *Review Environment*

The review environment is far less critical to the results of the study. However, maximizing participant engagement and image visibility is preferred. For this reason, a large powerwall setup was used that afforded a large high-resolution screen. The powerwall is a curved panoramic screen along one wall of a 10×10 meter room. The screen is approximately eight meters wide by three meters tall with a 50° curvature. The screen construction is similar to that of the stimulus environment where the screen is a coated silver, high-gain, retroreflective polyvinyl material stretched over a steel tubular frame. Imagery is front-projected by three Titan SX+ 3D projectors (Digital Projection, Kennesaw, GA) to provide a seamlessly blended 3182×1050 pixel image.

3 Panoramic Images

3.1 *Image Acquisition*

The panoramic images were captured at four locations at a typical surface stone operation: pit, plant, roadway, and shop. The images included both physically staged and digitally edited hazards. In order to accommodate the stimulus virtual environment and ensure as immersive an experience as possible, image composition and environmental conditions needed to be considered.

To ensure that images looked and felt realistic to the participants, the camera height, orientation, and position needed to be selected appropriately. First, the camera height was set to a reasonable standing height in order to give the participant a realistic perspective of the scene. The approximate eye height of the 50th percentile male—64.5 in.—was chosen in order to minimize the overall error of all the participants [10]. Since the stimulus environment had a level floor, it was also important to ensure that the camera was level on the tripod to maintain correct perspective. Similarly, in order to guarantee that near-field objects appeared to be the correct size in the image, they needed to be at least five meters away from the camera. Objects closer than that would be perceived as too large, and they would break the immersion; this is because the screen was five meters away from the participant in the stimulus environment. The 10-m diameter screen provides subjects with an open feeling, but limits the camera placement for more enclosed

locations such as the shop. Given that this requirement was not possible to meet in all instances, the perspective distortion was minimized by positioning the camera close to only large plain surfaces such as a wall or cabinet while maintaining the desired distance from all other salient objects and hazards within a scene. To ensure that the hazards would be present in the final cropped image, the camera was positioned such that the objects required to be in the scene were within $\pm 15^\circ$ of the camera vertically. Finally, to verify the accuracy of the projected panoramic images, the location and size of key objects were recorded. A laser rangefinder (Elite 1 Mile Arc, Bushnell, Overland Park, KS) was used to measure distance and inclination of objects. Inclination measures were used to ensure that objects were scaled properly in the vertical dimension and were located at the same inclination as represented in the actual setting. Object size was measured with a Digital Laser Distance Measurer (DLR165, Robert Bosch LLC, Farmington Hills, MI).

Changing environmental conditions and lighting were additional challenges to the realism and image quality of the panoramas. Flat, overcast lighting conditions would have been ideal to ensure even, well-lit scenes, but due to mine site availability, this was not always possible. The camera settings were optimized to minimize these effects as much as possible. The panoramic images were captured using a Nikon D3X (Tokyo, Japan) camera in conjunction with a GigaPan Epic Pro (GigaPan Systems, Portland, OR) mount. The GigaPan was configured to capture 180° vertically and 360° horizontally with an overlap of 30 %. With the fixed focal length of 14 mm, this amounted to 4×5 images, respectively, for each location. The aperture was set at f 5.6 to give sufficient depth of field for all images. The ISO was manually set for each location, where the ISO values ranged from 400 to 1600. The shutter speed was also manually adjusted depending on location and lighting, where inside shutter speeds were between 1/40 and 1/160 of a second and outdoor speeds ranged from 1/160 of a second to 1/3200. Shutter speeds in all conditions were fast enough to prevent workplace vibrations from interfering with the image quality. The camera was also configured for an exposure bracketing of three, where three exposures were taken for each image at \pm one exposure value step.

3.2 Image Editing

To create the panoramic images, the corresponding 20 images for each shot were imported into PTGui (New House Internet Services B.V., Rotterdam, The Netherlands), a panoramic stitching software. PTGui automatically assigns control points to align adjacent images and blend them into a seamless panorama. If the software encounters problems in matching adjacent features, these require user intervention was necessary. Some images required manual alignment using the control points due to a lack of unique detail. Objects in motion (i.e. people, vehicles, moving equipment, clouds) caused most issues. In these instances, masking was used to delete the objects in motion so that they only appeared in one of the

shots. The camera lens setting in the software was set at normal lens (rectilinear) and the final stitched panoramas were saved using equirectangular projection.

Adobe Photoshop (Mountain View, CA) was used for all the post-processing of the panoramas. Any additional lighting, contrast, and color issues were resolved, including the removal of image artifacts left by the camera such as lens flare. To keep the mine site anonymous, identifiers such as company signs and logos were removed from the panoramas. Although many hazards were staged and set up on the spot during the initial photo taking, several of the hazards could not be created at the site due to time, safety concerns, or other constraints. Therefore, hazards were digitally added into the panoramas during the editing process by additions or subtractions.

4 Stimulus Display

4.1 Calibration Setup

Spatial references were created for the display and motion tracking systems by creating a removable calibration plate at the center of the stimulus environment (see Fig. 4) and placing fixed reflective markers at various horizontal and vertical viewing angles with respect to the calibration plate origin. The calibration plate provided a repeatable, fixed origin and axes for calibrating the motion tracking system and aligning the projected images. The plate has three short pins that slip into holes drilled into the concrete floor. The plate was designed to catch the flanges on the standard Vicon active calibration wand to set the origin of the motion tracking system. A self-leveling laser level (HVL 100, Pacific Laser Systems, San Rafael, CA) with a 360° horizontal beam, two vertical beams at 90° angles, and a vertical plum beam was used to align the projection images with the calibration plate and fixed reflective markers. The fixed reflective markers consisted of a reflective sticker that was masked to the width of the laser beam to allow quick alignment of the laser level; these points were surveyed in using a Topcon QS-3R Robotic Total Station (Tokyo, Japan). The markers were placed above the screen and behind the screen door to provide absolute reference points every 15° for the vertical beams and every 5° for the horizontal, respectively. The laser level was set on a tripod with the plum beam centered on the calibration plate origin and aligned with the fixed markers. A texture map of a grid pattern with a 1° horizontal and vertical spacing was created to be used as a guide for aligning the projected images with the laser level beams during the image warping and blending calibration.

Image warping and blending was accomplished via a 3D Perception (3DP) display processor using Compact Designer (Orlando, FL). A 7 × 7 array of control points for each image channel was used to adjust the location of projected images on screen. Because the system does not have an array of alignment sensors,

adjustment to the warp and blend calibration must be done manually. In order to ensure the best calibration was achieved in the central area of the screen, the laser was first set to eye height and moved out from there. The 3DP display processor controlled the blend regions of all six projectors as well. The pixel alignment of the overlap and gamma alpha adjustment was changed for each blend region in order to achieve a seamless blend between projection images. This process was not only manual, but subjective as well, since no good metric was available for blend control. The circular shape and retroreflective coating on the screens made blending the projectors especially difficult because of the directional dependence. One must be sure to manipulate the blend settings from the viewing area. Due to ambient vibration and system drift despite the projectors being mounted on an independent structure, the system required daily calibration prior to use. In the development of this routine, it was also discovered that the projectors suffer from thermal drift and needed to warm up for at least an hour prior to image calibration.

To ensure proper color balance between projectors, a spectroradiometer (SpectraScan 650, Photo Research Inc., Chatsworth, CA) was used to measure color values for each projector. Measured X and Y values of red, green, and blue were used to calculate target RGB values used to calculate target RGB reference values based on an algorithm supplied by the projector manufacturer, Digital Projection. The reference values were directly used by the Titan projector processor to better match the color values projected on screen. Additional color balance was also subjectively manipulated using color and gamma adjustment layers via 3DP's Compact Designer. Color manipulation via Compact Designer was preferred over direct projector settings because it provides real-time feedback to the user as adjustments are being made.

4.2 Screen Survey

Following the development of the calibration procedure, a topographical survey of the stimulus environment's screen was performed using the Topcon Robotic Total Station. A total of 648 survey points were collected on the screen using a grid pattern, measuring every five horizontal and vertical degrees visible on the screen and along the edge of the buffer regions above and below the panoramic images (Fig. 1). The survey allowed for a validation of the calibration routine, such that the pixel error was no greater than five pixels in any location and was lower than two pixels on average.

4.3 Stimulus Cropping and Alignment

In order to generate seamless stimuli that perfectly match the visual field that the participant would have seen if standing in the original panorama location, the



Fig. 1 Photo depicting the wrap point of the stimulus display. As shown on the image, the panorama coordinate space begins at the lower left of the panorama, with the x (*horizontal*) and y (*vertical*) axes running from (0,0) at the bottom left to (1,1) at the top right. Also shown is the buffer region above and below the image, which exists to ensure the panoramic image is uniformly level on the top and bottom, despite any small variations in screen height and projection region

projected image needed to precisely match both the relative bearing and inclination where the image horizon line matches the participant's eye height. Because the top and bottom framing of the images could not be reliably controlled when exported from PTGui, additional panoramic test shots were collected at each location including three marker staffs, as depicted in Fig. 2, placed around the scene. Eye height was determined by matching background features at the same y -pixel value with the red tape mark. The marker staffs also contained black tape marks every two feet that were similarly used to verify object scale and distortion.

Given the located eye height position, the equirectangular source panoramic images acquired from PTGui were then down-sampled to 12288 pixels horizontally, while maintaining the aspect ratio. The resolution was chosen to exceed the display system's resolution, preventing aliasing, and to keep the texture within typical hardware limits. The vertical crop was positioned to align the image eye

Fig. 2 A section of a test shot containing a marker staff with eye height marked in *red* and every two feet marked with *black tape*. Features on the same pixel level (*white dashed arrow*) allowed researchers to vertically align images to these landmarks in the final image



height 64.5 in. above the floor. Because the floor of the theater was not perfectly level, all screen height measures were referenced to the eye height horizon. A black mask was added to the top and bottom of the images near the limits of the vertical projectable area. These masks precisely control the top and bottom of the stimulus image relative to other screen measures, and conceal blend artifacts at the corners of the projector overlaps (Fig. 2). Given the surveyed grid pattern with eye height correctly located, it was determined that the top and bottom masks should be positioned at 17.5° and -16.7° from eye height, respectively. The resulting resolution of the panoramic image was then calculated to be 12288×1160 , with a masked resolution of 12288×2048 to ensure full coverage.

4.4 *Stimulus Rendering*

Presenting stimuli within the stimulus environment requires more than simple image rendering, despite the panoramas being two-dimensional. The six-projector cylindrical display requires the image to be mapped onto an ideal cylinder and rendered for each projector. The rendered images then were passed to the 3DP display processor in order to map the image to the actual calibrated screen geometry. To create the image for each projector, in Unity, six cameras were generated and positioned inside the ideal cylinder to match the overlap of the projectors. The cropped and masked image was split into six 2048×2048 images that were then mapped on the ideal cylinder.

5 Synchronization

The data acquisition (DAQ) setup for the current study involved communication and synchronization between various systems. In this case, an in-house developed LabVIEW program was used to facilitate the study progression and synchronization of all data elements, including wired and wireless DAQ devices, optical motion tracking, video, eye tracking, and the stimulus display. The DAQ devices and motion tracking system had built in synchronization mechanisms that were handled via hardware triggers.

Because of the unpredictable drift of oscillator clocks used in computers, a simple one-time sync was not sufficient [11]. Clock drift was of particular importance in this study because oscillator clocks are notoriously sensitive to temperature changes such as that experienced by the eye tracking laptop used in this study, as it was semi-enclosed in a backpack [12]. Therefore, LabVIEW and the eye tracking laptop (X230, Lenovo, Morrisville, NC) were synchronized by calculating the clock offset before and after each two-minute stimulus trial. A simple two-way message paradigm was used that required 25 samples with 150 ms between each sample,

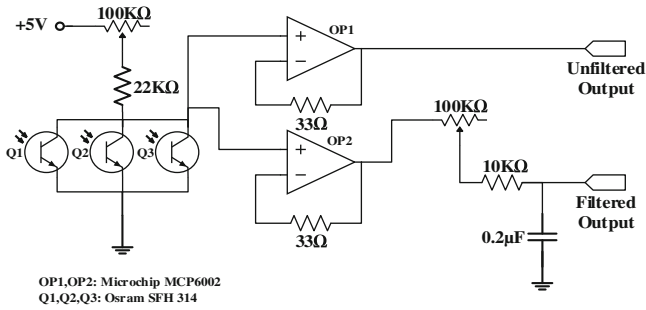


Fig. 3 This schematic drawing shows the circuit used in the photosensor. The circuit has an array of three phototransistors that, when exposed to light, pull the voltage at the collector towards ground. The signal is buffered by two op-amps, the output of one is then filtered through a low pass RC filter, and both outputs are recorded by an analog DAQ

discarding samples with a round trip time over seven milliseconds in order to eliminate any bad packets or network errors.

The display hardware, the rendering software, and the triggering mechanism used to display the panorama all have inherent latency. These fixed and variable latencies had to be accounted for to accurately determine when and how long a scene was displayed. To accomplish this, a photosensor device (Fig. 3) was mounted in the path of the light from the projector, and the output was wired to an analog DAQ (NI USB 6210, National Instruments, Austin, TX). The photosensor device consisted of several phototransistors biased with resistors to match the lighting conditions in the room and the light produced by the projector, such that when the stimulus was displayed, the voltage supplied to the DAQ would go low. Due to the digital light processing (DLP) projectors, the light produced was not continuous but rather pulsed, and two approaches were used to account for this. The output from the phototransistors was first buffered through two op-amps in a voltage-follower configuration, and one of the two outputs was then filtered through a resistor-capacitor low pass filter. The other output was sent directly to the DAQ, and both samples were recorded during the study. This allowed for the use of the analog filtered value directly, or analyzing the raw, photosensor data digitally to look for changes in peak value over a window.

To ensure that a good quality signal was supplied to the photosensor, it had to be mounted directly in the path of light from the projector to the screen, and the image projected on that portion of the projection needed to be of sufficient intensity to distinguish it from the background noise and ambient light between trials. To accomplish this, the photosensor device was mounted in the overprojection region of the projectors above the screen. Rather than fully mask this area as would normally take place, a white section of image was aligned with the position of the photosensor such that whenever time-critical stimuli were displayed, the photosensor would experience a strong transition from black to full white, thus encoding the stimuli start and stop.

6 Gaze Mapping

In order to combine the head position and eye tracking data, several systems needed to be synchronized and calibrated (Fig. 1 and Fig. 4). For future analysis, all systems had their clocks synchronized at multiple points during the study in post-processing by the methods described above. However, final gaze data in panorama space was needed for the debrief process immediately after stimulus data collection. Therefore, a simple real-time collection process was used for the first pass. Data from the eye tracking glasses was streamed over the network to the control computer that was recording the motion tracking and reaction time data, and everything was written out to a single file as it was received. While this did not account for differing latency between the eye and motion tracking systems, the fact that the latency was less than the fixation duration (75 ms) made it sufficient for debrief purposes.

In order to transform gaze data into panorama space, a static calibration was needed to create a reference between the two local coordinate systems. Functionally, this process was completed in two steps because the eye data and the motion tracking data were housed on separate hardware systems. Generally, the calibration accounted for both the orientation of the glasses relative to the participant's face (q_{etgCal} and q_{fwdCal}) and the orientation of the glasses rigid body in motion tracking space (q_{mtCal}). The static calibration was performed as the subject looked directly at a fixation + on the screen. Because the rotation from ETG space (physical coordinate system of the glasses) to local glasses space (local motion capture coordinate system) were separate during the static calibration, an arbitrary

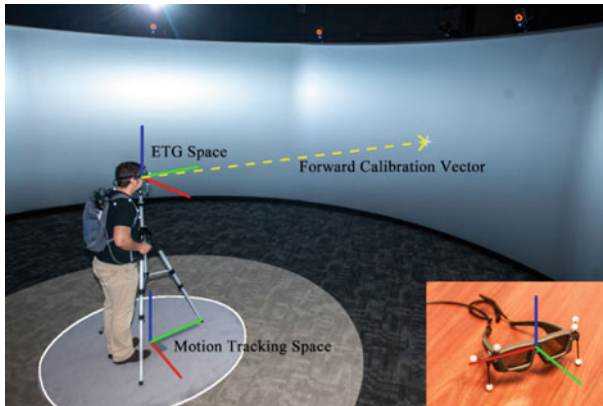


Fig. 4 Photo showing the calibration experimental setup. The participant stood in a fixed location at the center of the room with his or her head stabilized by a chin rest, while fixating on a + marker displayed on the screen. The forward calibration vector, used for calibration, is also shown (*dashed yellow line*). A close-up of the eye tracking glasses is shown (*lower right*). The *light gray, carpeted area (highlighted in white)* shows the movement area in which the participant was allowed to move freely

unit-y vector was chosen as a temporary calculation point. The two rotations were then defined as \mathbf{q}_{etgCal} , the rotation of the averaged ETG gaze vector during calibration to unit-y, and \mathbf{q}_{fwdCal} , the rotation of the unit-y to the normalized forward calibration vector ($\hat{\mathbf{v}}_f$), defined in Eq. 1 below.

$$\hat{\mathbf{v}}_f = \|\mathbf{p}_{fix} - \bar{\mathbf{p}}_{mtCal}\|. \quad (1)$$

where \mathbf{p}_{fix} is the static position of the fixation cross in global motion tracking space, and $\bar{\mathbf{p}}_{mtCal}$ is the average position of the origin of the eye tracking glasses in motion capture space during the static calibration. The rotation of the local glasses coordinate system in motion tracking space (\mathbf{q}_{mtCal}) was calculated as the average rotation of the rigid body during the static calibration. Figure 4 depicts these coordinate systems for clarity. The gaze vector in motion tracking space (\mathbf{v}_{gaze}) was computed for every ETG vector (\mathbf{v}_{etg}) during the trial as expressed in Eq. 2, where the correct vector was lastly rotated by its current orientation in motion tracking space (\mathbf{q}_{mt}):

$$\mathbf{v}_{gaze} = (\mathbf{q}_{mt}\mathbf{q}_{mtCal}) \left(\mathbf{q}_{fwdCal} \left(\mathbf{q}_{etgCal} \mathbf{v}_{etg} \mathbf{q}_{etgCal}^{-1} \right) \mathbf{q}_{fwdCal}^{-1} \right) (\mathbf{q}_{mt}\mathbf{q}_{mtCal})^{-1} \quad (2)$$

The next step in the process was to compute where on the screen the subject was looking. This was made more complex by the fact that the screen on which the image was projected was not a flat surface or a perfect cylinder, but an irregular parabolic toroid that flattens out as it approaches the door. Due to the irregular nature of the screen shape, a simple equation did not prove sufficient in mapping the projection surface. Instead, a mesh was created using the topographic survey points (see Sect. 4.2 Screen Survey); this allowed for a raycast to be performed to compute the screen position. The mesh was extended vertically beyond the survey points so that data would still be available when the subject was looking above or below the screen. A simple ray/triangle intersection test was then done using the origin and ray from the previous step to compute, in motion tracking space, where on the screen the subject was looking.

Given the ray intersection position in motion tracking space on the screen where the subject was looking, one final computation needed to be done to determine the panorama position in the panorama space (Fig. 1). This was made somewhat simpler by the fact that the projection system was calibrated to produce a near-perfect cylindrical image from the center of the room at eye height. Given a point on the screen, the vector from the center of the room to that point could be used to determine what portion of the image was projected onto that point by treating the screen as if it was a perfect cylinder. For the horizontal axis, this was the rotation of the gaze vector around the center of the room offset by the location of the origin of the panorama space with respect to the motion tracking space. The rotation was then normalized to [0, 1]. For the vertical axis, only the vertical height of the physical point was needed, which linearly maps to the vertical position in the panorama normalized to [0, 1]. Values below zero and above one are still allowed, but these values indicate a position outside the panoramic image.

7 Region of Interest Hit Calculation

Immediately following the stimulus data collection, the first pass at ROI hits were calculated to facilitate discussion about the hazards within the stimuli images. The debrief software uses the panorama position to compute where the subject fixated during each trial. The fixations were computed according to SMI's dispersion algorithm [13]. Once the fixations were determined, button press times were checked and the last fixation before a button press was used to determine if a hazard was hit or missed. In the interest of both processing time and avoiding false negatives, the hit/miss detection was relatively generous. Three tests were used to determine a hit, if any of them passed, the button press was considered to have identified the hazard. If the button press fixation was within the hit area of two ROIs, both hazards were considered hits. The three tests used to check for a hit were a simple bounds check, distance to vertices, and distance to line segments. All of the hazard ROIs were specified by polygons with a minimum of three vertices. The bounding box of these vertices was first computed and if the button press was within the bounding box, it was considered a hit. The second test found the smallest distance to any of the vertices that made up the polygon. If the distance was below a threshold value (in pixels), it was considered a hit. Finally, the perpendicular distance to each of the line segments was computed and the minimum was compared to the same threshold as the vertex test. If it was below the threshold, the distance was considered a hit. A threshold distance of 150 pixels was used for all hit calculations.

Acknowledgments NIOSH would like to thank Holly Tonini for her help in taking and editing the panoramic images.

Disclaimer The findings and conclusions are those of the authors and do not necessarily represent the views of NIOSH.

References

1. Mine Safety and Health Administration. United States Department of Labor. <http://arlweb.msha.gov/stats/charts/mnm-eoy-2015.asp>
2. United States. Department of Labor: Mine Safety and Health Administration. Program Policy Letter No. P15-IV-01. By Neal H. Merrifield. (2015)
3. Scharf, T., Vaught, C., Kidd, P., Steiner, L., Kowalski, K., Wiehagen, B., Rethi, L., Cole, H.: Toward a typology of dynamic and hazardous work environments. *Hum. Ecol. Risk. Assess. Int. J.* 7(7), 1827–1842 (2001)
4. Stinson, C., Kopper, R., Scerbo, B., Ragan, E., Bowman, D.: The effects of visual realism on training transfer in immersive virtual environments. In: *Proceedings of Human Systems Integration Symposium* (2011)

5. Bowman, D.A., McMahan, R.P.: Virtual reality: how much immersion is enough? *Computer* **40**(7), 36–43 (2007)
6. Gallop, S.: Peripheral visual awareness: the central issue. *J. Behav. Optim.* **7**(6), 151–155 (1996)
7. Patrick, E., Cosgrove, D., Slavkovic, A., Rode, J.A., Verratti, T., Chiselko, G.: Using a large projection screen as an alternative to head-mounted displays for virtual environments. In: *SIGCHI Conference on Human Factors in Computing Systems*, pp. 478–485. ACM (2000)
8. Lee, C., Rincon, G.A., Meyer, G., Hollerer, T., Bowman, D.A.: The effects of visual realism on search tasks in mixed reality simulation. *IEEE. Trans. Visual Comput. Graph.* **19**(4), 547–556 (2013)
9. Ni, T., Bowman, D., Chen, J.: Increased display size and resolution improve task performance in information-rich virtual environments. In: *Proceedings of the 2006 Conference on Graphics Interface*, pp. 139–146. Canadian Information Processing Society (2006)
10. Gordon, C.C., Blackwell, C.L., Bradtmiller, B., Parham, J.L., Hotzman, J., Paquette, S.P., Comer, B.D., Hodge, B.M.: *Anthropometric Survey of US Marine Corps Personnel: Methods and Summary Statistics*. No. TR-13/018. Army Natick Soldier Research Development and Engineering Center, Natick, MA (2013)
11. Sivrikaya, F., Yener, B.: Time synchronization in sensor networks: a survey. *IEEE Netw.* **18**(4), 45–50 (2004)
12. Marouani, H., Dagenais, M.R.: Internal clock drift estimation in computer clusters. *J Comput. Syst. Netw. Commun.* **2008**, 1–7 (2008)
13. SensoMotoric Instruments. *BeGaze Manual*. Version 3.5. (2015)

Interactive Landslide Simulator: A Tool for Landslide Risk Assessment and Communication

Pratik Chaturvedi, Akshit Arora and Varun Dutt

Abstract Understanding landslide risks is important for people living in hilly areas in India. A promising way of communicating landslide risks is via simulation tools, where these tools integrate both human factors (e.g., public investments to mitigate landslides) and environmental factors (e.g., spatial geology and rainfall). In this paper, we develop an interactive simulation model on landslide risks and use it to design a web-based Interactive Landslide Simulator (ILS) microworld. The ILS microworld is based on the assumption that landslides occur due to both environmental factors (spatial geology and rainfall) as well as human factors (lack of monetary investments to mitigate landslides). We run a lab-based experiment involving human participants performing in ILS and we show that the ILS performance helps improve public understanding of landslide risks. Overall, we propose ILS to be an effective tool for doing what-if analyses by policymakers and for educating public about landslide risks.

Keywords Early warning systems · Interactive landslide simulator (ILS) · Landslide risk communication · Feedback · Learning

P. Chaturvedi (✉)
Defence Terrain Research Laboratory (DTRL), Metcalfe House,
Delhi 110054, India
e-mail: prateek@dtrl.drdo.in

P. Chaturvedi · V. Dutt
Applied Cognitive Science Laboratory, Indian Institute of Technology (IIT) Mandi,
Mandi 175001, H.P, India
e-mail: varun@iitmandi.ac.in

A. Arora
Thapar University, Patiala 147004, Punjab, India
e-mail: akshit.arora1995@gmail.com

1 Introduction

Over the past few decades, catastrophic and disastrous effects of landslides have caused extensive damage to life, property, and public utility services world over. Thus, ensuring effective Early Warning Systems (EWSs) for landslides is essential for the survivability of people in case of occurrence of a disastrous event. To be effective, EWSs need to have not only a sound scientific and technical basis, but also a strong focus on people, who are actually exposed to risk. Unfortunately, such risk communication systems only address part of the existing challenge; the other important part being related to the properties of human perceptual-cognitive factors (cooperation; attitude; and effects of economic and educational background) [1–3]. Moreover, recent surveys in developing countries (like India) show only mediocre knowledge and awareness about causes and consequences of landslide disasters among the general public [4–6]. For example, a recent survey conducted in Mandi town of Himachal Pradesh, India, showed a big gap between experts and general public on understanding of hazard zonation maps and probability of landslides [4]. The existence of this gap is problematic because zonation maps, developed by landslide experts, are currently the common medium to communicate the susceptibility of a region to landslides.

An important aspect of EWSs is related to the development, evaluation, and improvement of risk communication, which helps in transferring risk related knowledge (like causes, consequences and what to do in case a disaster event takes place) and warnings in a manner easily understandable to the local community. A promising way of improving existing risk communication among EWSs is via simulation tools (also called microworlds), which are able to integrate human factors in landslide risk mitigation in addition to physical factors. Such simulation tools, and the models they are built upon, could help risk managers since personal experience and the visibility of processes are the two main influencing factors for improving people's mental models about natural disasters. Promising recent research has shown that regular feedback from a system likely provides an effective tool for people to improve their understanding about the system (Dutt and Gonzalez 2011, 2012). For example, research has documented some benefits of repeated feedback in computer-based microworlds in reducing people's misconceptions about Earth's climate [7]. Dutt and Gonzalez (2012) developed Dynamic Climate Change Simulator (DCCS) microworld and used it as an intervention to help participants understand basic characteristics of the climate system [8]. DCCS helped provide feedback to people about their decisions and enabled them to reduce their misconceptions compared to no DCCS intervention. As DCCS-like tools seem to be effective in improving people's understanding on problems, there is a need to develop simulation models that are able to integrate human factors in landslide risk mitigation in addition to physical factors. Such simulation models could be helpful for the risk managers since personal experience and the visibility of processes are the two main influencing factors explaining the content of people's mental models [9, 10].

Furthermore, affect or emotional response to stimuli is seen to influence risk perception and decision making [11, 12]. For example, Finucane et al. [12] have provided the “affect heuristic,” where this heuristic allows people to make decisions and solve problems quickly and efficiently, in which current emotions of fear, pleasure, and surprise influences decisions [12]. According to Finucane et al. [12], the orientation of one’s feelings (negative or positive) could be an effective tool for risk communication [12].

In the present work, an interactive simulation model of landslide is developed for understanding the influence of monetary contributions for landslide risk mitigation. Furthermore, the interactive simulation model is used to design a web-based Interactive Landslide Simulator (ILS) too. The ILS tool is based on the assumption that landslides occur due to the presence of both physical factors (spatial geology and rainfall) as well as human factors (monetary investments made for landslide risk mitigation). Thus, even in the presence of physical factors (which are outside of one’s control), the landslide risk could be reduced by increasing community investments towards landslide mitigation. Beyond considering human factors in the landslide problem, the ILS also models the damages due to the occurrence of landslide events in terms of fatality, injury, and loss of property. It considers how such damages might impact one’s daily income as well as property wealth. In summary, the ILS tool allows participants to make decisions on the landslide risk mitigation, observe the consequences of their decisions (via real-time feedback), and enable participants to try new decisions.

In this paper, we highlight the use of the interactive landslide model as well as the ILS tool in educating the general public about landslide risks. Specifically, we use affect heuristic in the ILS by creating affect-rich feedback to enable people to perceive risks and benefits for investments made against landslides. This will also enable them to develop a deeper causal understanding about landslide disasters and their consequences. Our hypothesis is that monetary contributions against landslides (which is an indicator of improved understanding) will be larger when affective feedback about monetary losses is high compared to low. Based on results of a lab-based experiment involving human participants, we propose a number of benefits of the ILS tool for educating people and for policymaking in terms of generating “what-if” analyses. As part of our outreach activities, we plan to popularize the use of the ILS tool among students in K-12 schools and colleges in mountain areas in India that are prone to landslide risks.

2 Interactive Simulation Model of Landslides

2.1 Interactive Landslide Simulator (ILS) Model

The ILS model focuses on calculation of total probability of landslides (due to natural factors and due to anthropogenic factors, i.e., investments made by people

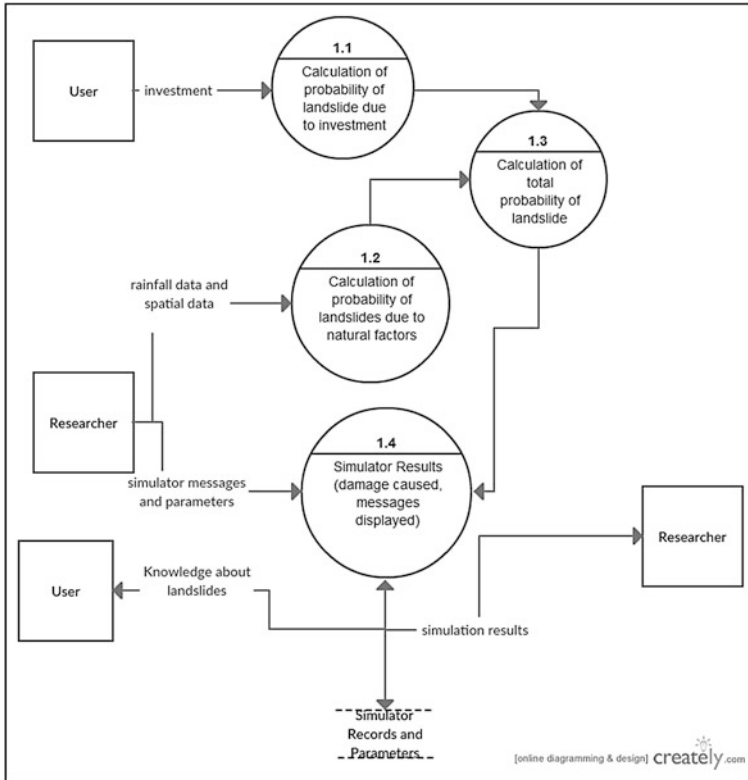


Fig. 1 Probabilistic model of the interactive landslide simulator microworld

against landslides). The model is also capable of simulating types of damages caused by landslides and their effects on people’s earnings.

Figure 1 shows the model of ILS proposed in the present research work. In this model, the probability of landslide is calculated as a weighted sum of probability of landslide due to environmental factors and probability of landslide due to people’s investments. Probability of landslide due to environmental (natural) factors is a combination of probability of landslide due to rainfall and probability of landslide due to slope and soil properties. Model also simulated the losses caused due to occurrence of landslide events.

The Calculation of Total Probability of Landslides.

$$\text{Total probability of landslide} = (W * P(I) + (1 - W) * P(E)) \tag{1}$$

where W is the weight factor, which is between [0, 1]. In the model, W have been assigned a value = 0.8, which indicates that investments against landslides will cause the system to respond rapidly and reduce the probability of landslide.

The total probability formula involves calculation of two probabilities, P(I) and P(E), which is described below:

Probability of Landslide Due to Investment P(I). The calculation used here is based on expected payoff equation used in Hasson (2009) [13], i.e.,

$$P(I) = 1 - \frac{M * \sum_{i=1}^n x_i}{n * B} \tag{2}$$

where,

- B Budget available towards addressing landslide (if a person earns a daily income or salary, then B is the same as this daily income or salary).
- n Number of time periods (days). In the default formulation of the game, n = 60 simulated days, i.e., the game is played for 60 simulated days.
- x_i Investments made by a person at each day i to mitigate landslides; x_i ≤ B,
- M Return to Mitigation, which captures the lower bound probability of P(I) when $\sum_{i=1}^n x_i = n * B$, i.e., people invest their entire daily income in mitigating landslides.

P(I) Probability of landslide after an investment is made.

Probability of Landslide Due to Natural Factors P(E). Natural factors include rainfall, soil type, slope profile, etc. These can be categorized into two parts:

- Probability of landslide due to rainfall (P(T))
- Probability of landslide due to soil type, slope profile etc. [spatial probability, P(S)]

The approach used to calculate both of them is based on a research paper [14]. Equation used for calculation of probability of landslide due to rainfall (P(T)):

$$z = -3.817 + DR * 0.077 + 3 DCR * 0.058 + 30 DAR * 0.009 \tag{3}$$

$$f(z) = \frac{1}{1 + e^{-z}} \tag{4}$$

$$z: -\infty \text{ to } +\infty, P : 0 \text{ to } 1$$

The logistic regression retains the daily (DR), 3-day cumulative (3 DCR) and 30-day antecedent rainfall (30 DAR) as significant predictors influencing slope failure. P(T) = f(z), that is the temporal probability of landslide. The rainfall data was collected as raw data from NASA’s TRMM project, from January 1, 2004 to April 30, 2013.

Now,

$$P(E) = P(T) * P(S) = f(z) * P(S) \tag{5}$$

Damage Modeling. The damage caused can be classified into 3 categories:

- (a) Property Loss
- (b) Injury
- (c) Fatality

All 3 of them have different kinds of effects on the player's wealth and income in the simulator. The data used for calculating probabilities of the above damage has been obtained from Parkash [15]. The stochastic nature of landslide occurrence and damages caused by it have thus also been considered. The exact assumptions about damages are detailed ahead in this manuscript.

2.2 *Interactive Landslide Simulator (ILS) Microworld*

Computer-based decision-making tasks have spread across disciplines and different levels of education [16]. Furthermore, these decision-making tasks have been long used in the study of dynamic decision making behaviour (also called Microworld, see Gonzalez et al. [17]), and many more specialized tasks have been created to provide decision makers with practice and training in organizational system's control; also called Management Flight Simulators [18, 19].

ILS microworld is a computer-based task, where a decision maker's goal is to maximize one's economic level. The economic level (defined by wealth due to income and property in ILS microworld) is influenced by exogenous environment circumstances (spatial and temporal conditions) and the past decisions made by humans. The economic level may decrease (by damages caused due to landslides, like injury, death or property damage) or increase (due to daily income and property wealth). However, the exact functional form governing these increases or decreases was unknown to decision makers. Decision makers could only observe the values that occurred in the previous time period. The level of wealth at time t depends upon the previous time period $t - 1$, a characteristic of dynamic systems called interdependency [20]. Also inherent in dynamic systems are feedback loops, where one observes the effect that one variable has on itself and others. Feedback loops can be positive or negative, "self-reinforcing" or "self-correcting" [21]. Both types of loops are present in ILS because decision makers make repeated investments so as to increase or decrease their economic level.

Figure 2 represents graphical user interface of ILS, which requires a decision maker controlling her economic level and keep it up as much as possible. The economic level is represented graphically as curve of 'Property wealth' and 'Total income not invested in landslides' versus number of times investment decision has been made (since the decision made is one per day the graph is plotted against number of days passed in the simulator). The plot of 'Total probability of landslide'



Fig. 2 ILS microworld graphical user interface [game] (source <http://pratik.acslab.org>)

versus number of days describes the cumulative effect of this variable on probability of landslide. The ‘Game Parameters’ table on the right hand side describes specific values like daily income, property wealth, probability of landslide, and damages due to landslide.

A decision-maker must enter the investment input in the text field specified on top left of the screen. The investment can only be made between zero (minimum) to the player’s current daily income (maximum). Once investment is made, the decision-maker can observe changes in the daily income, property wealth, and damages caused due to landslide [loss of daily income (due to death and injury) and loss of property wealth].

After a decision-maker enters the investment decision and clicks on the ‘Invest’ button, the system provides feedback on whether a landslide occurred or not. If a landslide occurs, then the system decides what kind of damage the landslide has caused and the resulting economic level is shown as a loss via a negative feedback screen (see Fig. 3). If landslide did not occur, however, a positive feedback screen is shown to the decision maker (see Fig. 4). The user can get back to investment decision screen by clicking on ‘Return To Game’ button.



Fig. 3 ILS microworld’s negative feedback screen where a landslide has occurred (source <http://pratik.acslab.org>)



Fig. 4 ILS microworld’s positive feedback screen where a landslide did not occur (source <http://pratik.acslab.org>)

Returning to game causes the player to come back to the main graphical user interface of ILS (see Fig. 2). Once a player has played multiple days in ILS (where the end-point is not known), the interface shows the amount of income and property wealth left at the end of the game. Although ILS is made to capture the dynamics of landslides, the tool can actually be deployed for other natural calamities so long as the geological data related to those calamities is available. Lastly, we have setup ILS as a web-application; therefore, it is accessible anywhere in the world at any time and on any web-browser compatible computing device.

3 ILS Experiment: Testing Affective Feedback in ILS

In order to showcase the effectiveness of the ILS tool, we performed a lab-based experiment where we used ILS with human participants. In this experiment, we manipulated the feedback, i.e., the effect of landslides on a person's income and property wealth using two different conditions: high-affect condition (i.e., high probability of death, injury, and property due to a landslide) and low-affect condition (low probability of death, injury, and property due to a landslide). The expectation was that participants will invest more and improve their understanding about landslides in the high-affect condition compared to the low-affect condition. These conditions and results are explained in greater detail below.

3.1 Methods

Experimental Design. Participants were randomly assigned to one of the two between-subjects conditions: high-affect and low-affect. In both conditions, participants were given daily income and were asked to make daily investment decisions. In high-affect condition, the probability of property damage, fatality and injury were set as 10, 3, and 30 %, respectively. In low-affect condition, the probability of property damage, fatality and injury were 3, 1, and 10 %, respectively. The goal was to maximize the net wealth (coming from property wealth and daily income combined) over multiple rounds of ILS (where the end-point was not known to participants). The nature of functional forms used in ILS were unknown to participants, and participants simply observed the values of the probability of human factors and natural factors and all the damages occurring in an event of a landslide.

The amount of damage (in terms of daily income and property wealth) that occurs in an event of fatality, injury and property damage was kept constant in both the affect conditions. The property wealth decreased to $\frac{1}{2}$ of its value every time property damage occurred in an event of a landslide. The daily income was reduced by 10 % of its latest value in case of injury and 20 % of its latest value in case of fatality loss. The initial property wealth was fixed to INR 2 million, which is the expected property wealth in Mandi district of Himachal Pradesh. The initial daily income of the person was kept 292 INR (taking into account the GDP and per-capita income of Himachal Pradesh, India where the study was carried out). The time duration of the simulation was 30 days (this duration was not known to participants). Weight of human factors in probability of landslide (W) was fixed to 0.8 and that of natural factors ($1 - W$) was fixed to 0.2. The W value was known to participants on the graphical user interface.

We used decision maker's average investment ratio as a dependent variable for the purpose of data analysis. The average investment ratio was defined as the ratio of investment made to total investment possible averaged across all participants and days. On account of Affect heuristic [12], we expected the average investment ratio to be greater in the high-affect condition compared to in the low-affect condition.

Participants. Forty-three participants at Indian Institute of Technology Mandi from diverse fields of study participated in the experiment. There were 20 participants in high-affect condition and 23 participants in low-affect condition to yield a medium to large effect size ($= 0.5$) in our results (for Alpha = 0.05 and a Power = 0.80). All participants were students from Science, Technology, Engineering, and Mathematics (STEM) backgrounds and their ages ranged in between 21 and 28 years (Mean = 23.54; Standard Deviation = 4.08). Twenty-eight participants were Master's students, 5 were Ph.D. students, and 10 were B. Tech. students. When asked about their previous knowledge about landslides, 20 participants mentioned having a basic understanding, 16 having little understanding, 5 being knowledgeable, and 3 having no idea. All participants received a base payment of INR 50 and an additional bonus according to their performance in the task.

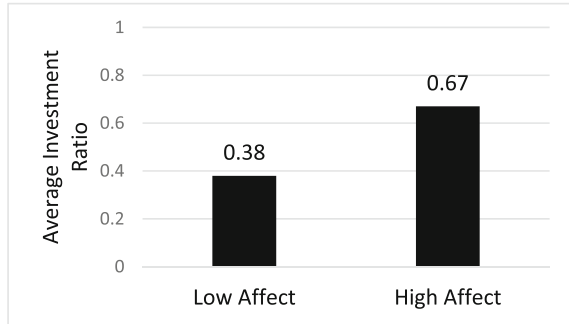
Procedure. Participants were recruited via an online advertisement circulated via an email at Indian Institute of Technology Mandi. Experimental sessions about 30 min long per participant. Participants were randomly assigned to one of the two conditions, and they were given instructions on the computer before entering the ILS microworld. Participants were encouraged to ask questions after reading instructions. Participants were not given any information concerning the nature of environment or conditions in the microworld. They were told that their goal was to maximize their final income and they were then asked to play ILS for 30 days.

3.2 Results

Data were analyzed for all participants in terms of their average investment ratio in both the high-affect as well as low-affect condition. The result was as per our expectation: Average investment ratios were significantly higher in high-affect condition compared to those in the low-affect condition (see Fig. 5).

As shown in Fig. 5, participants had lesser investment ratios in low-affect condition ($M = 0.38$, $SE = 0.05$) compared to those in high-affect condition ($M = 0.67$, $SE = 0.045$) [$t(41) = -4.1$, $p < 0.05$, $r = 0.54$]. Thus, our hypothesis related to affect heuristic was satisfied with these results from ILS.

Fig. 5 Average investment ratio in low- and high-affect conditions



4 Discussion and Conclusions

One way of improving existing risk communication practices for landslides is by training people about these risks via simulation tools. That is because personal experience and the visibility of processes are the two main factors for improving people's understanding and seriousness about natural disasters. Interactive Landslide Simulator (ILS) is an interactive simulation model, which could be used by policymakers to do what-if analyses. ILS can also be used as an educational tool for the general public to increase their understanding and awareness about landslides.

In order to showcase the performance of ILS in improving public's perception towards landslide risk, we conducted an experiment involving 43 students of different educational backgrounds and made them invest against landslides for 30 days in different affective conditions. As expected, the result from the experiment suggested that participants making investment decisions in high-affect condition invested much higher than the participants doing the same task in low-affect condition. This result can be explained by previous lab-based research on use of repeated feedback or experience (Cronin et al. 2009; Dutt and Gonzalez 2011) and affect heuristic (Fischhoff 2001; Finucane et al. [12]. Affect heuristic allows people to make decisions and solve problems quickly and efficiently, in which current emotions of fear, pleasure, and surprise influences decisions. As the emotional feedback is higher in high-affect condition, participants have made higher monetary contributions in this case. Thus, ILS has exhibited success in terms of improving public's seriousness and awareness towards landslide risk. In future, various other system-response parameters (e.g. w or M), feedback (e.g. numbers, text messages and images for damage) will be varied to study their effect on public's decision making. Here, we would like to evaluate affect and its ability to increase public contributions in the face of other system-response parameters.

Other uses of ILS include packaged education material for classroom and workshops that accounts for factors like feedback, affect, and social norms. We believe that such material, when tailored to specific individuals, will help improve decision making of individuals against landslides. ILS tool can be used for

communicating landslide risk in other landslide prone states by customizing the spatial probability (based on geology, soil properties etc.) and temporal probability (based on rainfall) of landslides in such areas. In future, we also plan to use ILS to understand the effects of social norms on people's investment decisions towards mitigation of landslide risk.

Acknowledgments This research was partially supported by Thapar University, Patiala and Indian Institute of Technology, Mandi, India. The authors thank Akanksha Jain and Sushmita Negi, Centre for Converging Technologies, University of Rajasthan for their contribution in collection of human data.

References

1. Basher, R.: Global early warning systems for natural hazards: systematic and people-centred. *Philos. Trans. R. Soc. London A Math. Phys. Eng. Sci.* **364**(1845), 2167–2182 (2006)
2. Meissen, U., Voisard, A.: Increasing the effectiveness of early warning via context-aware alerting. In: *Proceedings of the 5th International Conference, on Information Systems for Crisis Response and Management (ISCRAM)*, pp. 431–440 (2008)
3. Villagran de Leon, J.C., Pruessner, I., Breedlove, H.: *Alert and Warning Frameworks in the Context of Early Warning Systems* (2013)
4. Chaturvedi, P., Dutt V.: Evaluating the public perceptions of landslide risks in the Himalayan Mandi town. Accepted for Presentation in the 2015 Human Factor & Ergonomics Society (HFES) Annual Meeting, L.A (2015)
5. Oven, K.: *Landscape, livelihoods and risk: community vulnerability to landslides in Nepal*. Doctoral Dissertation, Durham University (2009)
6. Wanasolo, I.: *Assessing and Mapping People's Perceptions of Vulnerability to Landslides in Bududa, Uganda* (2012)
7. Dutt, V., Gonzalez, C.: Why do we want to delay actions on climate change? Effects of probability and timing of climate consequences. *J. Behav. Decis. Mak.* **25**(2), 154–164 (2012)
8. Dutt, V., Gonzalez, C.: Decisions from experience reduce misconceptions about climate change. *J. Environ. Psychol.* **32**(1), 19–29 (2012). doi:[10.1016/j.jenvp.2011.10.003](https://doi.org/10.1016/j.jenvp.2011.10.003)
9. Knutti, R., Joos, F., Müller, S.A., Plattner, G.K., Stocker, T.F.: Probabilistic climate change projections for CO₂ stabilization profiles. *Geophys. Res. Lett.* **32**(20) (2005)
10. Wagner, K.: Mental models of flash floods and landslides. *Risk Anal.* **27**(3), 671–682 (2007)
11. Baumeister, R.F., Vohs, K.D., Tice, D.M.: The strength model of self-control. *Curr. Dir. Psychol. Sci.* **16**(6), 351–355 (2007)
12. Finucane, M.L., Alhakami, A., Slovic, P., Johnson, S.M.: The affect heuristic in judgments of risks and benefits. *J. Behav. Decis. Mak.* **13**(1), 1–17 (2000)
13. Hasson, R., Löfgren, Å., Visser, M.: *Climate Change Disaster Management: Mitigation and Adaptation in a Public Goods Framework*, No. 178 (2010)
14. Geosciences Group: *Experimental Landslide Early Warning System for Rainfall Triggered Landslides along Rishikesh-Badrinath, Rishikesh-Uttarkashi-Gaumukh, Chamoli-Okhimath, Rudraprayag-Kedarnath and Pithoragarh-Malpa route corridors, Uttarakhand: Approach document*. http://bhuvan-noeda.nrsc.gov.in/disaster/disaster/tools/landslide/doc/landslide_warning.pdf (2015). Accessed 10 Mar 2016
15. Parkash, S.: Historical records of socio-economically significant landslides in India. *J. South Asia Disaster Stud.* **4**(2), 177–204 (2011)
16. Foss, B.A., Eikaas, T.I.: Game play in engineering education: concept and experimental results. *Int. J. Eng. Educ.* **22**(5), 1043–1052 (2006)

17. Gonzalez, C., Vanyukov, P., Martin, M.K.: The use of microworlds to study dynamic decision making. *Comput. Hum. Behav.* **21**, 273–286 (2005)
18. Paich, M., Serman, J.D.: Boom, bust, and failures to learn in experimental markets. *Manage. Sci.* **39**(12), 1439–1458 (1993)
19. Serman, J.D.: Teaching takes off, flight simulators for management education: “The Beer Game”. <http://web.mit.edu/jsterman/www/SDG/beergame.html> (2011). Accessed 18 Jan 2011
20. Edwards, W.: Dynamic decision theory and probabilistic information processing. *Hum. Factors* **4**, 59–73 (1962)
21. Serman, J.D.: *Business dynamics: systems thinking and modeling for a complex world*. McGraw Hill, Cambridge (2000)

The Human-Systems Integration (HSI) Concept, Applied in an Observation of a Car Crash Simulation

Nelson Matias, Natalha Carvalho, Paulo Sena, Claudia Araújo and Rosinei Ribeiro

Abstract The Human-systems Integration (HSI) is a concept which discusses the relation among several factors that influence and are influenced in a system. Aiming to identify all these factors, a car crash simulation is addressed in this paper, emphasizing all people and tasks involved, categorizing in their respective classifications, discussing how relevant they are during the emergency actions and how important is an integration to guarantee the efficiency and excellence in the rescue process.

Keywords Human-systems integration · Human factors · Accident simulation

1 Introduction

Several scenarios can be observed daily in our society, involving many professionals from different study areas, who apply their knowledge for health and safety. A car crash simulation occurred in September 2015 in Dutra highway, Km 79. All the tasks of emergency represent a small part of a huge system. The concept of

N. Matias (✉) · N. Carvalho · P. Sena · C. Araújo · R. Ribeiro
Faculdades Integradas Teresa D'Ávila—FATEA, Av. Peixoto de Castro,
539 Vila Celeste, Lorena, SP, Brazil
e-mail: nelson.matiaz@gmail.com

N. Carvalho
e-mail: natalhagmcarvalho@gmail.com

P. Sena
e-mail: pssena@gmail.com

C. Araújo
e-mail: claudialysia@gmail.com

R. Ribeiro
e-mail: rosinei1971@gmail.com

N. Matias
Universidade do Estado do Rio de Janeiro—UERJ, Rodovia
Presidente Dutra—Km 298, Resende, RJ, Brazil

Human-system Integration (HSI) applied to this simulation is the purpose of this paper, discussing its aspects.

During the simulation, 150 professionals worked aiming to explain the problems in a car crash accident and how the emergency team acts, as well as the proceedings to attend all people involved; the simulation included a bus that capsized and a crushed car. These professionals were from eight different state and federal organizations, including the Ergonomics Laboratory Anamaria de Moraes (LaErg) from Teresa D'Ávila Faculty such as Fire Department, The Brazilian Federal Highway Police, Military Police, Civil Defense, an Emergency Medical Service company, the private company responsible to manage the highway, Health Department of Sao Paulo and the nursing students from Teresa D'Ávila Faculty [1].

HIS is a strategy that focus on the human performance capability, including cognitive, physical and sensory skills used during the management in a system. The human machine interface applies five systems (Command, Control, Communications, Computers and Intelligence) [2]. It also includes the human factors engineering, personnel, manpower, habitability, system safety, health hazards, human survivability and training [3].

This process aims to identify how the human capacity and requirements can affect hardware and software, considering design and operations and how hardware and software can do the same to human behavior and performance [4]. Optimizing the system performance is its main purpose, once HIS establishes a connection among all the issues involved in a system [5]. The traditional engineering activities rarely are concerned with the end-user needs, assuming an instant acceptance of the new technology, forgetting the human limitations and incongruity with the unforeseen capabilities [6].

Therefore, this paper has as purpose, the discussion about HSI concept in the referred observed simulation, identifying all the approaches, issues and parts of the huge system existing, contributing to the comprehension of this simulation through a participative research.

2 Methodology

The implementation of a HSI process depends on the approaches related to the main system which is discussed, defining the guidelines to generate a Human-systems Integration Plan (HSIP).

Based on a simple structure, the following aspects might be addressed to achieve the objectives and create a HSIP [2]: (i) manpower, which refers to human resources, including both genders, being military or civilian, all required to operate and maintain a system; (ii) personnel, related to the human characteristics needed to optimize the performance, including four areas—cognitive (ability, knowledge), physical (sex, size, strength), psychomotor (coordination) and experience; (iii) training, which is the required knowledge and skills to operate the systems; (iv) human factors engineering (HFE), concerned with the decrease of human error,

during the operation or maintenance of a system; (v) system safety, defined as the inherent ability of a system to be operated, without accidents to personnel; (vi) personnel survivability, referred to the reduction of fratricide, by an individual or a system (e.g. eye and ear protection or microwave detection); and (vii) health hazards, defined as the conditions in the operation of a system that can cause death or reduce job performance.

Among all the issues comprehended, the HFE is one of the most complex, once it integrates several parts of the system. HFE is concerned with reducing the probability of a human error during an operation. Some problems related to HFE are: low light levels, environmental conditions, continuous operations, noise, disruptive wake/sleep cycles, mental overload and physical fatigue [2].

Aiming to comprehend all the activities categories related to HSI, the teams and human costs demanded were also evaluated.

2.1 Human-Systems Integration Plan

The HSIP is a necessary tool to define since the beginning, all the steps to be followed by the team involved in the systems, as well as their respective tasks and how they are concerned with the other elements of the systems. Moreover, these relations is important to mitigate ergonomic and economic problems, reducing unnecessary costs.

Some guidelines are suggested to elaborate a HSIP, as stated below [4]:

- Concept refinement phase: this step is based on the human-centered requirements (intrinsically related to human factors requirements and concepts);
- Technology development phase: HSIP inspection to reflect about the hardware, software and human results, besides specifications, strategies and results;
- System development and demonstration phase: identification of failures inhuman-machine integration. Development of strategies to solve problems; inclusion of latest system specifications, support requirements and analyses of training;
- Production and deployment phase: update HSIP with all the modifications related to system integration, defining the final strategies. This step is important to calculate potential Return on Investment (ROI), when it does exist.

3 Development

To evaluate the importance of this type of simulation, a parallel was traced between the observed accident in Brazil, in September 2015; and another simulation occurred in London, in February 2016; it simulated a subway disaster, involving



Fig. 1 This picture shows the scenario of the simulation occurred near London

eight carriages, and the scene was recreated in a disused power station at Dartford (Fig. 1), in Kent, a region near London [7].

The planning was realized during a period of 18 months, due to the complexity. It was a very important opportunity to London Fire Brigade practice the skills needed in large-scale accidents [7]. It is a part of a £800,000 four-day exercise, involving up to 4000 people, being 1000 of them, injured or killed during the simulation; 250 professionals worked in a temporary mortuary [8].

One of the most motivated events to this simulation was the involvement of the specially trained teams to assist previous accidents, as downing of Malaysia Airlines Flight MH17 in July 2014. As stated by Chief Constable Debbie Simpson, of the National Police Chiefs: “As frustrating as this can sometimes be, especially in a world of fast paced mainstream and social media, we have to be meticulous in our approach to ensure we achieve reliable scientific identification” [8].

In Brazil, the simulation performed was a car crash accident, since this is the main mode of transport in the country (Fig. 2). The venue was the Presidente Dutra highway, Km 79, considered the main road linking the two largest Brazilian cities. Moreover, the region hosts the second largest Catholic basilica in the world, which in October of each year celebrates the anniversary of its patron saint. Thus, there is an increase across highway vehicles, in particular by simulating passage chosen. There is also the presence of pilgrims who flock walk along the banks of the federal highway, increasing the complexity of any intervention on the road.

It is important to emphasize that LaErg was an observer of the simulated event. The Ergonomics Laboratory is located at Faculdades Integradas Teresa D’Ávila. The main LaErg mission is to offer Ergonomics concepts to community. LaErg



Fig. 2 During the simulation, the professionals had to deal with a bus capsized and all the inherent risks

participated in an observation approach, with members who evaluated the scene and took notes about risks and inappropriate postures, as well as other factors associated with human factors.

A comparative table is provided (Table 1), showing data about Brazilian and British events and their numbers, related to people and organizations involved.

Table 1 Comparison between quantitative and qualitative data about simulations

People involved description	Car crash simulation	Subway simulation
Environmental conditions	Side lane highway (operating during the simulation)	Closed metro station
Number of injured(i) and killed(k) people expected	37(i) 1(k) 1:35	1000 1:30
Injured and killed people volunteer	Nursing students—FATEA	Non described
Observation team	LaErg team—ergonomic	7 different countries
Accident vehicles involved	1 interstate bus; 1 private car	8—metro wagon
Total people involved	136	Up to 3000

3.1 *Human-Systems Integration and the Simulation*

Modeling and simulation have offered important methods and tools to support the systems and processes of engineering. “Models and simulations represent a more formal step in human-system design. They can reduce time and data gathering required for functional evaluation by screening alternatives and identifying the critical parameter ranges to rest. [...] Simulations are usually associated with the representation of systems or subsystems, [...] to represent the performance of a person-machine system”. They can reduce team and data gathering required for functional evaluation by screening alternatives and identifying the critical parameter ranges to rest [5].

3.2 *Complexity and Simulations*

Considering all the simulation studies to large scale accidents and the demands on the actors involved, it can be concluded the complexity about creating such events. There are two conditions about the concepts evolution, that is, the stability and instability and to engineering areas and physics existed the necessity to represent the rules and statements in their research activities, creating the following relation [9]:

$$g(f) = f(t) + n(t). \quad (1)$$

In the mentioned relation, ‘g(t)’ denotes a general process, ‘f(t)’ is a determinist component, being liable of predictability and ‘n(t)’ represent the ‘noise’, the unpredictable component, either the process or external conditions, is random, stochastic and chaotic. The model here described was associated with stable systems, which even disturbed, were able to return to their relaxation time. From the Thermodynamics and complexity sciences we can think of more appropriate equations as:

$$q = N(q, V, \alpha) + F. \quad (2)$$

Where ‘q’ is a set of variables describing the system, ‘N’ is a linear function, V represents the spatial derived and ‘α’ is an order parameter control, which describes the impact of the vicinity of the environment. ‘F’ describes fluctuations or noise, which according to Atlan and Prigogine, are necessary sources of growth of organization and complexity [9].

From that point of view we can say that the complex processes, such simulations are considered suitable for preparing the institutions and their representatives, precisely because of nonlinearity, though not necessarily chaotic, and a relationship between human action of those involved and the number of lives saved and

therefore met can be imagined, allowing a previous conclusion about the importance.

On the other hand, when the bus or the metro wagon were arranged in their respective scenarios, they had their positions set from concept or alleged initial action, being an explosion or impact. From that moment, we can say that there was randomness, since the positions were defined and not caused unpredictably. In this case, the picture tends to have a different complexity of that to be found in real accidents. Included in these cases their own communications and movements necessary for the performance of the teams.

Even considering the simulations, still distant of reality, it is undeniable that resemble this. In fact there is an incredible amount involved, especially in the applied products forward the demands and consequently the actions taken, as they may be rethought and changed.

“It’s like every living being was involved in a ‘fictitious bubble’, which is the interface developed by evolution to manage the adaptability and system survival.” The idea here recommended by Uexkull (1992) is called Umwelt, the ‘private universe’ of a living species [9].

Considering the various actors involved in the simulation, it can be assumed that the evolution of models exercised by different people and their institutions, from a critical realism, can generate an evolutionary construction of the Umwelt of those involved [9].

From a General Systems Theory we have the Evolon (Table 2) in which he describes the evolution through a crisis when a system transitions between two consecutive levels of stability [10].

“Instability is inherent in human beings. It reigns disorder, error, ambiguity. The zone of uncertainty between the brain and the environment is also the zone of uncertainty between subjectivity and objectivity, between the imaginary and the real [8].”

Table 2 Evolon steps, as mentioned by Vieira

Disruption or escape	Usually initiated by a combination of internal and external instabilities
Preparation or latent stage	Maximum search system for internal resources, their autonomy
Expansion	Exploration of resources in quantitative prominently finding solutions
Transition	When the best solutions are selected, the search for quality
Maturation	When the system acquires new structure
Climax	Acquisition of complex metastability
Instability	Usually initiated by a combination of internal and external instabilities

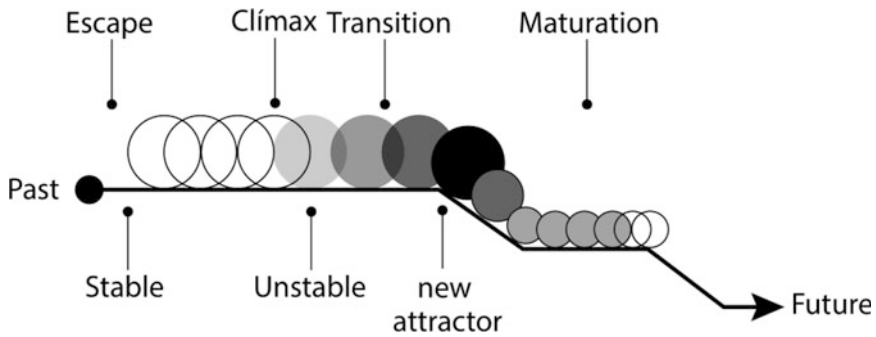


Fig. 3 Evolon proposal: *arrow* could indicate up or down situation

The Evolon (Fig. 3) develops itself through two different types of evolution: Type I, which would be connected to the escape of the level of stability (abandonment of an attractor). At this stage occur the phases of Disruption and Preparation or Latent stage. And Type II, in ‘approach to a new attractor’, comprising the steps of Expansion, Transition, Maturation, Climax and Instability [11].

“There are, of course, an old philosophical question regarding: the if we have access to something that is not phenomenal, i.e. which does not present itself to our sensibility. If not admit more planning that empirical strictly, then it is obvious that only phenomena are considered knowable; such is the thesis of phenomenalism or phenomenism. [...] Realism, however, [...] have to explain to the base of a wider world, though only indirectly knowable. [...] For the realism experience is a fact of class: each unique experience is an event that occurs in the knowing subject, which is considered in turn a concrete system that has expectations, and a body of knowledge with two consequences: deformation and enriching experience [9].”

Considering the approach realized in the Brazilian simulation, we can say that the fact that an assessment has not been conducted with all participants teams after the event important information ceased to be computed for the next simulation. We can say that only teams that had access to post-event data may, in their private worlds, establish new concepts of similar situations.

3.3 *Human-Systems Integration and the Simulation*

Modeling and simulation have offered important methods and tools to support the systems and processes of engineering. “Models and simulations represent formal more step in human-system design”. They can reduce team and data gathering required for functional evaluation by screening alternatives and Identifying the critical parameter ranges to rest [5].

Table 3 Teams evaluation, considering the ergonomic humans costs

	Brazilian simulation	Human costs ^a		
	Ergonomic macro areas	C	P	O
Coordination	Fire brigade	5	5	5
Manpower	Fire department	5	5	5
	The Brazilian federal Hwy police	2	1	5
	Military police	2	1	5
	Civil defense	3	1	2
	Emergency medical public organizations	5	5	2
	Private company responsible to manage the Hwy	4	5	5

^aHuman Costs considering Likert scale from 1 to 5, and level 5 suggests be the most important requirements. C Cognitive; P Physical, O Organizational

“The ultimate goal to be achieved is to live and feel better the world and our integration with the same [...]” [9].

4 Analysis and Results

Quantitative analysis in Table 3 was compiled from the main characteristics of each team and their involvement. At all stages of the simulation of the crash between the bus and the vehicle was certain perceived level interdependence between the different institutions, as when the metal clearance was required for the action of rescuers and firefighters, fitting to the Private Responsible the highway manage this action.

In Table 4 the effective applications of the different classes of HSI Activity Categories were identified. However, the documentation provided by the organizing team is not enough to inform the post simulation activity steps. Perhaps it is the absence of a meeting to discuss the perceptions of all teams involved.

The Simulated Exercise Report issued by the Fire Department has 6 topics: (a) Event Period (Scope), (b) Description of Simulated problem, (c) Held Activity Report, (d) Evaluation of Results, (e) Suggestions and criticisms and (f) Conclusion. Based on the identified steps, the item “d” reports without quantitative information, a disclosure obtained from different media of accidents on the highways. The topic “e” highlights how positive exposure achieved with the TV channels and consequent visibility by society. However, the topics “d” and “e” there is no mention of the comments from the partner institutions, probably due to lack of a conclusive meeting.

Table 4 Activities applied to the car crash simulation. *Y* yes; *N* no

#	HSI activity classes	Y/N	HSI methods
1	Envisioning opportunities	Y	Field observations and ethnography Participatory analysis
2	System scoping	Y	Organizational and environmental context analysis
		Y	Field observations and ethnography
		Y	Participatory analysis
3	Understanding needs	Y	Organizational and environmental context analysis
		Y	Field observations and ethnography
		Y	Task analysis
		N	Cognitive task analysis
		Y	Participatory analysis Contextual inquiry
		Y	Event data analysis—Prototyping
		Y	Models and simulations—Usability evaluation methods
4	Goals/objectives and requirements	Y	Usability requirements methods
		Y	Scenarios—Personas
5	Architecting solutions	Y	Task analysis
		Y	Usability requirements methods
		Y	Work domain analysis
		Y	Workload assessment
		Y	Participatory design
		Y	Contextual design
		N	Physical ergonomics
		Y	Situation awareness
		Y	Methods for mitigating fatigue
		Y	Prototyping
		Y	Models and simulations
6	Life-cycle planning	Y	Usability requirements methods (common industry format)
		N	Risk analysis
7	Evaluation	N	Usability requirements methods (common industry format)
		N	Prototyping
		N	Models and simulation
		N	Risk analysis
		N	Usability evaluation methods
8	Negotiating commitments	Y	Usability requirements methods (common industry format)
		N	Risk analysis

(continued)

Table 4 (continued)

#	HSI activity classes	Y/N	HSI methods
9	Development and evolution	Y	Usability requirements methods (common industry format)
		Y	Models and simulation
		N	Risk analysis
		N	Usability evaluation methods
10	Monitoring and control	Y	Organizational and environmental context analysis
		N	Risk analysis
11	Operations and retirement	N	Organizational and environmental context analysis
12	Organizational capability improvement	N	Organizational and environmental context analysis

5 Conclusion

After the analysis of all results obtained, from different sources and points of view, we can conclude that this type of simulation represents a complex system, addressing several aspects. This integration has to be considered since the planning of the simulation, avoiding biased factors, such as a controlled environment, in which the professionals can be influenced in their activities. With this, the training of the previous knowledge is provided, but not the acquirement of new skills, as psychological control, time control, deal with environmental phenomena, and other factors that instantly affect the whole system.

Considering the approach realized in the Brazilian simulation, we can say that the fact that an evaluation with all participants teams not have been held after the event important information will no longer be computed for the next simulation. Only the teams that had access to post-event report, may in their private universe “Umwelt” establishes new concepts of similar situations.

References

1. G1 Vale do Paraíba e Região: Simulação de acidente com romeiros envolve 150 pessoas na Via Dutra. [Online] Available at: <http://g1.globo.com/sp/vale-do-paraiba-regiao/festa-da-padroeira/2015/noticia/2015/09/simulacao-de-acidente-com-romeiros-envolve-150-pessoas-na-dutra.html> (2015). Accessed 20 Feb 2016
2. Clark, J.J., Goulder, R.K.: Human systems integration (HSI): Ensuring design & development meet human performance capability early in acquisition process. PM, pp. 88–91 (2002)
3. Dawes, S.M.: GSAW workshop: emerging issues in human systems integration (HSI). [Online] Available at: http://gsaw.org/wp-content/uploads/2014/04/s12c_dawes.pdf (2014). Accessed 20 Feb 2016

4. Directorate of Human Performance Integration: Air Force Human Systems Integration Handbook: Planning and Execution on Human Systems Integration. [Online] Available at: <http://www.wpafb.af.mil/shared/media/document/AFD-090121-054.pdf> (n.d.). Accessed 10 February 2016
5. Pew, R.W., Mavor, A.S. (eds.): Human-System Integration in the System Development Process: A New Look. Committee on Human-System Design Support for Changing Technology, Committee on Human Factors, National Research Council. Available at: <http://www.nap.edu/catalog/11893.html> (2007). Accessed 20 Feb 2016
6. Hebel, E.K., McKneely, J.A.B., Rigsbee, S.: The application of human-systems integration: designing the next generation of military global positioning system handheld devices. Johns Hopkins APL Technical Dig. **31**(1), 66–75 (2012)
7. BBC: Tube Disaster Exercise: ‘Tower Collapses into Station’. [Online] Available at: <http://www.bbc.com/news/uk-35686269> (2016) Accessed 3 Mar 2016
8. Morin, E.: O Enigma do Homem: para uma nova antropologia. Zahar, Rio de Janeiro (1979)
9. Vieira, J.A.: Rudolf Laban e as Modernas Ideias Científicas da Complexidade. Encontro Laban, São Paulo (1998)
10. Ramos, M.M.: New Complexities: Photography in Cyberspace (Translated from Portuguese by Bryan Brody, V!RUS, [online]) n. 8. Available at: <http://143.107.236.240/virus/virus08/?sec=4&item=2&lang=en> (2012). Accessed 10 Mar 2016
11. Pilchowski, A.C.: O papel da interatividade/crise na comunicação e criação em sistemas complexos: a ótica do clown. Dissertação de Mestrado em Comunicação e Semiótica, São Paulo (2008)

Digital Human Modeling Pipeline with a 3D Anthropometry Database

Peng Li, Jeremy Carson, Joseph Parham and Steven Paquette

Abstract This paper presents a digital human modeling pipeline with support from a 3D anthropometry database. The database is derived from the 2012 anthropometric survey of US Army personnel (ANSUR II) and provides search capabilities to query traditional anthropometric measurements and three-dimensional (3D) shape. The query results, which contain both measurements and 3D scans, facilitate further digital human modeling tasks. This paper first presents the implementation and functionality of this 3D database, then discusses some digital human modeling tasks relying on the query results from the database.

Keywords Digital human modeling · 3D anthropometry database · ANSURII

1 Introduction

Over the last three decades, there have been a number of large-scale 3D anthropometric data collection efforts around the world. These have greatly broadened the potential of many digital human modeling applications. However, we are still at the early stages of full exploitation of 3D shape data associated with these efforts [1]. The recently completed US Army anthropometric survey (ANSURII) [2] collected 3D scans of the whole body, head/face and feet, in addition to collecting 93 traditional anthropometric measurements from participating soldiers. To enable digital human modeling applications with this rich 3D resource, a database that enables users to query ANSURII data within the traditional anthropometric measurement domain as well as within the 3D shape domain has been developed [3]. In the following sections we introduce the implementation of the database (Sect. 2) and present a number of digital human modeling tasks based on ANSURII data

P. Li (✉) · J. Carson · J. Parham · S. Paquette
US Army Natick Research, Development and Engineering Center,
Natick, MA 01760, USA
e-mail: peng.li.civ@mail.mil

(Sect. 3). Section 4 summarizes some application specific programs for bridging a 3D anthropometric database and digital human modeling tasks.

2 The ANSURII 3D Anthropometric Database

A scientifically sampled working data set from the ANSURII survey contains 6068 subjects, 4082 male and 1986 female, respectively. The design consideration of a 3D anthropometric database is mainly based on two aspects: its contents and its query functions. In the database, the following information is stored for each subject:

- demographics (e.g., age, sex, race/ethnicity),
- anthropometric measurements,
- 3D whole body scan,
- a torso shape descriptor,
- thumbnail image of the 3D body scan.

The database implemented has three major query functions:

1. multiple variable query based on anthropometric measurements,
2. a shape query by example based on a shape descriptor,
3. a shape query by the shape generated from a statistical model (more specifically a model generated from principal component analysis of 3D shapes).

The database is implemented as a web based application as a user can query the database through a web browser. The first query function is based on demographic data and standard anthropometric measurements as shown in Fig. 1. This query is also called a filter search, and will return body measurements and thumbnail images of subjects who meet the query criteria. Users may also display those measurements not included in the query form. Simple descriptive statistics of all displayed

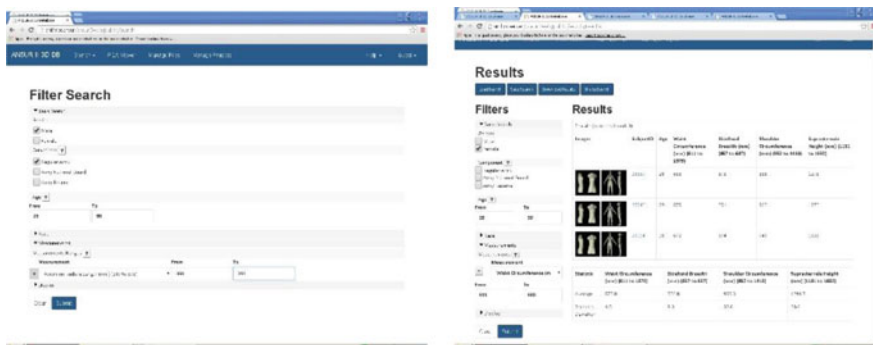


Fig. 1 Query based anthropometric measurements, input screen (left) and results displayed (right)

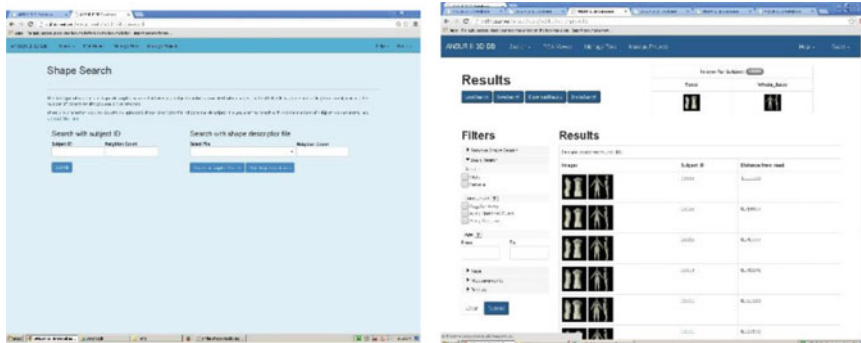


Fig. 2 Search by example input (left) and results displayed (right)

anthropometric variables are presented at the bottom of the results page. All search results include subjects' 3D image (torso and whole body) as a cue for later shape query.

The second query is a torso shape search by example (Fig. 2). Because the torso shape plays an important role in the development and evaluation of personal protective clothing and equipment, we created a separate torso form for each subject in the database. A torso form was extracted from a whole body scan by deleting the arm, leg, and head. The Discrete Cosine Transform (DCT) was then applied to quantify torso shape [4]. Coefficients of the DCT are taken as a 3D torso shape descriptor.

The shape search is based on the similarity of the torso shape descriptor. The users provide a shape example either a subject ID from a previous filter search, where a subject was identified based on standard anthropometry and demography, or a shape descriptor file of a new body scan from an external source. The database returns similar shapes based on their correlation distance to the example shape provided. A user can specify a maximum number of similar bodies to be returned. The search results are sorted by their similarity value in descending order.

The third query form uses a statistically generated torso shape as an example. The collection of torso 3D shape descriptors forms a shape space. We applied principal component analysis (PCA) to this shape space and decomposed the shape variation into a number of principal axes. We selected the first ten principal components (PC) for the shape generator. The ten components account for 77 % of torso variance. For each principal component there is a sliding value from -1 to 1 to control its blending weight for the corresponding extreme shapes chosen from the maximum positive and negative standard deviation (± 3 standard deviations) of that principal component. For example, Fig. 3 shows extreme shapes from the second principal component. The top ten most significant principal components provide twenty extreme shapes as constituent shapes for a shape generator.

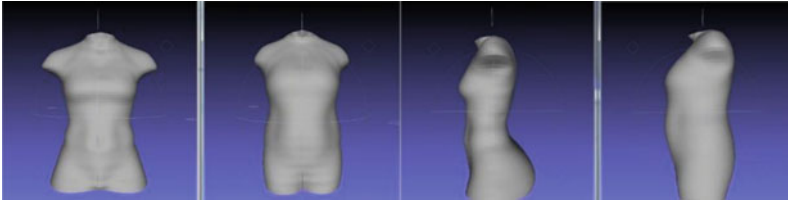


Fig. 3 Extreme shapes of PC2 (front and side view of $\pm 3D$)

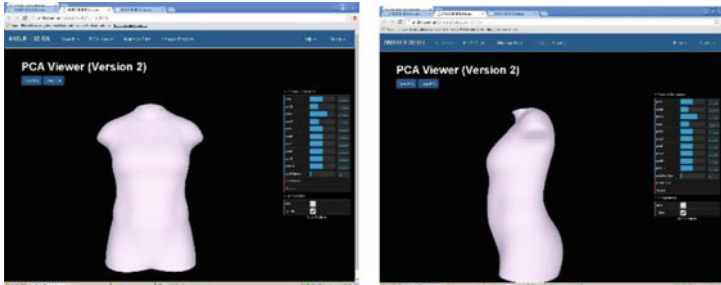
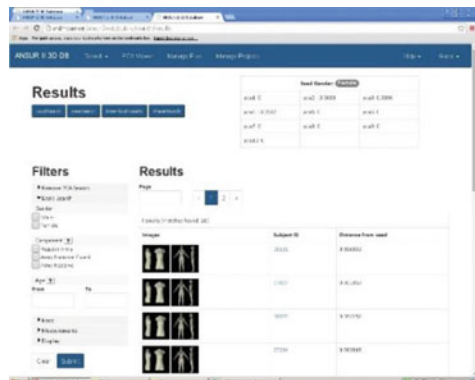


Fig. 4 PCA generated torso shape viewer. Sliders to manipulate the ten PC axis values within a range of ± 3 standard deviations are shown on the *right*

Fig. 5 Search results from PCA generated torso shape



Using an interactive interface to change the weights for selected PCs, we may blend across the constituent shapes derived from PCA. In this way, a user may generate a desired shape and use it to search for similar shapes in the database. The interface of the shape generator is shown in Fig. 4. The search results are shown in Fig. 5. These search results may also be filtered through selected anthropometric measurements.

3 Digital Human Modeling with Support of a 3D Anthropometric Database

The query results from the database include anthropometric measurements and 3D scans of relevant subjects, and can be downloaded to users' local computer. In order to generate digital human models from a number of 3D scans, it is necessary to uniformly re-sample the 3D scans and make a homological mesh structure across the whole data set. The raw 3D scans from the ANSURII survey comprise very dense point clouds with various number of points and void areas. To obtain a clean, uniform, watertight mesh, we applied a surface alignment tool [5] to register raw data into a uniform structure. The result is a watertight whole body mesh with a lower polygon count (low resolution at 11k vertices and 22k faces or high resolution at 43k vertices and 86k faces). The vertices of aligned scans are in full correspondence to each other. Therefore, in the 3D database aligned whole body scans are the only 3D data we export for a query activity.

Digital human modeling tasks around such a 3D database fall into three activities: (1) search for a specific body shape based on anthropometric measurements and generate an average shape (if multiple subjects are identified) from 3D scans as a digital model, (2) with a less restrictive filter search, gather a 3D data set for a larger population and create statistic models for that population, (3) search similar shapes based on a shape example and analyze their anthropometric meaning. A number of application cases are presented in the following sections.

3.1 Creating an Average Female Model for Constructing a Female Thermal Manikin

A 3D female body shape representing the US Army population was requested for making a female thermal manikin. We first chose a population mean of 18 anthropometric measurements as a starting point to query the ANSURII database. With added reasonable tolerance to each measurement, we are able to identify one subject within the population. At the same time, we generated an average female model from 3D scans of all female soldiers in the ANSURII working database and verified that the major measurements of the average shape are consistent with the selected population mean measurements. After comparing the individual scan and the average shape, we chose the average shape as the model for the female thermal manikin because the average shape has an overall smooth surface. An individual scan usually contains some unwanted details, for example, folded soft tissues due to waist band around abdomen area. The average female body surface is then sent to the manufacturer to make a prototype. Figure 6 shows the average female shape from the ANSURII database and the final product for the female thermal manikin.

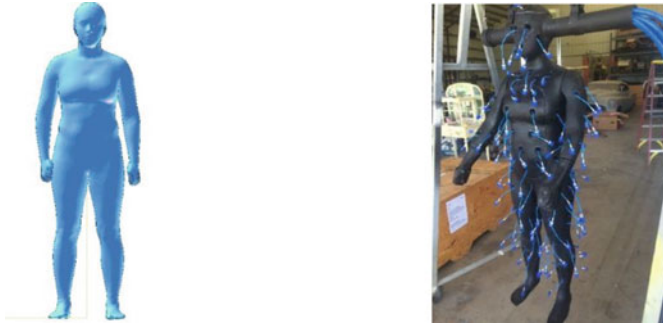


Fig. 6 The average female shape and the thermal manikin

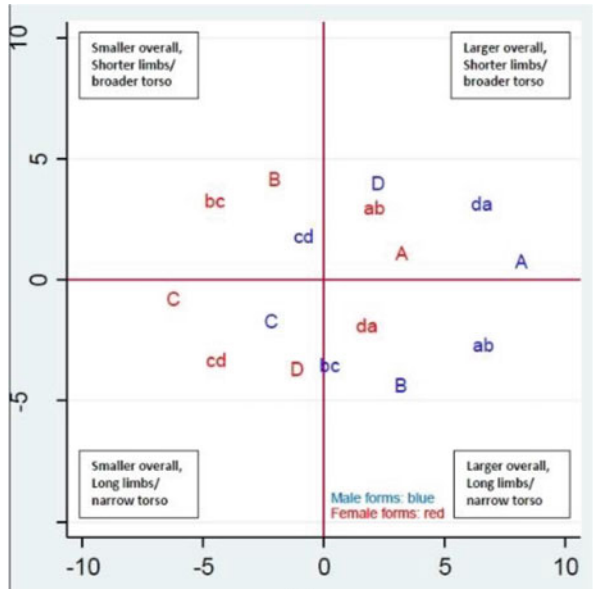
3.2 Boundary Human Models from Principal Component Analysis (PCA)

Creating a set of standard manikins for the development and evaluation of personal protective equipment (PPE) or for the clothing industry is a major outcome of a new anthropometric survey. Through PCA of selected anthropometric measurements relevant to a product, a set of so-called boundary manikins can be specified [6]. In the past, the results of such an analysis process are specifications for making the manikins. Now with a 3D anthropometric database it is possible to generate digital human models directly from the PCA generated specifications, either for a manikin manufacturer or a digital form for computer based design and simulation programs. Recently, researchers in our team conducted PCA on ANSURII survey data for deriving anthropometric specifications for creating digital human models of soldiers in a standing pose [7]. As a result, the analysis identified 27 boundary models for male soldiers and their corresponding nearest 3D scans in the database. Figure 7 shows the physical meanings of some boundary models and their 3D scans (only male model A, B, C, D and middle are shown).

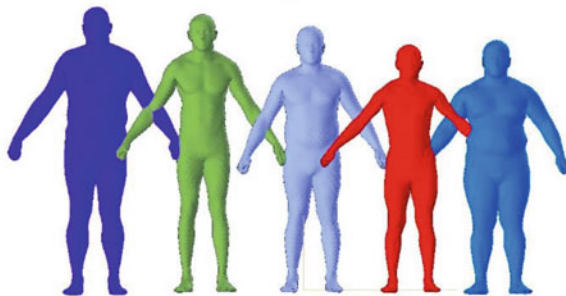
3.3 Shape Analysis of 3D Surface of Body Parts

With a homological mesh structure of 3D scans in the database, one can mark a specific body region (leg, arm, elbow, etc.) on a template as a mask and then obtain the same region from individual scans by applying the region masks for surface trimming. In this way if one is interested in only arm anthropometry and related 3D shapes, he/she can filter subjects with specific arm measurements and obtain arm geometry from exported 3D scans. One such application is to analyze leg shape variation of male soldiers. We create a leg region mask with a plane going through crotch and trochanterion point of the right leg and save all leg surfaces of male

Fig. 7 Physical meaning of boundary models (a) and their 3D scans (b)



(a)



(b)

subjects from the database. The principal component analysis of 3D leg surface revealed eight major principal components accounting for 95 % of the variance. However only the first two components account for dimensional variations and others are related to shape/pose variations (Fig. 8).

3.4 Creation of Digital Human Models in Non-standing Poses

Another application area for digital human modeling is the simulation and evaluation of workplace, cockpit design, etc., where a non-standing pose is usually

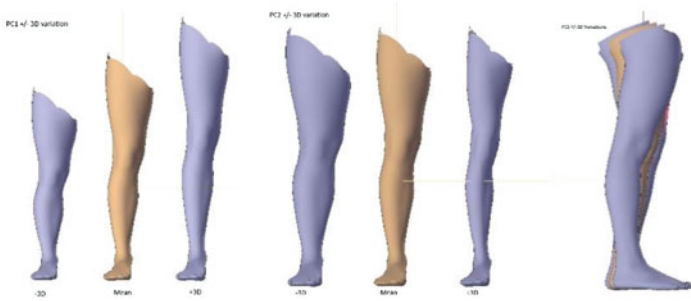
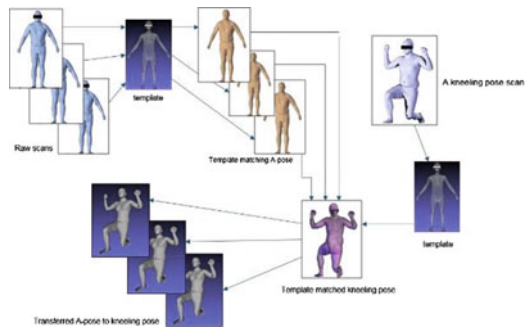


Fig. 8 PC1, PC2 and PC3 of leg shape variations

Fig. 9 Creation of a non-standing pose from a pose parameter mapping



required. Since the ANSURII survey took whole body scans in a standing pose only, if a non-standing pose model is needed, we have to use additional tools to generate the model. One of the tools we used is the alignment tool [5] from Bodylabs. This tool can align a template to a non-standing pose scan and then transfer other template aligned standing scans into the new non-standing pose (we call it pose parameter mapping). In this way, we can analyze shape variation and create models of non-standing poses at the population level without doing actual scanning. For example, we generated bending knee models from 2069 ANSURII standing scans by using the above approach [8] (Fig. 9).

3.5 A Digital Model in Pilot “Hunch” Pose for the Casualty Reduction Analysis

In this application a 3D male body shape representing the US Army population was requested for the creation of a digital human model in a pilot’s “hunch” position or the position pilots use when seated in an aircraft. To identify a mean body shape the ANSURII database was first filtered along several pilot-specific measurements to

best fit the 50th percentile for those respective measurements: e.g. torso length, seated height, arm length, weight. The first group of models was further reduced by finding the model with the closest Euclidean distance to the mean. To synthesize a “hunched” pose for the model, we scanned a subject in the lab in this pose. Using the above mentioned alignment tool in 3.4 the pose parameters were extracted from the new subject and then applied to the model identified during measurement down selection. The new pilot “hunch” model was digitally equipped with several protective components and evaluated for overall protection in the Integrated Casualty Estimation Methodology (ICEM) software suite.

4 Summary of Digital Human Modeling Pipeline

As shown in the previous section, there are many possible applications for query results from a 3D anthropometric database. From the point of view of digital human modeling, the end product is a digital human model. The database itself only contains individual scans of a standard pose. Thus, a number of model generation tools are needed to fill the gap between the database and the required model. Figure 10 illustrates a possible structure for a digital human modeling pipeline.

As we discussed in Sect. 3, these model generation tools include, to name a few, a program to average a group of surfaces, a program to perform principal component analysis on 3D surfaces and generate shapes by adjusting weights of principal components, a program to create surface masks and trim surface with the surface masks, a program to perform pose/shape manipulation, etc. We also anticipate the need to export digital human models to various CAD programs for garment or other product design, human factors/ergonomics evaluation programs such as JACK, RAMSIS, etc.

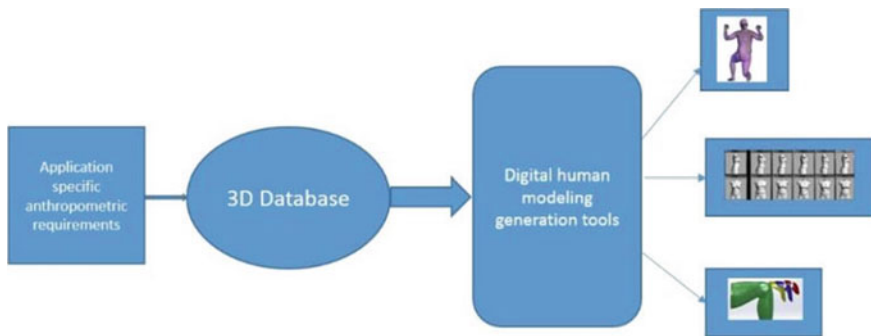


Fig. 10 A structural view of a digital human modeling pipeline

5 Conclusions

The 3D anthropometric database is an important front end for digital human modeling tasks. A 3D anthropometric database provides the basis in the selection of body sizes and shapes for the model generation. The 3D scans stored in a 3D anthropometric database should be in a standardized mesh format, uniformly sampled or template matched with full correspondence, so that it reduces the burden for later application programs. Since the current trend of the implementation of an anthropometric database is a web server based application, it will be difficult to gather all digital human modeling programs into a basket that resides on the server side. The best way is to deliver the query results with standardized 3D scan format to a client program and allows the end users to further process the data.

References

1. Trieb, R., Ballester, A., Kartsounis, G., Aleman, S., Uriel, J., Hansen, G., Fourli, F., Sanguinetti, M., Vangenabith, M.: EUROFIT—integration, homogenisation and extension of the scope of large 3D anthropometric data pools for product development. In: 4th International Conference and Exhibition on 3D Body Scanning Technologies, Long Beach, CA, USA, 19–20 Nov 2013
2. Gordon, C., Blackwell, C., Bradtmiller, B., Parham, J., Barrientos, P., Paquette, S., Corner, B., Carson, J., Venezia, J., Rockwell, B., Mucher, M., Kristensen, S.: 2012 Anthropometric Survey of U.S. Army Personnel: Methods and Summary Statistics. Technical Report NATICK/TR-15/007, US Army Soldier Systems Command, Natick Research, Development and Engineering Center (2014)
3. Li, P., Corner, B., Carson, J., Paquette, S.: A three-dimensional shape database from a large-scale anthropometric survey. In: Proceedings of 19th Triennial Congress of the IEA, Melbourne, Australia, 9–14 Aug 2015
4. Li, P., Corner, B., Paquette, S.: Shape description of the human body based on discrete cosine transform. In: Advances in Applied Human Modeling and Simulation, pp. 169–178. CRC Press, Boca Raton (2012)
5. Hirshberg, D.A., Loper, M., Rachlin, E., Black, M.J.: Coregistration: simultaneous alignment and modeling of articulated 3D shape. In: Computer Vision—ECCV 2012, Lecture Notes in Computer science, vol. 7577, pp. 242–255 (2012)
6. Gordon, C., Corner, B., Brantley, D.: Defining Extreme Sizes and Shapes for Body Armor and Load-bearing Systems Design: Multivariate Analysis of U.S. Army Torso Dimensions. Technical Report NATICK/TR-97/012, US Army Soldier Systems Command, Natick Research, Development and Engineering Center (1997)
7. Parham, J., Gordon, C., Blackwell, C., Paquette, S.: Derivation of the Anthropometric Specifications for the Creation of Digital Human Models for Soldiers in a Standing Posture. Internal Memo, US Army Soldier Systems Command, Natick Research, Development and Engineering Center (2014)
8. Li, P., Corner, B., Hurley, M., Powell, C., LaFleur, A.: Three-dimensional analysis of knee shape for designing a knee-pad. In: 6th International Conference on Applied Human Factors and Ergonomics and the Affiliated Conferences, Las Vegas, USA, Procedia Manufacturing 3, Elsevier, pp. 3689–3693 (2015)

Integrating Heterogeneous Modeling Frameworks Using the DREAMIT Workspace

Walter Warwick, Matthew Walsh, Stu Rodgers and Christian Lebiere

Abstract The history of agent development is a litany of expensive one-off solutions that are opaque to the uninitiated, difficult to maintain and impossible to re-use in novel contexts. This outcome is the unfortunate result of a tendency to apply monolithic “architectures” to agent development, which require specialists to build the models and extensive knowledge engineering and hand tuning to realize adequate performance. To address these shortcomings, we are developing methods to align agent development with best practices in software engineering. In this paper we describe an approach that promotes modularity and learning in the development and validation of intelligent agents. Specifically, our approach enables the modeler to decompose intelligent behavior as required by the problem (rather than the modeling environment), implement component behaviors using the tool best suited to those requirements and close the data loop between agent and environment early in the development process rather than as a post hoc validation step.

Keywords ACT-R · Diffusion model · C3Trace · Intelligent agents · Cognitive architectures

W. Warwick (✉) · M. Walsh · S. Rodgers
Tier1 Performance Solutions, 100 E Rivercenter Blvd., Suite 100,
Covington, KY 41011, USA
e-mail: w.warwick@tier1performance.com

M. Walsh
e-mail: m.walsh@tier1performance.com

S. Rodgers
e-mail: s.rodgers@tier1performance.com

C. Lebiere
Psychology Department, Carnegie Mellon University, Pittsburgh, PA, USA
e-mail: cl@cmu.edu

1 Introduction

Three fundamental lessons can be learned from the history of intelligent agent development:

First, the development and maintenance of intelligent agents and systems is very expensive. The cost of developing a model of a “moderately complex task” has been estimated at 3.4 years and \$400,000 [1]. This does not include the follow-up costs of upgrading the model as the systems it interacts with change. The problem is exacerbated by the fact that there are so few experts capable of building such models [2], and that the original designer is often the only one with the knowledge required to change the model.

Second, agent modelers have not always been willing to use the right tool for the job. Given its roots in cognitive science, the development of intelligent agents has often been pursued as an exercise in theory confirmation. Thus we see long-standing debates between, for example, connectionist and rule-based systems and the emergence of monolithic architectures as the theoretically preferred method for modeling behavior. The predictable result is a litany of one-off solutions, implemented in pet architectures, that are opaque to the uninitiated, difficult to maintain, and impossible to reuse in novel contexts. The more promising alternative is to acknowledge that many modeling formalisms exist, and that each has distinct strengths and weaknesses [3].

Third, knowledge engineering alone cannot support robust, sustainable agent development. Intelligent agents must also possess a mature capacity to *learn from experience*. Though some up-front knowledge engineering is needed, a truly intelligent agent must possess learning mechanisms to acquire the vast amounts of knowledge needed to accomplish complex tasks, and to cope with the non-stationary environments they face [4]. The psychological science community has identified learning in various forms as a core desideratum for a theory of cognition [5].

We see these lessons as underscoring the need for a *fundamentally different approach to intelligent agent development*. We maintain that the high cost of agent development is inexorably tied to (1) the tendency to apply monolithic solutions to agent development, and (2) the tendency to hand-tune knowledge representations in agents. We consider these points in turn.

1.1 Monolithic Solutions

All architectures come with a host of theoretical and methodological commitments. While these provide genuine leverage in some cases, they come at a cost. Not every aspect of intelligent behavior is performed equally well within any single architecture [3, 6]. For example, an architecture adept at pattern recognition may be less well suited to represent goal-oriented problem solving, and vice versa. Forcing the architecture to fit the behavior inevitably leads to a convoluted solution. Likewise, the same intelligent behavior may be represented at different levels of fidelity in

different architectures [7]. For example, one model may treat speed and accuracy as free parameters (e.g., *mean response time* and *probability of correct response*), while another may treat speed and accuracy as dependent measures produced by a series of intervening steps that represent the fine-grained detail of cognition. The high fidelity supported by such heavy machinery is sometimes needed to produce intelligent behavior. However, lower-fidelity solutions should be used when possible to reduce unnecessary pain and expense in the development process and improve computational efficiency and conceptual transparency.

1.2 Hand-Tuned Knowledge Representations

The capabilities of existing rule-based systems are well established [8]. Yet developing such systems is still difficult and costly. In particular, knowledge acquisition from subject matter experts can be costly and time consuming (cf. the knowledge acquisition bottleneck; [9]). An alternate approach is to incorporate learning mechanisms in intelligent agents. Intelligent agents trained using machine learning techniques can perform as well as—or better than—manually designed systems [10]. The main limitation of this approach is that machine learning techniques sometimes require prohibitively large training datasets. This has led researchers to incorporate some degree of knowledge engineering to create structured representations that tame the complexity of a domain, while providing the agent with experiences to learn from. This hybrid approach enables more economical design and greater adaptability than a pure rule-based approach, and it allows the agent to achieve expert-level performance using orders of magnitude fewer training examples than a pure machine learning approach [11].

2 The Approach

To overcome the shortcomings of the traditional approach to agent development, we are exploring novel methods predicated on three key ideas.

The first is to allow the development of component models using different modeling formalisms (Fig. 1). Component models can represent any one of the wide variety of human behaviors that underpin intelligence—from perception, through cognition, to action. The models are *basic* only in that they represent isolated processes; they potentially map to all levels of behavior. Examples include component models of vision, auditory processing, recognition, decision-making, and motor planning. Component models can be constructed using different modeling formalisms (e.g., ACT-R, SOAR, and C3TRACE) and programming languages (e.g., MATLAB and R).

Component models provide the basic blocks for assembling more sophisticated behaviors (Fig. 2). This enables *re-use*; the same component model can be used for

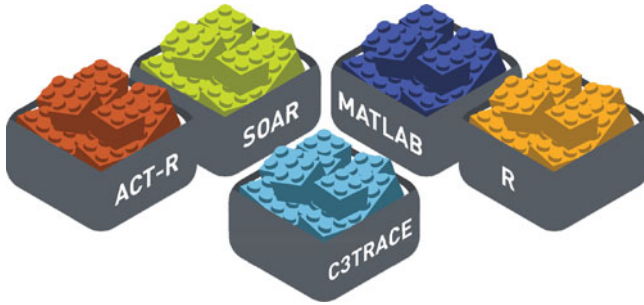


Fig. 1 Libraries of basic component building blocks created using different modeling formalisms

new behaviors. This also enables *composability*; complex agents can be assembled from simpler component models. Behaviors can be built using components from one modeling formalism (Fig. 2, Panel 1), two modeling formalisms (Panel 2), or many modeling formalisms (Panel 3). Finally, this enables *specialization*. Model plurality extends the capabilities of an intelligent agent beyond those supported by any single formalism. Additionally, it enables trade-offs between representational fidelity and computational cost. When multiple modeling formalisms can be used to represent the same process, the developer must choose among component models with fidelity and computational cost in mind. High-fidelity models may reproduce all aspects of behavior, but they are prohibitively expensive for all but the simplest tasks. Fortunately, some behavior can be characterized in precise terms following a definite pattern. In such cases, simple models are more appropriate. Different behaviors are best represented at different levels of abstraction: high-fidelity cognitive architectures such as ACT-R and Soar provide detailed accounts of human behavior at a significant complexity cost, while task network or mathematical models may provide an adequate low cost alternative.

The second key idea is to design a “workspace” that enables interactions among component models, and between component models and a software interface. This



Fig. 2 Composition of increasingly sophisticated agents from basic component building blocks

is the “glue” that holds the component models together. We call this the DREAMIT Workspace. The Workspace supports the definition of persistent local objects (i.e., local to the workspace) that define the input-output relationships among the component models, and between the component models and the interface (either to a constructive simulation or a computer mediated interface to the environment). For example, variables from a simulation environment are passed through the simulation interface to the DREAMIT Workspace (via a “get” function). The Workspace passes these to a component model, which returns a new model-derived variable. The Workspace subsequently passes the model-derived variable to another, different component model, or to the simulation interface in the form of a behavior to enact (via a “set” function).

The DREAMIT Workspace ensures *system level modularity*; a well-specified interface can allow different human behavior representations (HBRs) to “plug and play” with a given simulation. On the other hand, the DREAMIT Workspace ensures modularity internal to the HBRs as well. This second form of *architectural modularity* is powerful. Although it is commonplace to decompose tasks during the analysis of complex behavior, modelers often use a single computational architecture to develop the corresponding HBR. Even if the architecture provides some degree of modularity (e.g., separate modules to represent perceptual and cognitive function), the modularity of the architecture rarely recapitulates the decomposition of the task. The DREAMIT Workspace aligns the decomposition of complex behaviors with the modularity of the HBRs used to model them. This allows existing HBRs to be re-used and rearranged to construct novel complex behaviors.

The chief benefits of the DREAMIT Workspace are *scalable agent development* via the combination of multiple model components, *efficient agent development* via model re-use, and *enhanced agent capability* via model specialization. Aside from these benefits, the workspace creates greater transparency in the agent’s internal processes. Each of the component models that make up the agent receives inputs from and returns outputs to the DREAMIT Workspace. The meaning of these inputs and outputs are related to the component tasks, and are human-interpretable. A final benefit of the DREAMIT Workspace is that it potentially allows different component models to run on different systems connected by a network protocol. This could enable more efficient computation (e.g., using High Performance Computing resources) and integration of proprietary modeling frameworks.

The third key idea is to build a virtual data loop where agent(s) and human(s) act in a simulation environment, and data from the environment is passed back to the agent(s). The aim here is to capture data from training simulations, to apply computational methods (e.g., instance-based learning, reinforcement learning, regression, etc.) to the data to develop intelligent agent models more efficiently, and to close the loop by gathering additional data after embedding the agent models in the simulation environment. The data loop will reduce the resources (i.e., time and money) required for agent development and will produce agents capable of expressing prescribed tactics and adapting to either teammate or adversarial behaviors.

Beyond facilitating model training, the *validation loop* makes verification and validation an integral part of the modeling process rather than a postscript to model

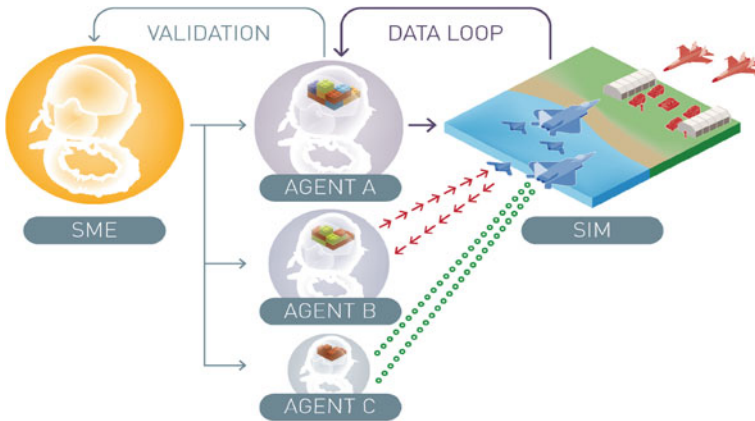


Fig. 3 Human and agent performance data is collected in the integrated training simulation environment and used to train and validate the agent

development. To validate the behavior of intelligent agents, the validation loop must include measures of fit to human data. We argue for using multiple types of data, ranging from quantitative data to SME input. In total, these sources of data give rise to an agent that learns from experience as human trainees do. The agent can be validated against the very same data that were used to train it (or other data that were withheld for validation), closing the loop on the authoring process (Fig. 3).

3 Instantiating the DREAMIT Workspace

Working under an Air Force Research Laboratory Phase I Small Business and Technology Transfer contract, we established proof of principle by developing three different models, each implemented in a different architecture, that interact to produce coherent agent behavior—the identification of an adversary’s tactical maneuvers in an air combat domain. Although the behavior could have been implemented entirely in any one of the modeling methodologies, we used multiple models to highlight the various avenues of data-driven model development available, and to pave the way for integration across multiple architectures.

3.1 *Basic Flight Maneuver (BFM) Identification Scenario and Task Decomposition*

Based on informal interviews with a subject matter expert, we identified some of the basic tactical decisions a pilot makes at the outset of an engagement. Given the pilot’s use of the multi-function display, the “input” to these decisions is based on



Fig. 4 Decomposition of basic fighter maneuver (BFM) identification

the sensed location, heading, and speed of the adversary. The outputs of these decisions are categorical judgments that, in turn, lead to other tactical decision making processes (e.g., whether and how to engage the adversary).

We decomposed the categorization problem into three distinct stages (Fig. 4): differentiation, integration, and recognition. Although there is some intuitive appeal in thinking about the problem in this way, we are not interested here in advancing a general theory of categorization. We are, however, interested in demonstrating how a complex behavior like tactical categorization can be decomposed into subtasks that can be addressed by different modeling formalisms.

3.2 Four Different Modeling Approaches

Working in parallel, the members of our team developed models for each stage in this decomposition using distinct modeling architectures. For example, a diffusion model was implemented in MATLAB. In the diffusion model, evidence is accumulated over time. Incoming information drives the process toward one of two decision bounds. The process terminates when accumulated evidence reaches a decision bound, at which time a decision is made. In this case, decision bounds were used to recognize changes in heading and altitude over time and, in turn, to recognize specific maneuvers defined by the conjunction of changes across multiple different dimensions (e.g., a *descending turn*).

The diffusion model has two main strengths. First, it accounts for a range of behavioral phenomena related to people's decisions and the time course of their responses [12]. Second, under certain parameterizations, it is equivalent to the sequential ratio probability test, a statistical test for optimal decision making. The main limitation of the diffusion model is that it lacks the control structure present in integrated cognitive architectures. This makes it suitable for simple decisions but not complex tasks. A key insight in our early research was that the DREAMIT Workspace and its other constituent models could provide the control structure necessary to perform complex tasks, allowing us to leverage the diffusion model's detailed predictions about the time course of decision making.

We also developed an agent in the ACT-R cognitive architecture. Again, each stage of the decomposition was represented in the model. Although the ACT-R

agent was developed to produce the same behavior as the diffusion model, the internal representation was completely different. For example, in the ACT-R model raw data prompts a retrieval from declarative memory so that the incoming data can be compared to previous data. The key cognitive functionality used in this model is the ability to retrieve the recent temporal context. This is accomplished by using the activation processes in declarative memory, specifically the base-level learning that captures the power laws of practice and recency [13]. This leveraging of the temporal statistics of the environment for decision making has proven to be one of the most robust features of the architecture, including in adversarial settings [14].

To ensure generality, we constructed chunk types that held a single attribute value for a given object. This representation consists of five very general components, listed here with their (arbitrary) names and functions:

- *Tag*: a link to the parent object, in this case the aircraft track identifier
- *Time*: the time stamp for this data item, either in terms of simulation cycle or real time
- *Field*: the name of the attribute (e.g., x, y, z, heading)
- *Value*: the piece of data itself (i.e., the current value of the given attribute)
- *Encoding*: a characterization of the nature of the data, *absolute* in this case

This basic representation is completely independent of the aviation domain, but it provides all the information needed for the differentiation process. Indeed, this model has been used *unchanged* to perform the same differentiation process in another model of fluid management in critical care, where the attributes are health-related values such as heart rate and blood pressure. This type of indirect representation has also been used in our model of list memory [15].

Our last approach to modeling BFM recognition uses a task network model and an R-based implementation of a recognition-primed decision (RPD) model. The task network model is used to perform the differentiation and integration steps while the R-RPD model performs the recognition step. Unlike the diffusion model and the ACT-R model, the task network model transforms the input data from an allocentric to an egocentric representation. In particular, the task network model takes the current location of ownship and each of the opposing red agents to determine a clock bearing (e.g., redship at my 1:00 o'clock), a rudimentary sense of the track crossing angle, and the distance to each redship. These calculations are based purely on the geometry of current and projected positions at each time step and are not intended to represent the cognitive processing of the ownship agent. So at a given time step, for a given redship the task network model outputs three variables: an integer between one and 12 that represents bearing to the redship; a string that indicates the relative motion of the redship to ownship: “closing,” “crossing ahead of my 9-3,” “in pursuit” (of redship), “crossing behind my 9-3,” or “pursued” (by redship); and a real-valued variable that indicates the range from ownship to redship.

Again, unlike the diffusion model and ACT-R model, the task network model combines the differentiation and integration stages under the calculations used to

transform the allocentric representation of latitudes, longitudes, heading, etc. Using the algorithms described in [16], we wrote an R package to implement a recognition-primed decision process. The R-package includes functionality to represent both interval and categorical variables along with a similarity-based recall routine that operates over a “long-term memory” data structure that records past situations, the course of action taken in that situation, and an outcome measure. The R-RPD model takes the output from the task network model and transform the clock bearing, track crossing angle, and distance for a given redship into a vector that represents the current situation (i.e., a particular time step in the scenario). This vector is then compared to past situations stored in long term memory, and a similarity value is calculated (essentially a dot product calculation) between the current situation and each of the remembered situations. The similarity value, in turn, is used to determine how strongly each of the remembered situations contributes to a composite sense of recognition over a set of discrete courses of action (i.e., recognized flight maneuvers).

4 Specification of DREAMIT Workspace and Communication Protocol

The primary purpose of the DREAMIT Workspace is to ensure communication of information to and from simulation and component models. For the prototype implementation, we adopted TCP/IP text sockets as the most flexible, low-overhead, platform-independent communication medium available. Efficient, lightweight socket implementations are available for all platforms and languages, including the implementation of the four architectures we used.

Our central conception of the Workspace is object-based, with each object composed of a set of attributes and values. This conception provides a natural match to other components of our framework, including common simulation application programming interfaces and the internal representation of many behavioral modeling frameworks (e.g., chunks in cognitive architectures). To communicate those objects to and from simulations and models, we adopted the JSON (JavaScript Object Notation) open standard for object serialization over text-based streams. As for TCP/IP, efficient, lightweight JSON implementations are available for all platforms and languages.

The current prototype of the DREAMIT protocol is quite simple. During the simulation runtime, objects are serialized using JSON then transmitted to the network over TCP/IP sockets. For each object, its attributes and values are mapped onto a JSON object name/value pairs. Basic values such as strings and numbers used in this simulation are also naturally mapped onto the corresponding basic JSON data types.

The Workspace takes as its initial input aircraft type, lat.-long. coordinates, altitude and heading information. These input data are presented to the Workspace

incrementally to emulate real-time interactions with a software interface (though the workspace can run in faster than real-time to speed up learning). The Workspace passes these values to the designated Stage 1 component model. The component model, in turn, returns model-derived values to the workspace, which are passed to the designated Stage 2 and 3 models, respectively. Using this Workspace and JSON specification, we have instantiated the following four heterogeneous agents for performing BFM identification:

- Stage 1 (ACT-R)—Stage 2 (Diffusion)—Stage 3 (Diffusion)
- Stage 1 (Diffusion)—Stage 2 (ACT-R)—Stage 3 (Diffusion)
- Stage 1 (ACT-R)—Stage 2 (ACT-R)—Stage 3 (Diffusion)
- Stage 1 (C3Trace)—Stage 2 (C3Trace)—Stage 3 (R-RPD)

Importantly, once the three-stage decomposition was complete, and the inputs and outputs of each stage were defined, the component models were designed independently from one another. The models were combined without further modification to create different heterogeneous agents. This demonstrates true model *re-use* and *composability*. A further step is to harness the distinct strengths of the different modeling formalisms to reflect the principle of *specialization*. For example, detection of change in noisy, continuously varying quantities is naturally modeled the diffusion framework, while categorization based on multiple dimensions and past experience is naturally modeled in ACT-R.

An important insight from this exercise is that even when two component models accomplish the same function (e.g., the Stage 2 ACT-R and diffusion models), their outputs may systematically vary in nuanced ways. The consequence is that performance of a downstream (i.e., Stage 3) model trained using input from one component model is degraded when an alternate component model is used as input instead. The solution to overcoming this fragility is to include learning mechanisms in component models that occupy later positions in the processing sequence. Although such mechanisms have traditionally allowed models to adjust following changes in environmental inputs, they are equally applicable to changes in sequences and steps in internal processing. The component models can be viewed locally as receiving (through the Workspace) inputs from the simulation and other models and sending outputs to other models and back to the simulation. Their learning mechanisms can thus locally adjust to that environment using whatever feedback signals are available as part of the overall data loop. This local learning is tractable, parallelizable and robustly adaptive.

5 Discussion

Our work focused on two objectives: the development of a methodology to align agent development with best practices in software engineering; and the application of that method to the development of intelligent behaviors. Though these two objectives are tightly related, the leverage that the DREAMIT Workspace provides

to intelligent agent development was not immediately clear. There are obvious practical benefits from encouraging modularity and encapsulation in any software development project, and we had these practices firmly in mind. But the extent to which those practices would influence our thinking about agent development only became clear as we began developing models.

One of the most significant shifts follows from the insight that agent development can be driven by the most natural decomposition of the desired behavior rather than by the requirements of a particular cognitive architecture or modeling approach. This shift is exemplified by the three-stage approach we took to the identification of basic flight maneuvers. In practical terms, this decomposition promotes modularity by allowing different component models to implement the various phases. On a deeper level, the decomposition of the behavior into differentiation, integration and recognition reflects a more general pattern of behavior representation in the sense that the techniques used to solve a tactical problem in the air combat domain might have direct application to behavior representations in entirely different domains. The true potential for model reuse follows from the identification of common patterns of human behavior across domains rather than from an otherwise contingent ability to re-apply a particular model.

A different but equally important shift in our thinking about agent development follows from the potential to develop heterogeneous behavior representations. Again, we originally saw this issue in practical terms: as a method for combining different models, the DREAMIT Workspace would provide efficiency gains by allowing the modeler to use the ‘right tool for the job’. But this approach also imposes a kind of discipline on the modeler; because the modeler can no longer assume that a monolithic approach will be applied to agent development, the modeler must take greater care to define the boundaries between behavior representation and “infrastructure.” Historically, given the ability to implement sub-routines, tune parameters or exploit quirks within a given architecture, it has been all too easy to ignore the crisp specification of input-output relationships and the division of labor between model and environment. A truly modular approach to agent development, in which different approaches might be integrated to achieve coherent behavior, requires that the modeler think very clearly about each step in the transformation of state information to overt action. Because that transformation might occur across multiple component models, the modeler cannot assume that there will be direct access to information or routines used earlier in the transformation. In short, the DREAMIT Workspace discourages the ‘useful cheating’ during both agent development and validation that has often been exploited when agents or behavior representations are developed monolithically.

There still is a good deal of effort needed to transition the DREAMIT Workspace from the proof of principle to a fully functional prototype. Most of that work, however, is straightforward software development and user interface design. The more interesting effort turns on establishing the extent to which the DREAMIT Workspace supports better agent development. Here, we require a constructive proof: the application of the DREAMIT Workspace to the data-driven development of a robust agent capable of effecting coherent behavior in a simulated environment.

Acknowledgments This work is funded in part by NSF award CNS1329878 to Christian Lebiere and by an Air Force Research Laboratory Phase I STTR award.

References

1. Gluck, K.A.: Cognitive architectures for human factors in aviation. In: Salas, E., Maurino, D. (eds.) *Human Factors in Aviation*, 2nd edn, pp. 375–400. Elsevier, New York (2010)
2. John, B.E., Prevas, K., Salvucci, D.D., Koedinger, K.: Predictive human performance modeling made easy. In: *Proceedings of the SIGCHI Conference on Human Factors in Computing Systems*, pp. 455–462. ACM (2004)
3. Pew, R.W., Mavor, A.S. (eds.): *Modeling Human and Organizational Behavior: Applications to Military Simulations*. National Academy Press, Washington, DC (1998)
4. Walsh, M.M., Gluck, K.A.: Mechanisms for Robust Cognition. *Cognitive Science* (in press)
5. Anderson, J.R., Lebiere, C.: The Newell test for a theory of cognition. *Behav. Brain Sci.* **26**, 587–601 (2003)
6. Gluck, K.A., Pew, R.W. (eds.): *Modeling Human Behavior with Integrated Cognitive Architectures: Comparison, Evaluation, and Validation*. Erlbaum, Mahwah (2005)
7. Walsh, M.M., Gunzelmann, G., Van Dongen, H.P.A.: Computational cognitive models of the temporal dynamics of fatigue from sleep loss. *Psychol. Rev.* (submitted)
8. Buchanan, B.G., Shortliffe, E.H. (eds.): *Rule-Based Expert Systems*, vol. 3. Addison-Wesley, Reading (1984)
9. Cullen, J., Bryman, A.: The knowledge acquisition bottleneck: time for reassessment? *Expert Syst.* **5**, 216–225 (1988)
10. Blum, A., Mitchell, T.: Combining labeled and unlabeled data with co-training. In: *Proceedings of the Eleventh Annual Conference on Computational Learning Theory*, pp. 92–100. ACM (1998)
11. Sanner, S., Anderson, J.R., Lebiere, C., Lovett, M.C.: Achieving efficient and cognitively plausible learning in Backgammon. In: *Proceedings of the Seventeenth International Conference on Machine Learning*. Morgan Kaufmann, San Francisco (2000)
12. Ratcliff, R., McKoon, G.: The diffusion decision model: Theory and data for two-choice decision tasks. *Neural Comput.* **20**, 873–922 (2008)
13. Anderson, J.R., Schooler, L.J.: Reflections of the environment in memory. *Psychol. Sci.* **2**, 396–408 (1991)
14. Lebiere, C., Jentsch, F., Ososky, S.: Cognitive models of decision making processes for human-robot interaction. In: *Virtual Augmented and Mixed Reality. Designing and Developing Augmented and Virtual Environments*, pp. 285–294. Springer, Berlin (2013)
15. Anderson, J.R., Bothell, D., Lebiere, C., Matessa, M.: An integrated theory of list memory. *J. Mem. Lang.* **38**, 341–380 (1998)
16. Warwick, W., McIlwaine, S., Hutton, R.J.B., McDermott, P.: Developing computational models of recognition-primed decision making. In: *Proceedings for the Tenth Conference on Computer Generated Forces*, Norfolk, VA (2001)

Lessons Learned in Development of a Behavior Modeling Tool for Health Intervention Design: BehaviorSim

Tylar Murray, Eric Hekler, Donna Spruijt-Metz, Daniel E. Rivera and Andrew Raij

Abstract The BehaviorSim Modeling Tool, a behavioral-scientist-facing software for development of Computational Human Behavior Models (CHBMs), has been developed in an effort to close the gap between Just-in-Time Adaptive Intervention researchers and dynamical systems modeling. We present a summary of our iterative methodology for creating the BehaviorSim Model Builder alongside insights and lessons learned at each stage of the process. Drawing from our lessons learned, we highlight and explain the following UI design guidelines as especially important in the development of future CHBM tools: (1) promote expertise development, (2) enable quick model iteration, (3) present high-level visualizations to de-internalize models, and (4) utilize adaptive interfaces. A focus on these design guidelines in the development of future CHBM tools, combined with the provided user persona, will allow developers to create systems that are more accessible and have more utility to JiTAI designers.

Keywords JiTAI · mHealth · Adaptive interventions · Behavior modeling

T. Murray (✉)
University of South Florida, Tampa, USA
e-mail: tylarmurray@mail.usf.edu

E. Hekler
Arizona State University, Phoenix, USA

D. Spruijt-Metz
University of Southern California, Los Angeles, USA

D.E. Rivera
Arizona State University, Tempe, USA

A. Raij
University of Central Florida, Orlando, USA

1 Introduction

With the increasing prevalence of wearable technologies and personal health data, behavioral researchers are becoming overwhelmed with data. This data offers researchers the potential to optimize a behavioral intervention to suit not only the user [1, 2], but also the context [3] as the user goes about his/her normal daily life. Sometimes called Just-in-Time Adaptive Interventions (JITAI)s, these in-context interventions promise to provide the optimal nudge at the optimal time to aid users looking to change their behavior [4]. Imagine, for example, an anti-stress application which knows not to interrupt work meetings, but also knows when to play a favorite song to help relieve stress on the drive home. Or consider a smoking cessation application that knows precisely when and where craving is most likely, and distracts with a game before the desire to smoke is noticeable. This impending wave of context-aware [5], affective computing [6] applications offers a unique opportunity to promote behavior change with technology. However, behavioral researchers are finding that existing models of human behavior are not sufficient for developing such applications.

Existing models of behavior do not offer the granularity and specificity needed for these applications [7]. Currently, psychological models of human behavior act as a guide for behavioral scientists looking to predict behavior, but are rarely computational in nature—making direct application to adaptive systems impossible. Methods for creating computational models of human behavior are not well defined, but some early concepts have been published [8].

Computational Human Behavior Models (CHBMs) provide a mathematical model “which describes how context is transformed into a behavioral outcome through the internal state of the human system” [9]. CHBMs are a more robust alternative to if-then-style decision rules used in proof-of-concept systems. As the level of intervention tailoring continues to rise and incorporates just-in-time and adaptive components, methods of modeling the relationships between sensor/EMA [10] data, user behavior, and application behavior will become increasingly important. Our research attempts to address this roadblock through the creation of methods and software which helps behavioral scientists use CHBMs in their research.

In this paper, we present a summary of our iterative methodology for creating the BehaviorSim Model Builder, which aims to be a behavioral-scientist-facing software for development of computational models of human behavior for use in JITAI)s. We present insights gained at each stage of the development process, followed by a discussion section which formulates generalizable knowledge from our specific lessons learned that may be of use to others designing JITAI) development support software, or those targeting behavioral scientists as a user group.

2 Methodology

2.1 Survey of Behavioral Scientists

A preliminary survey was given to a group of behavioral scientists in order to gauge the general perceptions and opinions on the development of behavioral models to support JiTAIs. In this survey we focused on a few key elements of the model building process to greatly simplify and shorten the modeling exercise. Contextual and behavioral outcomes based on physical activity were given, and user efforts were focused on defining the inner workings of the human system within these constraints. Participants were asked to describe the human system by sketching a time-series to represent their expectations, listing relevant constructs, and describing their constructs as they related to outcomes. Participants were also asked to complete survey items about the barriers facing modeling and simulation in behavioral science.

Approximately 50 surveys were distributed following presentations on behavioral modeling and simulation at the 35th Annual Conference of the Society of Behavioral Medicine. Out of these 50, 12 surveys were returned. In general, users had trouble with even the simplified modeling exercise. We also believe the low response rate to be indicative of the difficulty of the questionnaire, as it seemed as though all 50 participants who initially accepted the survey did attempt to complete it, but were unsatisfied with their answers and did not submit their responses. Of those few submitted, most did not stray far from the given example, and others provided very different solutions which—although helpful for conveying an abstract description of their model—could not be reconciled with the modeling paradigm presented. That is, the solutions provided abstract descriptions of the model, but they did not convey enough detail to form a CHBM. Participants seemed to find the sketching of time-series particularly challenging, and in the survey questions participants reported that the mathematics and programming concepts required for developing simulatable models were overwhelming. However, nearly all participants expressed a desire for increased collaboration between disciplines and a need for software tools to help them apply and validate these methods. These findings confirmed the need for modeling software tools to bridge the gap between systems theory and behavioral scientists.

2.2 BehaviorSim Model Builder v1

Using findings from the user study we developed proof-of-concept software to aid behavioral researchers with the task of building a computational behavioral model. The software—called the behaviorSim Model-Builder—took a step-wise approach towards the model-building process.



Fig. 1 In the “think” section, users list contextual variables, internal state variables (constructs), and behavioral measures to be used in their model

First, users are asked to list environmental inflows, internal state variables, and behavioral outflows of the model explicitly during the “think” stage. The “think” stage allows users to list the sensor measures as “context” or “behavioral”. “Context” is a measurement of the environment (e.g. location), and “behavioral measure” is a measure of a subject’s conscious or unconscious actions. “Constructs” are variables used to represent everything in between context and behavior which are not directly measured (Fig. 1).

Next, users are prompted to define the connections between nodes, “drawing” the model’s structure. This is accomplished by specifying the connections using a simple Diagram Specification Language (DSL) to denote connections between the context, state, and behavior variables given in the previous step.

Finally, users are required to “specify” the functional relationships at each node’s inflow(s). Nodes are highlighted one-at-a-time and the relevant section of the graph including only the node in question along with its direct inflows and outflows is shown. Users are asked to select a functional form which should be used to compute the highlighted node from its inflows. Users are also asked to specify a specific set of constants to use in a test instance of the model. These constants are used to compute a time-series representing the signal generated for this simulation instance.

As a very simple example, consider the following model of physical activity (PA): firstly we can name social pressure (SP) as an environmental inflow, normative belief (NB) as an internal state variable, and step count (SC) as a behavioral outflow; next we specify connections $SP \rightarrow NB \rightarrow SC$; lastly, we can specify that the connections ($SP \rightarrow NB$ and $NB \rightarrow SC$) both represent simple linear relationships.

The model builder was reviewed by an expert panel of 2 behavioral scientists and 1 human-computer interaction expert. Though the steps in the outlined model development process seemed appropriate, it quickly became obvious that a step-wise design is not optimal. Users who are forced to explore the process step-by-step have difficulty understanding how earlier choices related to later results, and feel constrained by previous choices rather than backtracking to revise the model. This design does not allow for quick iteration on models, and requires the user to maintain a great deal of planning information internally. Though the information flow diagram (Fig. 2) employed in this version worked well to convey information about the model to the users, the graph was also assumed to be interactive—reviewers made attempts to modify the graph by clicking. Similarly,

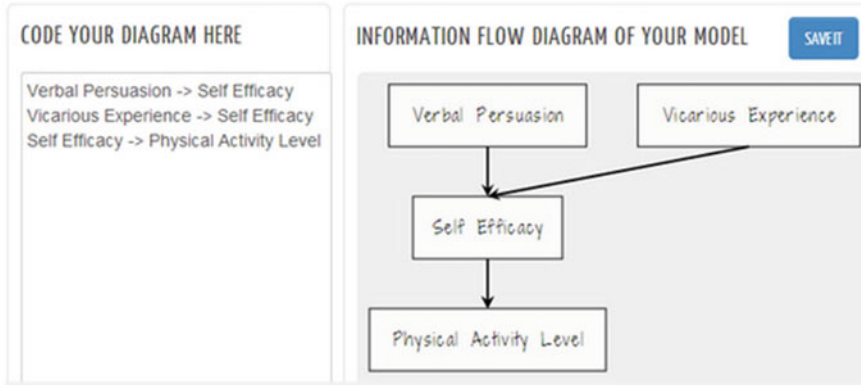
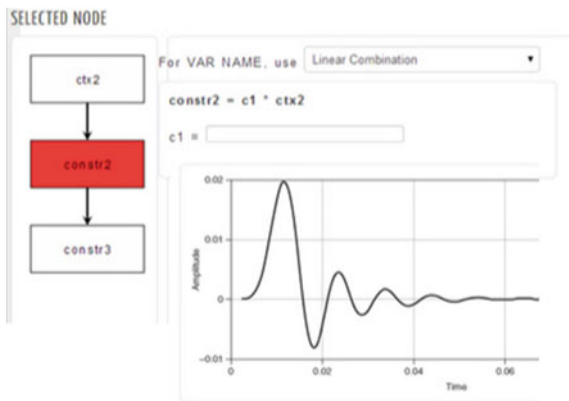


Fig. 2 The “draw” page showing DSL input box and resultant information-flow graph

Fig. 3 The “specify” UI for defining a node as a function of its inflows



reviewers attempted to select nodes in the specification stage (Fig. 3) by clicking on them. Our review concluded that a less constrained approach to the stages of the modeling process was needed, and a greater focus on the graphical model could greatly improve user experience. Furthermore, reviewers felt that the rift between behavioral scientists and the modeling methods had not been adequately addressed; more was needed to communicate the treatment of context, constructs, and behavioral measures as time-series in the “specify” stage.

2.3 BehaviorSim Model-Building Tutorial

After reviewing v1 of the behaviorSim Model Builder tool, a tutorial was designed to help bridge the knowledge gap for new modelers looking to use the tool.

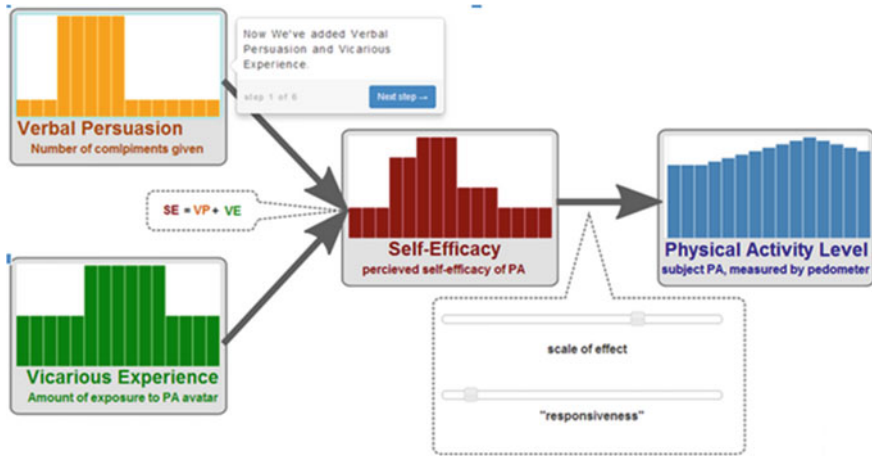


Fig. 4 BehaviorSim tutorial merging of time-series and information-flow graph

In theory, the tutorial would help users see the bigger picture before diving into the stepwise process. The tutorial was implemented as a walk-through of a simple example model's internals. The tutorial introduced a hybridized information-flow and time-series graph, wherein each node of the graph contains a time-series spanning a common time-frame. A user interface for adjusting model parameters and updating time-series values instantaneously was also overlaid onto this hybrid graph (see Fig. 4). This real-time parameter tweaking enables some degree of reconciliation with expectations of the data.

The same expert panel review process was used for the evaluation of the tutorial. Through this evaluation it became clear that, although we had taken a step in the right direction, an even more explicit definition of terms was needed in order to clarify persistent disciplinary differences. Reviewers also wanted better explanation of model input parameters and of the functional definition of the system. This tutorial included a specific scenario encoded as a set of time-series which defined the environment over time. Reviewers were not content with the hard-coded environmental inputs and wanted to be able to define how the contextual inflows changed over time. Though the hybrid graph was found helpful in conveying the connection between path diagram nodes and time series, the shared time-axis was not obvious, and reviewers expressed a need for more explicit x and y axes as well as a better explanation as to what "10 units of self efficacy" actually means. The time-series view was found to be both critical for the development of an accurate model, and valuable as a pedagogical exercise for users trying to internalize model formulations.

2.4 BehaviorSim Model Builder v2

Using what we had learned so far, the behaviorSim Model Building tool was re-designed and re-assessed. In this version all steps of the modeling process (think, draw, specify) are unified into a single-page application (see Fig. 5), allowing users to see how choices influence the model in real-time. This design allows users to iterate on their design more easily. The time-series charts popular in the tutorial were added as a “mini-simulation” to help users to visualize how variables change over time according to their model formulation. To address the terminology gap which plagued v1, a set of tool-tips were added which revealed detailed definitions for key terms used in the user interface. In addition, the second version incorporates findings from the v1 tutorial, adding a “miniature simulation” to the application to allow for “reconciliation” with model expectations.

In this version of the tool, users declare constructs and define the structure of their model simultaneously. In contrast to version 1, where the construct type had to be input by the user, the type of each node (contextual input, internal state, or behavioral measure) is inferred from the number of inflows and outflows. Source

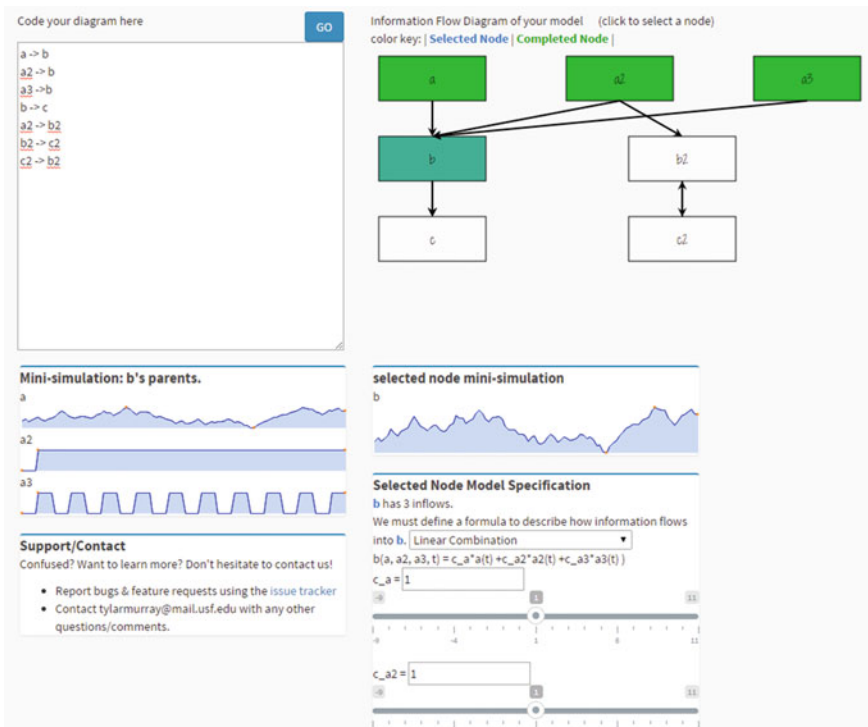


Fig. 5 BehaviorSim model builder v2 combines elements into a single view

nodes are assumed to be contextual input, sink nodes assumed to be behavioral measures, and all others are treated as internal state nodes.

The “miniature simulation” concept allows users to specify hypothetical contexts in which to explore the model dynamics, without the need to specify the full model. Users can specify environmental inflows for the simulation, choosing from adjustable presets (square wave, step function, random walk, or constant value). Selecting nodes on the graph by clicking, users can traverse the graph in any order. Time-series plots of inflows as well as the resulting outflow at each node are provided using the miniature simulation model instance. Internal state and behavioral measure nodes are specified similarly to environmental inflows through customization of function presets such as “linear combination” and “fluid flow analogy” [11].

To evaluate this design, this version was used as part of a structured exercise and interview outlining the design of a JiTAI to combat obesity. Based on recent work done to define the JiTAI design use-case [4], participants were asked to walk through a series of steps including “identify the distal outcome of your JiTAI”, “list the key factors affecting your distal outcome at the hour-to-hour level”, and “what tailoring variables will you use in your JiTAI”. Intermixed with these discussions, participants worked together with the staff to express these ideas as a CHBM using the behaviorSim Model Builder. As the exercise progressed, the staff took an increasingly passive role, ending with a fully unassisted modeling task. A think-aloud protocol was applied while the software was in use, and the concluding interview gives insight to what users find most valuable, least valuable, and most in need of improvement. Preliminary findings from this exercise completed with 4 behavioral researchers highlight both the strengths and the remaining weaknesses of our tool.

Though the single-page design of version two did seem to allow for increased ability to iteratively explore models, reviewers now found the user interface somewhat overwhelming. Upon starting the review, users often felt unsure where to start. Furthermore the connection between the information flow graph and the related interface elements below was not obvious. Reviewers did identify the relationship after some exploration, however. Additionally, the common user interface for specifying constructs regardless of node type broke down the distinction between environmental inflows, state variables, and behavioral outputs. This led to some confusion when specifying the various types of nodes. Further contributing to this problem, the meaning of the mini-simulation was not always clear to reviewers, though the inclusion of time-series graphs was found helpful for understanding the model functions and their parameters once explained. Nodes on the graph were made to change color when the specification process was complete, but reviews revealed that this was not a significant enough indicator of node “completeness”, and the user is sometimes unsure when they should feel free to move to the next node. Inclusion of a “next node” button which appears upon node specification completion may be all that is needed to help alleviate this issue.

3 Discussion

Our findings above reveal specific weaknesses in our design, and through analysis of these findings we present the following design guidelines for any software made to empower JiTAI developers. Firstly we outline a rough JiTAI developer user persona based on our assessment of the general population of researchers in behavioral intervention design. Next, we propose user stories and use-case details for the task of JiTAI design and evaluation. Lastly, we provide some generic design guidelines which we have found to be particularly relevant in this design space.

3.1 *JiTAI Developer User Persona*

In general, JiTAI developers are behavioral researchers who see the powerful potential of ubiquitous computing for high-frequency data collection, automated analysis, intervention deployment, and personalization. It is important to note that the research questions of a JiTAI researcher often differ significantly from the questions a behavioral scientist might typically have. The “traditional” way of modeling for behavior change relies primarily on statistical data analysis techniques to find relationships between variables on large time-scales. In contrast, the JiTAI researcher needs to translate these relationships into a small-time-scale model which provides guidance regarding which interventions are most effective at which specific time(s).

The JiTAI developer wants to turn a patient story into a set of equations that can be handled by an automated system. However, JiTAI developers typically do not have the level of familiarity with modeling systems to define computational psychological models mathematically. This is supported by our findings wherein we encounter more difficulty than expected using time-series as a common ground. Furthermore, the psychological models commonly used are ill-specified at the (small) timescales of greatest interest, and often do not fit commonly used modeling paradigms—making mathematical definition a unique challenge for even a systems engineer.

The JiTAI developer wants to deploy and test a hypothesis by comparing model predictions to experimental data. Statistical analysis techniques typically used to assess control vs experimental group differences are much less applicable to this problem, but the JiTAI developer often has little experience applying goodness-of-fit metrics.

3.2 *Adaptive Interface*

The science of JiTAIs is young, and—as our user persona shows—behavioral scientists looking to work with JiTAIs are likely to run into many new concepts. The potential complexity of a JiTAI system, however, may benefit from the use of

advanced and specialized graphs, charts, and user interfaces. Additionally, we found overlapping terminologies to be a common pain point; meaning that new users may not recognize the need to investigate the definition of a term. Thus, the needs of a novice user versus an expert user may be very different. Because of this, software to support JiTAI development needs to promote the development of expertise in both the system and the relevant concepts through steady changes to the user interface [12]. In our case, a guided walk-through of the software interface was sufficient, but we believe that a more graded approach would be more effective.

3.3 Enable Quick Iterations

The value of iterating on a design spans many domains, and is very applicable to the development of JiTAIs. Through our studies we have found that the development of even a simple JiTAI requires many iterations. Thus, a software to aid in JiTAI development must allow for quick and easy modification, comparison, and reversion. A comparison between the usage of our multi-staged model builder versus the single-page application showed a dramatic increase in the number of model iterations along with reported user comprehension. Iterations on the model tended to follow a moment of realization or the learning of a new concept. Thus, allowing for quick iterations allows for the user to more quickly apply newly gained expertise, yielding a better model and increased understanding.

To encourage iteration in the JiTAI development process, assessment tools available part-way through the process—like our mini-simulation time-series—allow users to test their mental model of the system against its digital representation. Allowing for more assessment points throughout JiTAI development allows users to identify problems early and iterate before the error cascades further through the process.

3.4 High-Level Visuals to De-Internalize Models

Traditionally, psychological models of human behavior are meant to be guidelines for thinking about human behavior. When using these models, the researcher must internalize the model and think through the subjects' state. With JiTAI models, internalization of the full system becomes impossible due to the rise in specificity and complexity. Thus, JiTAI development software must provide visualizations of the system to ease cognitive load on the user. Focus plus context displays [13] can be used to allow users to delve into the specifics of a portion of the model without losing the larger context. In the behaviorSim Model Builder, we focus on the specification of a single variable at a time, and highlight this variable's context in an information-flow path diagram of the model structure. This dual-viewing-area approach works well for comparing variable details, but the use of a zoom-able

interface such as is employed in some flow-based programming [14] tools may help alleviate the noted disconnect between specification and overview UIs.

3.5 *Customized Interface*

Though our JiTAI developer persona yields widely applicable general user stories, it is also important to recognize the diversity of the JiTAI developer user group. JiTAIs are applicable to any area of behavior change; just a few popular proposed JiTAI applications include management of eating behaviors, physical activity, smoking cessation, drug abuse, PTSD, and stress. Within each of these many application domains are a myriad of behavioral theories—further adding to the diversity of the user group. Each of these sub-user-groups may have slightly different needs as they develop a JiTAI. Furthermore, a JiTAI development software requires a standardized behavioral model or JiTAI format, and with that comes the opportunity to enable easy sharing and searching of JiTAI designs. Thus, personalization of the software interface—to adapt the process or to offer relevant information [15]—can greatly improve user experience in this domain.

4 Conclusion

In the quantified self era, we can now capture detailed, high frequency, context-specific measures of human behavior. Access to such data has the potential to change personal health, if only we could make sense of the hidden insights held within these data. Just-in-Time Adaptive Interventions are one application which stands to benefit from these insights and which may have great impact in applied behavioral health. One approach is to apply systems-thinking to help model and understand the data. The challenge is that health professionals and scientists do not usually have the experience or tools to apply systems thinking to health challenges.

In this paper, we describe preliminary work on understanding how HCI and user-centered iterative design can be used to transform these data into positive behavioral health outcomes. We ran several rounds of user-centered iterative design, and identified a driving user persona and design guidelines for next-generation tools for behavioral health. In particular, our qualitative analysis indicates behavioral scientists need: (1) ways to gain expertise in systems-thinking, (2) rapid iteration through multiple theoretical designs, (3) managed cognitive load when analyzing complex models using visualization of systems and their dynamics, and (4) personalization of such tools to the behavioral problem at hand, given the great diversity and complexity of human behavior. Taking these guidelines into account, we are evolving the BehaviorSim system to better enable behavioral health researchers and practitioners to leverage high frequency, context-specific measurements and design predictive, preventive, personalized and participatory health interventions.

References

1. Dallery, J., Raiff, B.R.: Optimizing behavioral health interventions with single-case designs: from development to dissemination. *Transl. Behav. Med.* **4**(3), 290–303 (2014)
2. Beck, C., McSweeney, J.C., Richards, K.C., Roberson, P.K., Tsai, P.F., Souder, E.: Challenges in tailored intervention research. *Nurs. Outlook* **58**(2), 104–110 (2010)
3. Brailsford, S.C., Desai, S.M., Viana, J.: Towards the holy grail: combining system dynamics and discrete-event simulation in healthcare. In: *Simulation Conference (WSC)*, pp. 2293–2303. IEEE Press (2010)
4. Nahum-Shani, I., Smith, S.N., Tewari, A., Witkiewitz, K., Collins, L.M., Spring, B., Murphy, S.: Just in Time Adaptive Interventions (JITAI)s: An Organizing Framework for Ongoing Health Behavior Support. Methodology Center Technical Report, pp. 14–126 (2014)
5. Schilit, B., Adams, N., Want, R.: Context-aware computing applications. In: *Mobile Computing Systems and Applications*, pp. 85–90. IEEE Press (1994)
6. Picard, R.W.: Perceptual user interfaces: affective perception. *Commun. ACM* **43**(3), 50–51 (2000)
7. Riley, W.T., Rivera, D.E., Atienza, A.A., Nilsen, W., Allison, S.M., Mermelstein, R.: Health behavior models in the age of mobile interventions: are our theories up to the task? *Transl. Behav. Med.* **1**(1), 53–71 (2011)
8. Nandola, N.N., Rivera, D.E.: An improved formulation of hybrid model predictive control with application to production-inventory systems. *IEEE Trans. Control Syst. Technol.* **21**(1), 121–135 (2013)
9. Murray, T., Hekler, E., Spruijt-Metz, D., Rivera, D.E., Raij, A.: Formalization of Computational Human Behavior Models for Contextual Persuasive Technology. *Persuasive Technology* (2016)
10. Shiffman, S., Stone, A.A., Hufford, M.R.: Ecological momentary assessment. *Annu. Rev. Clin. Psychol.* **4**, 1–32 (2008)
11. Martin, C.A., Rivera, D.E., Riley, W.T., Hekler, E.B., Buman, M.P., Adams, M.A., King, A.C.: A dynamical systems model of social cognitive theory. In: *American Control Conference (ACC)*, pp. 2407–2412. IEEE (2014)
12. Cockburn, A., Gutwin, C., Scarr, J., Malacria, S.: Supporting novice to expert transitions in user interfaces. *ACM Comput. Surv. (CSUR)* **47**(2), 31 (2015)
13. Baudisch, P., Good, N., Stewart, P.: Focus plus context screens: combining display technology with visualization techniques. In: *Proceedings of the 14th Annual ACM Symposium on User Interface Software and Technology*, pp. 31–40. ACM (2001)
14. Morrison, J.P.: *Flow-Based Programming: A New Approach to Application Development*. CreateSpace (2010)
15. Hood, L., Friend, S.H.: Predictive, personalized, preventive, participatory (P4) cancer medicine. *Nat. Rev. Clin. Oncol.* **8**(3), 184–187 (2011)

Experimentation System for Path Planning Applied to 3D Printing

Mateusz Wojcik, Iwona Pozniak-Koszalka, Leszek Koszalka
and Andrzej Kasprzak

Abstract This paper is focused on finding the efficient path generating algorithms. These algorithms can take part in the path planning process, which is the last stage in model processing for 3D printing. The paper provides the comparative analysis of the five implemented path generating algorithms, which are based on four strategies: ZigZag strategy, Contour strategy, Spiral Strategy, and Fractal strategy. The analysis is based on the results of experiments made with the designed and implemented experimentation system. The system allows carrying out two types of experiments: simulation experiments and physical one. The simulation experiment is performed with the programming application written in C#. The physical experiments utilized FDM technology for 3D printing. Basing on the obtained results, we can conclude that the algorithm based on the ZigZag strategy seems to be better than the algorithms based on other approaches.

Keywords Path generating · 3D printing · Optimization · Algorithm · Experimentation system

M. Wojcik · I. Pozniak-Koszalka (✉) · L. Koszalka · A. Kasprzak
Department of Systems and Computer Networks, Wrocław University
of Technology, Wrocław, Poland
e-mail: iwona.pozniak-koszalka@pwr.edu.pl

M. Wojcik
e-mail: wojcik.mateusz991@gmail.com

L. Koszalka
e-mail: leszek.koszalka@pwr.edu.pl

A. Kasprzak
e-mail: andrzej.kasprzak@pwr.edu.pl

1 Introduction

In the last years, the task of an efficient and accurate 3D printing is treated with the significant attention by the companies in many markets, e.g., biomedical market, jewellery market, textile market, automotive market, and even civil engineering markets. The practical users expect a tool which allows optimizing RP—the Rapid Prototyping process [1]. This process requires solving the four tasks called: object orientation, support generation, slicing, and path planning [2, 3]. This paper is focused on the last task, i.e., on finding the algorithm for effective planning the moves of an extruder. The objective is to present the tool for the practical users, i.e., the created computer experimentation system (simulator) with the implemented algorithms to path planning. The mathematical model of the considered optimization problem is formulated. The proposed process of solving the problem consists in the decomposition onto two stages (using the idea which is presented in [4, 5]), where the first consists in path generating, and the second one in path optimizing. At the first stage, the five algorithms were implemented, including PGZZ—based on ZigZag strategy, PGC—based on Contour strategy, PGS—based on Spiral strategy, and two algorithms: PGFH and PGFP—based on Fractal Strategy. The main role of these algorithms is to generate sub-paths, which after linking may create the final path. The detailed description of the considered strategies can be found in [6–8]. At the second stage, the final path may be found using the implemented algorithms based on so-called Artificial Intelligence methods, including Ant Colony strategy, Genetic approach, and Simulated Annealing idea, what was presented in [9].

The input-output experimentation system was designed and implemented in Java environment—it gives an opportunity for finding the optimal paths by the users in the practical cases. Moreover, the system allows for making investigations concerning properties of the tested algorithms. The system possesses a visualization module which allows observing the process of finding the solution in any case. In the paper, the analyses of the results of the investigations (made with the created system) are presented. They concern: (i) the properties of the considered algorithms, (ii) the comparison of the algorithms efficiency which is based on the data obtained from the simulation experiments and from the physical experiments.

The paper is organized as follows. In Sect. 2, the mathematical model of the considered problem is stated. Section 3 describes the implemented algorithms to solving the problem. The created experimentation system is presented in Sect. 4. The results of investigations, including the comparison based on simulations and physical measurements, are studied in Sect. 5. The conclusion and final remarks appear in Sect. 6.

2 Problem Statement

The main goal is to generate the shortest path which fulfils the whole printing area. The input is the single layer of the whole 3D model. Most likely it is impossible to find one path, which can do that. Therefore, the total, final path consists of the sub-paths found by the path generating algorithm. The model of the problem can be stated as follows:

Given: Printing layer as a set of the binary points (an example in Fig. 1):

$$X_{ij} = \begin{cases} 1 & \text{if printing point} \\ 0 & \text{otherwise} \end{cases} \quad i \in n \quad j \in m$$

where the length between two points is defined as

$$L_{X_{ab}X_{cd}} = \sqrt{(a - c)^2 + (b - d)^2}$$

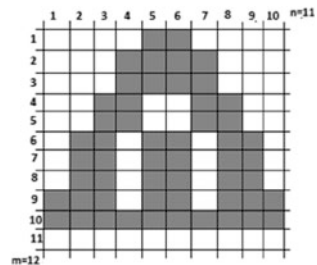
where: n is the length of the printing layer, and m is the width of the printing layer.

To find: $F = [V_1, V_2, \dots, V_s]$ —the final path, where $V_k = [X_{ab}X_{cd}X_{ef}\dots]$ is the order of the points inside k sub-path, $0 \leq k \leq S$, where S is the total number of sub-paths.

Such that: to minimize L_F —the total length of the found path.

$$\begin{aligned} & \sum_{k=1}^S \left(\sum_{j=1}^{P_k-1} \sqrt{(V_k[j]_x - V_k[j+1]_x)^z + (V_k[j]_y - V_k[j+1]_y)^z} \right) \\ & + \sum_{k=1}^{S-1} \sqrt{(V_k[p_k]_x - V_{k+1}[1]_x)^z + (V_k[p_k]_y - V_{k+1}[1]_y)^z} \\ & = L_F \end{aligned}$$

Fig. 1 An example of printing area (grey boxes refer to this area)



$L_F = L_{paths} + L_{switch\ path}$ is the sum of the length between the points in the sub-paths and the lengths between the last point in the one sub-path and the first point in the next sub-path. The parameter p_k is the number of points in k -th sub-path.

Subject to the constraint: Each point can be visited only once.

3 Algorithms

The implemented algorithms generate sub-paths, which after linking create the final path for covering the whole printing area. They use the image layer as input data. There is one assumption in the input data. The distance of one unit in horizontal and vertical direction is corresponded to the size of the extruder which is of 0.35 mm

3.1 Path Generating Algorithm Based on ZigZag Strategy (PGZZ)

- Step 1. Begin from top, left corner (Fig. 2-1). The extruder home position is (0.0), which corresponds to the top, left corner.
- Step 2. Move into the right corner (Fig. 2-2). In this step it selects all points which lay to the right of the first pixel.
- Step 3. Check the bottom pixels (Fig. 2-3). When there are no more pixels on the right, the algorithm checks, if there are pixels available below. It starts from the right corner below.
- Step 4. Check the pixels above. When previous step ends with no results, algorithm checks the pixels above. Otherwise the algorithm skips this step.
- Step 5. Choose the pixel in the rightmost position (Fig. 2-3). If any of those pixels is available—i.e. it has not been visited yet—the rightmost pixel is selected.
- Step 6. Check the pixels to the left (Fig. 2-4). After Step 4 the algorithm starts checking and selecting the pixels which lay to the left of the pixel which has been chosen in step 4.
- Step 7. Check the pixels below (Fig. 2-5). When there are no more pixels to the left, the algorithm checks if the pixels below are available. It starts from the lower left corner.
- Step 8. Check the pixel above. When the previous step ends with no results, the algorithm checks the pixels above. Otherwise, the algorithm skips this step.

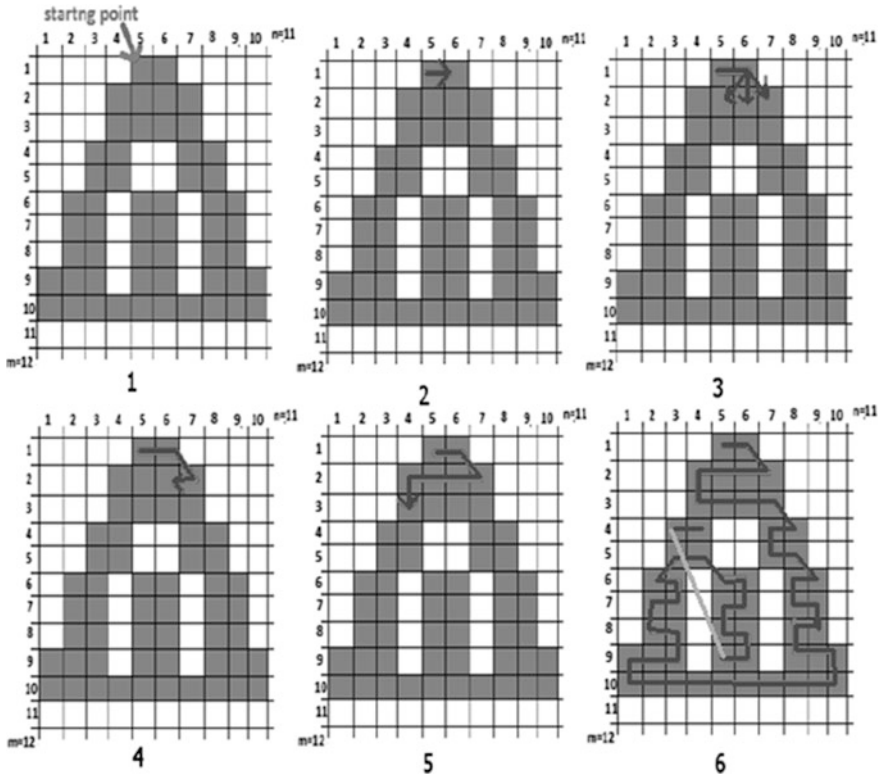


Fig. 2 An example of PGZZ algorithm

Step 9. Choose the pixel in the leftmost position (Fig. 2-5). If any of those pixels is available—i.e., it has not been visited yet the lower leftmost pixel is selected.

Step 10. Repeat the procedure. The algorithm repeats the steps from 2 to 9. This create ZigZag shaped path.

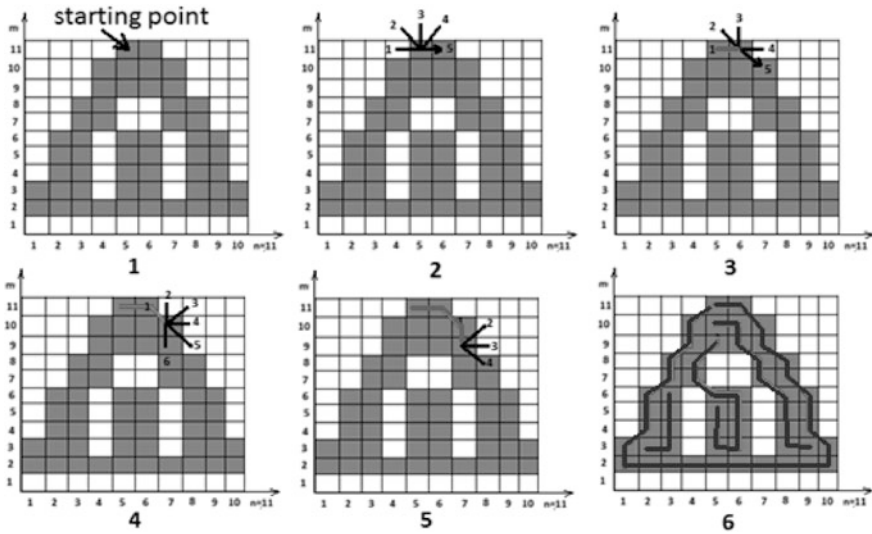


Fig. 3 An example of PGC algorithm

3.2 Path Generating Algorithm Based on Contour Strategy (PGC)

- Step 1. Begin from the first pixel in the top left corner, which is available to print. This pixel from now on is the starting pixel (Fig. 3-1).
- Step 2. Draw an imaginary line from the previous pixel. Then it rotates that imaginary line in clockwise direction till it finds next pixel which is available to print (Fig. 3-2). It starts drawing from 1 and checks till 5. The rest of the pixels are outside of the boundary.
- Step 3. Find the available pixel, the algorithm moves to this pixel and repeat step 2 (Fig. 3-3) Start drawing line from 1 and stop checking on 5.
- Step 4. If there are no available pixels, or algorithm finds again starting pixel, it ends searching contour and saves those pixels to sub-paths. If there are still pixels in layer go to step 1.

3.3 Path Generating Algorithm Based on Spiral Strategy (PGS)

This algorithm belongs to the radial sweep algorithm family, like PGC. The only difference between PGS and PGC is in the last step. Instead of ending the whole path as PGC, the algorithm PGS is continuing acting. When PGS finds the starting pixel, it does not stop but starts looking for the next pixel which belongs to the border.

3.4 Path Generating Algorithms Based on Fractal Strategy (PGFH and PGFP)







The difference between these two algorithms based on Fractal strategy is the curve which is to be used to create fractals. The first uses Hilbert curve [10] that way is called as Paths Generating Fractal Hilbert algorithm (PGFH). The second uses Peano curve [11], therefore is called as Paths Generating Fractal Peano algorithm (PGFP). The definition of fractal object says that fractal is rough or fragmented geometrical shape that can be sub-divided into parts, each of which is a reduced size copy of the whole [12]. The idea of using fractal curves in paths generating algorithms is to start those space filling curves from the minimum pixels. Moreover, the fractals have to grow till the layer will be inside of the fractal.

4 Experimentation System

When preparing the experiment design we took into consideration six different layers. All of these layers got different printing area. The tested objects are shown in Table 1—there are a very simple ones, as *t1.png*, and more complicated as *t6.png*. The first three layers are composed of one object without any holes or islands, but the next layers are more difficult for printing while possessing the holes and the islands.

The experiments were divided into two categories. The first category states the simulation experiments. We prepared the designed experimentation system, which contains as the hardware—the PC equipped with i5-3210M CPU 2.50 GHz and software. The software contains the implementations of the paths generating algorithms—they were written in Java programming language, in Eclipse IDE, version Kepler Service Release 2. The second category of experiments is the experiments made with a real 3D printer. The hardware part consists of the same elements like used for simulation, and additional elements, including Printron 2014.08.01 (software) and 3D printer equipped with RAMPS 1.4 with Marlin 1.0.2 firmware.

Table 1 The layers used in research

Layer ID	Shape	Horizontal (mm)	Vertical (mm)
t1.png		26.75	27.50
t2.png		45.25	48.50
t3.png		55.00	57.25
t4.png		70.00	65.75
t5.png		70.00	78.50
t6.png		184.00	90.25

5 Investigation

5.1 Simulation Experiment

Table 2 shows the results of the experiments for all path generating algorithms.

5.2 Physical Experiment

In the physical experiments, the paths found in the previous experiments were printed on the real device. In this test took part 5 layers. All printing processes were recorded by the video camera, what allowed a frame by frame analysis. The accuracy of such a method reaches 0.01 s when Smart Cutter Ver. 1.9.2f with Nikon COOLPIX S7000 camera was applied. Two indicators were considered: (i) the time of printing, (ii) the visual property of the printout. The obtained results of (i) are presented in Table 3.

Table 2 Comparison of paths generating algorithms—part I

Simulation experiment					
Layer	Algorithm	Time (s)	Path length (mm)	Layer size (mm ²)	Number of sub-paths
t1. png	PGFH	0.08	3564.71	2176.27	40
	PGFP	0.10	3696.51	2176.27	42
	PGS	0.09	3613.75	2176.27	1
	PGZZ	0.07	3559.10	2176.27	20
	PGC	0.10	3606.44	2176.27	1
t2. png	PGFH	0.12	4193.72	6492.58	57
	PGFP	0.18	4251.32	6492.58	69
	PGS	0.13	4752.70	6492.58	20
	PGZZ	0.10	3837.72	6492.58	36
	PGC	0.14	4702.29	6492.58	19
t3. png	PGFH	0.17	7133.15	9315.26	71
	PGFP	0.24	7072.67	9315.26	66
	PGS	0.22	7689.94	9315.26	9
	PGZZ	0.17	6995.36	9315.26	32
	PGC	0.22	7720.10	9315.26	9
t4. png	PGFH	0.34	14518.15	13616.04	272
	PGFP	0.41	14498.01	13616.04	258
	PGS	0.36	15206.17	13616.04	99
	PGZZ	0.30	13618.98	13616.04	101
	PGC	0.37	15321.88	13616.04	102
t5. png	PGFH	0.28	9950.81	16256.41	287
	PGS	0.28	13465.78	16256.41	124
	PGZZ	0.22	10470.43	16256.41	107
	PGC	0.29	13831.98	16256.41	128
t6. png	PGFH	1.26	55812.30	49127.19	530
	PGFP	1.80	55033.90	49127.19	443
	PGS	1.48	63849.14	49127.19	196
	PGZZ	1.08	50486.62	49127.19	35
	PGC	1.50	64122.41	49127.19	197

5.3 The Observed Relations

The time of processing in relation to the layer size. It can be observed that in the majority of cases all algorithms rise when the layer size grows. There is an exception from this rule and it appears for layer t5. In this case times of all algorithms bottom out. This can be explained by the low number of pixels which are printable in relation to all pixels. Next, it is evident that the shortest time of work of algorithm belongs to PGZZ. The biggest time had PHFP.

Table 3 Comparison of paths generating algorithms—part II

Physical experiments		
Layer	Algorithm	Time (s)
t1.png	PGFH	141.24
	PGFP	144.16
	PGS	123.04
	PGZZ	115.64
	PGC	123.28
t2.png	PGFH	160.76
	PGFP	164.64
	PGS	155.92
	PGZZ	132.08
	PGC	155.20
t3.png	PGFH	276.88
	PGFP	273.76
	PGS	261.76
	PGZZ	223.96
	PGC	262.28
t4.png	PGFH	557.60
	PGFP	555.00
	PGS	481.32
	PGZZ	434.96
	PGC	481.88
t5.png	PGFH	398.64
	PGFP	396.52
	PGS	361.68
	PGZZ	298.60
	PGC	366.15

The path length in relation to the layer size. The path length also grows when the layer size grows. That trend was expected. The algorithm which created the shortest paths is the PGZZ. The longest paths are created by: PGS and PGC. The fractal algorithms, in this case, have results in close agreement. The interesting is that the path length for layer t5 was for all of the algorithms bottom-up.

The sub-paths number in relation to the layer size. It can be observed that PGS and PGC created similar number of sub-paths. Moreover, those algorithms created the smallest value of this parameter for initial layers. For the complicated layers t5 and t6 PGZZ algorithm creates the smallest number of sub-paths. The algorithms with the biggest number of sub-paths are fractal algorithms. In this case the worst is fractal with Hilbert curve. This was expected, because fractal algorithms were adapting the shape of the object to the shape of the printed objects by deleting connection in the original paths.

The time of printing in relation to the layer size. It may be observed that, the fractals algorithms have the longest time of printing. However, the final path length of fractal algorithms was slightly shorter than paths found by PGC and PGS. This can be explained by the really short straight move of the printer without any turns in paths made by fractal algorithms and a lot of turns in whole final path. In paths made by PGC and PGS algorithms there are also a lot of turns, but the angles of those turns are not so big. In most cases it is less than or equal 45° . Also, their paths have much longer straight moves than in paths made by fractal algorithms. It is also evident that PGZZ is the algorithm that creates paths in the shortest printing time. On the other hand, paths made by fractal algorithms have the biggest printing time.

6 Conclusion and Final Remarks

The paths generating algorithms were tested on five layers with different levels of complexity. Three parameters were measured in the research: the final path length, the time of work of algorithm and sub-path which were found. Next, those paths were changed to GCode and printed on the 3D printer.

It may be concluded that the most efficient algorithm for 3D printing is the PGZZ. This algorithm founded much shorter paths than the rest of algorithms. Also, the time consuming for paths generating by PGZZ was one of the shortest. The results for fractal algorithms in this aspect were a little bit surprised and unexpected. Their final paths length was pretty short and the times required to find those paths, in case of Hilbert, were not so long. The results for paths made by PGFP curve were opposite to PGFH. The biggest disappointment in this aspect was related to the paths produced by PGS and PGC. The result of those paths was one of the worst, even though that for the simplest layers they seemed to be one of the best.

The research made gives us a lot of information, but there are many ideas for the feature work. For example, it can be supposed that printer can use different paths generating algorithms depending on the layer. To get necessary information, some more parameters of printout should be measured, such as the accuracy of printing, resistant for surface strength and tensile strength. Also, the speed of the printer should be tested for different algorithms. Next, the idea of feature work is to create the improved algorithms—the biggest disadvantages of PGZZ algorithm is that it can act in only one direction. In [13, 14], the authors showed that the proper direction can speed up printing. Such an improvement will be considered in our future work.

The experimentation system was tested as a good tool for the practical users. The system (simulator) is also serving as a tool for lab training and projects preparing for the MSc students in Wroclaw University of Technology.

Acknowledgment This work was supported by the statutory founds of the Dept. of Systems and Computer Networks, Wroclaw University of Technology, Poland.

References

1. Grimm, T.: User's Guide to Rapid Prototyping. Society of Manufacturing Engineers (2004)
2. Kulkarni, P., et. al.: A review of process planning techniques in layered manufacturing. *Rapid Prototyping J.* **6**, 18–35 (2000)
3. Farouki, R., et. al.: Path planning with offset curves for layered fabrication processes. *J. Manuf. Syst.* **14**, 355–368 (1995)
4. Wojcik, M.: Comparative analysis of algorithms for path finding in 3D printing. MSc. thesis, Report of Faculty of Electronics, Wroclaw University of Technology (2015)
5. Bogalinski, P., Davies, D., Koszalka, L., Pozniak-Koszalka, I., Kasprzak, A.: Evaluation of strip nesting algorithms: an experimentation system for the practical users. *J. Intel. Fuzzy Syst.* **27**(2), 611–623 (2014)
6. Misra, D., Sundararajan, V., Wright, P.K.: Zig-zag tool path generation for sculptured surface. In: *Geometric and Algorithmic Aspects of Computer-Aided Design and Manufacturing*, p. 265. American Mathematical Society (2005)
7. Park, S.C., Choi, B.K.: Tool-path planning for direction-parallel area milling. *Comput. Aided Design.* **32**, 17–25 (2000)
8. Rajan, V.T., Srinivasan, V., Tarabanis, K.A.: The optimal ZigZag direction for filling a two-dimensional region. *Rapid Prototyping J.* **7**(5), 231–240 (2001)
9. Wojcik, M., Pozniak-Koszalka, I., Koszalka, L., Kasprzak, A.: MZZ-GA algorithm for solving path optimization in 3D printing. In: *Proceedings to International Conference on Systems ICONS'15, Barcelona* (2015)
10. https://en.wikipedia.org/wiki/File:Hilbert_curve.svg
11. https://en.wikipedia.org/wiki/File:Peano_curve.svg
12. Chiu, W.K., Yeung, Y.C., Yu, K.M.: Toolpath generation for layer manufacturing of fractal objects. *Rapid Prototyping J.* **12**, 214–221 (2006)
13. Held, M.A.: *Geometry-Based Investigation of the Tool Path Generation for ZigZag Pocket Machine*. The Visual Computer, vol. 7, pp. 296–308. Springer, Berlin (1991)
14. Sarma, S.E.: the crossing function and its application to Zig-Zag tool paths. *Comput. Aided Des.* **31**(1), 881–890 (1991)

User Experience Design Based on Eye-Tracking Technology: A Case Study on Smartphone APPs

Qing-Xing Qu, Le Zhang, Wen-Yu Chao and Vincent Duffy

Abstract With the rapid development of mobile technology, smartphone has been becoming a part of our daily life. There are amounts of applications (APPs) developed for smartphone in the market, in order to meet the various needs of users. Recently, the user experience evaluation research of smartphone APPs is mainly based on subjective questionnaires, which might be relatively simple and lacking of the supporting evidence from objective data. This study aims at integrating subjective questionnaires and objective eye-tracking technology to evaluate user experience on instant message (IM) APPs. This study proposed that eye-tracking data could be used as objective criteria to evaluate user experience for smartphone APPs. A correlation model between smartphone APPs design variables and user experience was built based on Quantification Theory I.

Keywords User experience design · Smartphone APPs · Eye-tracking · Digital human modeling · Human factors

Q.-X. Qu (✉)
Department of Industrial Engineering, Northeastern University,
Shenyang 110819, People's Republic of China
e-mail: qqu@purdue.edu

Q.-X. Qu · L. Zhang · W.-Y. Chao · V. Duffy
School of Industrial Engineering, Purdue University, West Lafayette,
IN 47907, USA
e-mail: zhan1255@purdue.edu

W.-Y. Chao
e-mail: chaow@purdue.edu

V. Duffy
e-mail: duffy@purdue.edu

V. Duffy
Department of Agriculture and Biological Engineering, Purdue University,
West Lafayette, IN 47907, USA

1 Introduction

In recent years, smartphone APP design gets more and more attention both from industrial companies and academic researchers, which bring us not only great surprise but also abundant convenience to our daily life [1, 2]. The pros and cons of APP design directly affect the user experience, and large commercial interests of smartphone APPs encourage companies to continuously improve the performance of APPs [3]. However, the differentiation of functionality among same type smartphone APPs has been narrowed quickly in the competitive environment. To enhance the core competitiveness of smartphone APPs, improving the user experience has become an ideal option for companies. Recently, user experience evaluation research of smartphone APPs has been mainly based on the perspective of subjective questionnaires, which might be relatively simple and lacking of the support of objective evidence [4–6].

Given the above, in this paper, a systematic method was proposed to evaluate user experience, which integrated traditional subjective data collected by questionnaires and objective eye-tracking data collected by eye-tracking technology. A correlation model between smartphone APPs design variables and user experience was built. Hence, design recommendations for smartphone APPs can be concluded from the model.

In the following section, a systematic review of literature related to user experience and eye-tracking technology will be provided. The hypothesis of this study will be listed in section three. Section four describes the experimental design in detail. Section five is a scenario of the result of this study. Discussion and conclusion will be presented after section five.

2 Literature Review

In these days, user experience gets more and more attention from researchers in Human Computer Interaction (HCI), and been manifested as a quality of product design [7]. This experience recognized that user's needs go beyond functionality, and shift to experiential perspectives, not only contain usability, but also socio-cognitive and affective aspects of user experience such as pleasure, aesthetic experience, desire to reuse, positive feelings interacting with products and so on [7, 8]. The whole experience takes behavior, physiological reactions and psychological activities into account. A very official definition comes from ISO DIS 9241-210 [9]: "a person's perceptions and responses that result from the use or anticipated use of a product, system or service". Law et al. [10] pointed out that user experience measurement and its multiple definitions are two foundational issues and should be solved in tandem. But user experience subsumes a range of fuzzy, vague, elusive and ephemeral experience such as affective aspects, potential and intuitive feelings, or even without rational reasoning and hard to describe with words,

controversies and doubts about the definition and measurability of user experience are inevitable [10].

More and more research has applied eye-tracking method to product design by explaining the meaning of eye movements. Ares et al. [11] took food labels as examples, evaluated how consumers acquire information from food labels using eye tracking by analyzing eye movements (time to first fixation, percentage of consumers who fixated, total fixation duration, fixation count and visit count in each area of interest) when consumers directed their attention to selected areas. Their results discovered consumers' processing of food labels information, which can help designers understand how to grasp consumer' attention with a better visual display. Ho [12] investigated how people perceive handbags online with a task-free eye-tracking experiment. Participants were asked to look at randomly displayed pictures of handbags with predefined areas of interest. Their findings can provide eye-tracking evidence for the visual behavior of a consumer when he is looking at products online. Ho and Lu [13] found that pupil size can be measured to assess design product in emotional aspect. Positive and neutral products evoked significant pupil dilation than negative products. Although research was done on the visual perception of products, there is still a need in the study of information perception in real life, such as goal-oriented user experience and comparisons between different products displayed at the same time.

Kansei Engineering is also known as emotional/affective engineering, which aims at the development and improvement of products by translating the customer's emotional feelings into the domain of product design. It has been applied in user experience evaluation for product [14], website [15], mobile phone [16], and interface design [17]. Five senses, vision, hearing, smell, taste and skin, can present a person's feelings, emotions and intuition towards a certain object. Thus, Kansei engineering developed a triangulation approach to quantify and qualify an user's emotional responses in order to investigate the user responses gathered from questionnaires and eye tracking technique [18]. Aesthetic, physical, sensational and operational are four categories in Kansei concept for user experience evaluation. Semantic differential (SD) scale [15] and Likert scale [16] are commonly quantitative evaluation methods to collect user emotional condition of four Kansei categories. Combined with eye tracking feedback system, Kansei engineering extracts user experience factors from products to build scientific and high-efficient product evaluation standard system [14].

3 Hypotheses

When users are interested in using an APP, or in a stimulus, they usually give more attention to it, such as more fixation time and fixation duration [19, 20]. Various APPs combined with different design variables, result in different levels of user experience, arousing different affective emotional needs, which could make a significant effect on behavior performance [21]. Users with different occupations, age,

gender and culture, will pursue diverse user experience. How to design and improve an APP with better user experience may significantly add value to products both in theory and in practice [22]. Based on this motivation, some hypotheses are proposed.

- Hypothesis 1: User will give more attention to where they are interested in.
- Hypothesis 2: Various design levels on smartphone APPs can effectively affect user experience.
- Hypothesis 3: User experience has a positive effect on user behavior performance.
- Hypothesis 4: User characteristics (age, gender, nationality or others) have a moderating effect between design variables and user experience.

4 Methodology

4.1 Participants

The experiment targets at subjects who aged from 2 to 30. Those subjects are more likely to use smartphone IM APPs in their daily life. Participant who doesn't have experience with smartphone will be excluded from the experiment. The research requires at most 40 participants from 150 students who enrolled in IE 486 or IE 556.

4.2 Apparatus

The Tobii TX300 Eye Tracker, shown in Fig. 1, sets a new standard for remote eye trackers. Its unique combination of 300 Hz sampling rate with very high precision and accuracy, robust tracking and compensation for large head movements extends the possibilities for unobtrusive research of oculomotor functions and human

Fig. 1 Eye-tracking experiment



behavior by studying eye movements such as saccades and short fixations. It captures natural human behavior without the need for a chin-rest. Besides, Tobii TX300 offers maximum flexibility with numerous stimuli set-up and software options.

4.3 Stimuli

Eight instant messenger (IM) smartphone APPs (Available in App store and Google play) have been selected as experiment objects. The names of selected APPs are as shown below: Hangouts, Skype, WhatsApp, Line, Messenger, WeChat, QQ and Viber.

4.4 Eye-Tracking Measures

Fixation information can be used to measure the attention that individuals have paid to stimuli [23]. Fixation duration and fixation count are the most commonly used metrics to measure attention allocation. Stimuli with high levels of complexity provide diverse and numerous information cues that require considerable attention and time to view and comprehend [24]. So a complex stimulus will distract users' attention and trigger more fixations accordingly.

4.5 Procedure

All participant will firstly sign a consent form, and then, the experimenter will provide an instruction of the experiment. After the instruction, the subject will be first asked to sit in front a monitor with a Tobii Pro TX 300 Eye Tracker on it. The experimenter will ask the subject to adjust his seat and the distance to the monitor to make sure the eye-tracker sensor can read his eye movement. And then the subject will be asked to complete a calibration task. This would include staring nine points on the monitor. The experimenter may ask the subject to redo the calibration task until the eye-tracker can read the eye movements on all nine points. After the calibration, the experimenter will let the subject know when the experiment begins. During the experiment the subject will complete 2 tasks on eight different virtual IM APPs, the order of those APPs will be randomly given. The first task will ask the subject to search for a particular person in the contact list. The second task will ask the subject to send a message to that person. The subject is asked to repeat two tasks on each APP, every two tasks will take about 2 min. After every two task, the subject will be asked to fill in a subjective questionnaire to evaluate the user experience for that APP. The Tobii Pro TX 300 Eye Tracker will record the

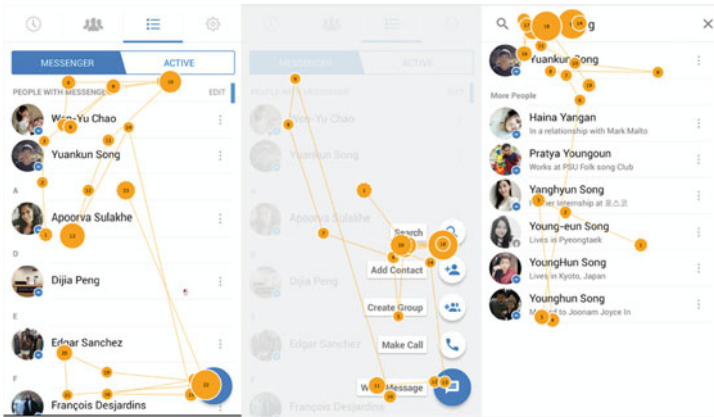


Fig. 2 An example of GazePlot for task 1 in Messenger APP

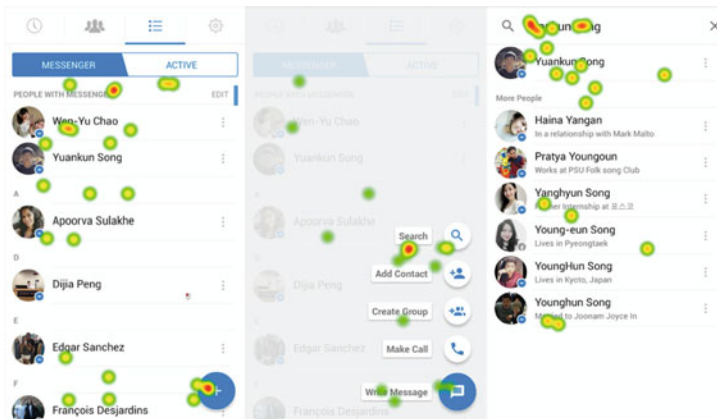


Fig. 3 An example of HeatMap for task 1 in Messenger APP

subject's eye movement during tasks, including Hit ratio in area of interest (AOI), Heat map, Scan path, First fixation location, Fixation duration, and Fixation count. After the subject completes the tasks, he will be asked to conduct a survey, including your age, gender, educational level, citizenship, the estimation of times he spend on a smartphone per day. After all tasks and questionnaires are completed, the subject needs to sign off the human subject log and exit the experiment. The subject could leave anytime if he has any known motion sickness or smartphone sickness problems during the experiment, and his data will be excluded from the study.

Two tasks (shown in Figs. 2, 3 and 4) have been designed for each APP. Participants need to complete two tasks and a follow up user experience evaluation questionnaire for each APP, refer it to Appendix.

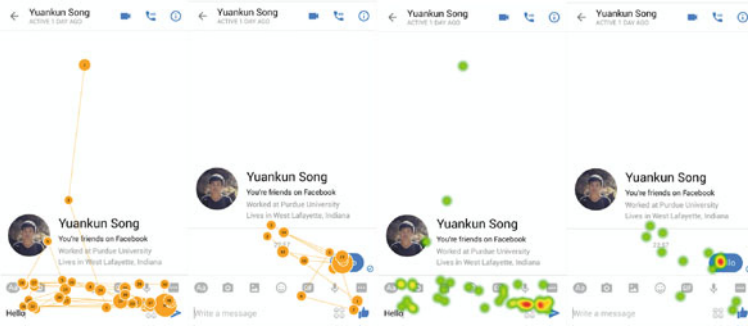


Fig. 4 An example of GazePlot and HeatMap for task 2 in Messenger APP

4.6 Eye-Tracking Outcomes

Use Messenger as an example, eye-tracker will collect data and establish a GazePlot and a HeatMap from participant’s eye movement, which can reflect users’ behavior, also provide some suggestions for companies if they want to improve the APP [25].

Task 1 In this mission, user will be asked to look for a friend from the contacts named “Yuankun Song”. Figures 2 and 3 show that how user browse the main interface to find the information. GazePlot can reflect the sequence how users browse the interface. HeatMap will be used for companies to analyze which part in the APP could arouse more attention from users.

Task 2 In this mission, user will be asked to open the message interface and type in “Hello” to “Yuankun Song”, using the “Message edit box”. GazePlot and HeatMap are shown in Fig. 4.

5 User Experience Evaluation: Quantification Theory I

5.1 Task 1

Search interface involves nine design variables as shown in Table 1. Each design variables can be divided into several levels, which could be encoded by “0–1” variables, in which way, we can get 8 representative objects encoding, as shown in Table 2.

A user experience evaluation model in search interface has been built using both eye tracking metrics and questionnaire-based data based on Quantification Theory I

Table 1 Design variables in search task

Interfaces	Design variables	Levels
Search (A)	Navigation location (A ₁)	Roof/bottom
	Labels in navigation (A ₂)	3/4/5 items
	Navigation styles (A ₃)	Figure/figure + text
	Navigation background (A ₄)	Dark/light
	Search box location (A ₅)	Roof/top-center/center
	Search styles (A ₆)	Figure/figure + text
	Portrait shapes (A ₇)	Circle/square
Click (B)	Click performance (B ₁)	Original/new interface
	History review (B ₂)	Yes/no

Table 2 0–1 encoding in search task design variables

Apps	Variables									
	A ₁₁	A ₁₂	A ₂₁	A ₂₂	A ₂₃	A ₃₁	A ₃₂	A ₄₁	A ₄₂	A ₅₁
Hangouts	0	1	1	0	0	0	1	0	1	0
Skype	0	1	0	0	1	0	1	1	0	0
WhatsApp	0	1	0	1	0	0	1	0	1	0
Line	1	0	1	0	0	1	0	0	1	0
Messenger	0	1	0	1	0	0	1	0	1	1
WeChat	0	1	0	1	0	0	1	1	0	1
QQ	1	0	0	0	1	1	0	0	1	1
Viber	0	1	0	0	1	0	1	1	0	0
Apps	Variables									
	A ₅₂	A ₅₃	A ₆₁	A ₆₂	A ₇₁	A ₇₂	B ₁₁	B ₁₂	B ₂₁	B ₂₂
Hangouts	1	0	1	0	1	0	0	1	1	0
Skype	1	0	1	0	0	1	1	0	0	1
WhatsApp	1	0	1	0	1	0	1	0	0	1
Line	1	0	1	0	0	1	1	0	0	1
Messenger	0	0	0	1	0	1	0	1	0	1
WeChat	0	0	0	1	1	0	1	0	0	1
QQ	0	0	0	1	1	0	1	0	0	1
Viber	0	1	1	0	0	1	0	1	0	1

[26, 27], as shown in Eq. (1). Y means user experience, which can be valued both questionnaire and eye tracking metrics. C is a constant in the model. The capital letters are design variables, while the lowercase letter mean their weights.

$$\begin{aligned}
 Y = C + & \begin{pmatrix} a_{11} & A_{11} \\ a_{12} & A_{12} \end{pmatrix} + \begin{pmatrix} a_{21} & A_{21} \\ a_{22} & A_{22} \\ a_{23} & A_{23} \end{pmatrix} + \begin{pmatrix} a_{31} & A_{31} \\ a_{32} & A_{32} \end{pmatrix} + \begin{pmatrix} a_{41} & A_{41} \\ a_{42} & A_{42} \end{pmatrix} \\
 & + \begin{pmatrix} a_{51} & A_{51} \\ a_{52} & A_{52} \\ a_{53} & A_{53} \end{pmatrix} + \begin{pmatrix} a_{61} & A_{61} \\ a_{62} & A_{62} \end{pmatrix} + \begin{pmatrix} a_{71} & A_{71} \\ a_{72} & A_{72} \end{pmatrix} + \begin{pmatrix} b_{11} & B_{11} \\ b_{12} & B_{12} \end{pmatrix} + \begin{pmatrix} b_{21} & B_{21} \\ b_{22} & B_{22} \end{pmatrix}
 \end{aligned}
 \tag{1}$$

5.2 Task 2

Chat interface involves ten design variables as shown in Table 3. Each design variables can be divided into several levels, which could be encoded by “0–1” variables, in the same way as the search interface, we can get 8 representative objects encoding, as shown in Table 4.

A user experience evaluation model in chat interface has been built using both eye tracking metrics and questionnaire-based data based on Quantification Theory I [26, 27], as shown in Eq. (2). Y means user experience, which can be valued both questionnaire and eye tracking metrics. C is a constant in the model. The capital letters are design variables, while the lowercase letter mean their weights.

Table 3 Design variables in chat task

Interfaces	Design variables	Levels
Main interface (C)	Search box (C_1)	Yes/no
	Portrait shapes (C_2)	Circle/square
	Time display (C_3)	Yes/no
Message interface (D)	Portrait display (D_1)	Yes/no
	Expression tools display (D_2)	Yes/no
	Time display styles (D_3)	Time/time + space
	Friend name location (D_4)	Medium/left
	Send key color is coincident with the background (D_5)	Yes/no
Interaction interface (E)	Editing state display (E_1)	Yes/no
	Sent key reshapes when message sent (E_2)	Yes/no

Table 4 0–1 encoding in chat task design variables

Apps	Variables									
	C ₁₁	C ₁₂	C ₂₁	C ₂₂	C ₃₁	C ₃₂	D ₁₁	D ₁₂	D ₂₁	D ₂₂
Hangouts	1	0	0	1	1	0	1	0	1	0
Skype	0	1	0	1	1	0	1	0	0	1
WhatsApp	0	1	0	1	1	0	1	0	0	1
Line	1	0	1	0	0	1	0	1	1	0
Messenger	1	0	0	1	1	0	1	0	1	0
WeChat	1	0	0	1	1	0	1	0	1	0
QQ	1	0	1	0	1	0	1	0	1	0
Viber	0	1	0	1	1	0	1	0	1	0

Apps	Variables									
	D ₃₁	D ₃₂	D ₄₁	D ₄₂	D ₅₁	D ₅₂	E ₁₁	E ₁₂	E ₂₁	E ₂₂
Hangouts	1	0	1	0	0	1	1	0	1	0
Skype	1	0	1	0	1	0	0	1	0	1
WhatsApp	1	0	1	0	0	1	0	1	1	0
Line	1	0	0	1	1	0	0	1	1	0
Messenger	1	0	0	1	0	1	1	0	1	0
WeChat	1	0	1	0	0	1	1	0	1	0
QQ	1	0	0	1	0	1	0	1	1	0
Viber	0	1	0	1	0	1	1	0	1	0

$$\begin{aligned}
 Y = C &+ \begin{pmatrix} c_{11} & C_{11} \\ c_{12} & C_{12} \end{pmatrix} + \begin{pmatrix} c_{21} & C_{21} \\ c_{22} & C_{22} \end{pmatrix} + \begin{pmatrix} c_{31} & C_{31} \\ c_{32} & C_{32} \end{pmatrix} + \begin{pmatrix} d_{11} & D_{11} \\ d_{12} & D_{12} \end{pmatrix} + \begin{pmatrix} d_{21} & D_{21} \\ d_{22} & D_{22} \end{pmatrix} \\
 &+ \begin{pmatrix} d_{31} & D_{31} \\ d_{32} & D_{32} \end{pmatrix} + \begin{pmatrix} d_{41} & D_{41} \\ d_{42} & D_{42} \end{pmatrix} + \begin{pmatrix} d_{51} & D_{51} \\ d_{52} & D_{52} \end{pmatrix} + \begin{pmatrix} e_{11} & E_{11} \\ e_{12} & E_{12} \end{pmatrix} + \begin{pmatrix} e_{21} & E_{21} \\ e_{22} & E_{22} \end{pmatrix}
 \end{aligned}
 \tag{2}$$

6 Discussion

Current methods, techniques and tools for user experience evaluation and measure are mainly drawn from usability research [7]. Among them, questionnaire with meaningful variables of products such as usability, emotion, and aesthetic and so on is one of the most versatile approach [28]. After assigning weights to each measure from questionnaires, the overall score for user experience can be easily calculated.

The Quantification Theory I is suggested as an alternative to those approaches described above [7]. Data collected from traditional methods is easily affected by the respondent’s surroundings, voluntary participation, difficulty of comparisons among product, false feeling of their inner state, or even give stated opinions object

wanted [29]. The results of such a survey will not always convey the truth of information, and then mislead the design [13].

As a physiological measurement, vision measure can effectively provide information about a product [30]. As stated by Davenport, “The eyes don’t lie. If you want to know what people are playing attention to, follow what they are looking at” [31]. The most of the feelings that are elicited by a product are mediated by initial visual perception. In addition, vision has been considered as the most important sense in the product-buying experience [32]. Research that focuses on eye movement of users has been widely applied in web design, advertisement, and brand extension. Wedel and Pieters [33] pointed out that more research is needed in product, brand packages and so on.

In order to improve APPs to meet various emotion needs from users, there is a need to select critical eye tracker metrics, which not only reflects the user experience significantly, but also serves as a novel tool for APP designer, to evaluate use experience. Future study may resolve the concept model built in Sect. 5 by applying analytic hierarchy process, structure equation modeling, partial least squares regression, and neural networks. Due to the complexity of the human cognition, how to obtain the optimal results deserves more discussion in the future.

7 Conclusion

Eye tracking technology had been proposed as an approach to collect objective data for user experience on smartphone APPs in this study. This approach can reduce the bias in subjective questionnaire-based measure of user experience. The proposed model can be used to detect weights for design variables for user interface design. Design variables that are assigned with higher weight (with more eye fixation) reveal sections that can attract more attention, which need to be redesigned to triumph over other competitors.

Acknowledgments This work was conducted in and supported by Discovery & Learning Research Center, Purdue University. Authors are grateful for the staffs and those shown in Figs. 1, 2, 3 and 4 for their permission to show their likeness in this article.

References

1. Park, J., Han, S.H., Kim, H.K., Oh, S., Moon, H.: Modeling user experience: a case study on a mobile device. *Int. J. Ind. Ergon.* **43**, 187–196 (2013)
2. Anuar, J., Musa, M., Khalid, K.: Smartphone’s application adoption benefits using mobile hotel reservation system (MHRS) among 3 to 5-star city hotels in Malaysia. *Procedia-Soc. Behav. Sci.* **130**, 552–557 (2014)

3. de la Vega, R., Roset, R., Castarlenas, E., Sánchez-Rodríguez, E., Solé, E., Miró, J.: Development and testing of painometer: a smartphone app to assess pain intensity. *J. Pain*. **15**, 1001–1007 (2014)
4. Chorianopoulos, K., Geerts, D.: Introduction to user experience design for TV Apps. *Entertain. Comput.* **2**, 149–150 (2011)
5. Haverila, M.: Mobile phone feature preferences, customer satisfaction and repurchase intent among male users. *Australas. Mark. J.* **19**, 238–246 (2011)
6. Engl, S., Nacke, L.E.: Contextual influences on mobile player experience—a game user experience model. *Entertain. Comput.* **4**, 83–91 (2013)
7. Law, E.L.-C., van Schaik, P.: Modelling user experience—an agenda for research and practice. *Interact. Comput.* **22**, 313–322 (2010)
8. Hassenzahl, M., Tractinsky, N.: User experience-a research agenda. *Behav. Inf. Technol.* **25**, 91–97 (2006)
9. ISO 9241-210: Ergonomics of human-system interaction—part 210: human-centred design for interactive systems. http://www.iso.org/iso/catalogue_detail.htm?csnumber=52075 (2010)
10. Law, E.L.-C., van Schaik, P., Roto, V.: Attitudes towards user experience (UX) measurement. *Int. J. Hum Comput Stud.* **72**, 526–541 (2014)
11. Ares, G., Giménez, A., Bruzzone, F., Vidal, L., Antúnez, L., Maiche, A.: Consumer visual processing of food labels: results from an eye-tracking study. *J. Sens. Stud.* **28**, 138–153 (2013)
12. Ho, H.-F.: The effects of controlling visual attention to handbags for women in online shops: evidence from eye movements. *Comput. Human Behav.* **30**, 146–152 (2014)
13. Ho, C.-H., Lu, Y.-N.: Can pupil size be measured to assess design products? *Int. J. Ind. Ergon.* **44**, 436–441 (2014)
14. Xiao, W., Cheng, J., Wang, X., Ye, J., Xi, L.: Analysis on universality evaluation standard system of product design on basis of Kansei Engineering and virtual reality. In: *HCI International 2015-Posters' Extended Abstracts*, pp. 439–443. Springer, Berlin (2015)
15. Goh, K.N., Chen, Y.Y., Daud, S.C., Sivaji, A., Soo, S.T.: Designing a checklist for an e-commerce website using Kansei Engineering. In: *Advances in Visual Informatics*, pp. 483–496. Springer, Berlin (2013)
16. Chen, K., Chiu, S., Lin, F.: Kansei design with cross cultural perspectives. *Usability Int. HCI Cult.* 47–56 (2007)
17. Ramakrisnan, P., Jaafar, A., Yatim, N.F.B.M.: Designing online discussion site (ODS) user interface for emotional user experiences: a proposed Kansei triangulation method. *J. Softw.* **8**, 3238–3245 (2013)
18. Ramakrisnan, P., Jaafar, A., Yatim, N.F.B.M.: Emotional user experiences in discussion board design: Kansei methodological triangulation approach. In: *2012 International Conference on Computer & Information Science (ICCIS)*, pp. 1073–1077. IEEE (2012)
19. Hutton, S., Crawford, T., Gibbins, H., Cuthbert, I., Barnes, T., Kennard, C., Joyce, E.: Short and long term effects of antipsychotic medication on smooth pursuit eye tracking in schizophrenia. *Psychopharmacology* **157**, 284–291 (2001)
20. Godijn, R., Theeuwes, J.: Programming of endogenous and exogenous saccades: evidence for a competitive integration model. *J. Exp. Psychol. Hum. Percept. Perform.* **28**, 1039 (2002)
21. Zain, N.H.M., Razak, F.H.A., Jaafar, A., Zulkipli, M.F.: Eye tracking in educational games environment: evaluating user interface design through eye tracking patterns. In: *Visual Informatics: Sustaining Research and Innovations*, pp. 64–73. Springer, Berlin (2011)
22. Kim, B., Dong, Y., Kim, S., Lee, K.-P.: Development of integrated analysis system and tool of perception, recognition, and behavior for web usability test: with emphasis on eye-tracking, mouse-tracking, and retrospective think aloud. In: *Usability and Internationalization. HCI and Culture*, pp. 113–121. Springer, Berlin (2007)
23. Vertegaal, R., Ding, Y.: Explaining effects of eye gaze on mediated group conversations: amount or synchronization? In: *Proceedings of the 2002 ACM Conference on Computer Supported Cooperative Work*, pp. 41–48. ACM (2002)

24. Deng, L., Poole, M.S.: Affect in web interfaces: a study of the impacts of web page visual complexity and order. *Mis Q.* 711–730 (2010)
25. Nielsen, J., Pernice, K.: *Eyetracking Web Usability*. New Riders (2010)
26. Qu, Q.-X.: Kansei knowledge extraction based on evolutionary genetic algorithm: an application to e-commerce web appearance design. *Theor. Issues Ergon. Sci.* **16**, 299–313 (2015)
27. Guo, F., Qu, Q., Chen, P., Ding, Y., Liu, W.L.: Application of evolutionary neural networks on optimization design of mobile phone based on user's emotional needs. *Hum. Factors Ergon. Manuf. Serv. Ind.* **26**, 301–315 (2015)
28. Vermeeren, A.P.O.S., Law, E.L.-C., Roto, V., Obrist, M., Hoonhout, J., Väänänen-Vainio-Mattila, K.: User experience evaluation methods: current state and development needs. In: *Proceedings of the 6th Nordic Conference on Human-Computer Interaction: Extending Boundaries*, pp. 521–530. ACM (2010)
29. Ariely, D., Berns, G.S.: Neuromarketing: the hope and hype of neuroimaging in business. *Nat. Rev. Neurosci.* **11**, 284–292 (2010)
30. Schifferstein, H.N.J., Desmet, P.M.A.: The effects of sensory impairments on product experience and personal well-being. *Ergonomics* **50**, 2026–2048 (2007)
31. Davenport, T.H., Beck, J.C.: *The Attention Economy: Understanding the New Currency of Business*. Harvard Business Press (2013)
32. Fenko, A., Schifferstein, H.N.J., Hekkert, P.: Looking hot or feeling hot: what determines the product experience of warmth? *Mater. Des.* **31**, 1325–1331 (2010)
33. Wedel, M., Pieters, R.: A review of eye-tracking research in marketing. *Rev. Mark. Res.* **4**, 123–147 (2008)

When Feedback Loops Collide: A Complex Adaptive Systems Approach to Modeling Human and Nature Dynamics

Zining Yang, Patrick deWerk Neal and Mark Abdollahian

Abstract In the context of sustainable development, complex adaptive systems frameworks can help address the coupling of macro social, environmental and economic constraint and opportunity with individual agency. Using a simple evolutionary game approach, we fuse endogenously derived socio-economic system dynamics from human and nature dynamics (HANDY) theory with Prisoner's Dilemma spatial intra-societal economic transactions. We then create a new human and nature dynamics agent based model to explore technological progression on population dynamics, economic development, social inequality and use of resources. We investigate the impact of technology proliferation on communications ease and the resulting compression of social space on individual wealth and societal sustainability. Our initial result shows complex adaptive or evolutionary systems approaches are necessary to understand both near and potentially catastrophic, far-from-equilibrium behavior and societal outcomes across all scales of human behavior and dynamics.

Keywords Sustainable development · Complex adaptive systems · Population dynamics · Agent-based modeling · System dynamics · Game theory

Z. Yang (✉) · P.d. Neal · M. Abdollahian
Claremont Graduate University, Claremont, CA 91711, USA
e-mail: zining.yang@cgu.edu

P.d. Neal
e-mail: patrick.d.neal@gmail.com

M. Abdollahian
e-mail: mark.abdollahian@cgu.edu

Z. Yang
La Sierra University, Riverside, CA 92505, USA

1 Introduction

From global warming to terrorism, there are widespread concerns that the current relationship between human and natural environment is unsustainable [1, 2] and the development process is likely to be punctuated and disrupted by short, sharp collapses that may fester and only amplify the dynamism of social forces [3–5]. The history of Mesopotamia—the very cradle of civilization, agriculture, complex society, and urban life—presents a series of rise-and-declines [6, 7]. In neighboring Egypt, this cycle also appeared repeatedly, while similar pattern of rise and collapse also occurred repeatedly in India [8], as well as the rise and fall of the Greeks, Romans and Maya among countless other societies. Scholars argue that despite the impression that societal collapse is rare, the emergent process is recurrent in history, and across the world in its distribution [3, 5, 9]. More specifically, according to Turchin and Nefedov [10] and Motesharrei et al. [1], there is a great deal of support for the hypothesis that secular cycles—demographic, social and political oscillations of a centuries long period are the norm rather than an exception. This begs the question of whether civilization and the modernization process in particular, is equally susceptible given the interdependence of economic development, migration and conflicts seen globally today.

Social scientists have long identified dynamic linkages between economic development, population dynamics, and environment [1, 11, 12]. Starting in ecological economics, the human and nature dynamics (HANDY) perspective is a quantitative, trans-disciplinary approach to understanding modernization and development through interdependent economic and social forces at the aggregate society level. Here we extend previous work by Motesharrei's [1] novel systems dynamic representation of the theory at the societal level towards integrated macro-micro scales in a complex adaptive systems framework using an agent based approach. As macroscopic structures emerging from microscopic events lead to entrainment and modification of both, co-evolutionary processes are created over time [13]. Similar to Abdollahian et al. [14–16] and Yang [17], we posit a new, approach where agency matters: individual game interactions, strategy decisions and outcome histories determine an individual's experience. These decisions are constrained or incentivized by the changing macro economic, cultural, social and political environment via human and nature dynamics theory, conditioned on individual attributes at any particular time. Emergent behavior results from individuals' current feasible choice set, conditioned upon past behavior and macro outcomes. Conversely, progress on economic development, the formation of cultural mores, societal norms and democratic preferences emerge from individuals' behavior interactions.

In order to create a robust simulation [18] platform, first we instantiate a system of equations that capture the core logic of HANDY macro-social theory. Second we fuse HD endogenous systems to agent attribute changes with a generalizable, non-cooperative Prisoner's Dilemma game following Axelrod [19–21] and Nowak and Sigmund [22, 23], to simulate intra-societal, spatial economic transactions.

Understanding the interactive demographic, social and political effects of macro-socio dynamics and individual agency in intra-societal transactions are key elements of a complex adaptive systems approach. Finally, we explore the model's initial behavioral dynamics via simulation methods to identify paths and pitfalls towards sustainable development.

2 HANDY Background

HANDY postulates a development process in which inequality and use of resources play a critical role. Brander and Taylor [24] developed an ancestor model of population and renewable resource dynamics and demonstrated that reasonable parameter values can produce cyclical feast and famine patterns of population and resources. Their model shows that a system with a slow-growing resource base will exhibit overshooting and collapse, whereas a more rapidly growing resource base will produce an adjustment of population and resources toward equilibrium values. However, this approach does not include a central component of population dynamics: economic stratification and the accumulation of wealth.

Inspired by a Lotka-Volterra model at the core, Motesharrei et al. [1] develop a human population dynamics model by adding accumulated wealth and economic inequality. They develop and measure “carrying capacity” and show it to be a potentially practical means for early detection of collapse. When a population surpasses the carrying capacity, starvation or migration can threaten to significantly impact population levels and rates of change. However, humans can also accumulate wealth and then draw down resources when production cannot match consumption needs. Empirically, they posit that accumulated surpluses are not evenly distributed throughout society. As elites control resources normally, they could leave the mass of the population, while producing a portion of generated wealth, with only a small portion of it usually at or just above subsistence levels [25, 26]. While the Brander–Taylor model has only two equations, Motesharrei et al's model adds an additional two equations to predict the evolution of nature, accumulated wealth, elites and commoners as an interdependent, asymmetric first order system. Their HANDY equations are given by:

$$\begin{cases} \dot{x}_C = \beta_C x_C - \alpha_C x_C \\ \dot{x}_E = \beta_E x_E - \alpha_E x_E \\ \dot{y} = \gamma y(\lambda - y) - \delta x_C y \\ \dot{w} = \delta x_C y - C_C - C_E. \end{cases} \quad (1)$$

In this system of equations, the total population is divided between the two variables, x_C and x_E , representing commoners and of elites respectively. The population grows at a birth rate β and decreases at a death rate α . In their model, β is assumed to be constant for both elites and commoners but α depends on wealth.

The equation for nature includes a regeneration or gain term $\gamma_y (\lambda - y)$, and a depletion or loss term $-\delta xCy$. Technological change can make the use of resources more efficient, but it also tends to raise both per capita resource consumption as well as resource extraction scales. Thus accumulated wealth increases with production, δxCy , and decreases with the consumption of the elites and the commoners

3 An Agent-Based, Complex Adaptive Systems Approach

While innovative in formalizing a systems approach for HANDY theory, a limitation of Motesharrei et al.'s [1] work lacks coupling and interdependence across human scales, from individuals to institutions and finally the societal outcomes they generate. Inspired by Motesharrei et al., our agent-based, complex adaptive systems HANDY model uniquely combines the interactive effects and feedbacks between individual human agency as well as the macro environmental constraints and opportunities that change over time for any given society. Decisions by individuals, including both elites and commoners, are affected by other individuals, social context, and system states, including accumulated wealth and resources. These decisions have variegated first and second order effects, given any particular system state or individual attributes. Such an approach attempts to increase both theoretical and empirical verisimilitude for some key elements of complexity processes, emergence, connectivity, interdependence and feedback [27] found across all scales of development.

Implemented in NetLogo [28], our model consists of three modules for the macro, meso and micro scales in complex systems. We maintain individual agent attribute relationships and postulated changes of birth rate and death rate for both commoners and elites following HANDY theory. These individual agent attributes impact how intra societal economic transaction games occur, either increasing or decreasing individual wealth and at increasing scales, ultimately societal productivity [29]. Thus we create heterogeneously mixed populations that cooperate and compete in a changing ecological and economic backdrop to model social co-evolutionary processes.

After capturing endogenous individual agent processes, we aggregate individual attributes from both elites and commoners to update accumulated societal wealth, which increases with productivity and decreases with consumption. Following the predator-prey mechanism and the original HANDY design, we model the consumption of the commoners to be a subsistence salary per capita, multiplied by the working population. The consumption of Elites is x times larger than the commoners', which represents the division of the output between elites and commoners, reflecting balance of class power between the two groups, as well as and the capacity of each group to organize and pursue their economic interests. This can easily be thought of as the top X % of society's population control Y % of wealth.

When the wealth level drops below the threshold to pay for consumption, payments are reduced and eventually stopped, and death rates start to increase dramatically.

In the last module, we incorporate evolutionary game theory to provide insights to understanding individual, repeated societal transactions in heterogeneous populations [30–32]. Social co-evolutionary systems allow each individual to either influence or be influenced by all other individuals as well as macro society [14–16, 33, 34], perhaps eventually becoming coupled and quasi-path interdependent. We have mixed populations of elites and commoners with explicit spatial contact networks, given population density, technology diffusion and agent attributes. Thus we explicitly recognize that the differential impact of heterogeneous, spatial structures matters in sustainable development. This design captures various individual preferences and relative socioeconomic attributes.

Accordingly, we instantiate a non-cooperative, socio-economic Prisoner's Dilemma (PD) transaction game given agent i 's attribute vector (A^i) of individual agent attributes similarity to agent j (A^j) for any A^{ij} pairs. The motivation behind this is that individuals are more likely to interact, engage and conduct transactions with other agents of similar norms [35] and produce different co-evolutionary behavior via frequency and rate dynamics [36]. To allow complexity, nonlinear and emergent behavior, we first randomly choose 50 % of spatially proximal agents as sources who can choose a partner at each iteration t . The remaining targets are chosen by other agents based on symmetric preference rankings and asymmetric neighborhood proximity distributions. Following Abdollahian et al. [14–16] and Yang [17], we explore communications reach, social connectivity and technology diffusion that constrains the potential set of A^{ij} game pairs through talk-span. Low values of talk-span constrain games to local neighborhoods among spatially proximate agents, while higher values expand potential A^{ij} pairs globally, modeling socially compressed space. This captures communications and technology diffusion for frequency and social tie formation [37]. It also reflects recent work on the importance of both dynamic strategies and updating rules based on agent attributes affecting co-evolution [38, 39]. Shorter attribute distances increase the probability that A^{ij} will enter into a socio-economic transaction and play the PD game. After each source agent calculates its probability of playing a game with all possible target agents, it chooses the target with the highest probability as its partner. Target agents also repeat the same process symmetrically. We then choose the A^{ij} pairing with the highest probability derived from its preference-proximity function at a particular iteration.

In the next step, agents who decide to play the socio-economic transaction game choose whether to cooperate or to defect, given the type of relationship they are in with the opponent: a cooperative relationship or a coercive relationship. Regardless of agent type, the relative wealth of two players is the determinant factor of the type of relationship. In other words, there can be cooperative relationship between an elite and a commoner, and also coercive relationship between two elites or two commoners, though it is more likely that an elite and a commoner are in a coercive relationship, and two agents of the same group are having a cooperative

relationship. Both agents select strategies probabilistically based on similarity of attributes. Relative payoffs for each agent are based on simple PD, non-cooperative game theory [22, 23, 40], with the cost as a function of the wealth ratio between elites and commoners.

We specifically model socio-economic transaction games as producing either positive or negative values to capture both upside gains or downside losses. Subsequently, A^{ij} games' V^{ij} outcomes condition agent W_{t+1}^i values, modeling realized costs or benefits from any particular interaction. The updated $W_{t+1}^i = W_t^i + A^{ij}$ game payoff for each agent subsequently gets added to the individual's attributes for the next iteration. We then repeat individual endogenous processing, aggregated up to society as a whole and repeat the game processes for $t + n$ iterations.

Aggregated wealth gets transformed into macro-society levels and impacts nature consistent with standard ecological economics as involving both inputs from, and outputs to nature, through depletion of natural sources and carrying capacity. The sum of all prior individual behavioral histories, evolutionary through iterations, does contribute to each individual and societal current states as an initial effort at a scale integrated framework. Thus agents simultaneously co-evolve as strategy pair outcomes at t to impact W^i at $t + 1$, thus driving both positive and negative feedback process through $t + n$ iterations. These shape A^i attributes which spur adaptation to a changing environment. Feedback into subsequent A^{ij} game selection networks and strategy choice yields a complex adaptive system representation across multiple scales.

4 Results

Figure 1 depicts our HANDY interface and a single sample run. The interface shows physical output space—heterogeneously mixed agents distributed spatially, where agent size indicates mean economic wealth W from populations, and agent color represents carrying capacity. A^{ij} game transactions V^{ij} are shown as links at each t and link color indicates different types of relationship. Solid circles are independent agents; hollow circles are agents paying tribute in a negative sum game to another agent. Red links indicate coercive relationships while blue links indicate cooperative relationships. For all agents' attributes, we setup initial conditions for population, elite commoner ratio, and techno-social connectivity via talk-span. Although not detailed herein, we also parameterize different agent birth and death rates and probability of game interactions in addition to strategies that can be randomized individually or in combinations to isolate dynamics in any specific subcomponent module.

Plots on the right bottom include time series for the core variables nature, wealth, elite population, and commoner population. The top right plot counts the number of

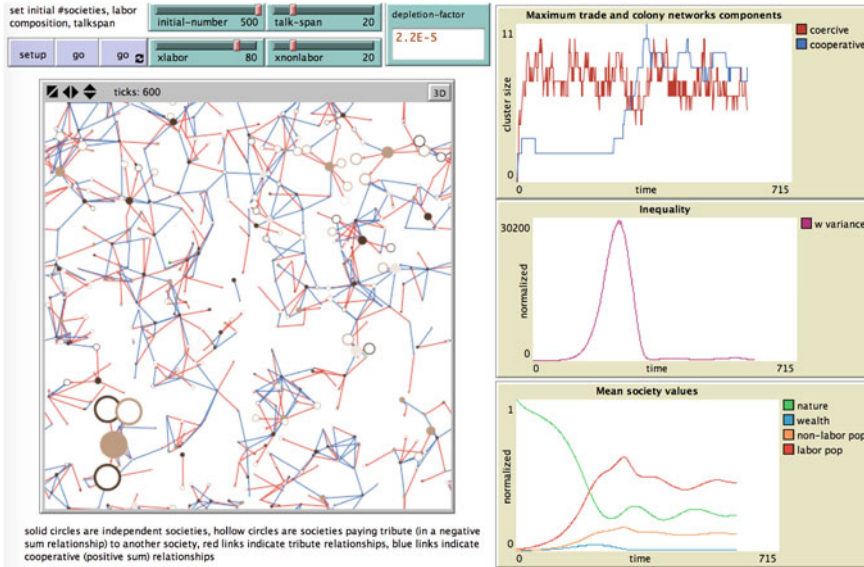


Fig. 1 NetLogo interface

cooperative relationship and coercive relationship; while the middle plot shows level of inequality measured by variance in wealth from all agents. This allows us to trace the development of wealth, income inequality, cultural dispositions, and political polarization. Besides the number of transactions games, the percentage of population interacting, and the number of different cooperative, mixed, or non-cooperative strategy pairs under different macro environmental conditions, we also track the evolution of network in the society.

We detail the result from our notional run in Fig. 2. Here a lesser developed society with 500 agents with decent communication technology develops more cooperative relationship than coercive relationship. Individual productivity and wealth, driven by successful cooperative strategy outcomes of individual transactions, help accelerate the emergence of network with more cooperative links. Spatial details at $t = 1, 100, 200, 300, 400$ and 500 snapshots are shown.

Initially, we find our society with low level of inequality or polarization along wealth continuum, resulting in cooperative relationship across the society, and nature's carry capacity starts at a high level. By $t = 100$, agents increase in individual wealth though more coercive relationships are found in economic transaction games played between individuals. By $t = 200$, we see continued heterogeneously mixed populations in terms of wealth level and choice in socio-economic transaction games. On average, agents who are independent seem to have more wealth than those who are punished from a coercive relationship. By $t = 300$, cooperative network starts to emerge. As a consequence, individual wealth gets accumulated to a

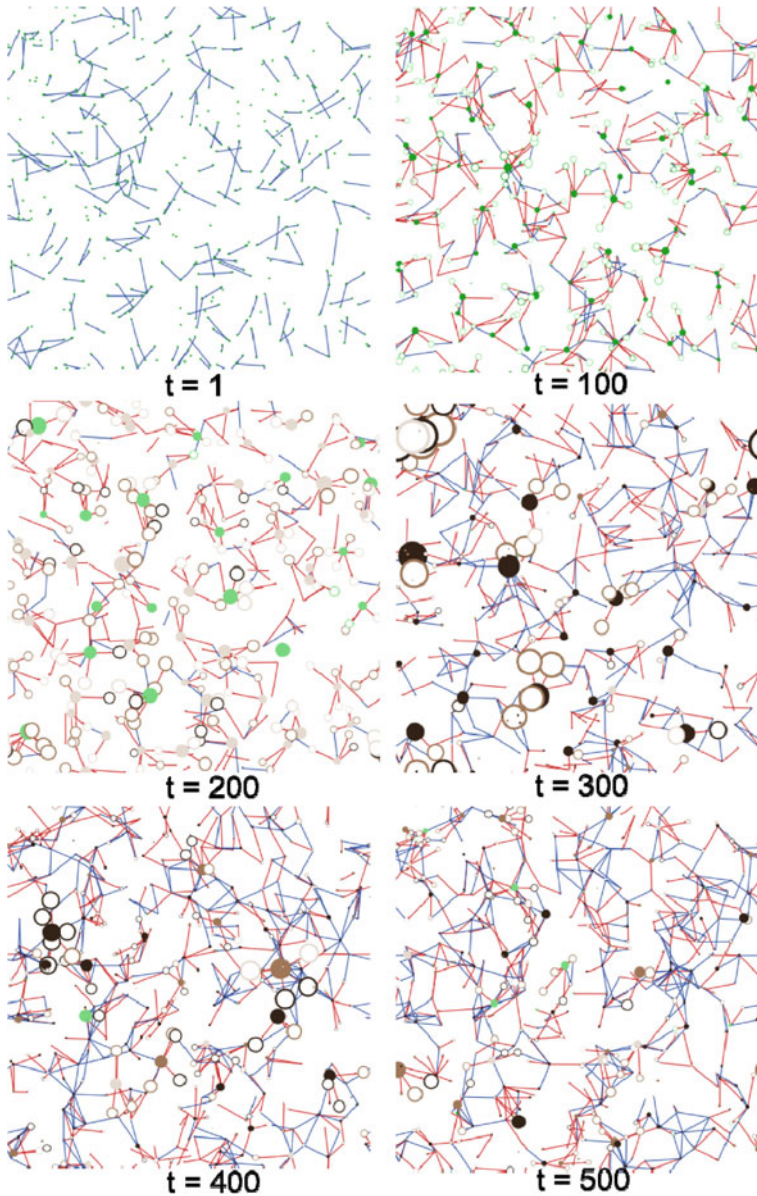


Fig. 2 Network evolution at $t = 1, 100, 200, 300, 400$ and 500

much higher level. By $t = 400$ and $t = 500$, the network becomes slightly denser, but with less wealthy agents, as negative relationship which leads to loss of wealth also emerges from the evolution. Although just one particular simulation, what is critical is that co-evolutionary behavior results in path dependence of economic and social

change as a key determinant for sustainable development outcomes. Moreover, as can also be seen from Fig. 1, the number of cooperative relationship and the number of coercive relationship between pairs of agents change in cycles.

5 Discussion

In the context of sustainable development, the complex adaptive systems framework can help address the coupling of nature constraint and opportunity with population dynamics and individual agency. Using a simple evolutionary game approach under a predator-prey framework, we fuse socio-economic system dynamics from human and nature dynamics (HANDY) theory with Prisoner's Dilemma spatial intra-societal economic transactions. We then create a new human and nature dynamics agent-based model to explore technological progression on population dynamics, economic development, social inequality, and use of resources. We investigate the impact of technology proliferation on communications ease and the resulting compression of social space on individual wealth and sustainability of societies. Our initial result shows complex adaptive or evolutionary systems approaches are necessary to understand both near and potentially catastrophic, far-from-equilibrium behavior and societal outcomes across all human and nature dynamics.

From a complex adaptive system perspective on HANDY theoretical processes, economic progress is a necessary condition for successful sustainable development and balance between human and nature. We find that inequality strongly impact economic growth and speed up the pace of development. Exploring the impact of societal conditions on transactions, compressing techno-social space by increased spatial proximity promotes co-evolutionary connection and mutual cooperation. Turning to the path dependence of development trajectories, our results show cycles in the number of cooperative relationship and coercive relationship.

Our next research step is to thoroughly empirically verify the entire HANDY model with real world data. Once validated, we will conduct sensitivity analysis as well as experiments to explore the conditions that lead to sustainable development or collapse. Another extension is to incorporate agent memory and learning following Quek et al. [41] and multi-player PD from evolutionary game theory to map the complex transaction networks that emerge over time. Another is to tackle far-from-equilibrium challenges by exploring the full dynamic characteristics of both ecological systems and human society. Key will be identifying behavioral symmetry breaks and formally testing for catastrophic or chaotic responses.

While only an initial, rough approximation at the complex, interdependent and highly nonlinear nature of ecological economics, our agent-based approach provides insights into the interactivity of individual agency, societal and ecological outcomes seen through the lens of evolutionary games. We hope such work motivates others to extend potential inquiries and insights with even greater

theoretical fidelity and empirical resolution. Perhaps complex adaptive system simulations like HANDY can assist policy makers and scholar alike, to better understand, anticipate and shape positive development outcomes for all.

References

1. Motesharrei, S., Rivas, J., Kalnay, E.: Human and nature dynamics (HANDY): modeling inequality and use of resources in the collapse or sustainability of societies. *Ecol. Econ.* **101**, 90–102 (2014)
2. Catton, W.R.: *Overshoot: The Ecological Basis of Revolutionary Change*. University of Illinois Press (1982)
3. Goldstein, J.S.: *Long Cycles: Prosperity and War in the Modern Age*, p. 268. Yale University Press, New Haven (1988)
4. Meadows, D.H., Meadows, D.L., Randers, J., Behrens, W.W.: *The Limits to Growth*, p. 102. New York (1972)
5. Tainter, J.A.: *The collapse of complex societies* (1988)
6. Redman, C.L., James, S.F., Paul, D.R.J. (eds.): *The Archaeology of Global Change: The Impact of Humans on Their Environment*. Smithsonian Books (2004)
7. Yoffee, N.: The decline and rise of Mesopotamian civilization: an ethnoarchaeological perspective on the evolution of social complexity. *Am. Antiq.* 5–35 (1979)
8. Kenoyer, J.M.: *Ancient Cities of the Indus Valley Civilization*. Oxford University Press, American Institute of Pakistan Studies (1998)
9. Yoffee, N., Cowgill, G.L. (eds.): *The Collapse of Ancient States and Civilizations*. University of Arizona Press (1988)
10. Turchin, P., Nefedov, S.A.: *Secular Cycles*. Princeton University Press, Princeton (2009)
11. Feng, Y., Kugler, J., Zak, P.J.: The politics of fertility and economic development. *Int. Stud. Quart.* **44**(4), 667–693 (2000)
12. Chua, A.: *World on Fire: How Exporting Free Market Democracy Breeds Ethnic Hatred and Global Instability*. Anchor (2003)
13. Prigogine, I., Stengers, I.: *Order Out of Chaos. Man's New Dialogue* (1984)
14. Abdollahian, M., Yang, Z., Coan, T., Yesilada, B.: Human development dynamics: an agent based simulation of macro social systems and individual heterogeneous evolutionary games. *Complex Adapt. Syst. Model.* **1**(1), 1–17 (2013)
15. Abdollahian, M., Yang, Z., deWerk Neal, P.: Human development dynamics: an agent based simulation of adaptive heterogeneous games and social systems. *Soc. Comput. Behav.-Cult. Model. Prediction* 3–10 (2014)
16. Abdollahian, M., Yang, Z., deWerk Neal, P., Kaplan, J.: Human development dynamics: network emergence in an agent based simulation of adaptive heterogeneous games and social systems. In: *Agent-Based Approaches in Economic and Social Complex Systems VIII*, pp. 3–14. Springer, Japan (2015)
17. Yang, Z.: An agent-based dynamic model of politics, fertility and economic development. In: *Proceedings of The 20th World Multi-Conference on Systemics, Cybernetics and Informatics* (2016)
18. Vespignani, A.: Predicting the behavior of techno-social systems. *Science* **325**(5939), 425 (2009)
19. Axelrod, R.: The evolution of strategies in the iterated prisoner's dilemma. *Dyn. Norms* 199–220 (1987)
20. Axelrod, R.M.: *The Complexity of Cooperation: Agent-Based Models of Competition and Collaboration*. Princeton University Press (1997)

21. Axelrod, R.: The dissemination of culture a model with local convergence and global polarization. *J. Conflict Resolut.* **41**(2), 203–226 (1997)
22. Nowak, M., Sigmund, K.: A strategy of win-stay, lose-shift that outperforms tit-for-tat in the Prisoner's Dilemma game. *Nature* **364**(6432), 56–58 (1993)
23. Nowak, M.A., Sigmund, K.: Evolution of indirect reciprocity by image scoring. *Nature* **393**(6685), 573–577 (1998)
24. Brander, J.A., Taylor, M.S.: The simple economics of Easter Island: A Ricardo-Malthus model of renewable resource use. *Am. Econ. Rev.* 119–138 (1998)
25. Drăgulescu, A., Yakovenko, V.M.: Exponential and power-law probability distributions of wealth and income in the United Kingdom and the United States. *Physica A* **299**(1), 213–221 (2001)
26. Banerjee, A., Yakovenko, V.M.: Universal patterns of inequality. *New J. Phys.* **12**(7), 075032 (2010)
27. Miller, J.H., Page, S.E.: *Complex Adaptive Systems: An Introduction to Computational Models of Social Life*. Princeton university press (2009)
28. Wilensky, U.: NetLogo. In: Evanston, I.L. (ed.) *Center for Connected Learning and Computer-Based Modeling*. Northwestern University (1999)
29. Binmore, K.: Game theory and the social contract. In: *Game Equilibrium Models II*, pp. 85–163. Springer, Berlin (1991)
30. Fudenberg, D., Maskin, E.: The folk theorem in repeated games with discounting or with incomplete information. *Econ. J. Econometric Soc.* 533–554 (1986)
31. Sigmund, K.: *Games of Life*. Oxford University Press, Oxford (1993)
32. Maynard-Smith, J., Szathmary, E.: *The Major Transitions in Evolution*. Freeman, Oxford (1995)
33. Snijders, T., Steglich, C., Schweinberger, M.: Modeling the Coevolution of Networks and Behavior, pp. 41–71 (2007)
34. Zheleva, E., Sharara, H., Getoor, L.: Co-evolution of social and affiliation networks. In: *Proceedings of the 15th ACM SIGKDD International Conference on Knowledge Discovery and Data Mining*, pp. 1007–1016. ACM (2009)
35. Schelling, T.C.: Dynamic models of segregation†. *J. Math. Soc.* **1**(2), 143–186 (1971)
36. McKelvey, B.: Avoiding complexity catastrophe in coevolutionary pockets: strategies for rugged landscapes. *Organ. Sci.* **10**(3), 294–321 (1999)
37. McPherson, M., Smith-Lovin, L., Cook, J.M.: Birds of a feather: homophily in social networks. *Ann. Rev. Soc.* 415–444 (2001)
38. Kauffman, S.A.: *The Origins of Order: Self-Organization and Selection in Evolution*. Oxford University Press, Oxford (1993)
39. Moyano, L.G., Sanchez, A.: Spatial prisoner's dilemma with heterogeneous agents: cooperation, learning and co-evolution. Arxiv preprint arXiv: 0805.2071 (2008)
40. Dixit, A., Reiley, D., Skeath, S.: *Games of Strategies*. Norton & Company, New York (2009)
41. Quek, H.Y., Tan, K.C., Abbass, H.A.: Evolutionary game theoretic approach for modeling civil violence. *Evol. Comput. IEEE Trans.* **13**(4), 780–800 (2009)